Applications of Aerobic Granular Sludge and Source-Separated Urine for Enhanced Nutrient Removal and Recovery

Stephany P. Wei

A dissertation
submitted in partial fulfillment of the
requirements for the degree of

Doctor of Philosophy

University of Washington
2022

Reading Committee:
Mari-Karoliina Winkler, Chair
David A. Stahl
Amy V. Mueller
Wei Qin

Program Authorized to Offer Degree:
Civil and Environmental Engineering

University of Washington

Abstract

Applications of Aerobic Granular Sludge and Source-Separated Urine for Enhanced Nutrient Removal and Recovery

Stephany P. Wei

Chair of the Supervisory Committee:
Mari-Karoliina Winkler
Civil and Environmental Engineering

Nutrient removal is one of the main goals of wastewater treatment plants (WWTP) to prevent eutrophication in the environment. The growing population and increasingly stringent discharge limits impose a need for intensification of existing wastewater infrastructure to maximize treatment capacity in the available space. The secondary goals of wastewater treatment are related to sustainability, such as reduced chemical usage and resource recovery. This thesis aims to find actionable maps for compact wastewater treatment solutions and new concepts for nutrient recovery with four specific objectives.

(1) Aerobic granular sludge (AGS) is an emerging technology that can enhance biological nutrient removal with reduced footprint. The current AGS technology is implemented in sequencing batch reactors (SBR) and its integration into existing full-scale continuous flow activate sludge (CFAS) systems is the next challenge to make this technology widely accessible. This thesis aims to address this research gap by understanding the selection factors contributing to granule growth in CFAS systems, investigating the partitioning of

microbial community between granules versus flocs, and exploring strategies for cultivating granules in a WWTP. The major conclusions from this work are the following: (i) Aerobic granules were discovered to naturally occur at 13 surveyed CFAS plants and their abundance were related to key design features such as high anaerobic food to mass ratios and influent soluble carbon fraction. Molecular analyses indicated that process configurations that select for slow-growing heterotrophs may also play an important role. (ii) In a hybrid granular activated sludge reactor, flocs offered better growth conductions for polyphosphate accumulating organisms while ammonia-oxidizing bacteria benefitted from the longer SRT in the granules. A complex relationship of microbial competition/cooperation between granules and flocs was demonstrated, highlighting the important role of small particles in maintaining the nutrient removal capacity of a hybrid granule/floc system. (iii) Full-scale application of a novel biocarrier technology for intensifying a CFAS plant was demonstrated with an all-organic media made of kenafs to facilitate biofilm attachment. The biofilm aggregates developed were comparable to SBR-type aerobic granules in terms of physical characteristics and activities of key microbial functional groups.

(2) Phosphorus recovery is gaining importance as the global phosphorus reserves is a finite resource. Struvite ($MgNH_4PO_4 \cdot 6H_2O$) is a proven slow-releasing fertilizer that can be obtained via precipitation. Struvite precipitation at WWTPs uses reject water from anaerobic digesters, but sludge thickening prior to digestion is needed to obtain high enough P concentrations in the struvite reactor as necessary to drive precipitation kinetics. This research aims to utilize the high thickening characteristics of AGS to demonstrate the production of a P-rich stream by simple anaerobic holding of the waste granular sludge. This

concept was tested with aerobic granules cultivated on aquaculture waste, achieving a P-rich stream without the need for sludge thickening equipment or anaerobic digester.

(3) Resource recovery at a WWTP can be limited by existing infrastructure and diluted concentrations. On the other hand, urine collected at the source (source-separated urine) offers an alternative stream for struvite recovery and is more favorable to centralized WWTP in terms of sustainable nutrient management. Struvite recovery from urine is well-demonstrated but due to the disproportionally high N/P ratio, significant amount of ammonia is remained after the struvite recovery step and requires additional treatment. The industrial production of nitrogen fertilizer via the Haber Bosch process consumes 1 – 2% of the global energy usage, and thus recycling of nitrogen from wastewater is desired. This thesis tested a chemical/physical process that combines air stripping and acid scrubbing at pilot-scale and demonstrated 93% N removal, from which 85% was recovered in the form of ammonium sulfate fertilizer.

(4) While nitrogen recovery via chemical/physical processes is a viable option (as identified in objective 3), the high energy demand is a major drawback. Biological nitrification offers a promising alternative as its energy input is lower than chemical/physical processes and the product (nitrified urine) is a good fertilizer. Urine can consist of varying compositions of ammonia and urea and in some cases (e.g., fresh urine), microbial hydrolysis of urea (ureolysis) is the first step towards obtaining a nitrified urine product. However, little is known about the ureolytic metabolism of nitrifying organisms and how their cellular regulations control the selective use of different nitrogen substrates. This thesis characterized the ureolytic physiology of five ammonia oxidizer isolates and showcased their varying

regulatory responses to alternative nitrogen substrates.

Table of Contents

List of Tables

List of Figures

Chapter 1. Overview

Wastewater treatment facilities are currently faced with increasing populations and stringent discharge limits, which stresses the need for intensification of existing infrastructure. In addition, human waste contains valuable resources and nutrients such as phosphorus and nitrogen that can be extracted to achieve a more sustainable nutrient loop. The main goal of this research is to advance nutrient removal and recovery from waste streams by adopting innovative biological technologies. This chapter reviews the current practices of nutrient management from wastewater, including biological nitrogen and phosphorus removal, struvite recovery, and the aerobic granular sludge technology. Then, the research objectives of this thesis will be identified for addressing the research gaps, along with an outline of the relevant thesis chapter(s).

1.1 The need for nutrient removal and recovery

Phosphorus and nitrogen are essential nutrients for all living organisms on earth and are consumed by humans via food. Healthy adults maintain a nutrient balance of zero (Kohlmeier, 2014; Liu & Jüppner, 2018), thus almost equal amount of consumed phosphorus and nitrogen are released within the excreta and discharged into the sewage system. In excess amount, these nutrients can cause destructive algal bloom leading to hypoxia in the receiving waters (Paerl et al., 2011). To avoid these environmental impacts, wastewater treatment plants (WWTP) have been upgraded to adopt nutrient removal technologies, but at a cost of significant space and energy consumption (Winkler & Straka, 2019). With the rapid population growth in urban areas and the projected increase in nutrient discharge limit stringency (Carey & Migliaccio, 2009), WWTP are faced with great challenges involving space and cost limitations. Another challenge faced by modern wastewater treatment is the desire for resource recovery and closed-loop nutrient cycling. While nitrogen fertilizer can be obtained by ammonia production from nitrogen

gas (N_2) via the energy-intensive Haber Bosch process, phosphorous is mined as a rock. With the diminishing phosphorus reserves, it is estimated that nearly all phosphorus generated from human waste must be recovered in order to meet future global food demand (Cordell et al., 2011). As a result, the main goals of wastewater treatment have shifted from solely protecting the human health and pollution control to energy optimization and resource recovery, and the development of new technologies and processes for meeting these goals have become essential.

1.2 Biological nitrogen removal

Nitrification is the biological oxidation of ammonia to nitrite and/or nitrate. The first step of nitrification is carried out by ammonia-oxidizing organisms (AOO) that convert ammonia (NH_3+NH_4^+) to nitrite (NO_2^-). The second step of nitrification involves the oxidation of nitrite (NO_2^-) to nitrate (NO_3^-) by the nitrite-oxidizing bacteria (NOB). The field of nitrification was pioneered by the isolation of the first ammonia-oxidizing bacteria (AOB) in the early 1890s (Frankland & Frankland, 1890) and the cultivation of *Nitrosomonas europaea* (Winogradsky, 1890), which is still used as a model AOB today. Our understanding in nitrification has since then expanded with the discovery and characterization of many phylogenetically distinct AOB and NOB, and further advanced with the groundbreaking isolation of the first ammonia-oxidizing archaea (AOA) (Konneke et al., 2005) and more recently complete ammonia oxidizer (comammox) (Daims et al., 2015; van Kessel et al., 2015). Denitrification is the process where nitrite or nitrate is biologically reduced to nitrogen gas (N_2), which is how nitrogen is ultimately removed from the wastewater into the atmosphere. In mainstream wastewater treatment processes, denitrification occurs in the anoxic zone of the treatment train, carried out by a diverse suite of heterotrophic bacteria (McIlroy et al., 2016) able to respire organic substrates anaerobically using nitrite or nitrate as electron acceptors. Denitrification can also occur

autotrophically, mediated by the anaerobic ammonium oxidizers (anammox) that anaerobically oxidize ammonia using nitrite as electron acceptor to produce N_2 (Kuenen, 2008; Strous et al., 1999). Anammox needs to be coupled with AOO so that half of the ammonia is first converted to nitrite (partial nitritation) as part of the substrate required for anammox. In WWTP, AOB are typically the dominant AOO supporting the anammox metabolism whereas the cooperation of AOA (not AOB) and anammox plays a significant role in the nitrogen turnover within the marine oxygen minimum zone (Lam et al., 2009; Pitcher et al., 2011). For a partial nitritation/anammox process to function properly, it is important that conditions are in place to favor the growth of AOB over NOB (i.e., NOB suppression, or also termed "nitrite shunt"), whose proliferation can outcompete the anammox for nitrite hence leading to undesirable nitrate accumulation in the effluent. While research on mainstream applications is underway (Cao et al., 2017; Winkler et al., 2012), full-scale anammox has mostly been applied in the sidestream of WWTP (Winkler & Straka, 2019), where high temperature and ammonia concentration are favorable for their slow metabolism.

1.3 Enhanced biological phosphorus removal

Enhanced biological phosphorus removal (EBPR) is a well-established engineering process that selects for polyphosphate-accumulating organisms (PAO), which are a group of bacteria that can store high amounts of phosphorus (up to 17% dry cell mass) in comparison to typical heterotrophic bacteria (1.5 to 2.0% dry cell mass) (Henze et al., 2008; Stensel, 1991). PAO are enriched under alternating anaerobic and anoxic/aerobic conditions, as required by their unique metabolism. Under anaerobic condition, the PAO consume carbon substrate and synthesize it into an intracellular storage product, which is then used as the electron donor in the subsequent aerobic/anoxic phase when oxygen or nitrite/nitrate are available (**Figure 1-1**). The energy

required for the anaerobic carbon uptake and conversion to storage product is harvested from the hydrolysis of intracellular polyphosphate, releasing ortho-phosphate into the bulk liquid. In the aerobic phase, PAO oxidize the carbon storage for cell growth and replenish the polyphosphate reserves, which results in phosphate uptake. Some PAO strains can also respire nitrite/nitrate (denitrifying PAO, or dPAO) to promote the same process under anoxic conditions, and thus contribute to the N-cycle by producing N_2. Due to additional cell growth in the aerobic/anoxic condition, phosphorus uptake is higher than the released phosphorus and as a result, a net phosphorus removal from the liquid is achieved.

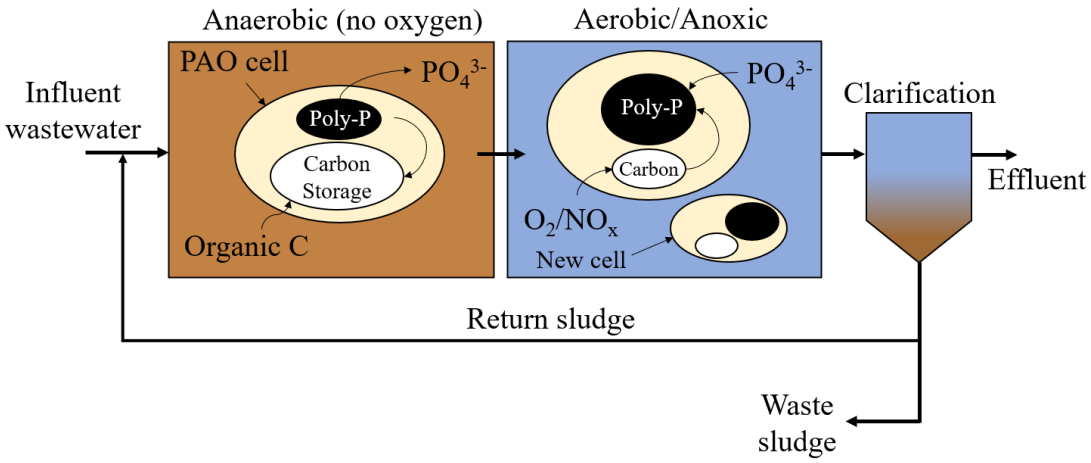

Figure 1-1. Conceptual scheme showing the P and C flows of the PAO metabolism.

PAO's carbon storage ability gives them the competitive advantage over other ordinary heterotrophs by consuming the carbon anaerobically, which allows the PAO to grow on the intracellular storage when electron acceptors are available while the ordinary heterotrophs starve. Metabolically similar to the PAOs, the glycogen-accumulating organisms (GAO) can also store carbon anaerobically but do not contribute to phosphorus cycling. PAO cells tend to form large

and tight clusters in activated sludge (Seviour et al., 2003) (**Figure 1-2**) and their growth on intracellular carbon storage is associated with slow-growing metabolism that is known to produce dense and well-settling flocs (de Kreuk & van Loosdrecht, 2004). Indeed, some WWTP adopt anaerobic selectors (which favor the growth of PAO) for purposes of improved floc settling, even when phosphorus removal is not required (Tchobanoglous et al., 2014).

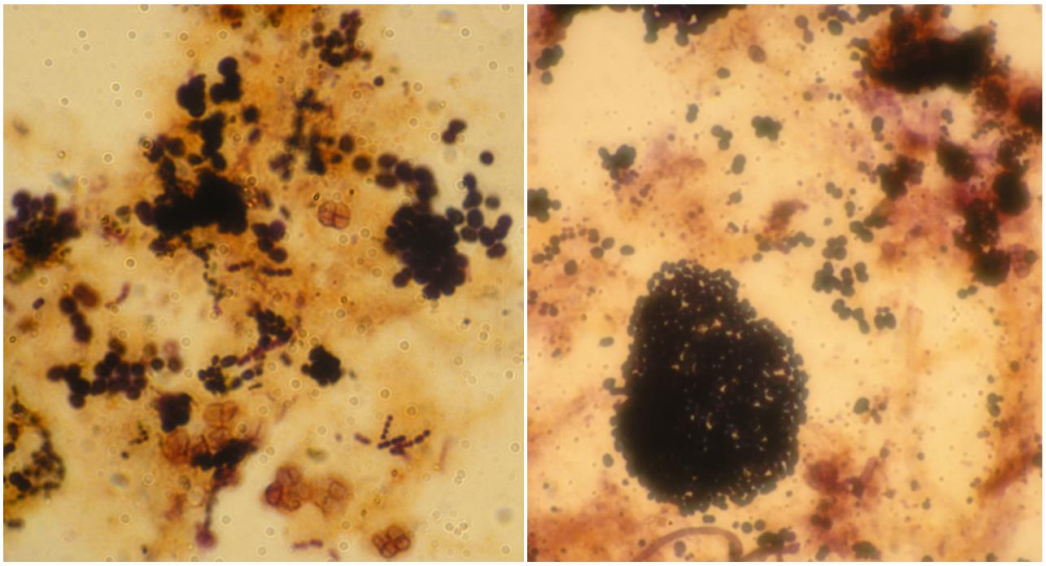

Figure 1-2. Neisser staining images of activated sludge samples. Left: Puyallup Pollution Control Plant, WA; Right: City of Idaho Falls WWTP, ID. Images were taken at 1000X with an Olympus BHS microscope. Dark purple cells are polyphosphate-positive showing PAO in clusters.

1.4 Putative polyphosphate accumulating organisms

Although all the PAO share the common metabolism of anaerobic P release and aerobic P uptake, they spread across multiple phyla and exhibit versatile physiology even within the same

genus. The most extensively studied PAO is the *Candidatus Accumulibacter phosphatis* (abbreviated to *Accumulibacter* thereafter), which was first named by (Hesselmann et al., 1999) and (Crocetti et al., 2000). Since then, *Accumulibacter* formed the basis of most metabolic models for PAOs (Martin et al., 2006; Oyserman et al., 2016; Smolders et al., 1995). Under anaerobic conditions, *Accumulibacter* take up volatile fatty acids (VFAs) (i.e., acetate and propionate) and store them intracellularly as polyhydroxyalkanoates (PHA). The reducing power required for the PHA synthesis step is obtained via glycolysis, the tricarboxylic acid cycle, or both (Oehmen et al., 2007). Under aerobic/anoxic conditions, *Accumulibacter* oxidize the intracellular PHA for cell growth and replenish the polyphosphate/glycogen reserves.

In 2005, (Kong et al., 2005) identified high abundance of the genus *Tetrasphaera* at a full-scale EBPR plant and demonstrated their ability to use amino acids anaerobically and uptake phosphorus aerobically. Since then, many studies had confirmed *Tetrasphaera* as a putative PAO and observed *Tetrasphaera* at higher abundance than *Accumulibacter* in some full-scale plants (Lanham et al., 2013; Marques et al., 2017; Nguyen et al., 2011). Compared to *Accumulibacter*, which primarily use VFA as the preferred carbon source, *Tetrasphaera* can use a wider range of complex carbon substrates. Some *Tetrasphaera* strains can even ferment glucose and amino acids for additional energy (Nguyen et al., 2011). Like *Accumulibacter*, the anaerobic P release of *Tetrasphaera* is coupled with uptake of organic substrates from the liquid and the aerobic phosphorus uptake capability is dependent upon the intracellular reserves stored during the anaerobic phase. However, the storage products of relevance for *Tetrasphaera* have yet to be identified (Liu et al., 2019).

Accumulibacter and *Tetrasphaera* are both important contributor to P removal in full-scale EBPR plants (Fernando et al., 2019). It has been suggested that *Accumulibacter* likely survive on fermentation products of *Tetrasphaera* (Marques et al., 2017), but their ecological niches are not well-understood. The important factors for determining the abundance of *Accumulibacter* versus *Tetrasphaera* may be the availability of organic substrates (acetate versus glucose) and anaerobic residence time (fermentation requires longer time) (Liu et al., 2019). Temperature is also a possible factor as the abundance of *Tetrasphaera* appears to be lower (0.23–1.8%) in tropical climate (Qiu et al., 2019) than temperate climate (3.6 – 28%) (Lanham et al., 2013; Stokholm-Bjerregaard et al., 2017).

1.5 Aerobic granular sludge

In the last two decades, aerobic granular sludge (AGS) is one of the most important innovations in the field of wastewater engineering. First developed in the late 1990s (Beun et al., 1999; Morgenroth et al., 1997), aerobic granules are self-forming biofilm aggregates with semi-spherical morphology and typical diameters of 0.5–3 mm. In comparison to activated sludge, aerobic granules are structured with bacteria and extracellular polymeric substances (EPS) in a denser manner (Figdore et al., 2017). The typical settling velocity and sludge volume index (SVI) of granular sludge are in the range of 30–90 m/hr and <50 ml/g with 5-min settling (SVI_5) whereas for activated sludge the ranges are 0.5–5 m/hr and 100–200 ml/g with 30-min settling (SVI_{30}) (Winkler et al., 2018). These fast settling and high thickening characteristics of AGS allow for much more compact wastewater treatment systems and high solids concentrations, leading to significant space reduction (de Bruin et al., 2004; Pronk et al., 2015).

In addition, all necessary redox conditions occur within micrometre-scale biofilm aggregates,

allowing for biological transformations of carbon, nitrogen, and phosphorus in one single reactor configuration (de Kreuk et al., 2005). Anaerobic condition is created during the anaerobic phase of reactor operation where PAO (or GAO) consume and store the carbon (**Figure 1-3a**). In the aerobic phase, oxygen concentration decreases with granule depth as a function of diameter due to diffusion limitations and aerobic consumption, thereby dividing the granule into aerobic and anoxic layers (**Figure 1-3b**). Thus, the distribution of different microbial populations within the granule is segregated by depth as depicted in **Figure 1-4**. AOB/NOB are localized to the outer oxygen penetrated shell where they oxidize NH_4 into NO_2 and NO_3, which diffuse into the interior of the granule where anoxic conditions enable denitrification (by denitrifying PAOs or GAOs).

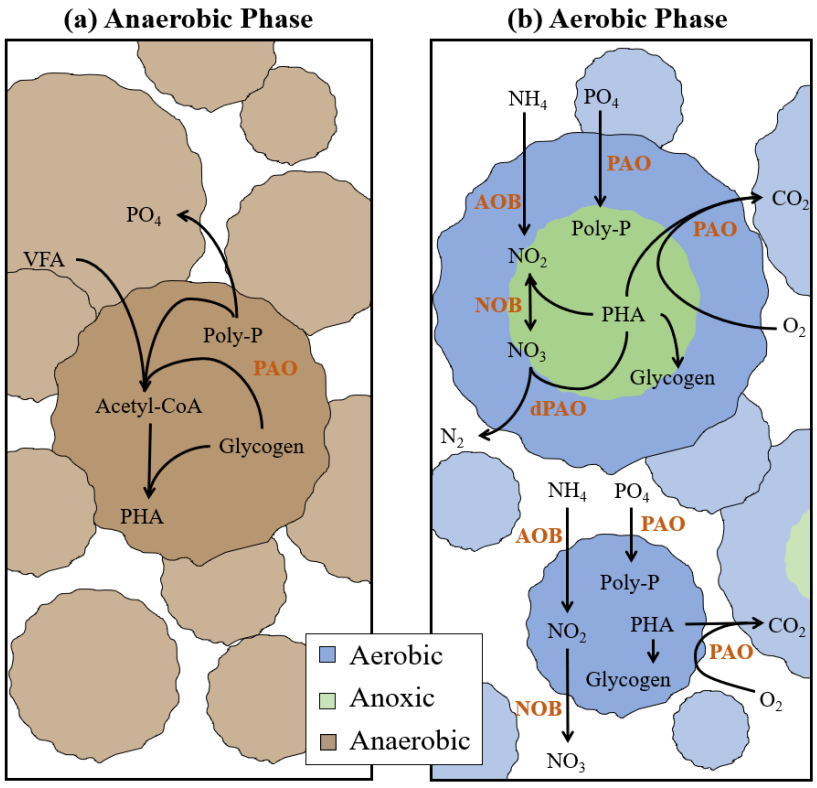

Figure 1-3. Transformations of C, N and P by the microbial consortium within a granule. (a) Anaerobic phase. (b) Aerobic phase; oxygen gradient is a function of granule size: larger

granules have higher anoxic volume fraction whereas smaller granules have higher aerobic volume fraction.

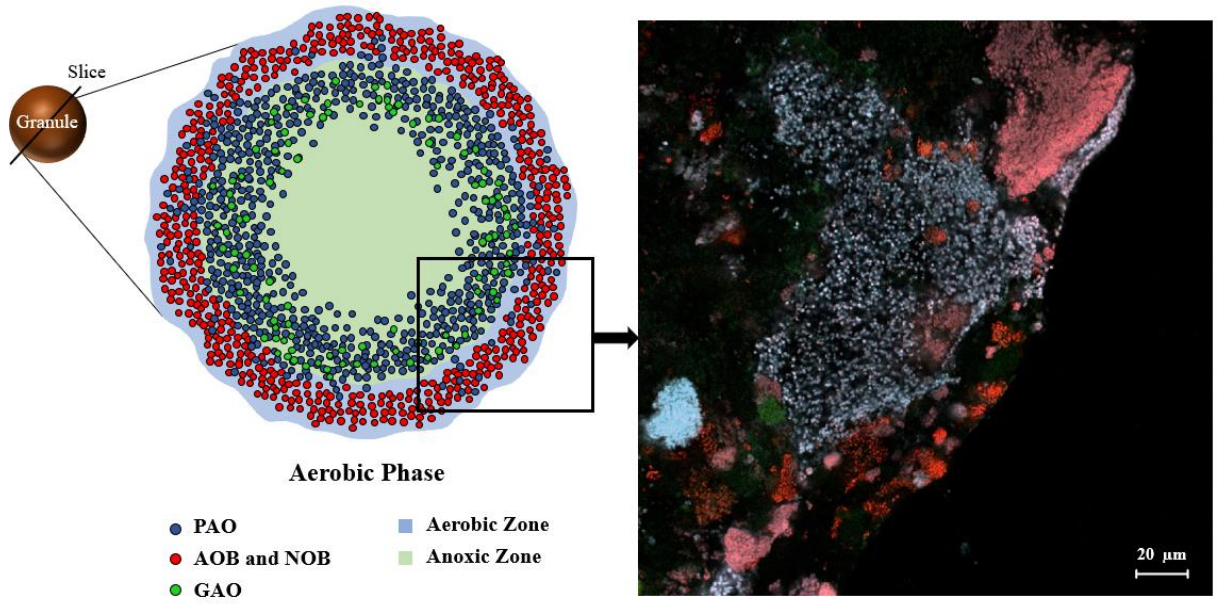

Figure 1-4. Microbial distribution within a granule. Schematic depiction (left) and a fluorescence in-situ hybridization image showing the edge of a 10 µm thick granule section (right) hybridized with fluorescent probes; PAO (blue), GAO (green) and AOB/NOB (red).

The most well-established AGS technology is demonstrated with sequencing batch reactors (SBRs) where influent wastewater is fed anaerobically through a settled sludge bed. This high food to mass (F/M) feeding regime reduces diffusion-limited growth by promoting substrate penetration into the granule core and enables a higher substrate concentration for faster anaerobic uptake rates by PAOs or GAOs. The enrichment of slow-growing heterotrophs (e.g., PAO and GAO) is known to aid in the formation of smooth and compact granules (de Kreuk & van Loosdrecht, 2004; Winkler et al., 2011). Additionally, the aeration period is followed by a short

settling time and subsequently the influent feed pushes the effluent over the top of the reactor, washing out the slow settling particles but retaining the larger AGS aggregates.

Research objective 1: Integration of aerobic granular sludge in continuous flow systems

The benefits of the AGS technology fit the current needs of the wastewater engineering industry of providing effective wastewater treatment in urban areas with growing population while reducing the economic and environmental costs. To date, full-scale demonstrations of AGS technology are limited to SBRs but most existing wastewater treatment plants (WWTP) have continuous flow activated sludge (CFAS) systems in place. In comparison to SBR-type AGS reactors, CFAS systems are operated with completely mixed feeding regime with diluted concentrations. As a result, *t*he AGS technology cannot be readily incorporated into most existing WWTPs, which clearly limits its broader application. This thesis aims to address this knowledge gap by understanding the selection factors contributing to granule growth in full-scale continuous flow systems (**Chapter 2**), investigating the partitioning and competition of key microbial functional groups between granules versus flocs (**Chapter 3**), and exploring strategies for cultivating granules in an activated sludge plant (**Chapter 4)**.

1.6 Phosphorus recovery

Struvite ($MgNH_4PO_4 \cdot 6H_2O$) is a proven slow-releasing fertilizer that can be precipitated from waste streams when all necessary ions (Mg^{2+}, NH_4^+, and PO_4^{3-}) are present and under the right pH conditions (Le Corre et al., 2009). High concentrations of ions lead to more favorable struvite precipitation kinetics and thus improves the operational costs of struvite reactors. A phosphorus concentration of at least 100 mg P/L is required for a struvite recovery rate that is economically feasible (Kehrein et al., 2020). Therefore, waste streams that contain high nutrient

concentrations, such as urine or livestock manure wastewater, have been investigated for their suitability for struvite recovery (Peng et al., 2018). The dewatering filtrate from anaerobic digested sludge (centrate) at WWTP is a common source of stream for struvite production (Bhuiyan et al., 2008; Lahav et al., 2013). Struvite precipitation from centrate is already commonly practiced at full scale WWTPs for benefits of preventing unwanted scaling issues, improved sludge dewaterability, and resource recovery (Kehrein et al., 2020; Saerens et al., 2021).

Research Objective 2: Enhance phosphorus recovery with aerobic granular sludge

The current practice of struvite recovery in activated sludge facilities are limited to sidestream where thickening of the activated sludge prior anaerobic digestion is required to obtain high phosphorus concentration. This greatly limits the application of phosphorus recovery as facilities smaller than 1 Mgal/day of capacity generally do not have specialized sludge thickening units (Metcalf & Eddy et al., 2014). With the integration of AGS, high solids concentration can be achieved without the need for separate equipment due to the inherently high thickening characteristics of the granules. Therefore, an alternative phosphorus recovery process could theoretically be adopted where high phosphorus concentration is obtained by simple anaerobic holding of the waste granular sludge, eliminating the need for thickening equipment. Such phosphorus recovery process is ideal for small facilities that wish to reduce their phosphate discharge, as it requires minimal equipment relative to other treatment methods. This thesis aims to demonstrate the production of high phosphorus concentration streams without the need for thickening with aerobic granules cultivated from aquaculture waste (**Chapter 5**).

1.7 Nitrogen management

In addition to phosphorus, nitrogen is another valuable nutrient in wastewater that can be recovered. Although the cost of nitrogen recovery does not offset the cost of industrial fertilizer production, the Haber Bosch process consumes more than 1% of the global energy (Cherkasov et al., 2015) and offsetting this energy consumption with resource recovered from wastewater is desirable. It should be noted that in addition to recovering phosphorus, struvite precipitation also recovers nitrogen. However, due to the high N/P ratio in many waste streams (e.g., centrate, liquid from anaerobic digestion of livestock manure, etc.), high ammonia concentrations typically remain in the effluent of the struvite reactor and requires additional treatment steps for nitrogen removal/recovery (e.g., in combination with other chemical nitrogen recovery methods or biological nitrogen removal).

1.7.1 The concept of source-separated urine for nutrient recovery

Technologies are available to recover nitrogen from wastewater but resource recovery from combined wastewater streams is challenging because it is limited to existing infrastructure, treatment technologies and diluted concentrations (Brands, 2014; Ishii & Boyer, 2015). On the other hand, urine collected at the source (source-separated urine) offers a promising alternative as it allows processing with a more concentrated stream and offers more flexible treatment and recovery options (Larsen et al., 2009; Maurer et al., 2006). Human urine has tremendous potential for nutrient recovery as it contributes most of the nutrient loads (80% of the total nitrogen and 45% of the total phosphorus) yet less than 1% of the volumetric flow to a WWTP (Wilsenach & van Loosdrecht, 2006). A logical approach would be to collect the urine separately from the feces, then recover the nitrogen and phosphorus from the urine. This concept of urine source separation is a more promising practice than conventional wastewater treatment systems

in terms of sustainable nutrient management (Larsen et al., 2007). Further, nutrient recovery from source-separated urine can alleviate the nutrient loads on downstream biological nutrient removal facility and increase the capacity of an existing plant by up to 60% (Wilsenach & Van Loosdrecht, 2004).

1.7.2 Nutrient recovery from urine via chemical methods

Fresh urine is slightly acidic (pH of around 6) and its total nitrogen content mainly consists of urea (4450 – 8750 mg N/L) (Etter et al., 2011; Udert et al., 2003). Due to non-sterile conditions during storage, the urea is hydrolyzed to ammonia by microbial ureolytic activity, which increases the pH of the urine solution to around 9. The resulting stored urine is high in PO_4^{3-} and NH_4^+ and is therefore a suitable stream for struvite ($MgNH_4PO_4 \cdot 6H_2O$) precipitation with the addition of Mg^{2+}. Struvite precipitation from urine is well-demonstrated and the influencing factors on crystal sizes and the fate of pharmaceuticals and heavy metals have been extensively covered in lab-scale studies (Ronteltap et al., 2007; Ronteltap et al., 2010; Tilley et al., 2008; Wilsenach et al., 2007).

Research Objective 3: Demonstrate complete N recovery from urine at pilot-scale

Despite the extensive amount of research conducted on struvite recovery from urine, pilot- and full-scale studies are limited to a few. In addition, due to the disproportionate molar ratio of NH_4^+ and PO_4^{3-} in urine, merely 3% of NH_4^+ can be removed along with 90% PO_4^{3-} removal via struvite precipitation (Etter et al., 2011; Maurer et al., 2006), and thus additional nitrogen removal/recovery are required. A method for nitrogen recovery is NH_3 stripping then the production of ammonium sulphate via acid scrubbing. This thesis aims to explore the feasibility

of nitrogen recovery from urine in the form of ammonium sulphate with a pilot-scale study (**Chapter 6**).

1.7.3 Nutrient recovery from urine using biological solutions

While the recovery of nitrogen can be accomplished via physical/chemical methods (e.g., with the production of ammonium sulphate), the high energy consumption is a major drawback. Therefore, alternative technologies with lower energy demand are needed. Partial nitritation/anammox can remove nitrogen from urine at a lower energy input than N production via the Haber Bosch process (Maurer et al., 2003), but the product is nitrogen gas that is lost into the air, offering no potential for nitrogen recovery. Urine nitrification is a promising alternative as nitrified urine is a good fertilizer and its energy requirement can compete with conventional nutrient removal at WWTP (Christiaens et al., 2019; Udert & Wachter, 2012). The total nitrogen in fresh urine is mostly urea, and thus the first step of the biological conversion to nitrified urine is urea hydrolysis. Urea hydrolysis can be catalyzed by the enzyme urea amidolyase or urease (also called urea amidohydrolase). Urea amidolyase is an ATP- and biotin-dependent enzyme system that consists of two components (i.e., urea carboxylase and allophanate hydrolase). Urease catalyzes the urea hydrolysis into ammonia and carbamate, which spontaneously splits to yield another ammonia molecule and carbonic acid:

$$NH_2CONH_2(urea) + H_2O \xrightarrow{urease} NH_3 + NH_2COOH(carbamate)$$

$$\xrightarrow{spontaneous} NH_3 + H_2CO_3$$

Depending on the time and condition during urine storage, the nitrifying organisms can be exposed to environments with varying urea and ammonia concentrations. Both the urea and ammonia can be used as nitrogen substrates for ammonia oxidation by the AOO, from which the

nitrite produced is utilized by the NOB for nitrite oxidation, resulting in the final product of a nitrified urine solution (**Figure 1-5**).

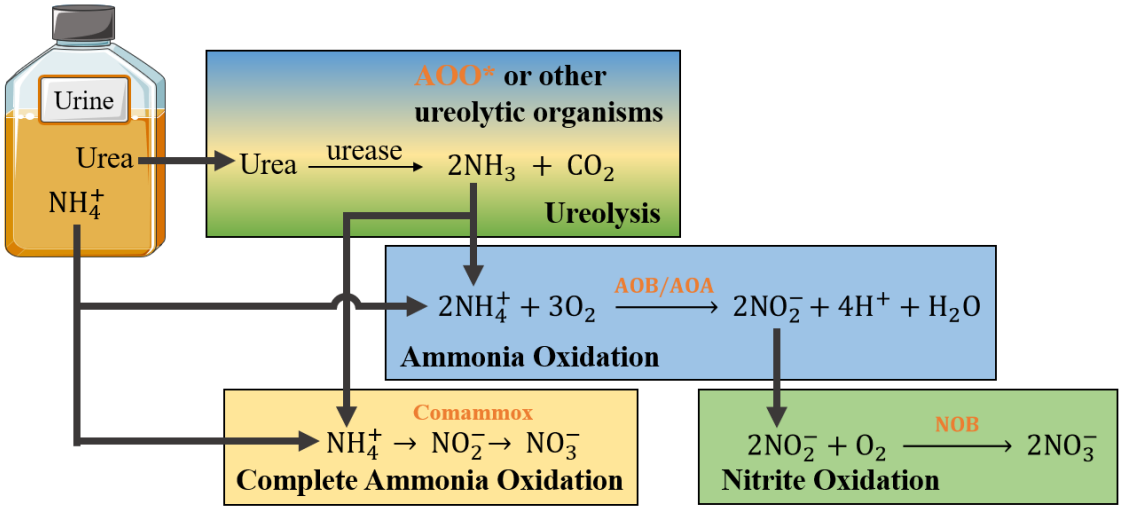

Figure 1-5. Schematic for the biological nitrification of urine. The total nitrogen in fresh urine is roughly 85% urea and 15% ammonia, and the conversion to nitrate is a multi-step process that involves urea hydrolysis, ammonia oxidation, and nitrite oxidation. *AOO can be AOB, AOA, or comammox.

1.7.4 Ureolytic metabolism of nitrifying microorganisms

Like most bacteria that have the ability to hydrolyze urea, many AOO and some canonical (strict nitrite-oxidizing) NOB contain the genes encoding the cytoplasmic nickel-dependent structural urease (UreABC) and the accessory urease proteins (UreEFGD) (Koch et al., 2019; Koper et al., 2004; Palomo et al., 2018; Qin et al., 2020). Even though the urea molecule, due to its small and uncharged nature, can diffuse passively across the cell membrane, some AOO (e.g., comammox) harbor the energy-dependent (ATP-dependent) urea uptake systems and encode the active urea transporter (UrtABCDE), which is related to high affinity for urea (Palomo et al., 2018). Using

the published genome of a few example AOO, the arrangement of these urea transport and utilization genes on the urea genomic region are displayed in **Figure 1-6**.

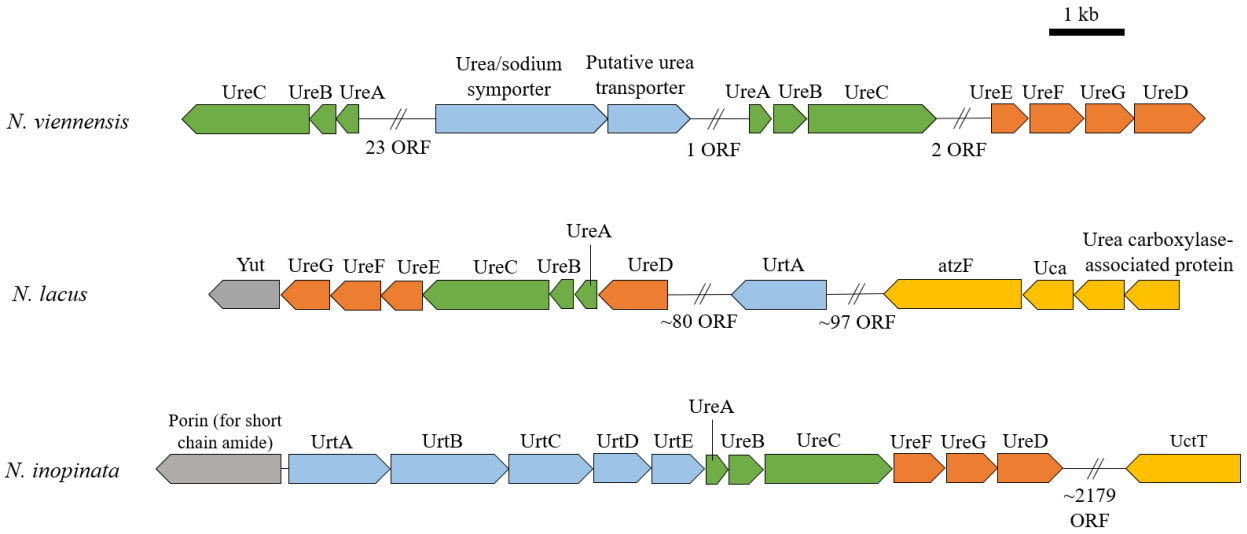

Figure 1-6. Schematic representation of the genomic regions for urea transport and utilization. The schematic was produced based on published genomes and annotations of *N. viennensis* (Tourna et al., 2011), *N. lacus* (Urakawa et al., 2015), and *N. inopinata* (Daims et al., 2015). UreABC, urease; UreEFGD, urease accessory proteins; UrtABCDE, urea ABC-type transporter; atzF, allophanate hydrolase; Uca, urea carboxylase; UctT, urea carboxylase-related amino acid permease; Yut, urea permease.

Research Objective 4: Enhance knowledge in ureolytic metabolism of nitrifiers

Many studies have confirmed the ureolytic activity of nitrifying microorganisms with batch incubations (Koch et al., 2015; Qin et al., 2014; van Kessel et al., 2015), including a few that showed a transient accumulation of ammonia in the medium when AOBs are grown on urea (Allison & Prosser, 1991; Jiang & Bakken, 1999). Surprisingly, little is known about how the AOO respond to changes in nitrogen substrates (i.e., ammonia versus urea), even baseline physiological characterizations of their ureolytic metabolism are lacking. In addition, little is

known about the control and regulation of the urease genes in the AOO. How the urease gene responds to environmental factors such as concentrations and availability of NH_4^+ and where the regulations occur on the cellular level are largely unknown. This thesis aims to strengthen our understanding in the ureolytic metabolism of the nitrifying microorganisms and how the phylogenetically distinct AOO respond to switches in nitrogen substrates (**Chapter 7**).

References

Allison, S.M., Prosser, J.I. 1991. UREASE ACTIVITY IN NEUTROPHILIC AUTOTROPHIC AMMONIA-OXIDIZING BACTERIA ISOLATED FROM ACID SOILS. *Soil Biology & Biochemistry*, **23**(1), 45-51.

Beun, J.J., Hendriks, A., Van Loosdrecht, M.C.M., Morgenroth, E., Wilderer, P.A., Heijnen, J.J. 1999. Aerobic granulation in a sequencing batch reactor. *Water Research*, **33**(10), 2283-2290.

Bhuiyan, M.I.H., Mavinic, D.S., Koch, F.A. 2008. Phosphorus recovery from wastewater through struvite formation in fluidized bed reactors: a sustainable approach. *Water Science and Technology*, **57**(2), 175-181.

Brands, E. 2014. Prospects and challenges for sustainable sanitation in developed nations: a critical review. *Environmental Reviews*, **22**(4), 346-363.

Cao, Y.S., van Loosdrecht, M.C.M., Daigger, G.T. 2017. Mainstream partial nitritation-anammox in municipal wastewater treatment: status, bottlenecks, and further studies. *Applied Microbiology and Biotechnology*, **101**(4), 1365-1383.

Carey, R.O., Migliaccio, K.W. 2009. Contribution of Wastewater Treatment Plant Effluents to Nutrient Dynamics in Aquatic Systems: A Review. *Environmental Management*, **44**(2), 205-217.

Cherkasov, N., Ibhadon, A.O., Fitzpatrick, P. 2015. A review of the existing and alternative methods for greener nitrogen fixation. *Chemical Engineering and Processing*, **90**, 24-33.

Christiaens, M.E.R., De Paepe, J., Ilgrande, C., De Vrieze, J., Barys, J., Teirlinck, P., Meerbergen, K., Lievens, B., Boon, N., Clauwaert, P., Vlaeminck, S.E. 2019. Urine nitrification with a synthetic microbial community. *Systematic and Applied Microbiology*, **42**(6).

Cordell, D., Rosemarin, A., Schroder, J.J., Smit, A.L. 2011. Towards global phosphorus security: A systems framework for phosphorus recovery and reuse options. *Chemosphere*, **84**(6), 747-758.

Crocetti, G.R., Hugenholtz, P., Bond, P.L., Schuler, A., Keller, J., Jenkins, D., Blackall, L.L. 2000. Identification of polyphosphate-accumulating organisms and design of 16S rRNA-directed probes for their detection and quantitation. *Applied and Environmental Microbiology*, **66**(3), 1175-1182.

Daims, H., Lebedeva, E.V., Pjevac, P., Han, P., Herbold, C., Albertsen, M., Jehmlich, N., Palatinszky, M., Vierheilig, J., Bulaev, A., Kirkegaard, R.H., von Bergen, M., Rattei, T., Bendinger, B., Nielsen, P.H., Wagner, M. 2015. Complete nitrification by Nitrospira bacteria. *Nature*, **528**(7583), 504-+.

de Bruin, L.M.M., de Kreuk, M.K., van der Roest, H.F.R., Uijterlinde, C., van Loosdrecht, M.C.M. 2004. Aerobic granular sludge technology: an alternative to activated sludge? *Water Science and Technology*, **49**(11-12), 1-7.

de Kreuk, M., Heijnen, J.J., van Loosdrecht, M.C.M. 2005. Simultaneous COD, nitrogen, and phosphate removal by aerobic granular sludge. *Biotechnology and Bioengineering*, **90**(6), 761-769.

de Kreuk, M.K., van Loosdrecht, M.C.M. 2004. Selection of slow growing organisms as a means for improving aerobic granular sludge stability. *Water Science and Technology*, **49**(11-12), 9-17.

Etter, B., Tilley, E., Khadka, R., Udert, K.M. 2011. Low-cost struvite production using source-separated urine in Nepal. *Water Research*, **45**(2), 852-862.
Fernando, E.Y., McLlroy, S.J., Nierychlo, M., Herbst, F.A., Petriglieri, F., Schmid, M.C., Wagner, M., Nielsen, J.L., Nielsen, P.H. 2019. Resolving the individual contribution of key microbial populations to enhanced biological phosphorus removal with Raman-FISH. *Isme Journal*, **13**(8), 1933-1946.
Figdore, B.A., Stensel, H.D., Winkler, M.K.H., Neethling, J.B. 2017. Aerobic Granular Sludge for Biological Nutrient Removal. Water Environment and Reuse Foundation.
Frankland, P.F., Frankland, G.C. 1890. V. The nitrifying process and its specific ferment.—Part I. *Philosophical Transactions of the Royal Society B*, **181**, 107–128.
Henze, M., Loosdrecht, M.C.M.v., Ekama, G.A., Brdjanovic, D. 2008. Chapter 7. Enhanced Biological Phosphorus Removal. in: *Biological Wastewater Treatment - Principles, Modelling and Design*, IWA Publishing.
Hesselmann, R.P.X., Werlen, C., Hahn, D., van der Meer, J.R., Zehnder, A.J.B. 1999. Enrichment, phylogenetic analysis and detection of a bacterium that performs enhanced biological phosphate removal in activated sludge. *Systematic and Applied Microbiology*, **22**(3), 454-465.
Ishii, S.K.L., Boyer, T.H. 2015. Life cycle comparison of centralized wastewater treatment and urine source separation with struvite precipitation: Focus on urine nutrient management. *Water Research*, **79**, 88-103.
Jiang, Q.Q., Bakken, L.R. 1999. Comparison of Nitrosospira strains isolated from terrestrial environments. *Fems Microbiology Ecology*, **30**(2), 171-186.
Kehrein, P., Van Loosdrecht, M., Osseweijer, P., Garfí, M., Dewulf, J., Posada, J. 2020. A critical review of resource recovery from municipal wastewater treatment plants–market supply potentials, technologies and bottlenecks. *Environmental Science: Water Research & Technology*, **6**(4), 877-910.
Koch, H., Lucker, S., Albertsen, M., Kitzinger, K., Herbold, C., Spieck, E., Nielsen, P.H., Wagner, M., Daims, H. 2015. Expanded metabolic versatility of ubiquitous nitrite-oxidizing bacteria from the genus Nitrospira. *Proceedings of the National Academy of Sciences of the United States of America*, **112**(36), 11371-11376.
Koch, H., van Kessel, M., Lucker, S. 2019. Complete nitrification: insights into the ecophysiology of comammox Nitrospira. *Applied Microbiology and Biotechnology*, **103**(1), 177-189.
Kohlmeier, M. 2014. *Nutrient Metabolism (Second Edition)*. Elsevier.
Kong, Y., Nielsen, J.L., Nielsen, P.H. 2005. Identity and ecophysiology of uncultured actinobacterial polyphosphate-accumulating organisms in full-scale enhanced biological phosphorus removal plants. *Applied and environmental microbiology*, **71**(7), 4076-4085.
Konneke, M., Bernhard, A.E., de la Torre, J.R., Walker, C.B., Waterbury, J.B., Stahl, D.A. 2005. Isolation of an autotrophic ammonia-oxidizing marine archaeon. *Nature*, **437**(7058), 543-546.
Koper, T.E., El-Sheikh, A.F., Norton, J.M., Klotz, M.G. 2004. Urease-encoding genes in ammonia-oxidizing bacteria. *Applied and Environmental Microbiology*, **70**(4), 2342-2348.
Kuenen, J.G. 2008. Anammox bacteria: from discovery to application. *Nature Reviews Microbiology*, **6**(4), 320-326.

Lahav, O., Telzhensky, M., Zewuhn, A., Gendel, Y., Gerth, J., Calmano, W., Birnhack, L. 2013. Struvite recovery from municipal-wastewater sludge centrifuge supernatant using seawater NF concentrate as a cheap Mg(II) source. *Separation and Purification Technology*, **108**, 103-110.

Lam, P., Lavik, G., Jensen, M.M., van de Vossenberg, J., Schmid, M., Woebken, D., Dimitri, G., Amann, R., Jetten, M.S.M., Kuypers, M.M.M. 2009. Revising the nitrogen cycle in the Peruvian oxygen minimum zone. *Proceedings of the National Academy of Sciences of the United States of America*, **106**(12), 4752-4757.

Lanham, A.B., Oehmen, A., Saunders, A.M., Carvalho, G., Nielsen, P.H., Reis, M.A.M. 2013. Metabolic versatility in full-scale wastewater treatment plants performing enhanced biological phosphorus removal. *Water Research*, **47**(19), 7032-7041.

Larsen, T.A., Alder, A.C., Eggen, R.I.L., Maurer, M., Lienert, J. 2009. Source Separation: Will We See a Paradigm Shift in Wastewater Handling? *Environmental Science & Technology*, **43**(16), 6121-6125.

Larsen, T.A., Maurer, M., Udert, K.M., Lienert, J. 2007. Nutrient cycles and resource management: implications for the choice of wastewater treatment technology. *Water Science and Technology*, **56**(5), 229-237.

Le Corre, K.S., Valsami-Jones, E., Hobbs, P., Parsons, S.A. 2009. Phosphorus Recovery from Wastewater by Struvite Crystallization: A Review. *Critical Reviews in Environmental Science and Technology*, **39**(6), 433-477.

Liu, E.S., Jüppner, H. 2018. Clinical Disorders of Phosphate Homeostasis. in: *Vitamin D (Fourth Edition)*, (Ed.) D. Feldman, Elsevier Inc.

Liu, R.B., Hao, X.D., Chen, Q., Li, J. 2019. Research advances of Tetrasphaera in enhanced biological phosphorus removal: A review. *Water Research*, **166**.

Marques, R., Santos, J., Nguyen, H., Carvalho, G., Noronha, J.P., Nielsen, P.H., Reis, M.A.M., Oehmen, A. 2017. Metabolism and ecological niche of Tetrasphaera and Ca. Accumulibacter in enhanced biological phosphorus removal. *Water Research*, **122**, 159-171.

Martin, H.G., Ivanova, N., Kunin, V., Warnecke, F., Barry, K.W., McHardy, A.C., Yeates, C., He, S.M., Salamov, A.A., Szeto, E., Dalin, E., Putnam, N.H., Shapiro, H.J., Pangilinan, J.L., Rigoutsos, I., Kyrpides, N.C., Blackall, L.L., McMahon, K.D., Hugenholtz, P. 2006. Metagenomic analysis of two enhanced biological phosphorus removal (EBPR) sludge communities. *Nature Biotechnology*, **24**(10), 1263-1269.

Maurer, M., Pronk, W., Larsen, T.A. 2006. Treatment processes for source-separated urine. *Water Research*, **40**(17), 3151-3166.

Maurer, M., Schwegler, P., Larsen, T.A. 2003. Nutrients in urine: energetic aspects of removal and recovery. *Water Science and Technology*, **48**(1), 37-46.

McIlroy, S.J., Starnawska, A., Starnawski, P., Saunders, A.M., Nierychlo, M., Nielsen, P.H., Nielsen, J.L. 2016. Identification of active denitrifiers in full-scale nutrient removal wastewater treatment systems. *Environmental Microbiology*, **18**(1), 50-64.

Metcalf & Eddy, Abu-Orf, M., Bowden, G., Burton, F.L., Pfrang, W., Stensel, H.D., Tchobanoglous, G., Tsuchihashi, R., AECOM. 2014. *Wastewater engineering: treatment and resource recovery*. McGraw Hill Education.

Morgenroth, E., Sherden, T., van Loosdrecht, M.C.M., Heijnen, J.J., Wilderer, P.A. 1997. Aerobic granular sludge in a sequencing batch reactor. *Water Research*, **31**(12), 3191-3194.

Nguyen, H.T.T., Le, V.Q., Hansen, A.A., Nielsen, J.L., Nielsen, P.H. 2011. High diversity and abundance of putative polyphosphate-accumulating Tetrasphaera-related bacteria in activated sludge systems. *Fems Microbiology Ecology*, **76**(2), 256-267.

Oehmen, A., Lemos, P.C., Carvalho, G., Yuan, Z.G., Keller, J., Blackall, L.L., Reis, M.A.M. 2007. Advances in enhanced biological phosphorus removal: From micro to macro scale. *Water Research*, **41**(11), 2271-2300.

Oyserman, B.O., Noguera, D.R., del Rio, T.G., Tringe, S.G., McMahon, K.D. 2016. Metatranscriptomic insights on gene expression and regulatory controls in Candidatus Accumulibacter phosphatis. *Isme Journal*, **10**(4), 810-822.

Paerl, H.W., Hall, N.S., Calandrino, E.S. 2011. Controlling harmful cyanobacterial blooms in a world experiencing anthropogenic and climatic-induced change. *Science of the Total Environment*, **409**(10), 1739-1745.

Palomo, A., Pedersen, A.G., Fowler, S.J., Dechesne, A., Sicheritz-Ponten, T., Smets, B.F. 2018. Comparative genomics sheds light on niche differentiation and the evolutionary history of comammox Nitrospira. *Isme Journal*, **12**(7), 1779-1793.

Peng, L.H., Dai, H.L., Wu, Y.F., Peng, Y.H., Lu, X.W. 2018. A comprehensive review of phosphorus recovery from wastewater by crystallization processes. *Chemosphere*, **197**, 768-781.

Pitcher, A., Villanueva, L., Hopmans, E.C., Schouten, S., Reichart, G.J., Damste, J.S.S. 2011. Niche segregation of ammonia-oxidizing archaea and anammox bacteria in the Arabian Sea oxygen minimum zone. *Isme Journal*, **5**(12), 1896-1904.

Pronk, M., de Kreuk, M.K., de Bruin, B., Kamminga, P., Kleerebezem, R., van Loosdrecht, M.C.M. 2015. Full scale performance of the aerobic granular sludge process for sewage treatment. *Water Research*, **84**, 207-217.

Qin, W., Amin, S.A., Martens-Habbena, W., Walker, C.B., Urakawa, H., Devol, A.H., Ingalls, A.E., Moffett, J.W., Armbrust, E.V., Stahl, D.A. 2014. Marine ammonia-oxidizing archaeal isolates display obligate mixotrophy and wide ecotypic variation. *Proceedings of the National Academy of Sciences of the United States of America*, **111**(34), 12504-12509.

Qin, W., Zheng, Y., Zhao, F., Wang, Y.L., Urakawa, H., Martens-Habbena, W., Liu, H.D., Huang, X.W., Zhang, X.X., Nakagawa, T., Mende, D.R., Bollmann, A., Wang, B.Z., Zhang, Y., Amin, S.A., Nielsen, J.L., Mori, K., Takahashi, R., Armbrust, E.V., Winkler, M.K.H., DeLong, E.F., Li, M., Lee, P.H., Zhou, J.Z., Zhang, C.L., Zhang, T., Stahl, D.A., Ingalls, A.E. 2020. Alternative strategies of nutrient acquisition and energy conservation map to the biogeography of marine ammonia-oxidizing archaea. *Isme Journal*, **14**(10), 2595-2609.

Qiu, G.L., Zuniga-Montanez, R., Law, Y.Y., Thi, S.S., Nguyen, T.Q.N., Eganathan, K., Liu, X.H., Nielsen, P.H., Williams, R.B.H., Wuertz, S. 2019. Polyphosphate-accumulating organisms in full-scale tropical wastewater treatment plants use diverse carbon sources. *Water Research*, **149**, 496-510.

Ronteltap, M., Maurer, M., Gujer, W. 2007. The behaviour of pharmaceuticals and heavy metals during struvite precipitation in urine. *Water Research*, **41**(9), 1859-1868.

Ronteltap, M., Maurer, M., Hausherr, R., Gujer, W. 2010. Struvite precipitation from urine - Influencing factors on particle size. *Water Research*, **44**(6), 2038-2046.

Saerens, B., Geerts, S., Weemaes, M. 2021. Phosphorus recovery as struvite from digested sludge - experience from the full scale. *Journal of Environmental Management*, **280**.

Seviour, R.J., Mino, T., Onuki, M. 2003. The microbiology of biological phosphorus removal in activated sludge systems. *Fems Microbiology Reviews*, **27**(1), 99-127.
Smolders, G.J.F., Vandermeij, J., Vanloosdrecht, M.C.M., Heijnen, J.J. 1995. A Structured Metabolic Model for Anaerobic and Aerobic Stoichiometry and Kinetics of the Biological Phosphorus Removal Process. *Biotechnology and Bioengineering*, **47**(3), 277-287.
Stensel, H.D. 1991. Principles of Biological Phosphorus Removal: Principles and Practice. 2nd Edition ed. in: *Phosphorus and Nitrogen Removal from Municipal Wastewater*, (Ed.) R. Sedlak. New York, NY., pp. 141-166.
Stokholm-Bjerregaard, M., McIlroy, S.J., Nierychlo, M., Karst, S.M., Albertsen, M., Nielsen, P.H. 2017. A Critical Assessment of the Microorganisms Proposed to be Important to Enhanced Biological Phosphorus Removal in Full-Scale Wastewater Treatment Systems. *Frontiers in Microbiology*, **8**.
Strous, M., Fuerst, J.A., Kramer, E.H.M., Logemann, S., Muyzer, G., van de Pas-Schoonen, K.T., Webb, R., Kuenen, J.G., Jetten, M.S.M. 1999. Missing lithotroph identified as new planctomycete. *Nature*, **400**(6743), 446-449.
Tchobanoglous, G., Stensel, H.D., Tsuchihashi, R., Burton, F. 2014. *Wastewater Engineering: Treatment and Resource Recovery*. *5th ed*. Metcalf & Eddy, Inc., McGraw-Hill Education, New York.
Tilley, E., Atwater, J., Mavinic, D. 2008. Recovery of struvite from stored human urine. *Environmental Technology*, **29**(7), 797-806.
Tourna, M., Stieglmeier, M., Spang, A., Könneke, M., Schintlmeister, A., Urich, T., Engel, M., Schloter, M., Wagner, M., Richter, A. 2011. Nitrososphaera viennensis, an ammonia oxidizing archaeon from soil. *Proceedings of the National Academy of Sciences*, **108**(20), 8420-8425.
Udert, K.M., Larsen, T.A., Biebow, M., Gujer, W. 2003. Urea hydrolysis and precipitation dynamics in a urine-collecting system. *Water Research*, **37**(11), 2571-2582.
Udert, K.M., Wachter, M. 2012. Complete nutrient recovery from source-separated urine by nitrification and distillation. *Water Research*, **46**(2), 453-464.
Urakawa, H., Garcia, J.C., Nielsen, J.L., Le, V.Q., Kozlowski, J.A., Stein, L.Y., Lim, C.K., Pommerening-Roser, A., Martens-Habbena, W., Stahl, D.A., Klotz, M.G. 2015. Nitrosospira lacus sp nov., a psychrotolerant, ammonia-oxidizing bacterium from sandy lake sediment. *International Journal of Systematic and Evolutionary Microbiology*, **65**, 242-250.
van Kessel, M., Speth, D.R., Albertsen, M., Nielsen, P.H., Op den Camp, H.J.M., Kartal, B., Jetten, M.S.M., Lucker, S. 2015. Complete nitrification by a single microorganism. *Nature*, **528**(7583), 555-+.
Wilsenach, J.A., Schuurbiers, C.A.H., van Loosdrecht, M.C.M. 2007. Phosphate and potassium recovery from source separated urine through struvite precipitation. *Water Research*, **41**(2), 458-466.
Wilsenach, J.A., Van Loosdrecht, M.C.M. 2004. Effects of separate urine collection on advanced nutrient removal processes. *Environmental Science & Technology*, **38**(4), 1208-1215.
Wilsenach, J.A., van Loosdrecht, M.C.M. 2006. Integration of processes to treat wastewater and source-separated urine. *Journal of Environmental Engineering-ASCE*, **132**(3), 331-341.
Winkler, M.K.H., Bassin, J.P., Kleerebezem, R., de Bruin, L.M.M., van den Brand, T.P.H., van Loosdrecht, M.C.M. 2011. Selective sludge removal in a segregated aerobic granular

biomass system as a strategy to control PAO-GAO competition at high temperatures. *Water Research*, **45**(11), 3291-3299.
Winkler, M.K.H., Kleerebezem, R., van Loosdrecht, M.C.M. 2012. Integration of anammox into the aerobic granular sludge process for main stream wastewater treatment at ambient temperatures. *Water Research*, **46**(1), 136-144.
Winkler, M.K.H., Meunier, C., Henriet, O., Mahillon, J., Suarez-Ojeda, M.E., Del Moro, G., De Sanctis, M., Di Iaconi, C., Weissbrodt, D.G. 2018. An integrative review of granular sludge for the biological removal of nutrients and recalcitrant organic matter from wastewater. *Chemical Engineering Journal*, **336**, 489-502.
Winkler, M.K.H., Straka, L. 2019. New directions in biological nitrogen removal and recovery from wastewater. *Current Opinion in Biotechnology*, **57**, 50-55.
Winogradsky, S. 1890. Recherches sur les organisms de la nitrification. *Ann. Inst. Pasteur*, **4**, 213-231,257-275,760-771.

Chapter 2.

Flocs in Disguise? High Granule Abundance Found in Continuous-Flow Activated Sludge Treatment Plants

Abstract

To date, high performance of full-scale aerobic granular sludge (AGS) technology has been demonstrated on a global scale. Its further integration with existing continuous flow activated sludge (CFAS) treatment plants is the next logical step. All granular sludge reactors operated in sequencing batch reactors (SBR) mode with anaerobic feeding conditions select for growth of phosphorus and glycogen accumulating organisms (PAO and GAO, respectively), which are known to enhance sludge settling characteristics. Therefore, we hypothesized that AGS are commonly present at full-scale CFAS processes with enhanced biological phosphorus removal (EBPR) and low sludge volume index (SVI). This hypothesis was confirmed at 13 EBPR plants, where granules were found present (at plants where SVI was lower than 100 ml/g) with a strong correlation between high granule abundance and low SVI. A wide range of granule abundance was found among the plants, ranging from 0.5% to as high as 80%. Evaluations of the EBPR plant process configurations showed that high granule abundances may be related to selector design features such as high anaerobic food to mass (F/M) ratios, unmixed in-line fermentation, and high influent soluble COD fraction. Granules were also observed at a non-EBPR plant with an aerobic selector receiving high F/M feeds. Quantitative PCR and 16S rRNA gene sequencing analyses revealed higher relative gene abundance of *Accumulibacter* PAO and *Competibacter* GAO in the granules over flocs, as well as a correlation between granule abundance and some possible EPS producers such as *Flavobacterium* and *Competibacter*. Our results indicated that

process configurations that select for slow-growing or EPS-producing heterotrophs play an important role for granule formation in full-scale CFAS systems as previously shown in SBR configurations.

Published as:

Wei, S. P., H. D. Stensel, B. N. Quoc, D. A. Stahl, X. W. Huang, P. H. Lee and M. K. H. Winkler (2020). "Flocs in disguise? High granule abundance found in continuous-flow activated sludge treatment plants." Water Research **179**.

2.1 Introduction

Aerobic granular sludge (AGS) is gaining interest as a biological treatment process more efficient for nutrient removal than the activated sludge process, requiring less reactor volume, energy, and recycle pumping. Aerobic granules are self-forming dense biofilm aggregates with high content of extracellular polymeric substances (EPS) exhibiting greater adhesive and stronger gel properties than flocs (Nancharaiah and Reddy 2018, Seviour et al. 2009). They are semi-spherical and defined operationally as having a minimum diameter of 0.2 mm (de Kreuk et al. 2007) but most typically range from 0.5 mm to 3.0 mm (Figdore et al., 2017). The larger size and spherical morphology of granular sludge result in a much greater settling velocity and thickening ability compared to flocculent activated sludge (Adav et al. 2008). In AGS sequencing batch reactors (SBRs), granules have a sludge volume index (SVI) of about 30 - 50 ml/g with an SVI_5/SVI_{30} near 1.0 whereas flocculent sludge has a typical SVI_{30} of >100 ml/g and an SVI_5/SVI_{30} value in the range of 1.6 to 2.0 (Figdore et al. 2017, Winkler et al. 2018). Thus, AGS systems can be operated with a much higher mixed liquor suspended solids (MLSS) concentration and shorter detention time to greatly improve system capacity, reducing plant construction costs and footprint (Giesen et al. 2013).

Various types of aerobic granules have been grown, including heterotrophic (Liu et al. 2003), enhanced biological phosphorus removal (EBPR) (Pronk et al. 2015), nitrifying (Belmonte et al. 2009), nitrifying/denitrifying (Wang et al. 2012), and nitritation/anaerobic ammonium oxidation granules (Winkler et al. 2012). The existing literature has shown that anaerobic feeding conditions are not required for cultivation of aerobic granules but, as yet, granular sludge with EBPR and nitrification/denitrification capability (PAO-NDN granules) is the preferred type for

biological nutrient removal (Figdore et al. 2018a). There are also reports in the literature suggesting that selection of slow-growing heterotrophs, such as the polyphosphate and glycogen accumulating organisms (PAOs and GAOs, respectively), tends to form granules that are denser and smoother in comparison to heterotrophic granules (de Kreuk and van Loosdrecht 2004). The well-established treatment systems that select for PAO-NDN granules have been mostly limited to SBR, such as the full-scale AGS Nereda® technology, and therefore cannot be easily integrated in existing continuous flow activated sludge (CFAS) infrastructure. In SBR systems, the readily biodegradable chemical oxygen demand (rbCOD) is used by slow growing heterotrophs to generate internal energy reserves as it is fed through the settled sludge bed anaerobically. During the subsequent aeration phase the internal storages are used for phosphorus uptake and denitrification. This anaerobic feast and famine operation favors the growth of slow-growing PAOs and GAOs that form the compact and smooth granule structure (Winkler et al. 2011). The high food to mass (F/M) feeding regime reduces diffusion-limited growth by promoting substrate penetration into the granule core. Additionally, the aeration period is followed by a short settling time and subsequently the influent feed pushes the effluent over the top of the reactor, washing out the slow settling particles but retaining the larger AGS aggregates (Pronk et al. 2015). Selective wasting of smaller particles is also done manually.

Although CFAS processes do not inherently have the key selective mechanisms of the AGS SBR operation, they have incorporated “selector” designs to favor growth of floc-forming over filamentous organisms to avoid poor settling sludge. Such selectors have been categorized as either kinetic or metabolic selectors (Jenkins et al. 2004), with the latter having an anaerobic or anoxic reactor in which the influent wastewater is in contact with recycle mixed liquor prior to

entering the downstream aerobic reactor. The anaerobic selector favors PAO growth and is a necessary feature for the commonly used EBPR process designs in flocculent activated sludge processes. Despite the very low SVI values (as low as 49 ml/g (Parker et al. 2004)) reported for some CFAS EBPR facilities, there has been no initiative to determine the presence of granules. Additionally, the conventional microscopic practice at wastewater treatment plants uses a magnification too high (generally >100X) to visualize granules (Jenkins et al. 2004). As a result, granule occurrence at CFAS facilities has remained largely unexplored for the 100 years plus history of activated sludge.

Granules were speculated to be present in CFAS plants with SVIs below 60 ml/g (Martin et al. 2016) and large dense particles with granular like appearance had also been observed in a CFAS system (SVI < 45 ml/g) operated with an anoxic selector (Andreasen et al. 1999). However, no confirmation with clear images of granules were provided by these studies. Downing et al. (2017) were first to report on granule formation at a CFAS plant with a high F/M in an initial aerated zone and SVI_5/SVI_{30} values of about 1.0. Large particles were observed by light microscopy and sieve analysis showed that 80% of particles in the mixed liquor were greater than 0.20 mm. Thus, we examined microscopically a sample from an A^2O EBPR facility in Washington State that utilized surface wasting for solids retention time (SRT) control and reported periods of SVI near 40 ml/g. Our observation of small granules (212 - 500 μm diameter) in this facility then led us to survey other CFAS plants for the presence of granules.

In this work, we collected sludge samples from 13 EBPR and 4 non-EBPR CFAS plants to investigate if granules are (1) commonly present at full-scale continuous flow EBPR facilities

with low SVIs, and (2) related to the abundance of PAOs and GAOs. For each sludge sample the percentage of granules and flocs, their relative sizes, and their microbial community were analyzed. The objective of this work was to determine if granule presence was common in CFAS plants and if their presence could be related to process design and/or operational factors. The outcome of this research should aid in further understanding of the potential for implementing or improving granular growth in existing CFAS facilities for plant treatment capacity and nutrient removal enhancement.

2.2 Methods

2.2.1 Sample Collection and Plant Data

A mixed liquor grab sample was collected at the end of aeration basin from 13 EBPR plants and shipped overnight on ice to the University of Washington. A second sample was collected from 3 of the 13 plants resulting in a total of 16 mixed liquor samples (**Table 2-1**). Samples were immediately stored at 4 °C upon arrival and analyzed within 24 hours. Each plant provided information on their process flow scheme, operating conditions, and secondary treatment influent and effluent data, which typically included daily measurements of BOD, TSS, TKN, NH_3-N, total and/or ortho-P for influent and effluent. There was no data for influent volatile fatty acids (VFAs). Influent soluble COD (sCOD) data was available for only the ID and SP plants. We used data collected for the 3-SRT period just prior to sample collection. Additional information of the plants are provided in the supplementary information, including aeration basin design and hydraulic retention times (Table S1), influent characteristics and performance data (Table S2 and S3), and process schematics (Table S4). Five mixed liquor samples were also collected from 4 non-EBPR plants (Table S5) to check for presence of granules.

Table 2-1. Summary of the 16 samples from 13 EBPR plants (3 plants had 2 samples collected): process configurations and averaged operational parameters over a 3-SRT period prior to time of sampling.

Facility	Sample ID	Process[a, b]	Flow (MGD)	SRT (day)	Influent BOD (mg/L)	F/M of 1st Anaerobic Stage (gBOD/gVSS·hr)	Temperature (°C)	MLSS (mg/L)
Henderson, NV (East)	HE1	JHB	6.0	7.1	246	10.3	29.0	1552
	HE2		5.5	4.3	260	13.5	26.5	1226
Idaho Falls, ID[c]	ID1	JHB	9.6	9.7	217	2.00	19.8	3218
	ID2		9.4	11.6	241	2.42	15.0	3532
Henderson, NV (West)	HW	JHB	15.1	5.7	263	14.0	26.8	1300
Crooked Creek, GA	CrC	AO	6.5	9.4	179	0.82	22.3	2591
Cashmere, WA[d]	CM	A2O	0.39	12.0	415	0.65	16.0	5483
Clark County, NV	ClC	A2O	109	13.8	320	4.50	29.9	3078
Puyallup, WA	Puy1	A2O	7.5	15.1	170	4.70	13.5	3525
	Puy2		3.2	17.8	313	4.89	21.6	2566
West Boise, ID	WB	JHB	17	10.7	204	4.80	23.0	2881
South Plant, WA	SP	AO	66	3.7	347	2.90	22.0	2360
Durham, OR	Dur	A2O	21.2	5.5	168	3.50	23.3	2125
Pocatello, ID	Poc	A2O	5.9	12.9	356	1.39	13.3	2179
Kalispell, MT	Kal	JHB	2.5	11	300	5.70	15.9	2146
Ballenger McKinney, MD[e]	BM	4-Stage Bardenpho	6.3	23.8	292	10.5	21.2	2468

[a] JHB = Johannesburg Process (return activated sludge goes to anoxic zone before entering first anaerobic zone); A2O = anaerobic/anoxic/aerobic; AO = anaerobic/aerobic. See Table S4 for plant schematics.
[b] HE, HW, CM and CrC do not have primary treatment; all other plants do.
[c] Receives flow from a fruit processing plant.
[d] Receives flow from a malting plant.
[e] A membrane bioreactor plant; receives glycerol as supplemental carbon.

2.2.2 Percent Granule Determination

The percent of granule solids in a mixed liquor sample was based on the fraction of mixed liquor solids retained on a 212-µm sieve. The suspended solids retained and passing through the sieve were measured separately and equaled the total suspended solids of the sample. The presence of granules versus wastewater influent inert particulates was also confirmed by observing granular morphologies of mixed liquor at 6X-10X magnification under a Zeiss Stemi SV11 (and Zeiss Stemi 508 for later samples) stereomicroscope in dark field mode. In addition, Neisser staining was performed as described in Jenkins et al. (2004) to detect the presence of PAOs in the granules.

2.2.3 Granular Size Distribution

Additional analysis was done for plant samples with a granular sludge content greater than 30% to determine the granular size distribution by image processing of stereo-microscopic images taken in dark field mode. The area of each granule was traced and measured manually using the Fiji image processing package of ImageJ. The diameter of the granule was then calculated from the area ($A = d^2\pi/4$) assuming a spherical granule. Granule size distribution was based on the calculated diameter values.

2.2.4 Analytical Methods

Suspended and volatile solids (TSS and VSS) were analyzed according to Standard Methods 2540D and 2540E. The SVI_5 and SVI_{30} (ml/g) were determined from the settled volume (ml) of a mixed liquor sample, after 5 and 30 min settling in a 1-L graduated cylinder, divided by g TSS.

2.2.5 DNA Extraction

Flocs and granules were separated with a 212-µm sieve for 14 of the 16 EBPR mixed liquor samples (ID2 and Puy1 were not included; see Table S6 for details). DNA was extracted for the granule and floc samples separately following the method described in Tatti et al. (2016) with a few exceptions: samples were lysed for 25 seconds at the speed of 4 m/s using the FastPrep®-24 bead beater (MP Biomedical) and the cleanup step was repeated twice; first with phenol-chloroform-isoamyl alcohol (25:24:1) then with chloroform-isoamyl alcohol (24:1). Concentrations of the DNA samples were measured using a Qubit 2.0 fluorometer. For comparison purposes, DNA was also extracted from one non-EBPR plant (Ed) having no granule fraction.

2.2.6 Quantitative PCR

DNA extracted from 12 flocs and 12 granules from the EBPR plants were characterized with the quantitative polymerase chain reaction (qPCR), excluding plants with granule abundance of less than 1% (Table S6). Quantitative PCR was done on triplicate DNA extractions, except for those extracted only in duplicate (HE2, ID1, and Poc granules). Quantitative PCR targeted three populations, using primers 341f/534r for total bacterial 16S rRNA genes (He et al. 2007), 651f/846r for *Candidatus* Accumulibacter (Crocetti et al. 2000), and GBf/GAOQ989r for *Candidatus* Competibacter (Kong et al. 2002) (Table S7). All reactions were run on the Roche Light Cycler 96 using the FastStart Essential DNA Green Master reaction mix for SYBR Green-I. Technical duplicates were conducted for each DNA extraction in 10 µl total volume containing 0.2 ng/µl DNA and 0.25 µM each for forward and reverse primers. Amplification efficiencies and starting concentrations (N_0) were calculated for each primer set using the LinRegPCR program (Ruijter et al. 2009). Relative gene copies were estimated by taking the ratio of N_0 (of

PAO or GAO)/N_0 (total bacteria).

2.2.7 Amplicon Sequencing and Bioinformatics

The V4-V5 region of the 16S rRNA gene was amplified from 24 DNA extractions (11 granule and 13 floc samples) using primers 515F-Y/926R (Parada et al. 2016) for PCR. The amplification products were sequenced on a 2×300bp Illumina MiSeq (BGI Genomics, Hong Kong). Amplicon reads were processed following the Divisive Amplicon Denoising Algorithm 2 (DADA2) pipeline (Callahan et al. 2016), a model-based approach yielding amplicon sequence variants (ASVs) as the end product instead of the traditional operational taxonomic units (OTU). The forward and reverse reads were first trimmed at 290 and 240 bp, respectively while using 2 as the DADA2 maximum expected error allowed in a read. Next, 20 sub-sample sets were used to conduct iterations for estimating the error rates and sample composition until they matched. The samples were then denoised using the error parameters followed by identification of sequence variances and merging of forward and reverse reads. Taxonomy of the sequence variants were assigned from domain to genus level against the Silva Project's v. 128 dataset using the Ribosomal Database Project Classifier (Wang et al. 2007). The relative gene abundance of each ASV was calculated by the amplicon read counts of each ASV (×100%) divided by the total amplicon read counts. The R package phyloseq version 1.28.0 was used to analyze the phylogenetic sequencing data, calculate alpha diversity measures, and perform non-metric multi-dimensional scaling and canonical correspondence analyses (McMurdie and Holmes 2013). Heatmaps were generated using the R package pheatmap version 1.0.12.

2.2.8 Estimation of Gene Copies in Granule Relative to Floc

Using the relative gene abundances determined from qPCR and the percent granules, Eq. 1 was

applied to estimate the ratio of absolute gene abundance in granules relative to flocs. The approach for arriving at Eq.1 can be found in Supplementary Note 1 and the motivation for why this calculation was important was discussed in Section 2.3.5.

$$\frac{X_g}{X_f} = \frac{(\%X_g)(\%\ granule)}{(\%X_f)(\%\ floc)} \qquad \text{Eq. 1}$$

Where:

$\frac{X_g}{X_f}$ = gene copies in the granules relative to flocs in the mixed liquor

$\%X_g$ and $\%X_f$ = relative gene abundance to total bacterial gene copies in granules and flocs, respectively (known from qPCR results, Section 2.2.6).

%granule = percent MLSS retained on 212-μm sieve (known from %granule determination, Section 2.2.2).

%flocs = 100% - %granules

2.3 Results and Discussions

2.3.1 High Granule Abundance is Correlated with Low SVI

The percent granules from the 16 EBPR samples ranged from 0.5 – 80% while the SVI_{30} ranged from 39 to 209 ml/g (**Figure 2-1**). Granules could not be observed with the traditional light microscopic approach for activated sludge at typical magnifications of >100X, which are too high for granule observations. Instead, granules were observed with a stereomicroscope with darkfield illuminations at 6 – 20X magnifications (**Figure 2-2**). The granules exhibited semi-spherical morphology and dense core as contrasted to flocculent sludge. Because CFAS systems are not designed for granulation, the granules were smaller in diameter (mostly less than 0.5 mm)

than the typical 0.5 – 3.0 mm observed in granular sludge SBR systems having higher F/M feeding and washout regimes (Figdore et al. 2017). Due to the small sizes of the granules, their presence and abundance at CFAS plants appears to have been generally overlooked. Non-degraded influent particulates could contribute to the fractional granule determination based on the 212-µm sieve method, especially at plants without primary treatment. However, our microscopic observations of the smooth morphology and dense core of the granules and enrichment of PAOs in these particles (confirmed with Neisser staining, Figure S1) indicated that granule growth dominated influent particulates. Size distribution analyses were conducted for samples with the highest percent granules (**Figure 2-3**). Note that not all CFAS granules were small, as 15% of HE1's mixed liquor fell into the >0.5 mm size range. The imaging technique used for obtaining the size distributions was not suitable for samples that were mostly flocs because outline tracing of the small and irregular aggregates was difficult. If size distribution of highly flocculent samples is desired, an alternative method (e.g., using series of sieves) would be needed.

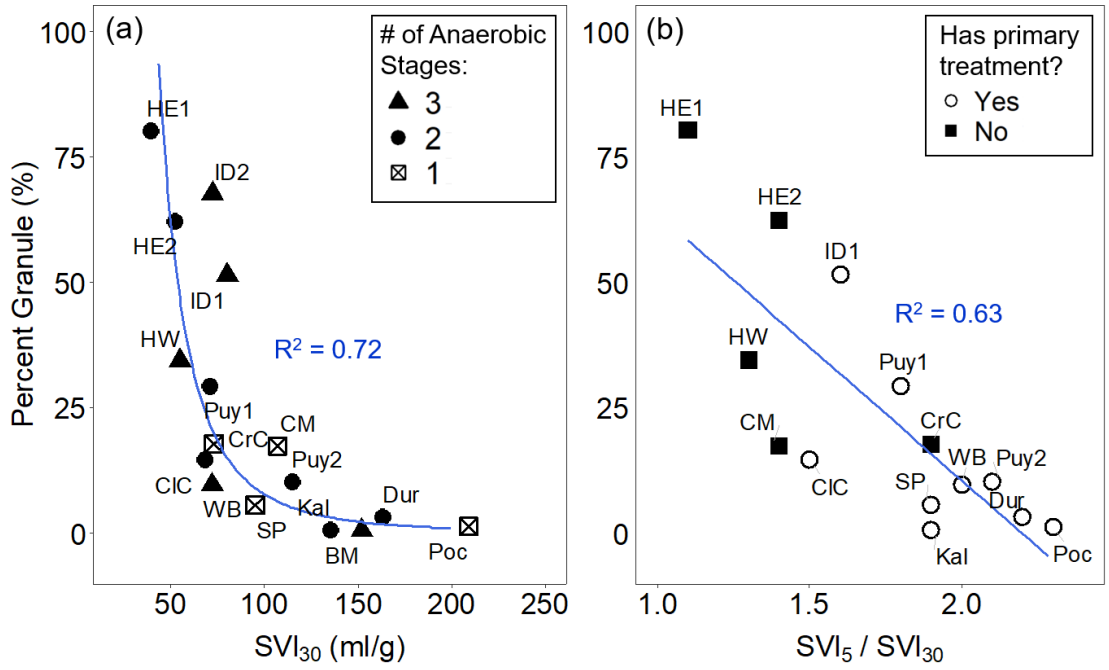

Figure 2-1. Correlation of percent granules versus (a) SVI30 and (b) SVI5/SVI30 ratios for EBPR plants. BM was omitted in (b) due to excessive filamentous growth and minimal settling even after 30 minutes. ID2 was not included in (b) due to unavailable SVI5 data.

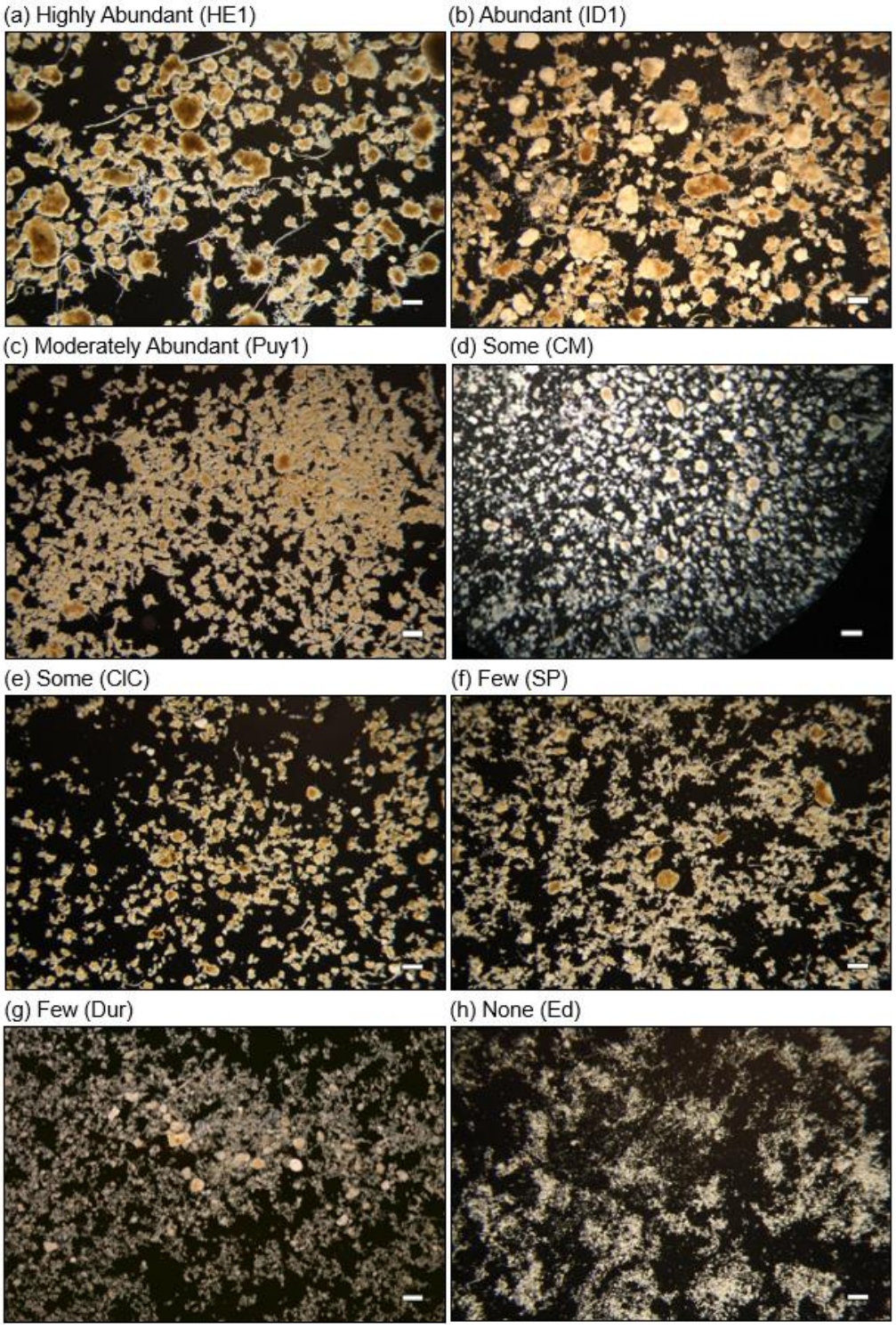

Figure 2-2. Stereomicroscopic images of mixed liquor samples taken at 6X magnification; scale bar = 500 µm; percent granules: (a) 80.2%; (b) 51.5%; (c) 29.3%; (d) 17.4%; (e) 15%; (f) 5.6%; (g) 3.3%; (h) 0%.

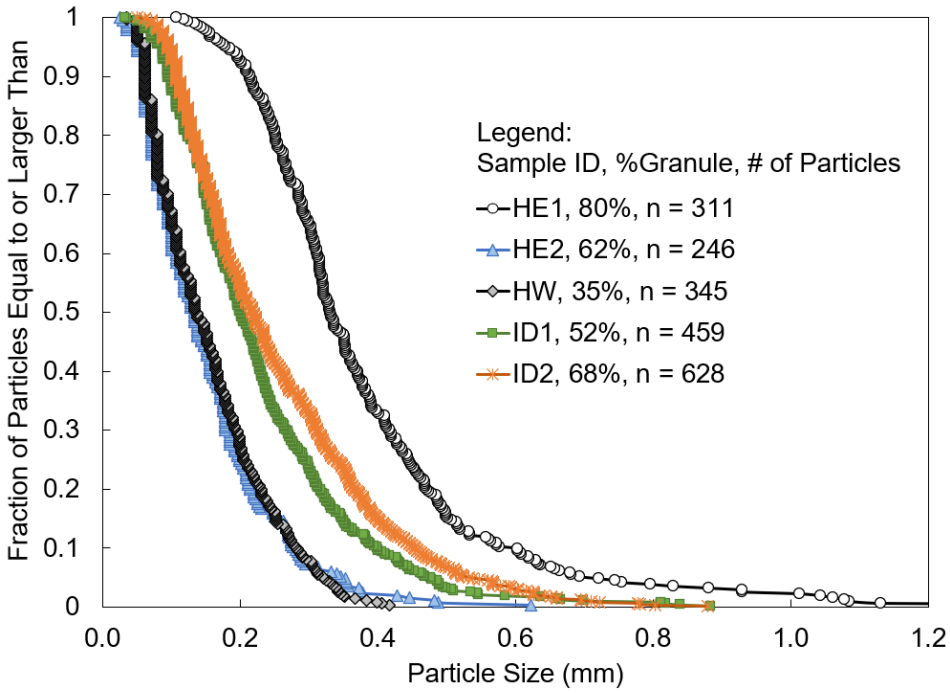

Figure 2-3. Mixed liquor particle size distributions of samples with high granule percentage.

Three of the non-EBPR plants (ED, Lyn, WP) with SVI_{30} of 193 to 475 ml/g were filamentous and had minor or no granules (Table S5, Figure S2). For the Pasco plant, the Pas1 sample had 3.4% granules with high SVI (193 ml/g) whereas Pas2 sample had 44% granules with low SVI (67 ml/g). Neisser staining images (not shown) could not detect polyphosphate in both Pas samples. The Pas plant had an aerobic selector that received only 10% of the return sludge flow (see Table S4 for configuration), and thus the F/M ratio of the aerobic selector was very high (18.3 - 28.8 gBOD/gVSS·d). Under this high F/M operation, a feast phase (high availability of electron donor and acceptor) is followed by a famine phase (carbon-depleted). Such an aerobic feast/famine operational regime is known to select for polyhydroxyalkanoates (PHA)-storing organisms such as in bioplastic research (Mannina et al. 2020). Therefore, even though PAOs were not detected at Pasco, it is possible that granule growth at this plant was related to the selection of other slow-growing PHA-storing organisms. Additional data for the Pas plant can be

found in Supplementary Note 2. Our observation of granules at Pas confirmed the understanding that granulation can be achieved under aerobic operations without anaerobic or anoxic selectors (Li et al. 2011, Liu et al. 2003) and that EPS formation or other heterotrophs (perhaps PHA-storing organisms other than PAO) may be contributing to granule growth at Pas.

Higher granule abundances were clearly correlated with lower SVI values (**Figure 2-1a**) and granule abundance of >1% were observed at all EBPR plants except Kal and BM, which were the two EBPR plants with the highest SVI values. It appears that granules are commonly present in EBPR plants with low SVIs. The SVI_5/SVI_{30} ratio is a common indicator for the settling characteristics of the sludge with granules; the closer the SVI_5/SVI_{30} ratio is to 1, the higher the amount of granules (Świątczak and Cydzik-Kwiatkowska 2018). This relationship was confirmed by our results with the significant correlation between higher granule abundance and SVI_5/SVI_{30} as this ratio approached 1 (**Figure 2-1b**).

2.3.2 Possible Importance of F/M Ratio and rbCOD Fraction

Anoxic and anaerobic selectors are typically used to improve settleability at CFAS plants to suppress the growth of aerobic filamentous bacteria. In AGS systems the anaerobic zone is accompanied by high F/M ratios to allow rbCOD to reach the granule core by diffusion, which speeds up granulation and supports granule stability (Li et al. 2011, Liu et al. 2003, Wu et al. 2018). The ranges of nominal F/M ratios are 0.15 – 1.3 g rbCOD/gMLSS·d in lab-scale acetate-fed SBRs and 0.1 – 0.3 kg COD/kgVSS·d in full-scale AGS SBRs, but much higher F/M values can be expected as the influent is fed by plug flow in direct contact with the settled sludge bed (rather than diluting it with the mixed liquor) (Figdore et al. 2017). In this study, the F/M ratios

of the first anaerobic stage ranged from 0.65 – 14.0 gBOD/gVSS·d (**Figure 2-4**). We found no correlation between these F/M ratios and the percent granules (Figure S3a). It should be noted that the lack of correlation could be partly due to having only net BOD data for most of the plants, even though rbCOD or VFAs would be more representative as the electron donor for anaerobic metabolism (of PAO and GAO). The difference in process configurations also increased the variability. For example, CM had the highest influent BOD (**Table 2-1**) but the lowest F/M ratio due to the lack of anaerobic staging. BM was also an outlier, having a high F/M feed with multiple anaerobic stages but a mixed liquor lacking granules and barely settled after 30 minutes. This discrepancy may be related to BM being the only MBR plant characterized in this study, having the longest SRT and a different sludge wasting regime than the other plants with secondary clarifiers. In addition, BM was the only plant using glycerol as supplemented carbon source. Thus, additional studies to provide more detailed COD characterizations in the F/M analysis and to minimize plant-to-plant operational variables would likely improve understanding of factors contributing to granule formation.

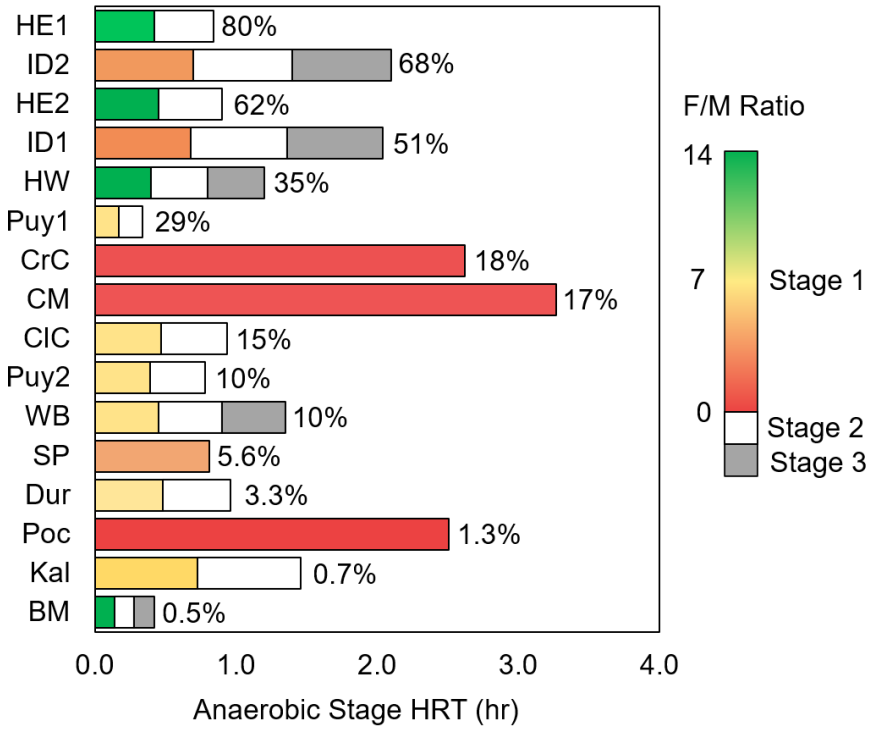

Figure 2-4. Anaerobic selector configurations: number of stages, hydraulic retention times, and the F/M ratio (gBOD/gVSS·hr) in the first stage. Numbers in % denotes the percent granule.

However, it should not be overlooked that the Henderson plants (HE1, HE2, and HW) had the highest F/M ratios and highest granule abundance. HE and HW also utilized an unmixed in-line fermenter (UMIF) design by turning off the mixer in their second anaerobic zone to produce additional rbCOD (Barnard et al. 2012). Although ID had high granule abundance (68%) but low F/M, it had a longer anaerobic hydraulic retention time (**Figure 2-4**), which could promote additional rbCOD/VFA formation. Additionally, ID had very high sCOD/COD fraction (82 ± 18%), which serves as a precursor for a high rbCOD fraction, and thus a possibly higher F/M (if based on rbCOD) than some other plants. As a comparison, SP's sCOD/COD fraction was 30 ± 3% (the only other plant with sCOD data) and had lower granule percentage (5.6%). The importance of F/M ratio for improved settleability and granule growth had been noted by

previous research. At a full-scale biological nitrogen removal plant, Wilen et al. (2008) observed significant improvement in settleability (SVI of 30 – 70 ml/g) along with occurrence of PAOs (although not an EBPR plant) and elevated sludge EPS content during a period when F/M was increased due to bypassing primary settler. Similarly, dense and granular-like flocs with low diluted SVIs of 39 – 47 ml/g were observed at a pulp and paper plant with an anoxic selector and very high F/M ratios of 17 - 30 g sCOD $gVSS^{-1}$ d^{-1} (Andreasen et al. 1999). Although not yet conclusive, these data have identified high F/M ratios and high sCOD (or rbCOD) fraction as factors relating to granule growth at CFAS systems.

In addition to high anaerobic F/M conditions (feast), a prolonged starvation (famine) phase has also been shown to enhance cell adhesiveness and granule stability in AGS SBR systems (Wilen et al. 2018). We explored the effect of starvation phase based on the plant's total SRT, anoxic and aerobic fraction of the SRT ($SRT_{anoxic+aerobic}$), and ratio of $SRT_{anoxic+aerobic}$ to minimum SRT required for EBPR. However, no correlations could be found between these starvation parameters versus granule abundance (Figure S3b - d). It is possible that the effect of famine phase could not be seen with the range of SRTs in this study.

2.3.3 Microbial Community Compositions

The amplicon reads from 16S rRNA gene sequencing of 24 DNA extractions were analyzed using DADA2, resulting in a total of 397,146 amplicon reads and 4,325 unique ASVs. The sequencing depth of each sample is shown in Figure S4. After taxonomic assignment and prefiltering (Supplementary Note 3), a total of 28 phyla and 385 genera were kept for subsequent analyses. Proteobacteria was the most dominant phylum across all samples with relative

abundance ranging from 33.0 – 61.3% (Figure S5). Within the Proteobacteria phylum, β-Proteobacteria (10.3 – 48.1%), α-Proteobacteria (3.1 – 35.6%) and γ-Proteobacteria (3.1 – 21.4%) were the dominant classes. The other dominant phyla were Bacteroidetes (11.2 – 45.6%), Actinobacteria (0.3 – 31.9%), Chloroflexi (0.0 – 13.7%), and Planctomycetes (none Anammox type) (0.2 – 8.6%). These phyla are the common dominating microbial groups in full-scale activated sludge treatment plants (Coats et al. 2017, Qiu et al. 2019). At the genus level, the genera exhibiting high abundance varied for each plant (Figure S6), but the most common dominating groups included *Flavobacterium*, *Candidatus* Competibacter (*Competibacter*), *Zoogloea*, and *Candidatus* Accumulibacter (*Accumulibacter*).

Accumulibacter was detected at all EBPR plants with relative gene abundances from 0.1 – 5.9% (Figure 5). Puy2 floc was the only sample from an EBPR plant with no *Accumulibacter* detected. Relative *Accumulibacter* gene abundances of 0.2 – 6% had been reported for full-scale EBPR plants (Coats et al. 2017, Lanham et al. 2013, Qiu et al. 2019, Stokholm-Bjerregaard et al. 2017). Except HE1 and BM, *Tetrasphaera* was detected at all EBPR plants at relative gene abundances of 0.04 to 1.22%. Previous studies had reported *Tetrasphaera* abundances of 3.6 – 28% in full-scale plants in temperate climate (Lanham et al. 2013, Stokholm-Bjerregaard et al. 2017) and 0.23 – 1.8% in tropical climate (Qiu et al. 2019). The DNA extraction method used here might have caused underestimation of the *Tetrasphaera* abundances due to a shorter bead beating time utilized (25 s at 4 m/s) than the recommended protocols (160 s at 6 m/s) for extracting DNA from Gram-positive Actinobacteria (e.g. *Tetrasphaera*) (Albertsen et al. 2015). Putative PAOs *Obscuribacter* and *Candidatus* Accumulimonas were not detected in any samples. *Candidatus* Competibacter was the dominate putative GAO (0.04 – 17%) for most of our EBPR plant

samples (**Figure 2-5**). *Defluviicoccus* was the dominant putative GAO in CM (both granules and flocs) and ID floc. Lab-scale studies had shown that *Competibacter* cannot metabolize propionate efficiently whereas *Defluviicoccus* GAOs can assimilate both acetate and propionate at relatively high rates (Dai et al. 2007). CM and ID received wastewater from a local fruit plant and malting plant, respectively, which can lead to higher VFAs. Although the composition is unknown, these industrial loads may explain the high influent BOD of CM (**Table 2-1**) and high influent sCOD/COD fraction of ID (discussed in Section 2.3.2). The actinobacterial genus *Micropruina* was the only putative GAO detected at BM. Unlike the classical *Competibacter* and *Defluviicoccus* GAOs, *Micropruina* is a fermentative GAO that can utilize a broad range of substrates, including glucose, amino acids, and glycerol (McIlroy et al. 2018). BM was the only plant in this study that used glycerol as a supplemental carbon source, which may explain the dominance of *Micropruina* GAO.

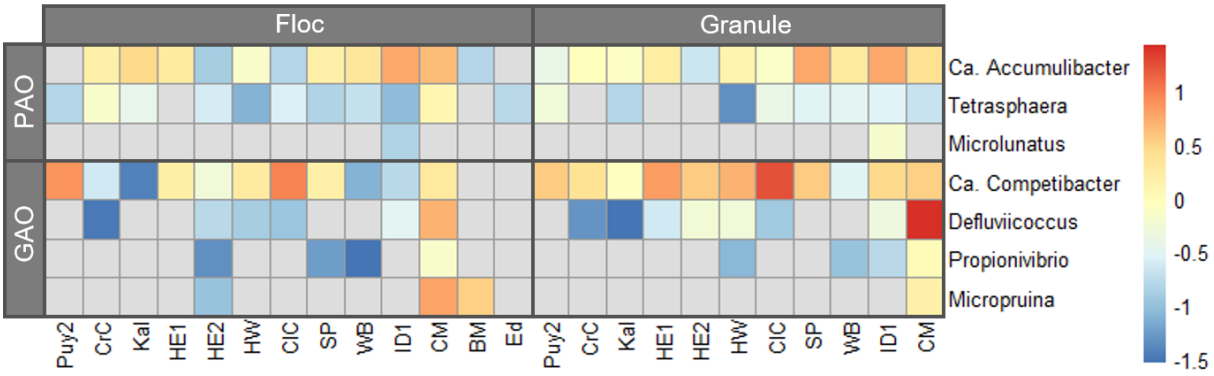

Figure 2-5. Relative gene abundance of putative PAOs and GAOs on log 10 scale based on 16S rRNA gene sequencing. Note that BM and Ed had granule fraction of 0.5% or less and thus only floc samples were submitted for sequencing.

Comparison of alpha diversity measures showed no discernible differences between granules and flocs in terms of richness and evenness (Figure S7), which is in alignment with the literature

(Winkler et al. 2013a). Similarity analyses with non-metric multidimensional scaling (NMDS results) (Figure S8) showed that floc and granule samples did not form separate clusters. Instead, samples from the same plant tended to ordinate closer together (i.e., having more similar microbial community structure). This observation suggested that the difference in microbial structure between granule and floc samples from the same plant is relatively small in comparison to the difference between two separate plants. At a full-scale AGS SBR plant, Ali et al. (2019) found that the percent of shared OTUs between flocs (<0.2 mm) and small granules (0.2 – 1 mm) was 62% while this similarity was reduced for large granules, sharing only 36% OTUs with flocs and 39% OTUs with small granules. They concluded that the lack of a clear phylogenetic separation between floc and small granule communities was due to their similar SRTs. On the other hand, large granules had much higher SRT and were enriched with putative functional groups for nitrogen and phosphorus removal. Due to the small granule size and lack of selective wasting at the plants in this study, we can expect similar SRTs and high percent of shared ASVs between granules and flocs, which was found to be 83 ± 7% among all the plants (excluding ASVs with <0.1% relative abundance).

2.3.4 EPS Producing and Filamentous Organisms are Related to Granule Abundance

Canonical correspondence (CCA) was performed to correlate environmental factors with microbial community structure and to determine the major microbial groups related to granule abundance. **Figure 2-6** is the resulted CCA plots showing the ordinations of abundance gradient across the 11 plants (with more than 0.5% granules) constrained by environmental factors. Top 100 abundant genera were used for producing the CCA plots but only the 10 genera showing the highest correlations with environmental factors (furthest away from the origin) were displayed for ease of visibility. The strong positive correlation between temperature and %granule was

likely due to the high granule abundance at the Henderson plants (samples HE1, HE2, and HW), where temperature was also high. Genera that correlated with the %granule were *Competibacter*, *Roseiflexus, Nitrospira, Thermomonas, Flavobacterium,* and *Azospira*. The ratio of granule abundance over floc abundance (**Figure 2-7**) for the genera identified in the CCA plots similarly showed that *Competibacter*, *Roseiflexus,* and *Nitrospira* were commonly more abundant in the granules than flocs.

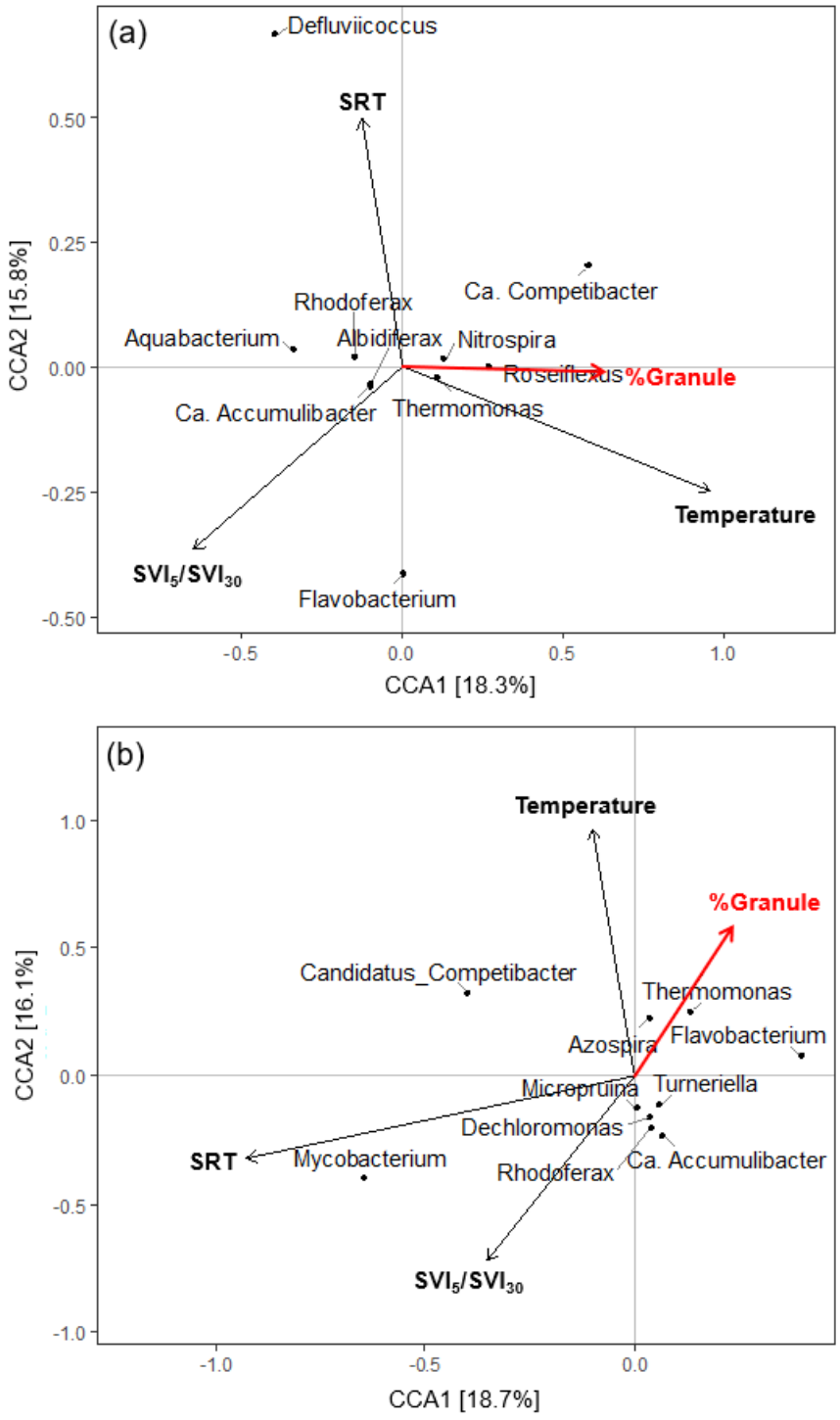

Figure 2-6. Canonical correspondence analysis (CCA) ordination diagram of relative gene abundance based on 16S rRNA gene sequencing at the Genus level together with environmental variables for (a) granule samples and (b) floc samples.

Competibacter has been demonstrated to be an important EPS producer during the granulation process, which will be further discussed in Section 2.3.5. *Roseiflexus* is a filamentous bacterium closely related to the Type 1851 morphotype. Filamentous bacteria have been shown to serve as the backbone of aerobic granules (Liu and Liu, 2006), which may explain the correlation of *Roseiflexus* with granule abundance. For all the plants where *Nitrospira* was detected, it was more dominant in the granules in comparison to flocs (**Figure 2-7**). As *Nitrospira* are not the main EPS producers in activated sludge systems, they are likely not the cause of granulation. Their higher abundance in the granules may be explained by the preference of some complete ammonia oxidizing (comammox) *Nitrospira* species for biofilm environments (Cotto et al. 2019). *Flavobacterium* are commonly present at relatively high abundance (1 – 2%) in lab- and full-scale AGS systems fed with real wastewater and appeared to be associated with EPS production and/or substrate hydrolysis (Fan et al. 2018, Świątczak and Cydzik-Kwiatkowska 2018, Szabo et al. 2017). Except the high amount of *Thermomonas* observed in a lab-scale AGS SBR treating synthetic wastewater (Song et al. 2009), other mentions of *Thermomonas* and *Azospira*, which are both heterotrophic denitrifiers (Heylen et al. 2006, Mcllroy et al. 2016), in AGS systems are very limited.

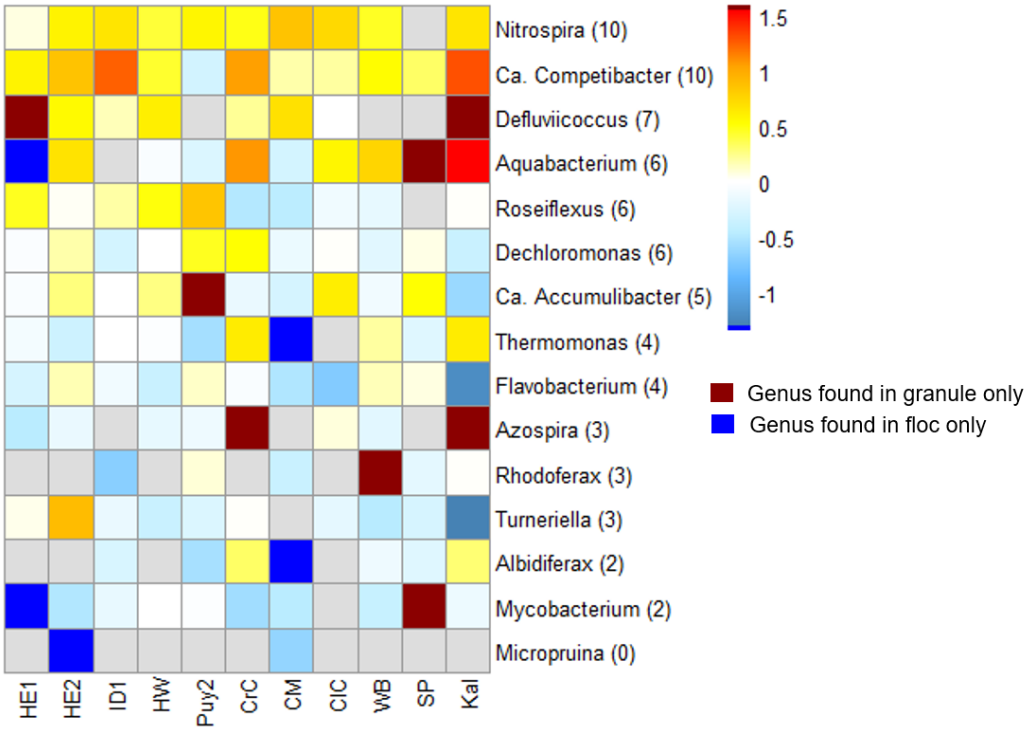

Figure 2-7. Ratio of relative gene abundance in the granule over floc on log 10 scale based on 16S rRNA gene sequencing. The number in parenthesis after each genus name is the number of plants with ratio higher than 1 (or higher than 0 on log scale) for that genus

2.3.5 Abundance of Accumulibacter and Competibacter in Granules over Flocs are Highly Correlated with %Granule

The qPCR results showed that the relative abundances of *Accumulibacter* PAO and *Competibacter* GAO were typically higher in the granules than in flocs (Supplementary Note 4). Relative abundances only represent the enrichment of PAO or GAO relative to other bacteria within an ecosystem (e.g. granule or floc) and cannot be used to compare abundances between granules versus flocs in the mixed liquor. For example, relative *Accumulibacter* abundance in HE1 granules was 2% more than the flocs, whereas this difference was 10% for SP. However, HE1 had 80% granules and SP only had 6% granules, thus the absolute *Accumulibacter* PAO

abundance in granule over floc is higher for HE1. Therefore, an estimation approach was taken (Section 2.2.3) to compare the absolute abundances in granule relative to floc in the mixed liquor sample. After this estimation, the percent granules were significantly correlated with the estimated abundance ratio of granule over floc for *Accumulibacter* and *Competibacter* as shown in **Figure 2-8**.

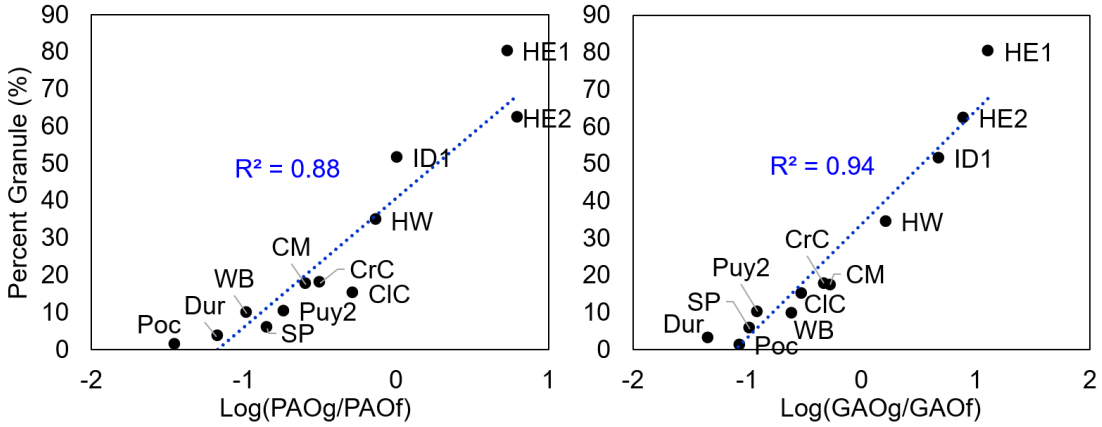

Figure 2-8. Correlation of percent granules with estimated log ratio of (a) *Accumulibacter* PAO and (b) *Competibacter* GAO abundance in granules relative to flocs.

Our results confirmed that PAO and GAO were more dominant relative to other bacteria in the granules than flocs. Additionally, a higher distribution of PAO or GAO abundance in the granules relative to flocs in a mixed liquor sample was associated with higher granule abundance. Undoubtedly, the selection of slow-growing heterotrophs such as PAO and GAO is known to induce granulation in AGS SBRs (de Kreuk and van Loosdrecht 2004). Higher inert content (e.g., polyphosphate) of PAO cells had been associated with higher biomass density and thus better sludge settleability (Schuler and Jang 2007, Winkler et al. 2013b), corroborating our findings on the correlation of PAO abundance as related to low SVI and granule growth in CFAS systems. The ability of PAO aggregates to withstand higher shear stress than other floc-forming

populations (Larsen et al. 2006) and produce denser granules in comparison to other granule types (Figdore et al. 2018a, Winkler et al. 2011) may contribute to the occurrence of granules at these CFAS facilities. Although GAOs do not accumulate polyphosphate, *Competibacter* enrichment was found to be related to the synthesis of "granulan," an exopolysaccharide important for the EPS structural change during the granulation process in lab-scale AGS SBRs (Seviour et al. 2011). In addition, flocs in a *Competibacter*-dominated SBR without fast washout had been shown to self-granulate during a period of increased physiological stress due to over aeration (Weissbrodt et al. 2013).

Further research is needed to understand the role of PAO and GAO in EPS production as related to granulation in CFAS systems. In addition, the qPCR analyses of this study were limited to *Accumulibacter/Competibacter* and did not capture other important putative PAO/GAO populations, such as *Tetrasphaera* and *Micropruina*, of which *Tetrasphaera* is as important as *Accumulibacter* for biological P removal in full-scale systems (Nielsen et al. 2019). Despite this limitation, it can be concluded hereof that the abundances of *Accumulibacter* and *Competibacter* are associated with granule growth in full-scale CFAS systems.

2.4 Conclusions

Sludge samples were collected from 13 EBPR and 4 non-EBPR CFAS plants to determine the presence of granules and identify the factors related to granule growth. We found that granules were commonly present in existing CFAS treatment systems with low SVIs. Our evaluations of plant process configurations indicated that granule growth may be related to feeding characteristics such as high F/M ratios and sCOD (or rbCOD) fraction in the anaerobic selectors. This observation was consistent with the high correlation of %granule versus PAO and GAO

abundances in the granules over flocs. Ongoing efforts for integrating AGS technologies into CFAS systems, such as the use of hydrocyclones (Sturm et al. 2017) or granule/floc separator (Figdore et al. 2018b), could benefit from adopting strategies that increase the feed F/M ratio or rbCOD fractions. Granules were also observed at a facility with an aerobic selector receiving high F/M feeds, indicating that other heterotrophs (other than PAO) were related to granule growth. In addition, the abundance of EPS producers such as the *Flavobacterium* was found to be correlated with granule abundance. Our result indicated that process configurations that select for the slow-growing or EPS-producing heterotrophs may be factors contributing to granule growth in full-scale CFAS systems.

Acknowledgements

This work was supported by the National Science Foundation (ID# 1510665 and 1603707). The authors would like to express our gratitude to all the plant staff and engineers for providing samples and plant data, as well as Dr. James Barnard for helping us identify plants to sample from. We would like to thank Sunny Wei and Li-Wen (Audrey) Wang for their contributions to lab work.

References

Adav, S.S., Lee, D.J., Show, K.Y. and Tay, J.H. (2008) Aerobic granular sludge: Recent advances. Biotechnology Advances 26(5), 411-423.

Albertsen, M., Karst, S.M., Ziegler, A.S., Kirkegaard, R.H. and Nielsen, P.H. (2015) Back to Basics - The Influence of DNA Extraction and Primer Choice on Phylogenetic Analysis of Activated Sludge Communities. Plos One 10(7).

Ali, M., Wang, Z.W., Salam, K.W., Hari, A.R., Pronk, M., van Loosdrecht, M.C.M. and Saikaly, P.E. (2019) Importance of Species Sorting and Immigration on the Bacterial Assembly of Different-Sized Aggregates in a Full-Scale Aerobic Granular Sludge Plant. Environmental Science & Technology 53(14), 8291-8301.

Andreasen, K., Agertved, J., Petersen, J.O. and Skaarup, H. (1999) Improvement of sludge settleability in activated sludge plants treating effluent from pulp and paper industries. Water Science and Technology 40(11-12), 215-221.

Armenta, M., Stensel, H.D., Bucher, B., Sukapanpotharam, P., Quoc, B.N. and Winkler, M.K.H. (2019) Operation and Performance of Sidestream Aerobic Granular Sludge Nitrifying Reactor, WEF Nutrient Removal and Recovery Symposium, Minneapolis, MN, USA.

Barnard, J., Houweling, D., Analla, H. and Steichen, M. (2012) Saving phosphorus removal at the Henderson NV plant. Water Science and Technology 65(7), 1318-1322.

Belmonte, M., Vazquez-Padin, J.R., Figueroa, M., Franco, A., Mosquera-Corral, A., Campos, J.L. and Mendez, R. (2009) Characteristics of nitrifying granules developed in an air pulsing SBR. Process Biochemistry 44(5), 602-606.

Callahan, B.J., McMurdie, P.J., Rosen, M.J., Han, A.W., Johnson, A.J.A. and Holmes, S.P. (2016) DADA2: High-resolution sample inference from Illumina amplicon data. Nature Methods 13(7), 581-+.

Coats, E.R., Brinkman, C.K. and Lee, S. (2017) Characterizing and contrasting the microbial ecology of laboratory and full-scale EBPR systems cultured on synthetic and real wastewaters. Water Research 108, 124-136.

Cotto, I., Dai, Z., Huo, L., Anderson, C.L., Vilardi, K.J., Ijaz, U., Khunjar, W., Wilson, C., De Clippeleir, H., Gilmore, K., Bailey, E. and Pinto, A.J. (2019) Long solids retention times and attached growth phase favor prevalence of comammox bacteria in nitrogen removal systems. bioRxiv, 696351.

Crocetti, G.R., Hugenholtz, P., Bond, P.L., Schuler, A., Keller, J., Jenkins, D. and Blackall, L.L. (2000) Identification of polyphosphate-accumulating organisms and design of 16S rRNA-directed probes for their detection and quantitation. Applied and Environmental Microbiology 66(3), 1175-1182.

Dai, Y., Yuan, Z.G., Wang, X.L., Oehmen, A. and Keller, J. (2007) Anaerobic metabolism of Defluviicoccus vanus related glycogen accumulating organisms (GAOs) with acetate and propionate as carbon sources. Water Research 41(9), 1885-1896.

de Kreuk, M.K., Kishida, N. and van Loosdrecht, M.C.M. (2007) Aerobic granular sludge - state of the art. Water Science and Technology 55(8-9), 75-81.

de Kreuk, M.K. and van Loosdrecht, M.C.M. (2004) Selection of slow growing organisms as a means for improving aerobic granular sludge stability. Water Science and Technology 49(11-12), 9-17.

Downing, L., Redmond, E., Klopping, P. and Young, M. (2017) Selective Pressures for Granulation in Full-scale, Flow through Activated Sludge System, WEFTEC Conference Proceedings, Chicago, IL, USA.

Fan, X.Y., Gao, J.F., Pan, K.L., Li, D.C., Zhang, L.F. and Wang, S.J. (2018) Shifts in bacterial community composition and abundance of nitrifiers during aerobic granulation in two nitrifying sequencing batch reactors. Bioresource Technology 251, 99-107.

Figdore, B.A., Stensel, H.D. and Winkler, M.K.H. (2018a) Comparison of different aerobic granular sludge types for activated sludge nitrification bioaugmentation potential. Bioresource Technology 251, 189-196.

Figdore, B.A., Stensel, H.D., Winkler, M.K.H., Armenta, M., Bucher, B., Sukapanpotharam, P. and Smyth, J. (2018b) Aerobic Granular Sludge Bioaugmentation in Low SRT Flocculent Activated Sludge: Bench Scale Demonstration and Pilot Testing, *WEFTEC*, New Orleans, LA, USA.

Figdore, B.A., Stensel, H.D., Winkler, M.K.H. and Neethling, J.B. (2017) Aerobic Granular Sludge for Biological Nutrient Removal, Water Environment and Reuse Foundation.

Giesen, A., de Bruin, L.M.M., Niermans, R.P. and Van der Roest, H.F. (2013) Advancements in the Application of Aerobic Granular Biomass Technology for Sustainable Treatment of Wastewater. Water Practice and Technology 8(1), 47-54.

He, S., Gall, D.L. and McMahon, K.D. (2007) "Candidatus Accumulibacter" population structure in enhanced biological phosphorus removal sludges as revealed by polyphosphate kinase genes. Applied and Environmental Microbiology 73(18), 5865-5874.

Heylen, K., Vanparys, B., Wittebolle, L., Verstraete, W., Boon, N. and De Vos, P. (2006) Cultivation of denitrifying bacteria: Optimization of isolation conditions and diversity study. Applied and Environmental Microbiology 72(4), 2637-2643.

Jenkins, D., Richard, M.G. and Daigger, G.T. (2004) Manual on the causes and control of activated sludge bulking, foaming, and other solids separation problems, Lewis Publishers, Boca Raton, Fla.

Kong, Y.H., Ong, S.L., Ng, W.J. and Liu, W.T. (2002) Diversity and distribution of a deeply branched novel proteobacterial group found in anaerobic-aerobic activated sludge processes. Environmental Microbiology 4(11), 753-757.

Lanham, A.B., Oehmen, A., Saunders, A.M., Carvalho, G., Nielsen, P.H. and Reis, M.A.M. (2013) Metabolic versatility in full-scale wastewater treatment plants performing enhanced biological phosphorus removal. Water Research 47(19), 7032-7041.

Larsen, P., Eriksen, P.S., Lou, M.A., Thomsen, T.R., Kong, Y.H., Nielsen, J.L. and Nielsen, P.H. (2006) Floc-forming properties of polyphosphate accumulating organisms in activated sludge. Water science and technology 54(1), 257-265.

Li, A.J., Li, X.Y. and Yu, H.Q. (2011) Effect of the food-to-microorganism (F/M) ratio on the formation and size of aerobic sludge granules. Process Biochemistry 46(12), 2269-2276.

Liu, Y. and Liu, Q.S. (2006) Causes and control of filamentous growth in aerobic granular sludge sequencing batch reactors. Biotechnology Advances 24(1), 115-127.

Liu, Q.S., Tay, J.H. and Liu, Y. (2003) Substrate concentration-independent aerobic granulation in sequential aerobic sludge blanket reactor. Environmental Technology 24(10), 1235-1242.

Mannina, G., Presti, D., Montiel-Jarillo, G., Carrera, J. and Suarez-Ojeda, M.E. (2020) Recovery of polyhydroxyalkanoates (PHAs) from wastewater: A review. Bioresource Technology 297.

Martin, K., Shaw, A., Clippeleir, H. and Sturm, B. (2016) "Accidental Granular Sludge?": Understanding process design and operational conditions that lead to low SVI-30 values through a survey of full scale facilities in North America, WEFTEC Conference Proceedings, New Orleans, LA, USA.

McIlroy, S.J., Onetto, C.A., McIlroy, B., Herbst, F.A., Dueholm, M.S., Kirkegaard, R.H., Fernando, E., Karst, S.M., Nierychlo, M., Kristensen, J.M., Eales, K.L., Grbin, P.R., Wimmer, R. and Nielsen, P.H. (2018) Genomic and in Situ Analyses Reveal the Micropruina spp. as Abundant Fermentative Glycogen Accumulating Organisms in Enhanced Biological Phosphorus Removal Systems. Frontiers in Microbiology 9.

McIlroy, S.J., Starnawska, A., Starnawski, P., Saunders, A.M., Nierychlo, M., Nielsen, P.H. and Nielsen, J.L. (2016) Identification of active denitrifiers in full-scale nutrient removal wastewater treatment systems. Environmental Microbiology 18(1), 50-64.

McMurdie, P.J. and Holmes, S. (2013) phyloseq: An R Package for Reproducible Interactive Analysis and Graphics of Microbiome Census Data. Plos One 8(4).

Nancharaiah, Y.V. and Reddy, G.K.K. (2018) Aerobic granular sludge technology: Mechanisms of granulation and biotechnological applications. Bioresource Technology 247, 1128-1143.

Nielsen, P.H., McIlroy, S.J., Albertsen, M. and Nierychlo, M. (2019) Re-evaluating the microbiology of the enhanced biological phosphorus removal process. Current Opinion in Biotechnology 57, 111-118.

Parada, A.E., Needham, D.M. and Fuhrman, J.A. (2016) Every base matters: assessing small subunit rRNA primers for marine microbiomes with mock communities, time series and global field samples. Environmental Microbiology 18(5), 1403-1414.

Parker, D., Appleton, R., Bratby, J. and Melcer, H. (2004) North American performance experience with anoxic and anaerobic selectors for activated sludge bulking control. Water Science and Technology 50(7), 221-228.

Pronk, M., de Kreuk, M.K., de Bruin, B., Kamminga, P., Kleerebezem, R. and van Loosdrecht, M.C.M. (2015) Full scale performance of the aerobic granular sludge process for sewage treatment. Water Research 84, 207-217.

Qiu, G.L., Zuniga-Montanez, R., Law, Y.Y., Thi, S.S., Nguyen, T.Q.N., Eganathan, K., Liu, X.H., Nielsen, P.H., Williams, R.B.H. and Wuertz, S. (2019) Polyphosphate-accumulating organisms in full-scale tropical wastewater treatment plants use diverse carbon sources. Water Research 149, 496-510.

Ruijter, J.M., Ramakers, C., Hoogaars, W.M.H., Karlen, Y., Bakker, O., van den Hoff, M.J.B. and Moorman, A.F.M. (2009) Amplification efficiency: linking baseline and bias in the analysis of quantitative PCR data. Nucleic Acids Research 37(6).

Schuler, A.J. and Jang, H. (2007) Causes of variable biomass density and its effects on settleability in full-scale biological wastewater treatment systems. Environmental Science & Technology 41(5), 1675-1681.

Seviour, T., Pijuan, M., Nicholson, T., Keller, J. and Yuan, Z.G. (2009) Gel-forming exopolysaccharides explain basic differences between structures of aerobic sludge granules and floccular sludges. Water Research 43(18), 4469-4478.

Seviour, T.W., Lambert, L.K., Pijuan, M. and Yuan, Z.G. (2011) Selectively inducing the synthesis of a key structural exopolysaccharide in aerobic granules by enriching for Candidatus "Competibacter phosphatis". Applied Microbiology and Biotechnology 92(6), 1297-1305.

Song, Z.W., Ren, N.Q., Zhang, K. and Tong, L.Y. (2009) Influence of temperature on the characteristics of aerobic granulation in sequencing batch airlift reactors. Journal of Environmental Sciences 21(3), 273-278.

Stokholm-Bjerregaard, M., McIlroy, S.J., Nierychlo, M., Karst, S.M., Albertsen, M. and Nielsen, P.H. (2017) A Critical Assessment of the Microorganisms Proposed to be Important to Enhanced Biological Phosphorus Removal in Full-Scale Wastewater Treatment Systems. Frontiers in Microbiology 8.

Sturm, B., Faraj, R., Figdore, B.A., Willoughby, A., Ford, A., Bott, C., Shiskowski, D., McFall, L. and Downing, L. (2017) Balancing Granular Sludge with Activated Sludge Systems for Biological Nutrient Removal, WEFTEC Conference Proceedings, Chicago, IL, USA.

Świątczak, P. and Cydzik-Kwiatkowska, A. (2018) Performance and microbial characteristics of biomass in a full-scale aerobic granular sludge wastewater treatment plant. Environmental Science and Pollution Research 25(2), 1655-1669.

Szabo, E., Liebana, R., Hermansson, M., Modin, O., Persson, F. and Wilen, B.M. (2017) Microbial Population Dynamics and Ecosystem Functions of Anoxic/Aerobic Granular Sludge in Sequencing Batch Reactors Operated at Different Organic Loading Rates. Frontiers in Microbiology 8.

Tatti, E., McKew, B.A., Whitby, C. and Smith, C.J. (2016) Simultaneous DNA-RNA Extraction from Coastal Sediments and Quantification of 16S rRNA Genes and Transcripts by Real-time PCR. Jove-Journal of Visualized Experiments (112).

Wang, Q., Garrity, G.M., Tiedje, J.M. and Cole, J.R. (2007) Naïve Bayesian Classifier for Rapid Assignment of rRNA Sequences into the New Bacterial Taxonomy. Applied & Environmental Microbiology 73(16), 5261-5267.

Wang, X.H., Jiang, L.X., Shi, Y.J., Gao, M.M., Yang, S. and Wang, S.G. (2012) Effects of step-feed on granulation processes and nitrogen removal performances of partial nitrifying granules. Bioresource Technology 123, 375-381.

Weissbrodt, D.G., Neu, T.R., Kuhlicke, U., Rappaz, Y. and Holliger, C. (2013) Assessment of bacterial and structural dynamics in aerobic granular biofilms. Frontiers in Microbiology 4.

Wilen, B.M., Liebana, R., Persson, F., Modin, O. and Hermansson, M. (2018) The mechanisms of granulation of activated sludge in wastewater treatment, its optimization, and impact on effluent quality. Applied Microbiology and Biotechnology 102(12), 5005-5020.

Wilen, B.M., Lumley, D., Mattsson, A. and Mino, T. (2008) Relationship between floc composition and flocculation and settling properties studied at a full scale activated sludge plant. Water Research 42(16), 4404-4418.

Winkler, M.-K., Bassin, J., Kleerebezem, R., De Bruin, L., Van den Brand, T. and Van Loosdrecht, M. (2011) Selective sludge removal in a segregated aerobic granular biomass system as a strategy to control PAO–GAO competition at high temperatures. Water Research 45(11), 3291-3299.

Winkler, M.K.H., Kleerebezem, R., de Bruin, L.M.M., Verheijen, P.J.T., Abbas, B., Habermacher, J. and van Loosdrecht, M.C.M. (2013a) Microbial diversity differences

within aerobic granular sludge and activated sludge flocs. Applied Microbiology and Biotechnology 97(16), 7447-7458.
Winkler, M.K.H., Kleerebezem, R., Strous, M., Chandran, K. and van Loosdrecht, M.C.M. (2013b) Factors influencing the density of aerobic granular sludge. Applied Microbiology and Biotechnology 97(16), 7459-7468.
Winkler, M.K.H., Kleerebezem, R. and van Loosdrecht, M.C.M. (2012) Integration of anammox into the aerobic granular sludge process for main stream wastewater treatment at ambient temperatures. Water Research 46(1), 136-144.
Winkler, M.K.H., Meunier, C., Henriet, O., Mahillon, J., Suarez-Ojeda, M.E., Del Moro, G., De Sanctis, M., Di Iaconi, C. and Weissbrodt, D.G. (2018) An integrative review of granular sludge for the biological removal of nutrients and recalcitrant organic matter from wastewater. Chemical Engineering Journal 336, 489-502.
Wu, D., Zhang, Z.M., Yu, Z.D. and Zhu, L. (2018) Optimization of F/M ratio for stability of aerobic granular process via quantitative sludge discharge. Bioresource Technology 252, 150-156.

Appendix A. Supplementary Material for Chapter 2

Table S1. Summary of aeration basin stages in series, nominal hydraulic retention times and F/M ratio of first anaerobic zone.

	Anaerobic			Anoxic		Aerobic	
Sample	# of Stages	HRT per stage, hr	1st Stage F/M, gBOD/gVSS d	# of Stages	HRT per stage, hr	# of Stages	Total HRT, hr
HE1	2	0.42	10.3	4	0.42	1	12.2
HE2	2	0.45	13.5	4	0.45	1	13.2
ID1	3	0.68	2.00	-	-	3	11.6
ID2	3	0.70	2.42	-	-	3	12.0
HW	3	0.40	14.0	4	0.40	1	13.9
CrC	1	2.62	0.82	-	-	1	18.7
CM	1	3.27	0.65	3	5.59	3	15.5
ClC	2	0.47	4.50	-	-	6	4.70
Puy1	2	0.17	4.70	3	1.44	4	7.45
Puy2	2	0.39	4.89	3	3.37	4	17.4
WB	3	0.45	4.80	2	0.54	3	7.18
SP	1	0.81	2.90	-	-	4	5.65
Dur	2	0.48	3.50	2	0.39	7	3.53
Poc	1	2.51	1.39	4	3.31	2	11.3
Kal	2	0.73	5.70	2	1.81	3	10.5
BM	3	0.14	10.5	2	1.76	4	7.04

Table S2. Summary of lab and operational data for sample collected from HE, ID, HW, CrC, CM and ClC.

Parameter	Unit	HE1	HE2	ID1	ID2	HW	CrC	CM	ClC
UW Lab Measurements									
Sample Date	-	8/30/17	11/9/17	10/11/17	1/7/19	Jan	12/1/17	11/8/17	8/30/17
Percent Granule	%	80.2	62.2	51.5	67.7	34.5	17.8	17.4	14.6
SVI_{30}	ml/g	39	52	80	72.3 ± 8.2[i]	55	73	107	68
SVI_5	ml/g	43	70	127	-	70	137	154	101
Plant Operational Data									
# of Anaerobic Stages	-	2		3	3	3	1	1	2
Has Primary Treatment?	-	No		Yes	Yes	No	No	No	Yes
Has Fermenter?	-	ML Ferment[d]		No	No	No	No	No	No
Anaerobic Zone Mixer[a]	-	S		I	I	S	VSP	I	VSP
Month of Average SRT[b]	-	Aug/2017	Oct/2017	Oct/2017	Dec/2018	Oct/2017	Nov/2017	Oct/2017	Aug/2017
Average SRT	day	7.1 ± 3.8	4.3 ± 1.0	9.7 ± 0.8	11.6 ± 1.5	5.7 ± 0.6	9.4 ± 0.1	12.0 ± 0.0	13.8 ± 4.8
Plant Performance Data									
Data Range for Averages[c]	-	21 days before 8/30/17	13 days before 11/9/17	29 days before 10/11/17	35 days before 1/1/19	17 days before 11/9/17	28 days before 12/1/17	36 days before 11/8/17	41 days before 8/30/17
Flow	MGD	6.0 ± 0.0	5.5 ± 1.3	9.7 ± 1.0	9.4 ± 0.4	15.1 ± 1.9	6.4 ± 0.2	0.39 ± 0.2	109 ± 2.2
Temperature	°C	29.0 ± 1.3	26.5 ± 1.9	19.8 ± 0.7	15.0 ± 0.0	26.8 ± 0.6	22.3 ± 1.0	16.0 ± 0.9	29.9 ± 0.8
Influent BOD	mg/L	246 ± 21	260 ± 18	217 ± 27	241 ± 44	263 ± 18	179 ± 25[f]	415 ± 76	320 ± 29
Influent TP	mg/L	5.4 ± 0.3	5.2 ± 0.1	N/A	N/A	5.2 ± 0.1	6.2 ± 0.8	5.6 ± 0.6	5.8 ± 0.4
Influent TKN	mg/L	40.7 ± 3.1	44.3 ± 1.6	N/A	N/A	44.2 ± 1.3	42.4 ± 3.9	35.2	45.1 ± 2.9
PE COD	mg/L	N/A	N/A	N/A	N/A	N/A	N/A	N/A	N/A

Table S2 Continued. Summary of lab and operational data for sample collected from HE, ID, HW, CrC, CM and ClC.

PE sCOD	mg/L	N/A	N/A	188 ± 43	283 ± 46	N/A	N/A	N/A	N/A
PE BOD	mg/L	N/A	N/A	137 ± 45	188 ± 42	N/A	N/A	N/A	212 ± 5
PE TP	mg/L	N/A	N/A	4.5 ± 0.6[e]	5.6 ± 0.9	N/A	N/A	N/A	5.3 ± 0.4
PE TKN	mg/L	N/A	N/A	>16.0	28.5 ± 2.1	N/A	N/A	N/A	31.7 ± 1.2[h]
SVI_{30}	ml/g	79.9 ± 15	80.8 ± 19	65.3 ± 4	72.3 ± 8.2	62.6 ± 12	69.7 ± 3.5	55.7 ± 2.6	63.2 ± 19
MLSS	mg/L	1552 ± 344	1226 ± 156	3218 ± 221	3532 ± 410	1300 ± 131	2591 ± 102	5483 ± 470	3078 ± 141
SE sCOD	mg/L	N/A	N/A	47.7 ± 25.8	32.1 ± 5.2	N/A	N/A	N/A	N/A
SE TP	mg/L	1.15 ± 0.32	2.10 ± 0.25	<0.51	0.99 ± 0.49	0.6 ± 0.09	N/A	N/A	0.45 ± 0.06
SE PO_4^{3-}	mgP/L	0.87 ± 0.30	1.86 ± 0.49	N/A	N/A	0.54 ± 0.73	N/A	N/A	N/A
SE TKN	mg/L	2.75 ± 1.46	3.73 ± 1.60	N/A	N/A	2.45 ± 0.52	N/A	N/A	N/A
SE NH_4^+-N	mgN/L	0.57 ± 1.27	0.24 ± 0.31	N/A	N/A	0.09 ± 0.06	N/A	N/A	N/A
SE NO_x	mgN/L	13.2 ± 2.6	13.1 ± 3.0	N/A	N/A	14.9 ± 0.85	N/A	N/A	N/A
Effluent TP	mg/L	0.72 ± 0.33	1.14 ± 0.30	0.24 ± 0.06	0.32 ± 0.09	N/A	0.10 ± 0.02[g]	0.25 ± 0.06	0.09 ± 0.01
Effluent PO_4^{3-}	mgP/L	0.42 ± 0.26	0.69 ± 0.27	N/A	N/A	0.09 ± 0.03	0.05 ± 0.02	N/A	N/A
Effluent NH_4^+-N	mg/L	N/A	N/A	0.05 ± 0.01	0.06 ± 0.02	N/A	0.25 ± 0.09	0.20 ± 0.27	0.10 ± 0.01
Effluent NO_x	mgN/L	N/A	N/A	10.7 ± 1.3	8.2 ± 1.6	N/A	16.4 ± 3.3	N/A	14.2 ± 0.9

[a] I = Invent; VSP = vertical shaft propeller; CBD = coarse bubble diffuser; SP = submersible propeller.
[b] The month of data used for calculating the average SRT.
[c] The range of data (approximately 3 SRTs) used for calculating the averaged plant performance data.
[d] Mixer in second anaerobic zone is on only 5 – 10 mins a day.
[e] Upper TP detection limit was 5.0 mg/L. Actual averaged primary effluent TP was likely higher.
[f] cBOD
[g] Roughly 55 mg/L of alum is added to the aeration basin effluent for supplemental P removal.
[h] Total nitrogen
[i] Due to the lack of sample volume collected from ID2, SVI_5 and SVI_{30} could not be measured in our lab. Therefore, we used the averaged SVI reported by the plant for a period of 3 SRTs prior to sample date.

Table S3. Summary of lab and operational data for sample collected from Puy1, Puy 2, WB, SP, Dur, Poc, Kal and BM.

Parameter	Unit	Puy1	Puy2	WB	SP	Dur	Poc	Kal	BM
UW Lab Measurements									
Sample Date	-	4/11/17	8/11/17	8/25/17	7/26/17	7/24/18	1/5/18	11/16/17	11/22/17
Percent Granule	%	29.3	10.3	9.7	5.6	3.3	1.3	0.7	0.5
SVI_{30}	ml/g	71	115	72	95	163	209	135	152
SVI_5	ml/g	128	241	146	178	357	487	260	158
Plant Operational Data									
# of Anaerobic Stages	-	2[d]		3	1	2	1	2	1
Has Primary Treatment?	-	Yes		Yes	Yes	Yes	Yes	Yes[e]	Yes
Has Fermenter?	-	No		Yes	No	Yes	No	Yes	No
Anaerobic Zone Mixer[a]	-	CBD		VSP	SP	VSP	SP	I	SP
Month of Average SRT[b]	-	Apr/2017	Aug/2017	Aug/2017	Jul/2017	Jul/2018	Dec/2017	N/A	Nov/2017
Average SRT	day	15.1 ± 1.5	17.8 ± 2.6	10.7 ± 1.3	3.7 ± 0.4	5.5 ± 1.0	12.9 ± 2.0	11[f]	23.8 ± 5.0
Plant Performance Data									
Data Range for Averages[c]	-	41 days before 4/11/17	53 days before 8/11/17	32 days before 8/25/17	11 days before 7/26/17	16 days before 7/24/18	39 days before 1/5/18	33 days before 11/16/17	71 days before 11/22/17
Flow	MGD	7.5 ± 1.9	3.2 ± 0.2	15.8 ± 0.4	65.4 ± 2.3	21.2 ± 0.9	6.0 ± 0.2	2.5 ± 0.1	6.4 ± 0.4
Temperature	°C	13.5 ± 0.8	21.6 ± 1.0	23.0 ± 0.2	22.0 ± 0.2	23.3 ± 0.4	13.3 ± 1.0	15.9 ± 0.9	21.2 ± 1.5
Influent BOD	mg/L	170 ± 42	313 ± 49	204 ± 28	347 ± 34	168 ± 13	356 ± 76	300 ± 24	292 ± 90
Influent TP	mg/L	N/A	N/A	N/A	8.3 ± 0.9	7.6 ± 0.9	7.4 ± 0.5	5.9 ± 0.4	9.0 ± 2.1
Influent TKN	mg/L	N/A	N/A	N/A	62.5 ± 2.9	N/A	N/A	41.2	43.7 ± 6.3[g]
Influent NH_4^+-N	mg/L	N/A	N/A	24.7 ± 1.4	37.2 ± 0.6	31.7 ± 4.4	29.4 ± 1.0	43.6 ± 8.9	33.5 ± 3.7[g]
PE COD	mg/L	217 ± 46	405 ± 28	N/A	322 ± 15	324 ± 44	N/A	N/A	N/A

Table S3. Continued. Summary of lab and operational data for sample collected from Puy1, Puy 2, WB, SP, Dur, Poc, Kal and BM.

PE sCOD	mg/L	N/A	N/A	N/A	166 ± 13	N/A	N/A	N/A	N/A
PE BOD	mg/L	N/A	N/A	155 ± 13	188 ± 19	N/A	263 ± 33	150 ± 27	135 ± 46[g]
PE TP	mg/L	N/A	N/A	N/A	5.5 ± 0.3	5.2 ± 0.6	7.0 ± 0.5	N/A	5.0 ± 0.9[g]
PE PO_4^{3-}	mgP/L	N/A	N/A	5.0 ± 0.4	3.3 ± 0.6	3.7 ± 0.7	N/A	N/A	N/A
PE TKN	mg/L	N/A	N/A	N/A	N/A	N/A	N/A	N/A	36.6 ± 3.8[g]
PE NH_4^+-N	mg/L	N/A	N/A	N/A	38.7 ± 0.6	32.7 ± 3.1	29.6 ± 1.6	N/A	32.0 ± 1.5[g]
SVI_{30}	ml/g	69.6 ± 2.6	88.0 ± 12	55.6 ± 7.4	83.5 ± 2.8	114 ± 6.5	238 ± 35	151 ± 6.4	N/A
MLSS	mg/L	3525 ± 207	2566 ± 292	2881 ± 172	2360 ± 77	2125 ± 293	2179 ± 243	2146 ± 57	3027 ± 472[h]
SE TP	mg/L	N/A	N/A	N/A	N/A	0.26 ± 0.07	N/A	N/A	0.87 ± 0.45
Effluent TP	mg/L	0.4	3.16 ± 0.14	2.12 ± 0.80	2.93 ± 0.32	0.14 ± 0.10	0.18 ± 0.01	0.09 ± 0.02	0.23 ± 0.15
Effluent NH_4^+-N	mg/L	1.2 ± 0.9	0.19 ± 0.10	0.43 ± 0.95	50.3 ± 0.8	3.28 ± 4.91	0.43 ± 0.71	0.25 ± 0.15	0.02 ± 0.1
Effluent NO_3^- + NO_2^-	mgN/L	7.4	7.0 ± 1.4	15.8 ± 2.7	<0.2	10.6 ± 1.6	8.56	6.31 ± 0.94	1.28 ± 1.16

[a] I = Invent; VSP = vertical shaft propeller; CBD = coarse bubble diffuser; SP = submersible propeller.
[b] The month of data used for calculating the average SRT.
[c] The range of data (approximately 3 SRTs) used for calculating the averaged plant performance data.
[d] 1/3 of internal return is recycled to the first anaerobic selector. Mixed liquor sample was abundant in PAOs (shown by Neisser staining images), indicating anaerobic conditions in the selector.
[e] With both inline ML ferment and primary sludge fermenter. Inline ML ferment: mixer in first RAS anoxic zone is on a timer 2-hour off and 5-min on.
[f] An estimated number from plant staff.
[g] Data for 25-mm fine screen effluent
[h] This MLSS is lower than what is expected of a typical MBR plant. The reason is that the MBR at BM was installed for improving effluent quality, not for increasing plant capacity.

Table S4. Plant process schematics

(a) Henderson East

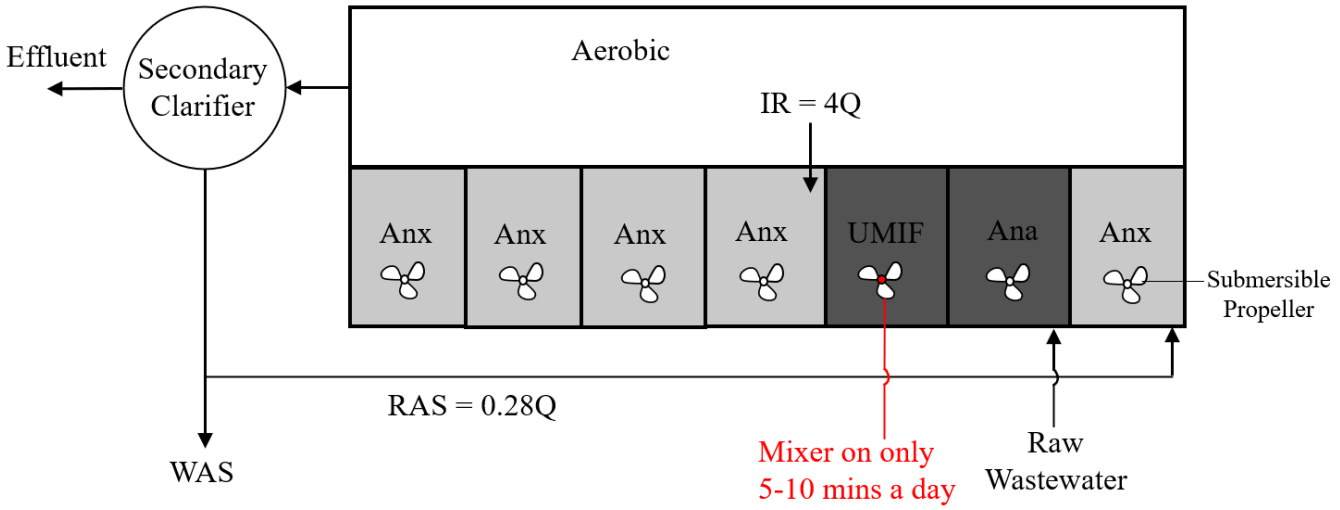

(b) Idaho Falls

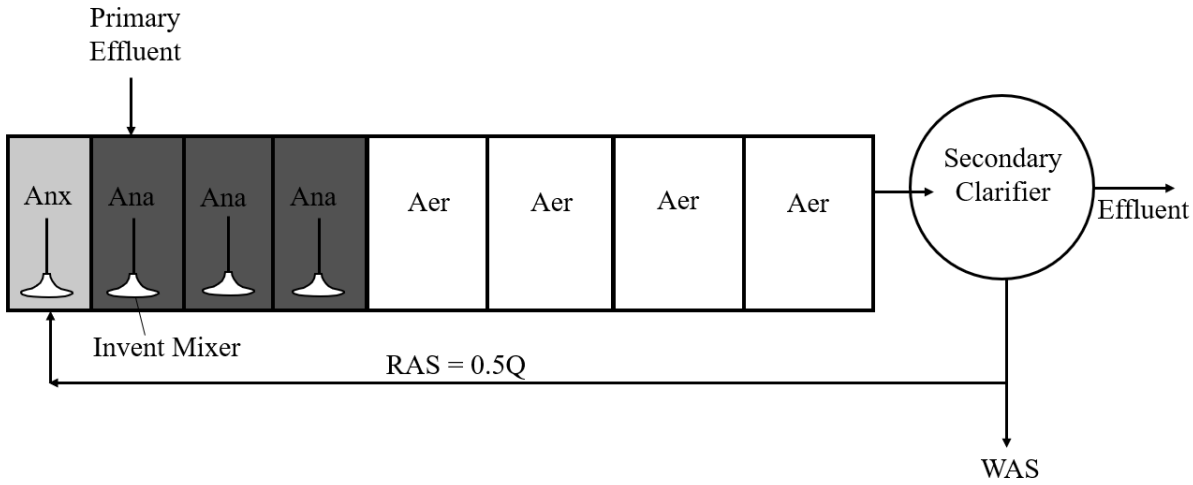

(c) Henderson West

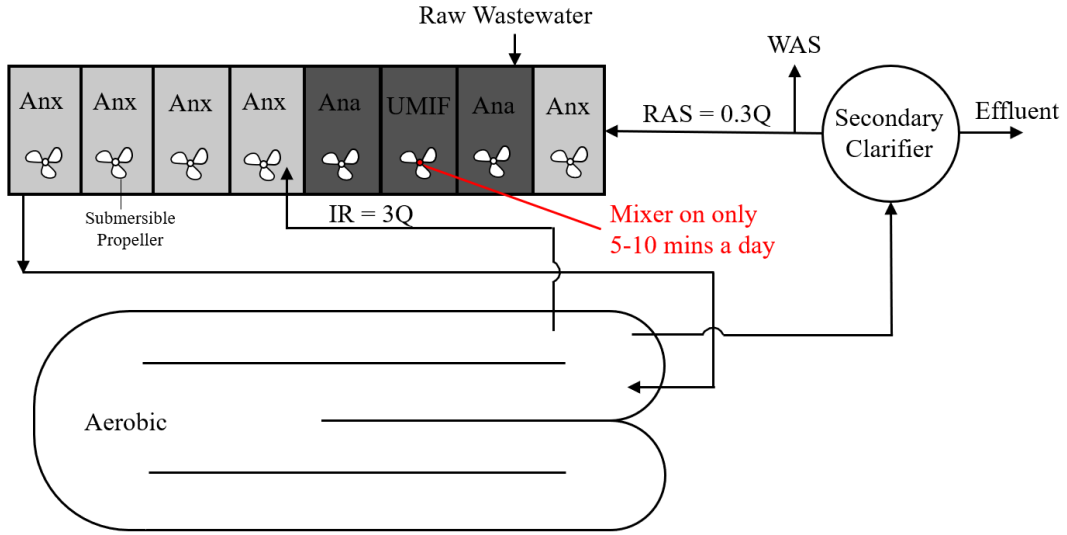

(d) Crooked Creek

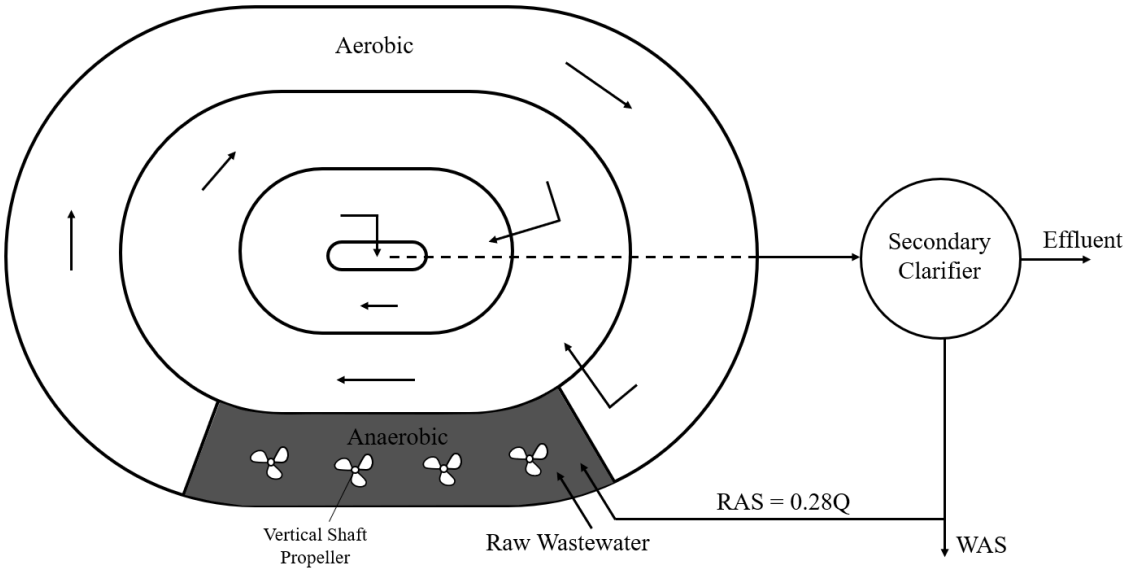

(e) Cashmere

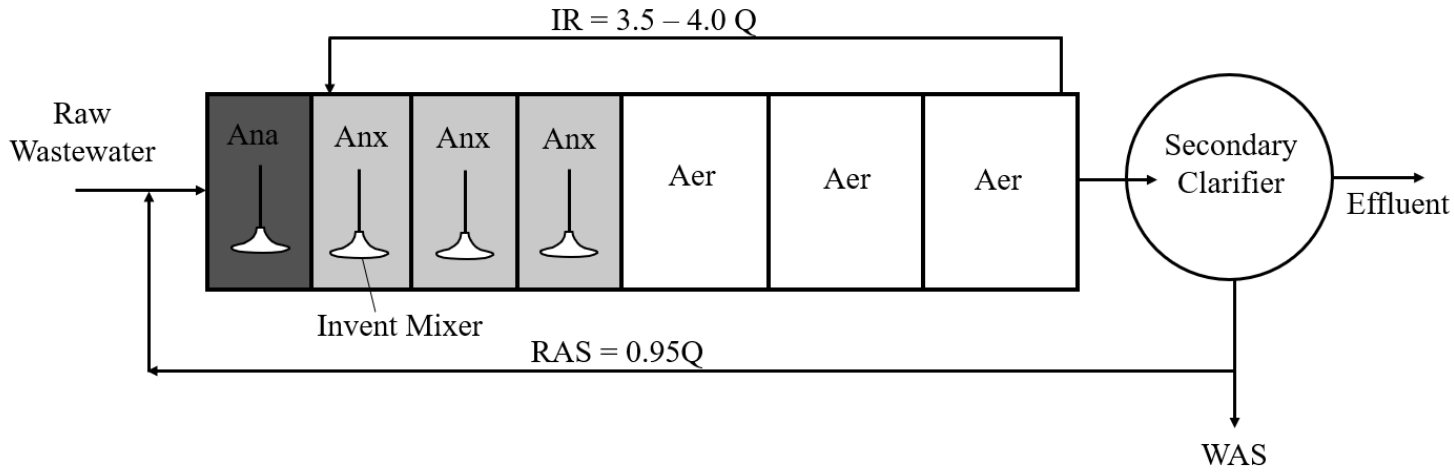

(f) Clark County

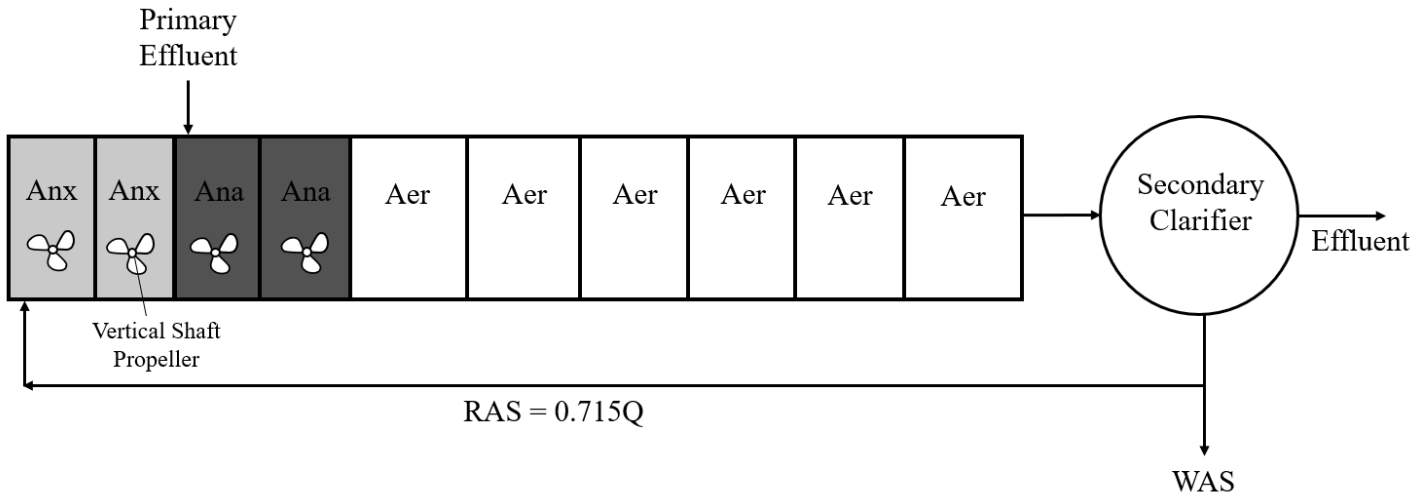

(g) Puyallup

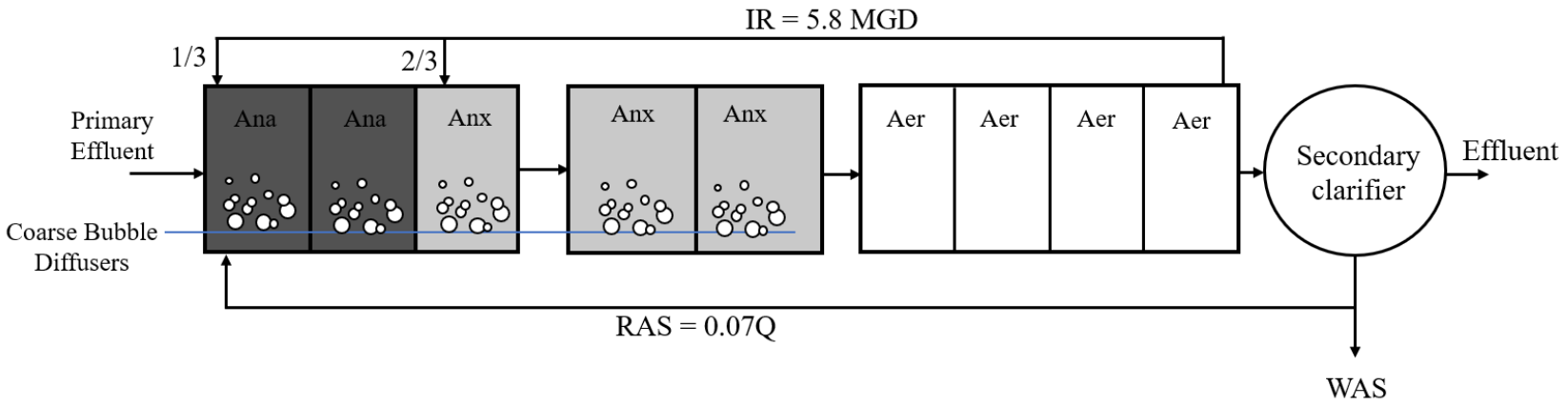

(h) West Boise

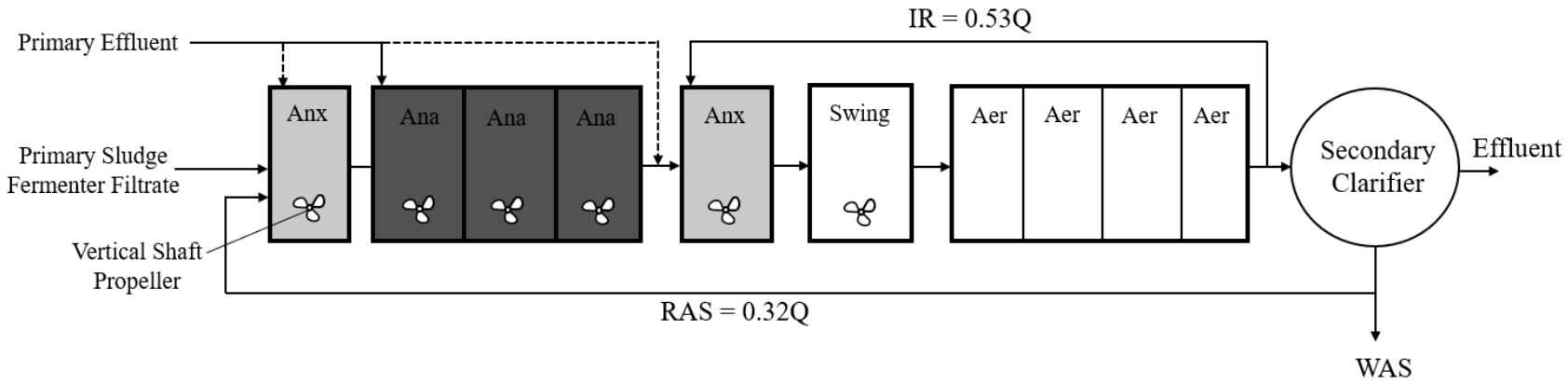

(i) South Plant

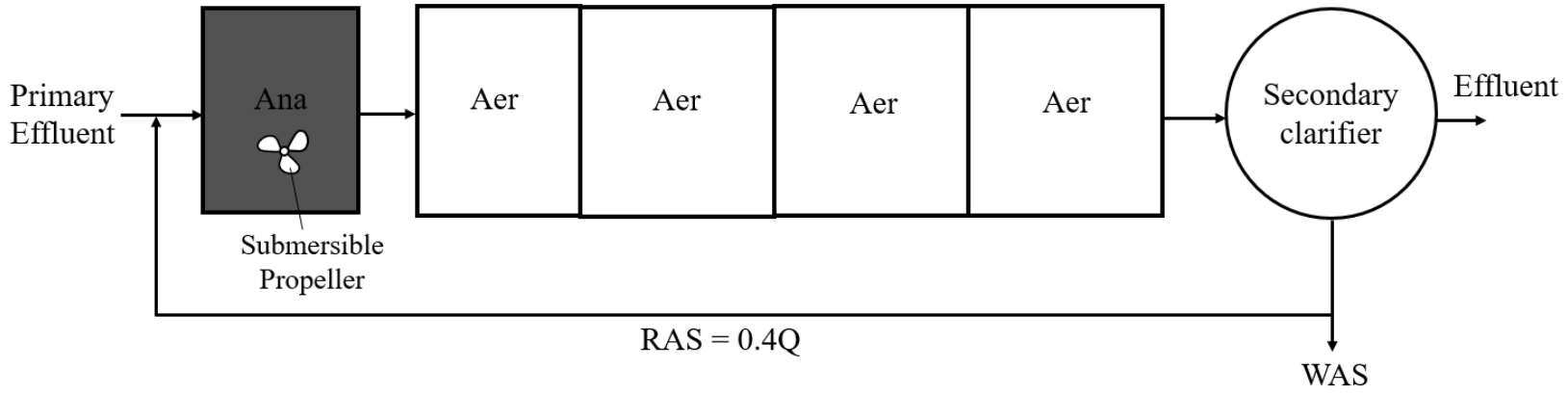

(j) Durham

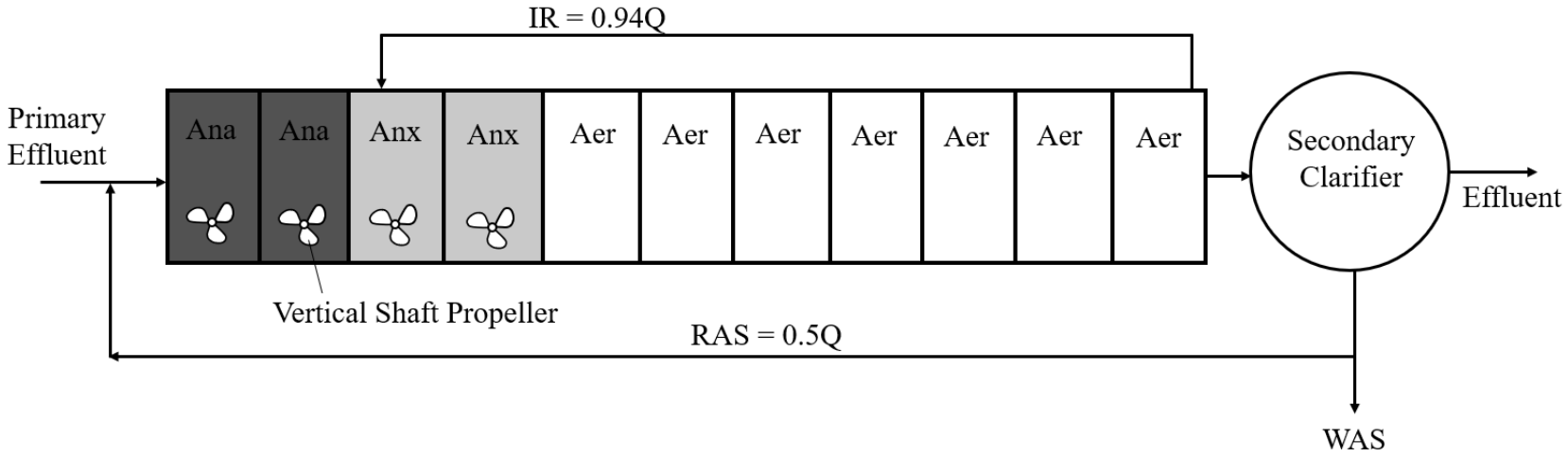

(k) Pocatello

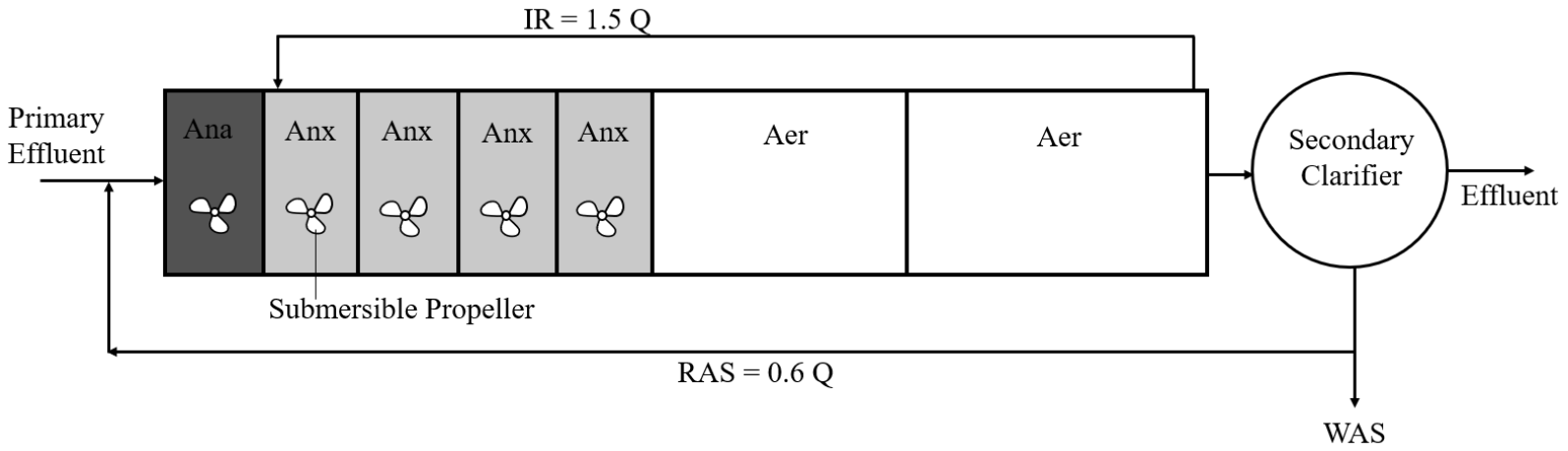

(l) Kalispell

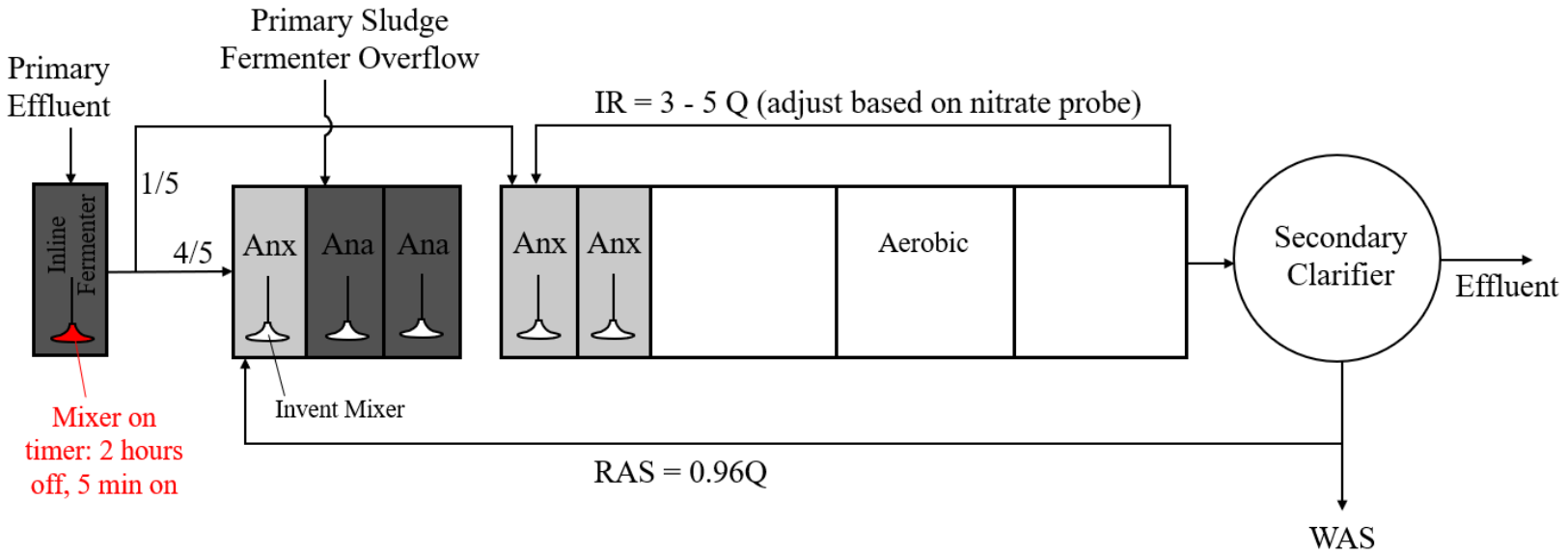

(m) Ballenger McKinney

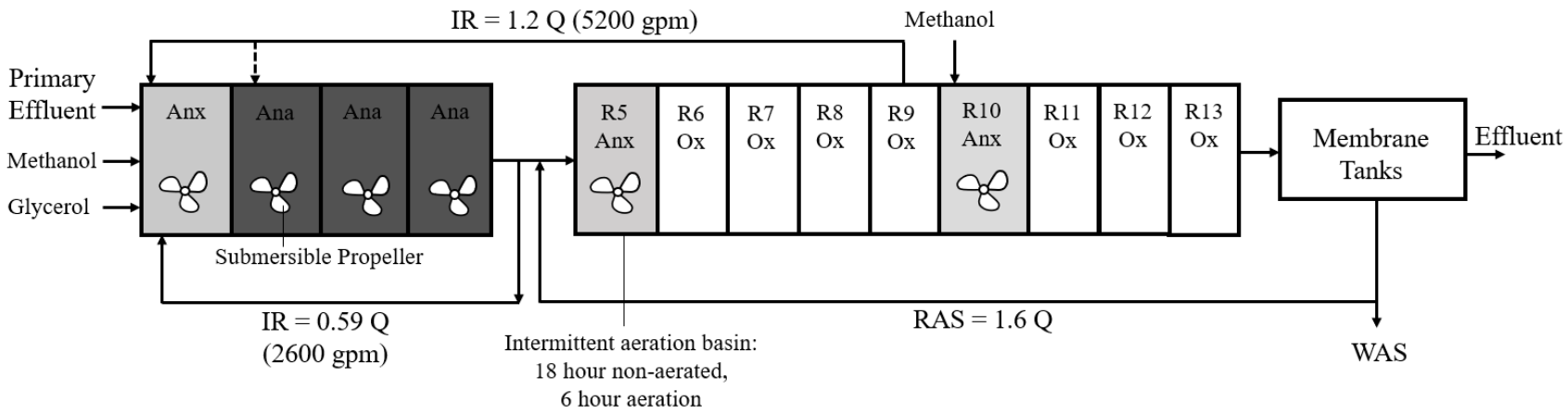

(n) Pasco

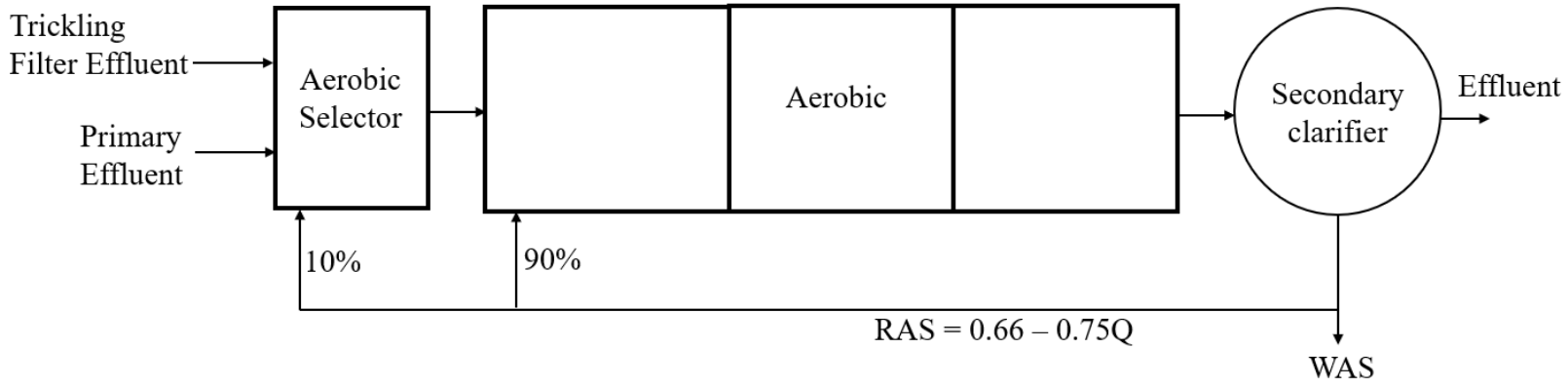

Table S5. Summary of lab data for samples collected from non-EBPR plants

Facility	Sample ID	Sample Date	Percent Granule	SVI_{30}	SVI_5
-	-	-	%	ml/g	ml/g
Edmonds, WA	Ed	9/12/17	F[a]	241	509
Lynnwood, WA	Lyn	9/12/17	F[a]	475	526
West Point, WA	WP	9/12/17	F[a]	193	394
Pasco, WA	Pas1	9/22/17	3.4	193	358
	Pas2	10/4/18	44.1	67	96

[a] F = sample was too filamentous for sieving.

Table S6. Summary of chosen samples for DNA extraction, qPCR analyses, and 16S rRNA gene sequencing.

Sample	EBPR or non-EBPR	Percent Granule, %	DNA Extracted	qPCR Analyses Conducted	16S rRNA Gene Sequencing Conducted
HE1	EBPR	80.2	Floc and Granule	Floc and Granule	Floc and Granule
HE2	EBPR	62.2	Floc and Granule	Floc and Granule	Floc and Granule
ID1	EBPR	51.5	Floc and Granule	Floc and Granule	Floc and Granule
ID2	EBPR	67.7	No[a]	No	No
HW	EBPR	34.5	Floc and Granule	Floc and Granule	Floc and Granule
CrC	EBPR	17.8	Floc and Granule	Floc and Granule	Floc and Granule
CM	EBPR	17.4	Floc and Granule	Floc and Granule	Floc and Granule
ClC	EBPR	14.6	Floc and Granule	Floc and Granule	Floc and Granule
Puy1	EBPR	29.3	No[a]	No	No
Puy2	EBPR	10.3	Floc and Granule	Floc and Granule	Floc and Granule
WB	EBPR	9.7	Floc and Granule	Floc and Granule	Floc and Granule
SP	EBPR	5.6	Floc and Granule	Floc and Granule	Floc and Granule
Dur	EBPR	3.3	Floc and Granule	Floc and Granule	No[e]
Poc	EBPR	1.3	Floc and Granule	Floc and Granule	No[e]
Kal	EBPR	0.7	Floc and Granule	No[d]	Floc and Granule
BM	EBPR	0.5	Floc only[b]	No[d]	Floc only
Ed	non-EBPR	F[c]	Floc only[b]	No	Floc only
Lynn	non-EBPR	F[c]	No	No	Yes
WP	non-EBPR	F[c]	No	No	Yes
Pas1	non-EBPR	3.4	No	No	Yes
Pas2	non-EBPR	44.1	No	No	Yes

[a] Sample received did not have enough volume for floc/granule separation.
[b] Insufficient granule fraction for DNA extraction from granules.
[c] F = sample was too filamentous for sieving.
[d] qPCR was not conducted because granule abundance was less than 1%.
[e] 16S rRNA sequencing analysis was not conducted due to limits in project scope.

Table S7. Primers and amplification conditions used

Primer	Sequence (5’ – 3’)	Reference	Target	qPCR Conditions
Bac 341f	CCTACGGGAGGCAGCAG	(He et al., 2007)	Bacterial 16S	95°C: 60s, 35×(95°C: 10s; 64°C: 10s; 72°C: 30s)
Bac 534r	ATTACCGCGGCTGCTGG			
PAO 651f	CTGGAGTTTGGCAGAGGG	(Crocetti et al., 2000)	*Accumulibacter* PAO 16S	95°C: 60s, 35×(95°C: 10s; 64°C: 10s; 72°C: 30s)
PAO 846r	GTTAGCTACGGCACTAAAAGG			
GBf	GAGTGGGCTAGAGGATCGTG	(Fukushima et al., 2010; Kong et al., 2002)	*Competibacter* GAO 16S	95°C: 60s, 35×(95°C: 10s; 63°C: 10s; 72°C: 30s)
GBr	TTCCCCRGATGTCAAGGCC			

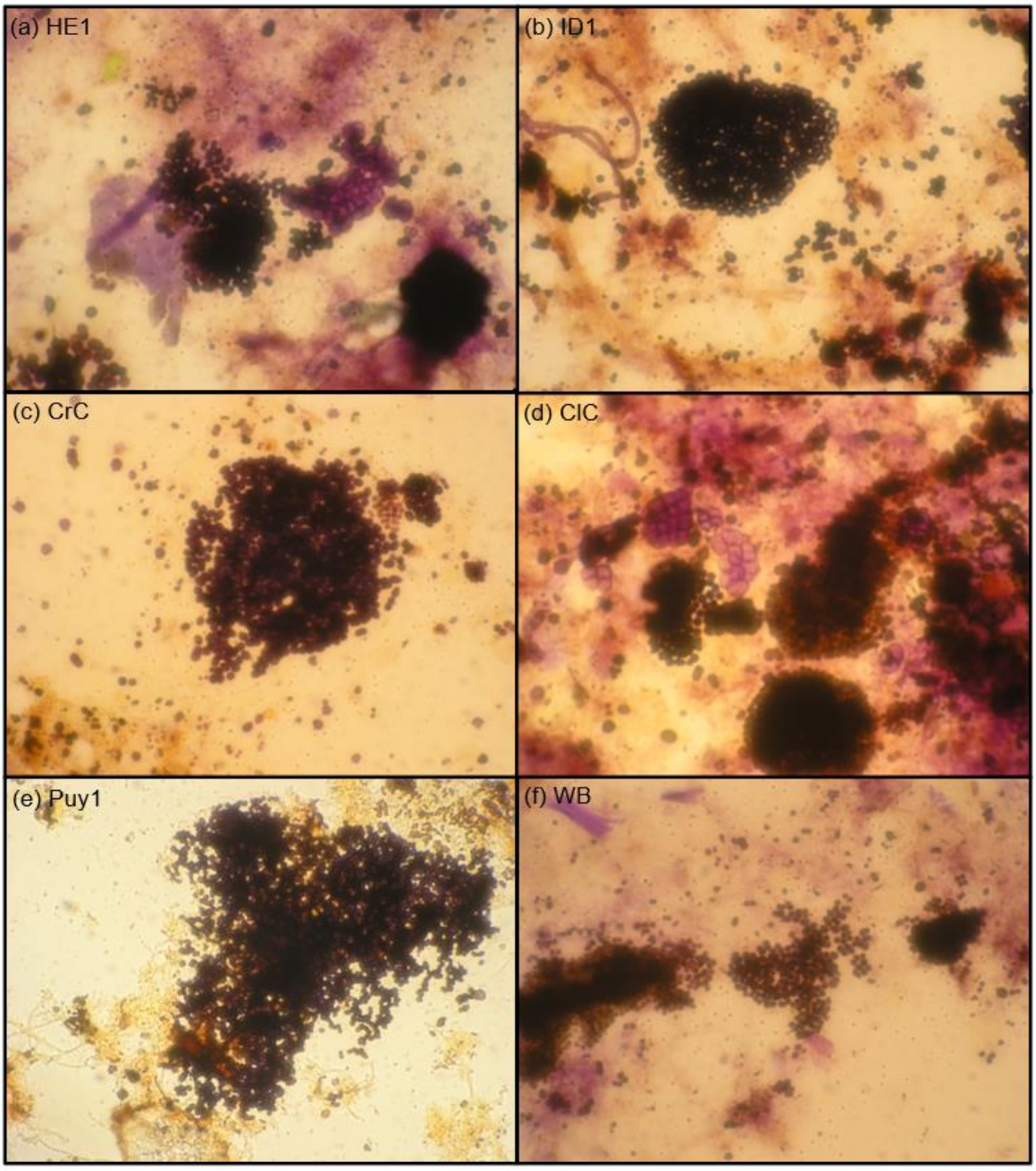

Figure S1. Neisser Staining images at 1000X magnification of solids retrained on 212-µm sieve (granules). Dark purple cells are polyphosphate-positive showing high PAO abundance in granules.

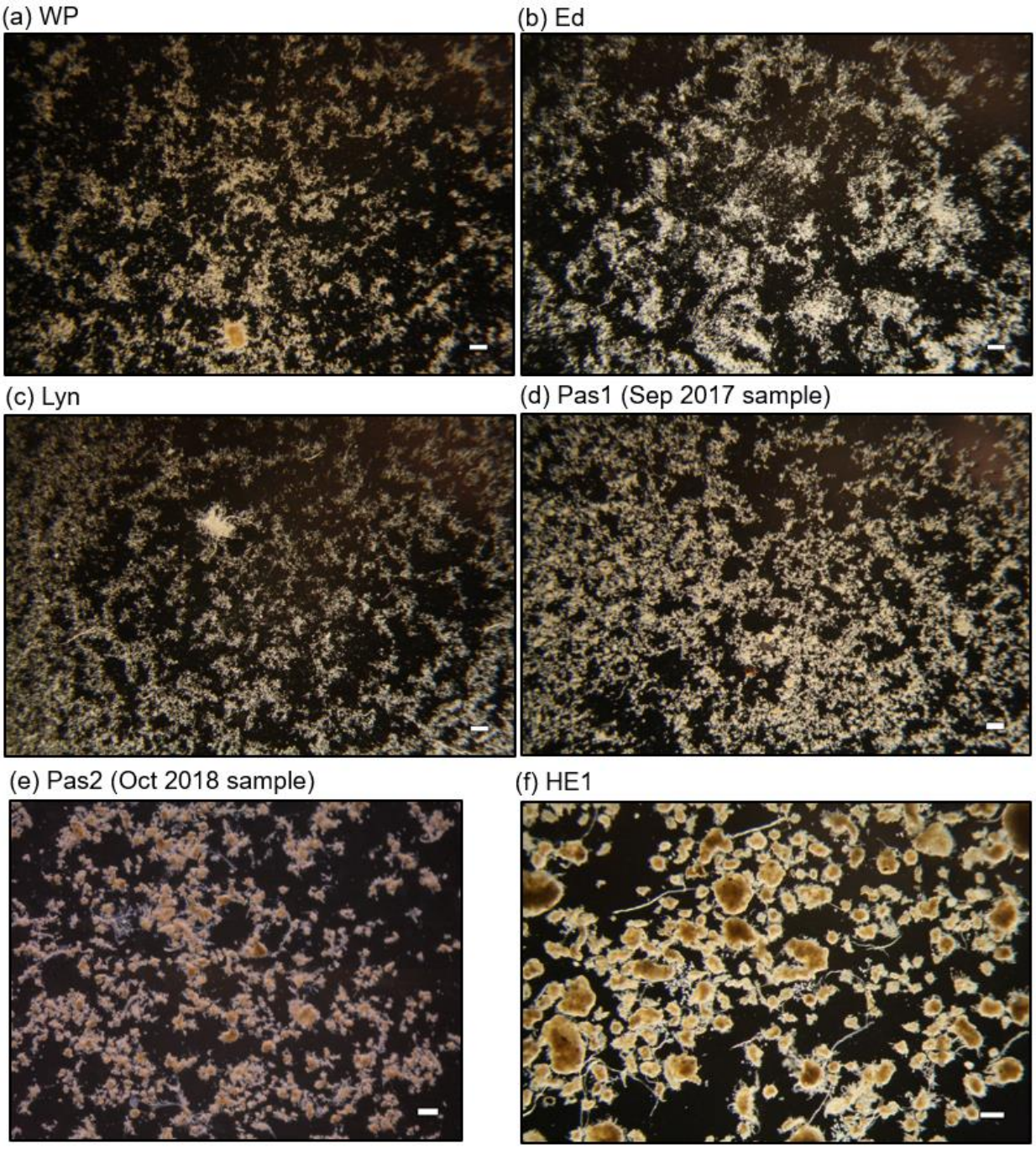

Figure S2. Micrographs of (a) - (e) non-EBPR plants and (f) one EBPR plant for comparison; scale bar = 0.5 mm.

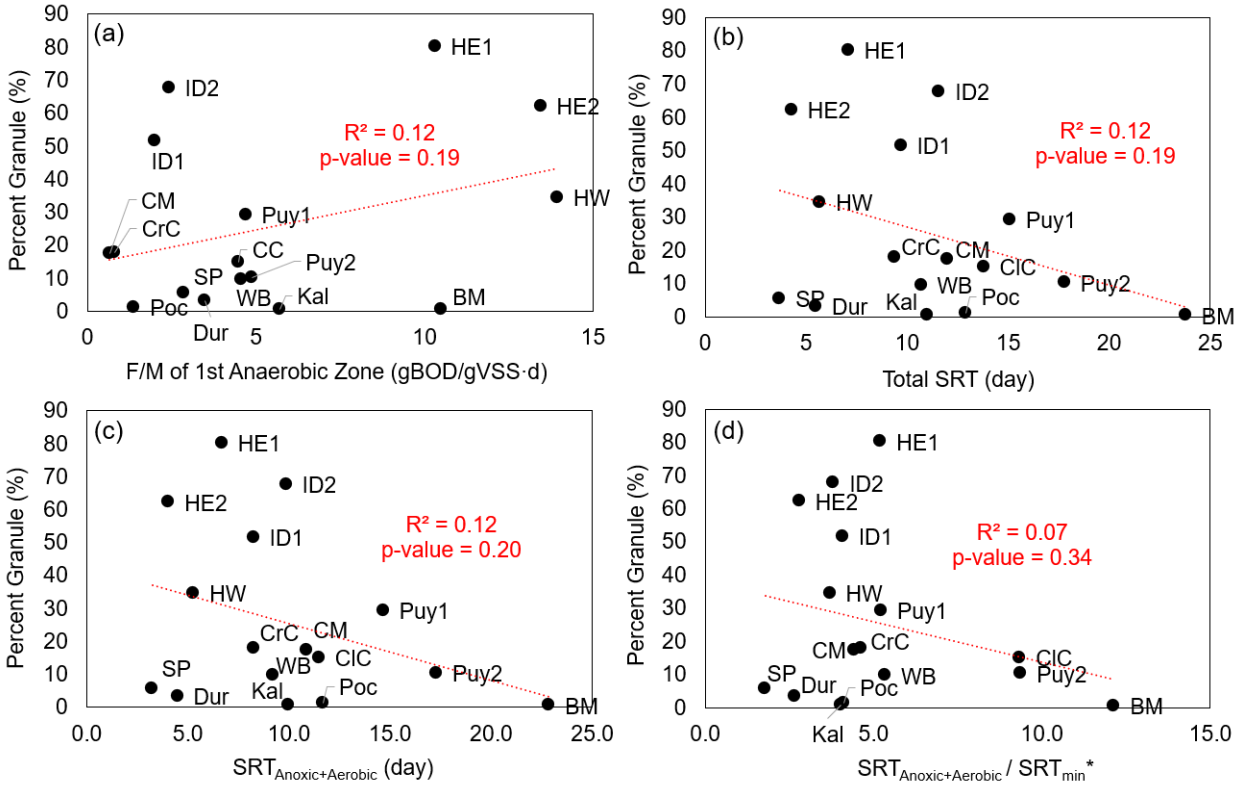

Figure S3. Correlation of percent granule versus (a) F/M ratio of 1st anaerobic zone, (b) total SRT, (c) anoxic and aerobic fraction of the SRT, and (d) ratio of anoxic and aerobic fraction of the SRT over minimum SRT for EBPR. *Minimum SRT for EBPR was determined based on Mamais and Jenkins (1992).

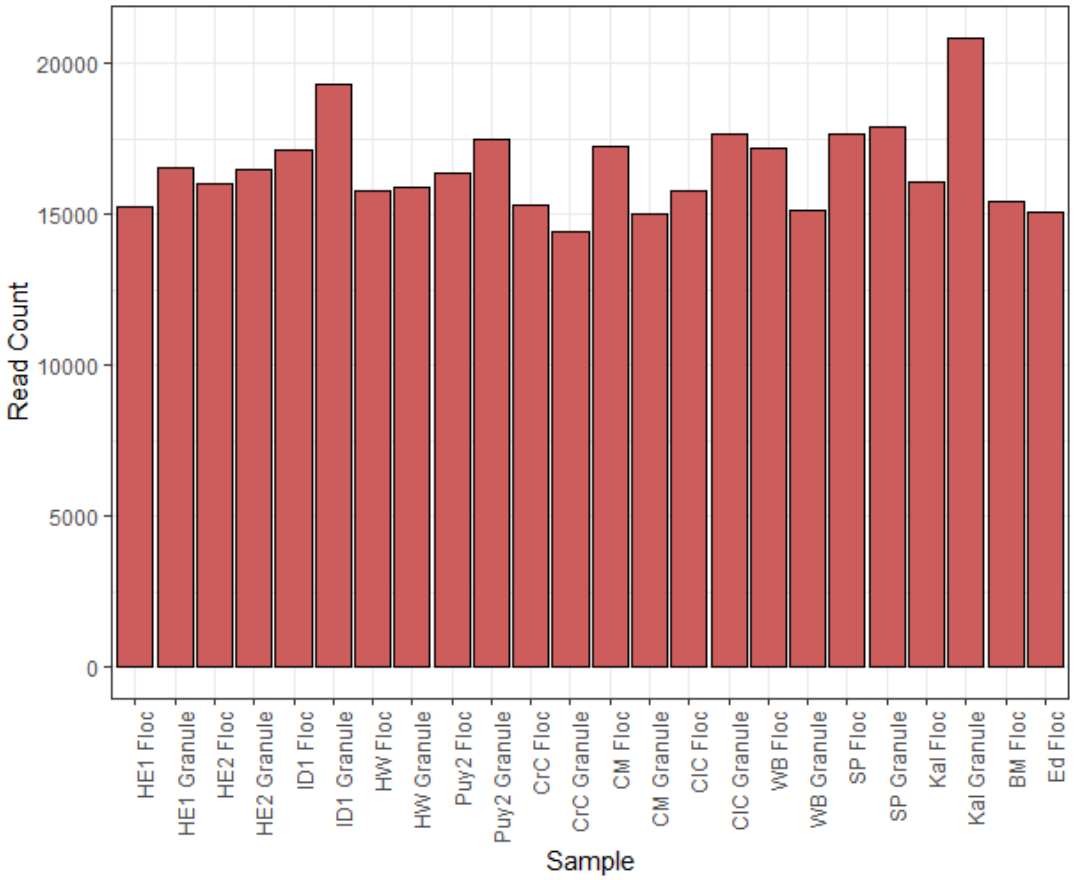

Figure S4. 16S rRNA gene sequencing depth of each sample. BM and Ed had minimal or no granule fraction.

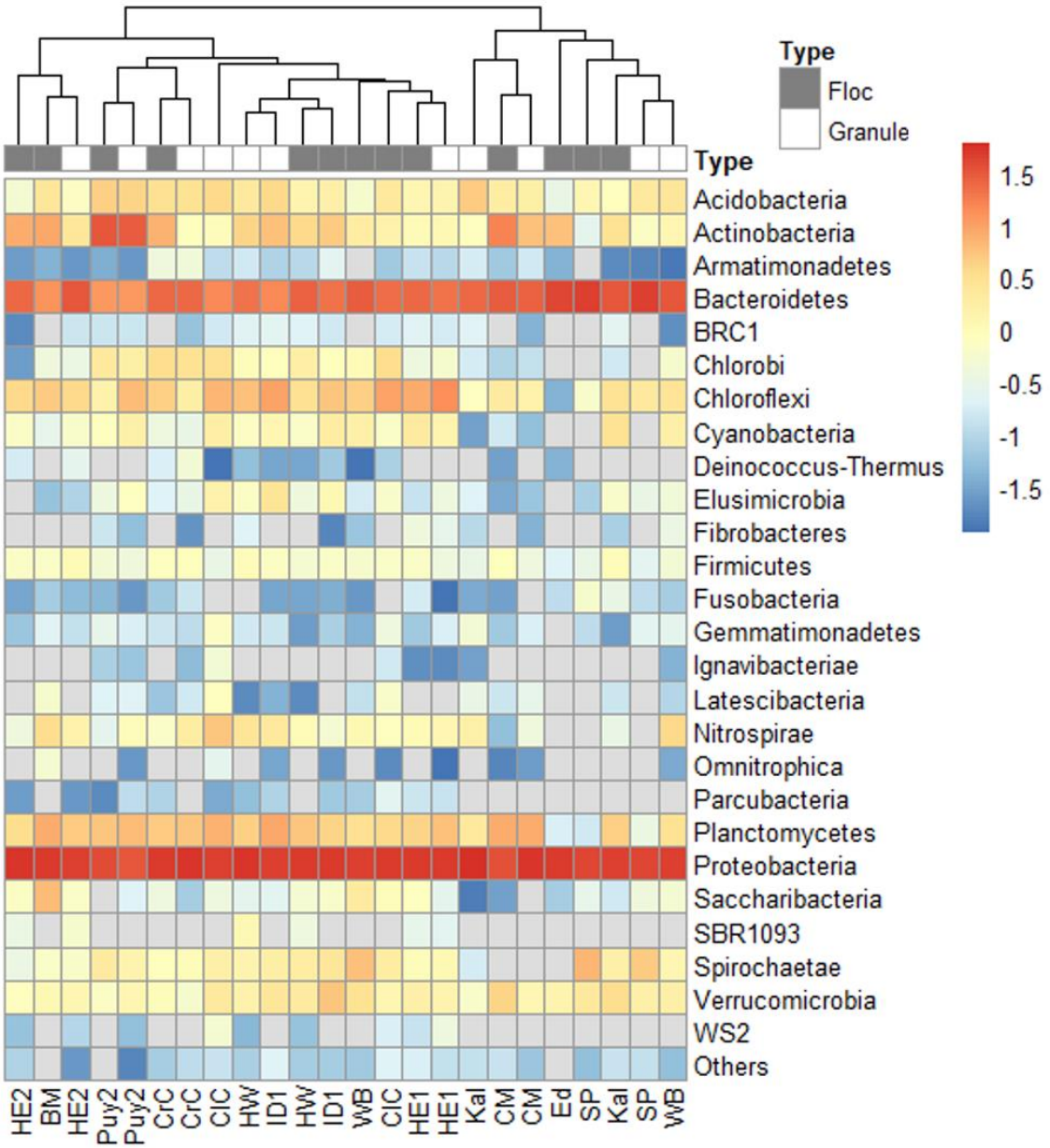

Figure S5. Relative gene abundance at the Phylum level on log 10 scale based on 16S rRNA gene sequencing. Phyla with less than 0.2% relative gene abundance are grouped into "Others." Clustering of the columns was based on Euclidean distances.

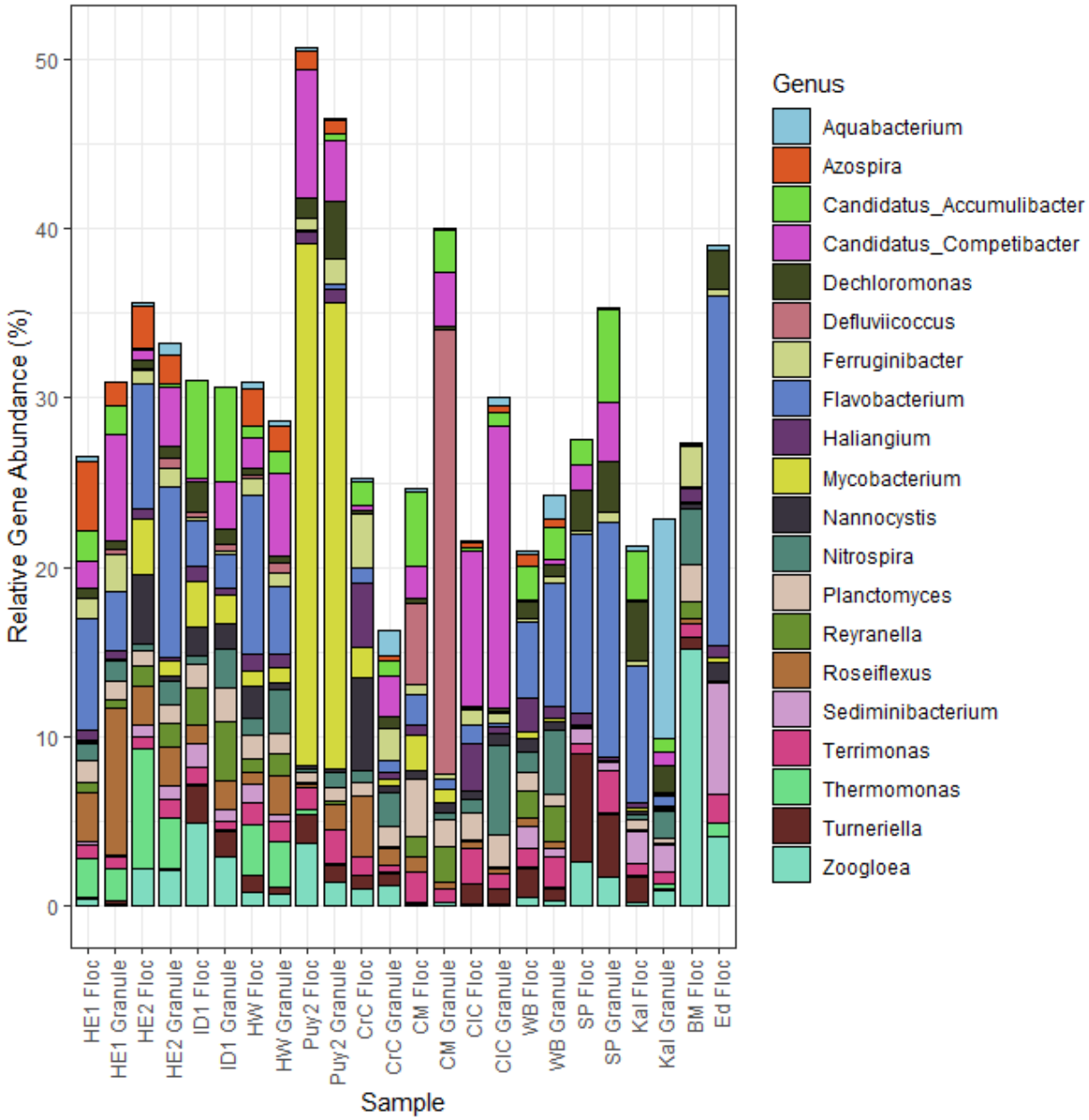

Figure S6. Top 20 most abundant genera based on 16S rRNA sequencing.

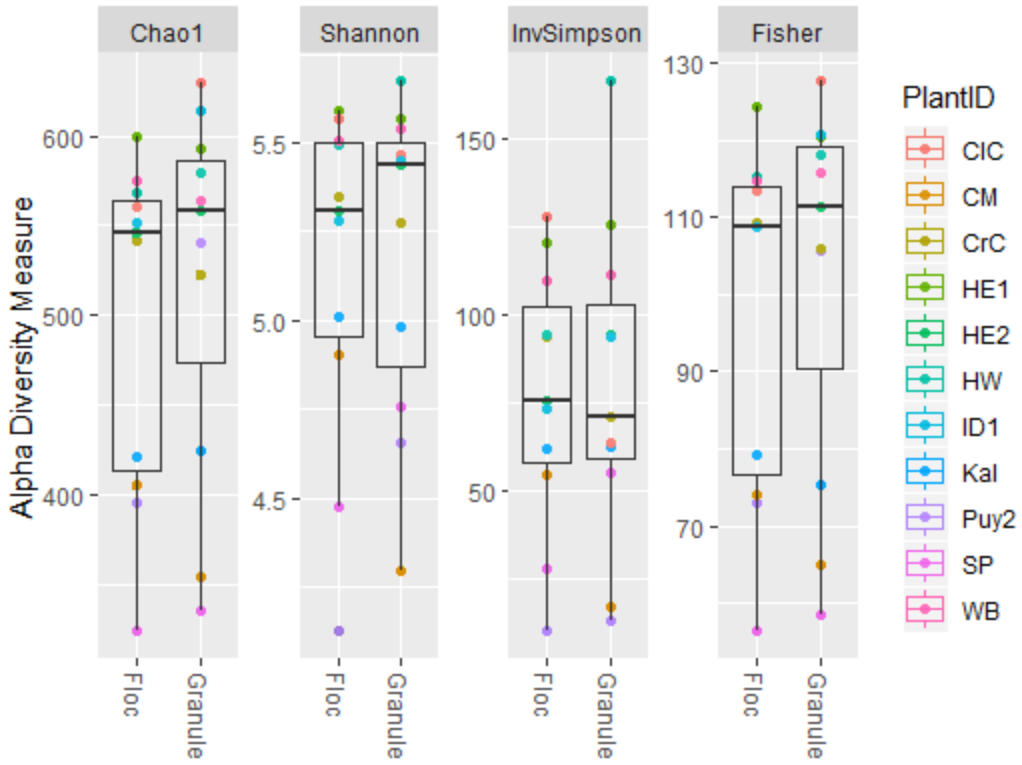

Figure S7. Boxplots comparing distributions of the four alpha diversity measures for the 16S rRNA amplicon sequences of granules versus flocs.

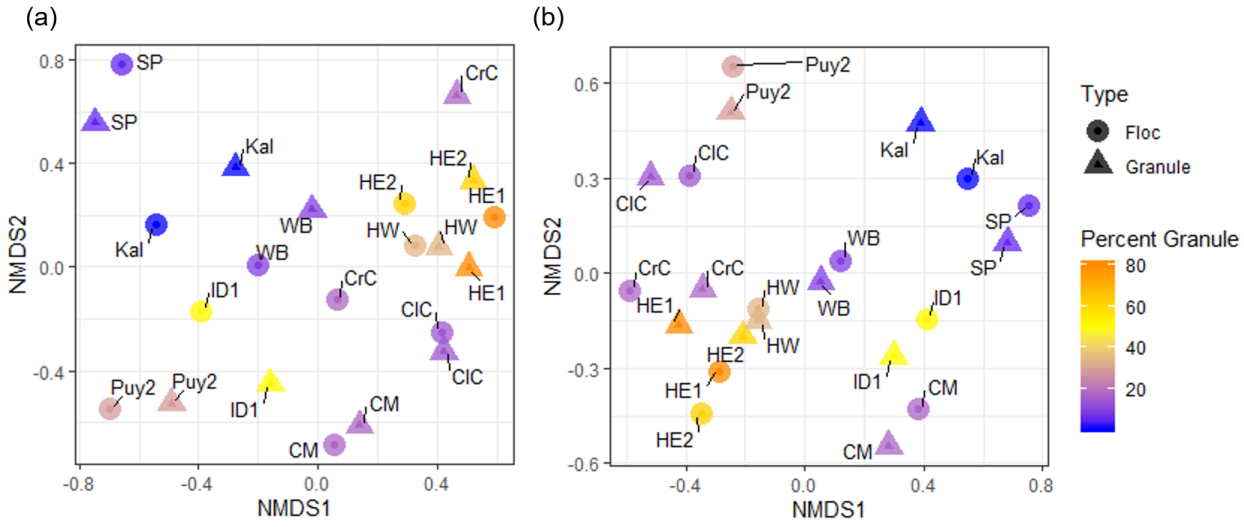

Figure S8. Ordinations of the 24 16S rRNA sequencing datasets based on non-metric multidimensional scaling of (a) all genera (stress = 0.207) and (b) top 30 most abundant genera (stress = 0.204).

Supplementary Note 1

From the qPCR analysis we obtained relative gene abundance of a taxon to total bacterial gene copies in granules and flocs separately. To estimate the absolute gene copies in the granules relative to flocs in the mixed liquor sample, the following approach was taken.

The number of gene copies for a taxon in the granule within a mixed liquor sample can be written as:

$$\frac{X_{c,g}}{mg\ MLVSS} = \left(\frac{X_{c,g}}{TB_{c,g}}\right)\left(\frac{TB_{c,g}}{mg\ VSS_g}\right)\left(\frac{mg\ VSS_g}{mg\ MLVSS}\right) \quad \text{Eq. S1}$$

Where:

$X_{c,g}$ = number of gene copies of a taxon X in granules
mg MLVSS = mg of VSS of the mixed liquor sample
$TB_{c,g}$ = number of gene copies of total bacteria in granules
mg VSS_g = mg of granule VSS

Eq. S1 can be rewritten as:

$$\frac{X_{c,g}}{mg\ MLVSS} = (\%X_g)\left(\frac{TB_{c,g}}{mg\ VSS_g}\right)(\%\ granule)$$

Where:

$\%X_g$ = relative gene abundance of a taxon X to total bacterial gene copies in granules (known from relative qPCR results).
% granule = % of total mg MLSS retained on 212-µm sieve (known from % granule analysis).

The same equation can be applied for flocs:

$$\frac{X_{c,f}}{mg\ MLVSS} = (\%X_f)\left(\frac{TB_{c,f}}{mg\ VSS_f}\right)(\%\ flocs) \quad \text{Eq. S2}$$

Where:

$\%X_f$ = relative gene abundance of a population X to total bacterial gene copies in flocs (known from relative qPCR results).
% flocs $= 100\% - \%$ granules (known)

Therefore, to know the gene abundance in the granules relative to flocs, we can apply $\frac{Eq.S1}{Eq.S2}$:

$$\frac{Eq.S1}{Eq.S2} = \frac{\left(\frac{X_{c,g}}{mg\ MLVSS}\right)}{\left(\frac{X_{c,f}}{mg\ MLVSS}\right)} = \frac{X_{c,g}}{X_{c,f}} = \frac{(\%X_g)\left(\frac{TB_{c,g}}{mg\ VSS_g}\right)(\%\ granule)}{(\%X_f)\left(\frac{TB_{c,f}}{mg\ VSS_f}\right)(\%\ Flocs)} \quad \text{Eq. S3}$$

We assume that the total bacterial gene copies per mg VSS is the same for granules and flocs, and thus:

$$\left(\frac{TB_{c,g}}{mg\ VSS_g}\right) = \left(\frac{TB_{c,f}}{mg\ VSS_f}\right) \quad \text{Eq. S4}$$

Then, Eq. S3 can be rewritten as:

$$\frac{X_{c,g}}{X_{c,f}} = \frac{(\%X_g)\left(\frac{TB_{c,g}}{mg\ VSS_g}\right)(\%\ granule)}{(\%X_f)\left(\frac{TB_{c,f}}{mg\ VSS_f}\right)(\%\ Flocs)} = \frac{(\%X_g)(\%\ granule)}{(\%X_f)(\%\ Flocs)} \quad \text{Eq. S5}$$

As an example, applying Eq. S5 to PAO will yield the following:

$$\frac{PAO_{c,g}}{PAO_{c,f}} = \frac{(\%PAO_g)(\%\ granule)}{(\%PAO_f)(\%\ Flocs)}$$

Eq. S5 was used to produce Figure 8 in the main manuscript.

Supplementary Note 2

The configuration of Pasco's aeration basin can be found in Table S4 and the plant's data summary can be found in Table S8. Because only 10% of the RAS flow is going to the aerobic selector, the MLVSS in the selector was very low. This low MLVSS was the reason for the high F/M ratio in the selector. The plant experienced very low SVIs (< 50 ml/g) after a month of receiving flows from an industrial food processor, which overlapped with the time of Pas2 (44% granules) sample collection (Figure S9). However, this same industrial load did not influence the plant's SVIs during which Pas1 (3.4% granules) was collected. The effect of industrial load on granule growth remains unclear.

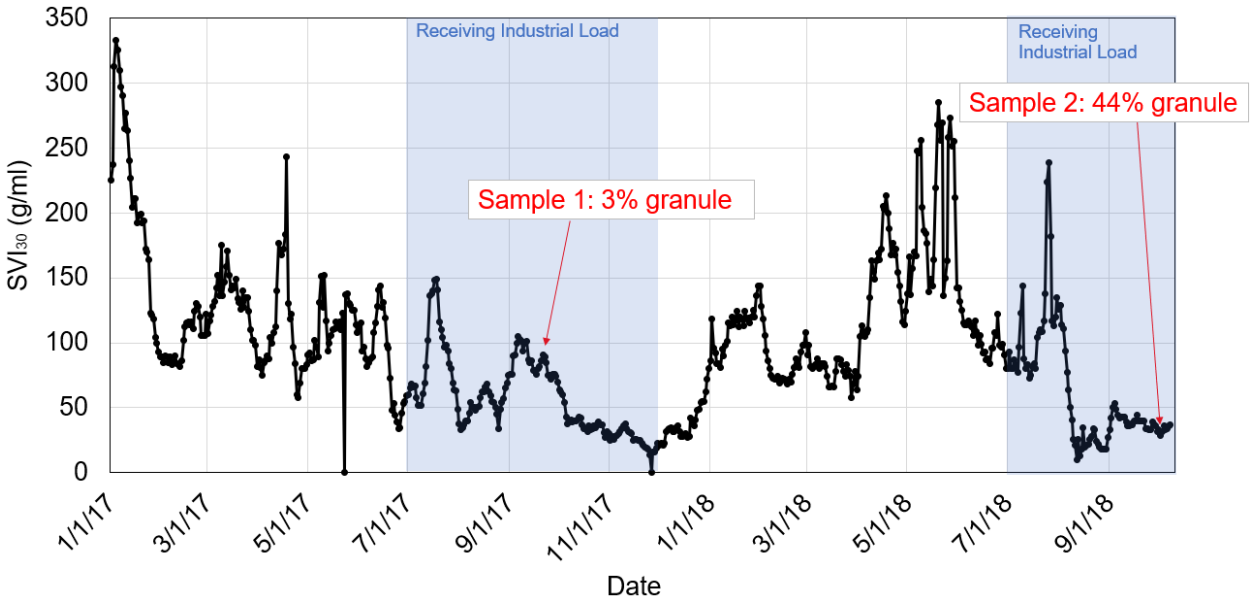

Figure S9. SVI_{30} of the Pasco plant.

Table S8. Summary of lab and operational data for samples collected from Pasco.

Parameter	Unit	Pas1	Pas2
UW Lab Measurements			
Sample Date	-	9/22/2017	10/4/2018
Percent Granule	%	3.4	44.1
SVI_{30}	ml/g	193	67
SVI_5	ml/g	358	96
Plant Operational Data			
Has Primary Treatment?	-	Yes	Yes
Has Fermenter?	-	No	No
Month of Average SRT[a]	-	Sep/2017	Sep/2018
Average SRT	day	6.8 ± 0.7	5.0 ± 1.0
Aeration Basin Stages			
# of Aerobic Selector Stages	-	1	1
HRT of Aerobic Selector	hr	0.50	0.40
Aerobic Selector F/M	gBOD/gVSS d	18.3	28.8
% of Aerobic Stages	-	3	3
HRT per Aerobic Stage	hr	1.68	1.36
Plant Performance Data			
Data Range for Averages[b]	-	20 days before 9/22/2017	15 days before 10/4/2018
Flow	MGD	5.2 ± 0.2	6.4 ± 0.1
Temperature	°C	24.6 ± 0.9	24.0 ± 0.6
Influent BOD	mg/L	253 ± 42	288 ± 21
Influent TP	mg/L	13.0 ± 0.5	9.0
Influent NH_4^+-N + NH_3	mg/L	31.8 ± 3.4	38.5 ± 7.2
AB Influent BOD	mg/L	97.9 ± 4.2	133.9 ± 4.3
AB Influent sBOD	mg/L	60.1 ± 5.4	69.2 ± 3.1
SVI_{30}	ml/g	103 ± 24	35.5 ± 3.7
MLSS	mg/L	2615 ± 115	2642 ± 121
MLVSS	mg/L	1585 ± 94	1772 ± 53
Effluent BOD	mg/L	3.5 ± 0.6	9.3 ± 1.9
Effluent TP	ml/g	6.1 ± 0.2	3.3
Effluent NH_4^+-N + NH_3	mg/L	0.75 ± 0.57	2.4 ± 1.3

[a] The month of data used for calculating the average SRT.

[b] The range of data (approximately 3 SRTs) used for calculating the averaged plant performance data.

Supplementary Note 3

The amplicon reads from 16S rRNA gene sequencing of 24 DNA extractions were analyzed. Pre-filtering at the Phylum level was conducted to make sure we eliminate phyla that were poorly represented and with low abundance. Before pre-filtering, a total of 4325 unique amplicon sequence variances (ASVs) and 46 unique phyla were identified. The prevalence of each phylum was determined and listed in Table S9. Definitions for the columns are as follows:

Column 1. Sum of the number of samples each ASV appeared at least once.
Column 2. The different ASVs a phylum has.
Column 3. Sum of the read counts of each ASV (sum of read counts for each phylum).
Column 4. Column 1 divided by Column 2.

The # of Samples / # of ASV ratio (Column 4) gives the averaged prevalence of each phyla while accounting for the number of different ASVs. Phyla with a ratio of 2.0 or less were omitted from the dataset. A poorly represented phyla can have a relatively high ratio if there are only a few ASVs that appeared in many samples. Therefore, we also filtered out phyla with read counts of 100 or less.

Table S9. Prevalence of each phylum based on 16S rRNA sequencing. Rows highlighted in red indicate poorly represented phyla that were omitted from dataset.

Phylum	# of Samples	# of ASV	Read Counts	# of Samples / # of ASV
Acidobacteria	331	112	8910	2.96
Actinobacteria	492	196	24513	2.51
Aminicenantes	5	2	20	2.50
Armatimonadetes	55	21	395	2.62
Ascomycota	1	1	4	1.00
Bacteroidetes	2488	811	107368	3.07
BRC1	40	11	433	3.64
Ca. Berkelbacteria	5	2	32	2.50
Chlamydiae	11	10	55	1.10
Chlorobi	112	32	4233	3.50
Chloroflexi	618	230	17778	2.69
Ciliophora	2	1	84	2.00
Cloacimonetes	2	1	8	2.00
Cyanobacteria	84	31	3938	2.71
Deinococcus-Thermus	23	15	224	1.53
Diapherotrites	1	1	4	1.00
Elusimicrobia	78	29	1938	2.69
Euryarchaeota	9	6	32	1.50
FBP	2	1	80	2.00

Fibrobacteres	20	13	277	1.54
Firmicutes	230	89	2373	2.58
Fusobacteria	23	4	348	5.75
Gemmatimonadetes	52	12	771	4.33
Gracilibacteria	13	10	70	1.30
Hydrogenedentes	37	9	260	4.11
Ignavibacteriae	15	7	157	2.14
Latescibacteria	30	11	655	2.73
Microgenomates	20	18	73	1.11
Miscellaneous Euryarchaeotic Group	2	1	12	2.00
Nitrospirae	60	9	5192	6.67
Omnitrophica	16	8	155	2.00
Parcubacteria	32	20	179	1.60
Peregrinibacteria	1	1	2	1.00
Planctomycetes	1110	427	18754	2.60
Proteobacteria	5642	1944	194428	2.90
RBG-1_(Zixibacteria)	1	1	4	1.00
Saccharibacteria	75	28	2679	2.68
SBR1093	6	1	459	6.00
Spirochaetae	153	37	6881	4.14
SR1_(Absconditabacteria)	1	1	5	1.00
Synergistetes	5	3	39	1.67
TM6_(Dependentiae)	17	12	101	1.42
Verrucomicrobia	420	155	7322	2.71
Woesearchaeota_(DHVEG-6)	1	1	9	1.00
WS2	9	2	252	4.50
WWE3	7	6	39	1.17

Supplementary Note 4

Quantitative PCR analyses were conducted to quantify the relative abundance of *Accumulibacter* and *Competibacter* in granules and flocs, and the results are shown in Figure S10. Out of the 12 plants, higher relative abundances of *Accumulibacter* and *Competibacter* were observed at 9 and 8 plants, respectively. The other plants (3 for *Accumulibacter* and 4 for *Competibacter*) showed no statistical difference between granules and flocs (based on two-tailed Z-test with 95% confidence interval). The higher abundance of *Competibacter* in the granules over flocs was a consistent observation based on both qPCR and 16S rRNA gene sequencing analyses. However, *Accumulibacter* did not have a positive correlation with the granule composition based on 16S rRNA gene analyses (Figure 6 and Figure 7 in the main paper) with the possible explanation that our 16S rRNA gene sequencing results were less quantitative for their abundances or that some PAO organisms were targeted by the PCR primers but not the primers used for sequencing.

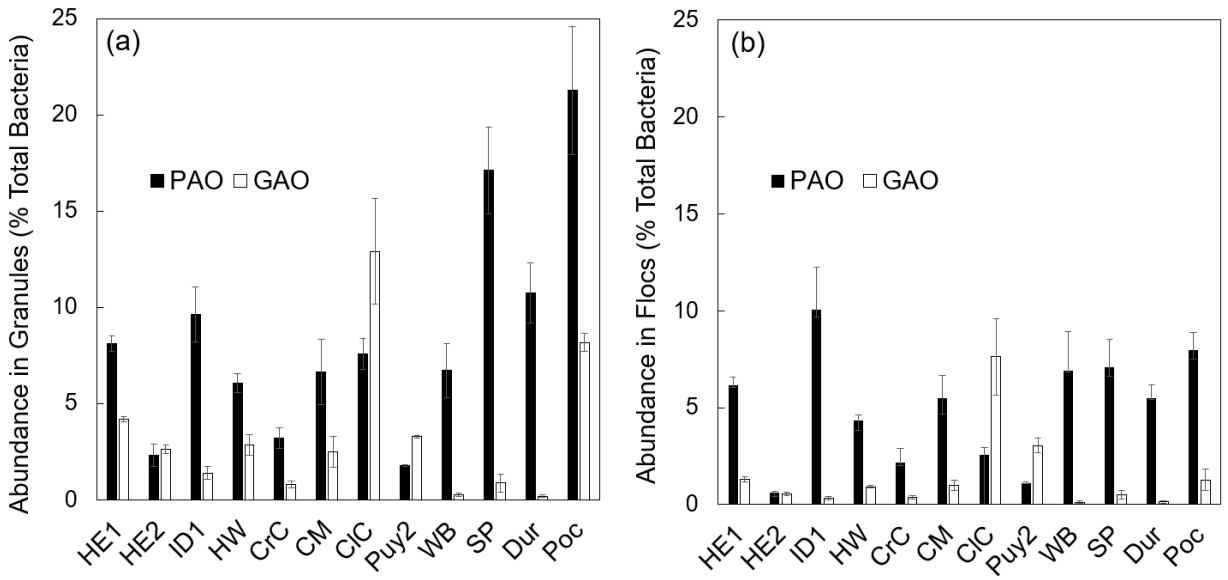

Figure S10. Relative 16S rRNA gene copies of *Accumulibacter* PAO and *Competibacter* GAO to total bacteria in (a) granules and (b) flocs based on qPCR.

References

Crocetti, G.R., Hugenholtz, P., Bond, P.L., Schuler, A., Keller, J., Jenkins, D., Blackall, L.L. 2000. Identification of polyphosphate-accumulating organisms and design of 16S rRNA-directed probes for their detection and quantitation. *Applied and Environmental Microbiology*, **66**(3), 1175-1182.

Fukushima, T., Onuki, M., Satoh, H., Mino, T. 2010. Effect of pH reduction on polyphosphate- and glycogen-accumulating organisms in enhanced biological phosphorus removal processes. *Water Science and Technology*, **62**(6), 1432-1439.

He, S., Gall, D.L., McMahon, K.D. 2007. "Candidatus Accumulibacter" population structure in enhanced biological phosphorus removal sludges as revealed by polyphosphate kinase genes. *Applied and environmental microbiology*, **73**(18), 5865-5874.

Kong, Y.H., Ong, S.L., Ng, W.J., Liu, W.T. 2002. Diversity and distribution of a deeply branched novel proteobacterial group found in anaerobic-aerobic activated sludge processes. *Environmental Microbiology*, **4**(11), 753-757.

Mamais, D. and Jenkins, D. 1992. The Effects of MCRT and Temperature on Enhanced Biological Phosphorus Removal. *Water Science and Technology*, **26**(5-6), 955-

Chapter 3.

Partitioning of Nutrient Removal Contribution Between Granules and Flocs in a Hybrid Granular Activated Sludge System

Abstract

Sludge granulation in continuous-flow systems is an emerging technology to intensify existing activated sludge infrastructure for nutrient removal. In these systems, the nutrient removal contributions and partitioning of microbial functions between granules and flocs can offer insights into process implementations. To this end, a reactor system that simulates the continuous-flow environment using an equal amount of initial granule and floc biomass was investigated. The two operational strategies for maintaining granule growth in the continuous-flow system were (a) the higher solids retention time (SRT) for the granules versus flocs, as well as (b) selective feeding of carbon to the granules. The SRT of the large granule fractions (>425 μm, LG) and floc/small granule fractions (<425 μm, FSG) were controlled at 20 and 2.7–6.0 days, respectively. Long term operation of the hybrid granule/floc system achieved high PO_4^{3-} and NH_4^+ removal efficiencies. Higher polyphosphate-accumulating organisms (PAO) activity was observed in the FSG than LG, while ammonia-oxidizing bacteria (AOB) activities were similar in the two biomass fractions. Nitrite shunt was observed in the FSG, possibly due to out-competition by the high NOB activity in LG. More importantly, washing out the FSG caused a reduction in LG's AOB and PAO activity, indicating a possible dependency of LG on FSG for maintaining its nutrient removal capacity. Our findings highlighted the partitioning and potential competition/cooperation of key microbial functional groups between LG and FSG, facilitating

nutrient removal in a hybrid granular activated sludge system, as well as implications for practical application of the treatment platform.

Published as:

Wei, S. P., H. D. Stensel, R. M. Ziels, S. Herrera, P. H. Lee and M. K. H. Winkler (2021). "Partitioning of nutrient removal contribution between granules and flocs in a hybrid granular activated sludge system." Water Research **203**.

3.1 Introduction

Aerobic granular sludge (AGS) is one of the major latest innovations in wastewater treatment for enhanced nutrient removal. The fast-settling and high-thickening properties of AGS allow for the increase in solids inventory without additional secondary clarifiers (Pronk et al., 2015). AGS technology is therefore an attractive alternative for future expansions at any wastewater facilities that must meet increased capacity with population growth but are limited by space. The current AGS technology is based on sequencing batch reactors (SBRs), where plug-flow feeding and washout of slow-settling particles (i.e., tall reactors with short settling time) can be conveniently applied. These selection stresses are needed for sludge granulation but cannot be easily adapted in continuous-flow systems (CFS) where reactors are shallow and completely-mixed, making the integration of AGS technology into existing wastewater infrastructure an ongoing challenge. Research efforts are therefore underway to develop alternative processes that enable granule growth in CFS. The main strategy utilized thus far has been based on settling velocity, where fast-settling particles are continuously separated from the slow-settling particles and retained in the system. This washout of slow-settling particles is accomplished with equipment such as solids/liquid separator, external settler, or other designs of similar concept, which are reviewed in detail by Kent et al. (2018). More recently, Sun et al. (2019) demonstrated granulation in a pilot-scale CFS with ten completely stirred tank reactors in series (to mimic plug-flow condition) and two external settlers to wash out the slow-settling particles.

The inclusion of the enhanced biological phosphorus removal (EBPR) process may further improve the feasibility of achieving granulation in CFS. EBPR-based systems select for slow-growing microorganisms such as polyphosphate- and glycogen-accumulating organisms (PAO

and GAO, respectively) that form denser and stronger granules than ordinary heterotrophs (de Kreuk & van Loosdrecht, 2004; Figdore et al., 2018). These benefits of PAO/GAO granules are well-established in AGS SBRs and have also been utilized for granule selection in some continuous-flow studies (Devlin & Oleszkiewicz, 2018; Li et al., 2016; Liu et al., 2014). Moreover, high abundance of PAO/GAO-based granules was unexpectedly observed at existing full-scale continuous-flow EBPR plants, suggesting the feasibility of widespread adaptation of AGS at CFS where EBPR capacity is already present (Wei et al., 2020). Leveraging the growth of PAOs in granules may be a simple way to integrate AGS technology in CFS. Various studies had demonstrated this concept in continuous-flow EBPR systems by adding a granule/floc separator that receives a portion of the mixed liquor flow, from which lighter particles are selectively wasted whereas larger particles are retained and recycled to the anaerobic zone (Carter, 2020; Stinson et al., 2019; Sturm et al., 2017). These continuous-flow configurations can have varying floc/granule separation methods but share the common strategy of favoring growth of PAOs within the granules.

The principle of AGS revolves around granulation, but flocs still constitute a major portion (20–40%) of the biomass in AGS systems and is important for treating non-diffusible substrates and removing colloids to achieve low effluent TSS concentrations (Layer et al., 2019). It is therefore expected that regardless of the various CFS configurations with integrated AGS, it will be a hybrid system consisting of both granules and flocs, and their respective roles in system performance must be better understood. In AGS SBR systems, flocs and granules have different solids retention time (SRTs) due to the selective retainment of larger particles (Ali et al., 2019). A similar selection pressure is imposed when CFS are modified with a granule/floc separator,

where flocculent/granular SRTs can be decoupled to enable selective wasting of small particles. Various process schemes and methods for granule/floc separations have been proposed and are being tested in large-scale (Carter, 2020; Stinson et al., 2019; Sturm et al., 2017), but there is a lack of fundamental knowledge in the role of flocs or the microbial segregation/dependencies between flocs and granules in these systems.

In this study, a reactor system simulating a continuous-flow environment was inoculated with a combined granule/floc biomass and operated for 157 days. Selective feeding of carbon to the granules was adopted and SRTs of the large/small particles were differentially controlled. The primary goal of this study was to understand differences in nutrient removal performance, partitioning of functional groups, and microbial community structure between small/large particle fractions in continuous-flow systems integrated with granular sludge. Based on the results, a secondary goal was to hypothesize potential competitions and dependencies between flocs/granules and to inform implementation of granular sludge in CFS.

3.2 Materials and Methods

3.2.1 Experimental phases

The study included five experimental phases with two operational modes as listed in **Table 3-1**. The two operational modes (AGS SBR and continuous-flow simulation) are described in Sections 3.2.2 and 3.2.3. Initially, the reactor was operated in AGS SBR mode with granular sludge only (pre-experiment phase). Then, Phase I started by switching to the continuous-flow simulation mode in which we continued the operation of the granular sludge column but added a second reactor for floc recycling purposes. During the switch to continuous-flow operation, 2000

mg/L of flocculent MLSS were added to the original 2000 mg/L of granular MLSS. The flocculent sludge was collected from the City of Puyallup Water Pollution Control Plant (WA, USA), an anoxic/aerobic nitrogen removal facility. A 425-µm sieve was used to separate large/small particles to decouple the SRT of granules/flocs. This slightly larger cutoff size than the original definition of 0.2 mm for aerobic granules (de Kreuk et al., 2007) was chosen initially to ensure that no large flocs were included in the 'granular' category. SRT of the >425-µm size fraction was controlled at 20 days for the entire study while SRT of the <425-µm size fraction were varied for Phase I–III (**Table 3-1**). Methodology for SRT control is detailed in SI 1.2. After Phase III, the reactor was returned to AGS SBR mode ("floc removed" phase). The same synthetic wastewater feed with acetate/propionate as sole carbon source was used for all phases. The feed concentrations were 433 mg/L COD, 42 mg/L NH_4^+-N and 21 mg/L PO_4^3-P (detailed composition listed in SI 1.3). For all phases, the DO and pH during the aerobic phase were controlled at 2.0 mg/L and 7.5, respectively, and temperature was controlled at 16°C.

Table 3-1. Operational phases of this study.

Phase	Operation mode	SRT of >425 µm fraction (days)	SRT of <425 µm fraction (days)	Duration (days)
Pre-experiment	AGS SBR	20	-	39
I	Continuous-flow	20	6.0	50
II	Continuous-flow	20	4.0	64
III	Continuous-flow	20	2.7	43
Flocs removed	AGS SBR	20	-	17

3.2.2 AGS SBR mode

A 3-L reactor column (column reactor) was operated in SBR cycles consisting of 60-min anaerobic feeding (900 ml), 13-min idle, 4-min dilution water fill (750 ml with deionized water),

242-min aeration, 3-min settling, 5-min decant (55% volume exchange ratio), and 3-min idle. Instead of plug-flow feeding through the sludge bed, as is typical in AGS SBRs, the reactor was mixed continuously with N_2 gas during anaerobic feeding. Anaerobic mixing was done to better simulate a continuous-flow feeding condition similar to previous research (Nguyen Quoc et al., 2021) and to avoid a substrate gradient where larger particles are exposed to higher carbon concentrations.

3.2.3 Continuous-flow simulation mode

The continuous flow operation was set up to simulate conditions in a conceptual hybrid granule/floc process scheme (Figure S1a), which is a conventional anaerobic/aerobic process except 55% of the mixed liquor flow is routed to a granule separator where particles of different sizes are partitioned. From the granule separator, larger particles are recycled to the anaerobic zone whereas lighter fraction are recycled to the aerobic zone. This operation allows for (1) bypassing 55% of the flocs away from the anaerobic zone to achieve selective feeding of carbon to the granules and (2) decoupling controls of flocculent/granular SRTs. To simulate this conceptual scheme in the lab, the same column reactor and cycles as the AGS SBR mode were used, but with the following modifications: (1) decant from the column reactor (top 55% of volume) was pumped to a side reactor (floc reactor) to settle for 60 mins, while sludge remained in the column reactor was fed anaerobically; and (2) after the anaerobic feeding/idle period, effluent was withdrawn from the top of floc reactor, and the remaining sludge was pumped back to the column reactor. Figure S1b deciphers a detailed schematic of reactor operations.

3.2.4 Biomass-specific activity tests

Batch tests were conducted for <425 µm and >425 µm size fraction separately to determine the maximum specific ammonia and nitrite oxidation rates (SAR and SNR, respectively) and the specific phosphorus release rate (SPR). SAR and SNR tests were done at air saturation and SPR test was done anaerobically. Briefly, a 150-ml biomass sample was spiked with 20 mg NH_4^+-N/L ammonia, 10 mg NO_2^--N/L, or 90 mg COD/L acetate then monitored for changes in ammonia, nitrite, or phosphate concentrations over time for the SAR, SNR, and SPR test, respectively. The specific activities were determined from the slope of concentrations versus time and normalized to g volatile solids. See SI 1.4 for detailed methods.

3.2.5 Analytical methods

Suspended and volatile solids (TSS and VSS) were analyzed according to Standard Methods 2540D and 2540E (APHA, 2005), respectively. The sludge volume index was determined from the settled volume (ml) of a mixed liquor sample, after 5 and 30 min settling in a graduated cylinder, divided by g TSS (SVI_5 and SVI_{30}, respectively). Ammonia (ISO 15923-1), nitrite (EPA Method 354.1), and phosphate (EPA Method 365.1) concentrations were measured using the Gallery™ Automated Photometric Analyzer (Thermo Fisher Scientific). Acetate and propionate concentrations were analyzed with an ion-chromatography Dionex ICS-5000 system with the IonPac® ICE-AS6 column (Thermo Scientific). Granule and floc morphologies were observed at 6X-10X magnification under a Zeiss Stemi 508 stereomicroscope in darkfield mode. Particle size distribution of >425 µm fraction was obtained by sieving analysis (SI 1.5).

3.2.6 16S rRNA gene amplicon sequencing and bioinformatics

Samples were collected at the end of each experimental phase, and DNA was extracted using the Qiagen DNeasy PowerBiofilm Kit following the manufacturer's procedure except that homogenization was performed using a FastPrep®-24 (MP Biomedicals, USA) at 4 m/s for 30 s. The V4-V5 region of the 16S rRNA gene was amplified by polymerase chain reaction (PCR) using primers 515F-Y/926R (Parada et al., 2016). The PCR products were sequenced on an Illumina MiSeq in 2×300bp mode by BGI Genomics (Hong Kong) and the Molecular Research Lab (Texas, USA). Amplicon reads were processed following the Divisive Amplicon Denoising Algorithm 2 (DADA2) pipeline (Callahan et al., 2016) (v. 1.16) implemented in R v. 4.0.2. Parameters used for data trimming and filtering are detailed in SI 1.6. Taxonomy of the sequence variants were assigned against the Silva Project's v.132 database using the Ribosomal Database Project Classifier (Wang et al., 2007). All amplicon sequence variants (ASV) of a phyla with less than 50 reads were omitted from the analysis. The relative abundance of each ASV was calculated by the read counts of each ASV (×100%) divided by the total read counts in a sample. The R packages phyloseq v. 1.32.0 (McMurdie & Holmes, 2013) and pheatmap v. 1.0.12 were used for further data analysis and visualization. STAMP v. 2.1.3 (Parks et al., 2014) was used for statistical analysis.

3.2.7 PCR amplification for detection of comammox

To detect the presence of complete ammonia oxidizing bacteria (comammox) within the *Nitrospira* species, PCR was performed using primer sets cmx_amoB 148F/485R (Cotto et al., 2019) and NTS 232F/1200R (Lim et al., 2008). DNA extraction from a pure *Nitrospira inopinata* culture was used as positive control. Detailed information on PCR reaction setup and thermal profiles can be found in SI 1.7.

3.2.8 Fluorescence in-situ hybridization

Fluorescence in-situ hybridization (FISH) was conducted on granule slices to observe the distribution of ammonia-oxidizing and nitrite-oxidizing bacteria (AOB and NOB, respectively). Detailed methods and the FISH probes used can be found in SI 1.8.

3.3 Results

3.3.1 System Performance

The overall performance data are plotted in **Figure 3-1** and the typical cycle profiles of nutrient concentrations are shown in **Figure 3-2**. In the pre-experimental phase, the average effluent ammonia concentration of the AGS reactor was 3.7 ± 1.0 mg N/L with 91% NH_4^+ removal efficiency. As soon as the continuous-flow simulation started (Phase I), the effluent ammonia dropped below 0.05 mg N/L, while the effluent nitrate increased to around 10 mg N/L (**Figure 3-1b**). Complete nitrification was sustained for the rest of the study based on the low effluent ammonia/nitrite concentrations (except a brief increase at the end of Phase II). The reactor did not have an anoxic phase, and thus denitrification took place within the anoxic layer of the granules during the aerobic phase via simultaneous nitrification/denitrification (SND). It was estimated that roughly 11 ± 5% of the nitrogen was removed via SND (see S2.1 for calculations). Denitrification also occurred during the anaerobic phase of a reactor cycle where any remaining nitrate was removed with the influent carbon as electron donor (**Figure 3-2d**). P removal performance was stable, except for a period of perturbation between Phase II and III (grey highlighted area in **Figure 3-1a**) caused by an error during carbon media preparation. Stable reactor performance was attained again before Phase III began. Excluding the period of

operational issues, the system achieved removal efficiencies of 96.2–98.9% for PO_4^{3-} and 99.1–99.9% for NH_4^+ (Table S5).

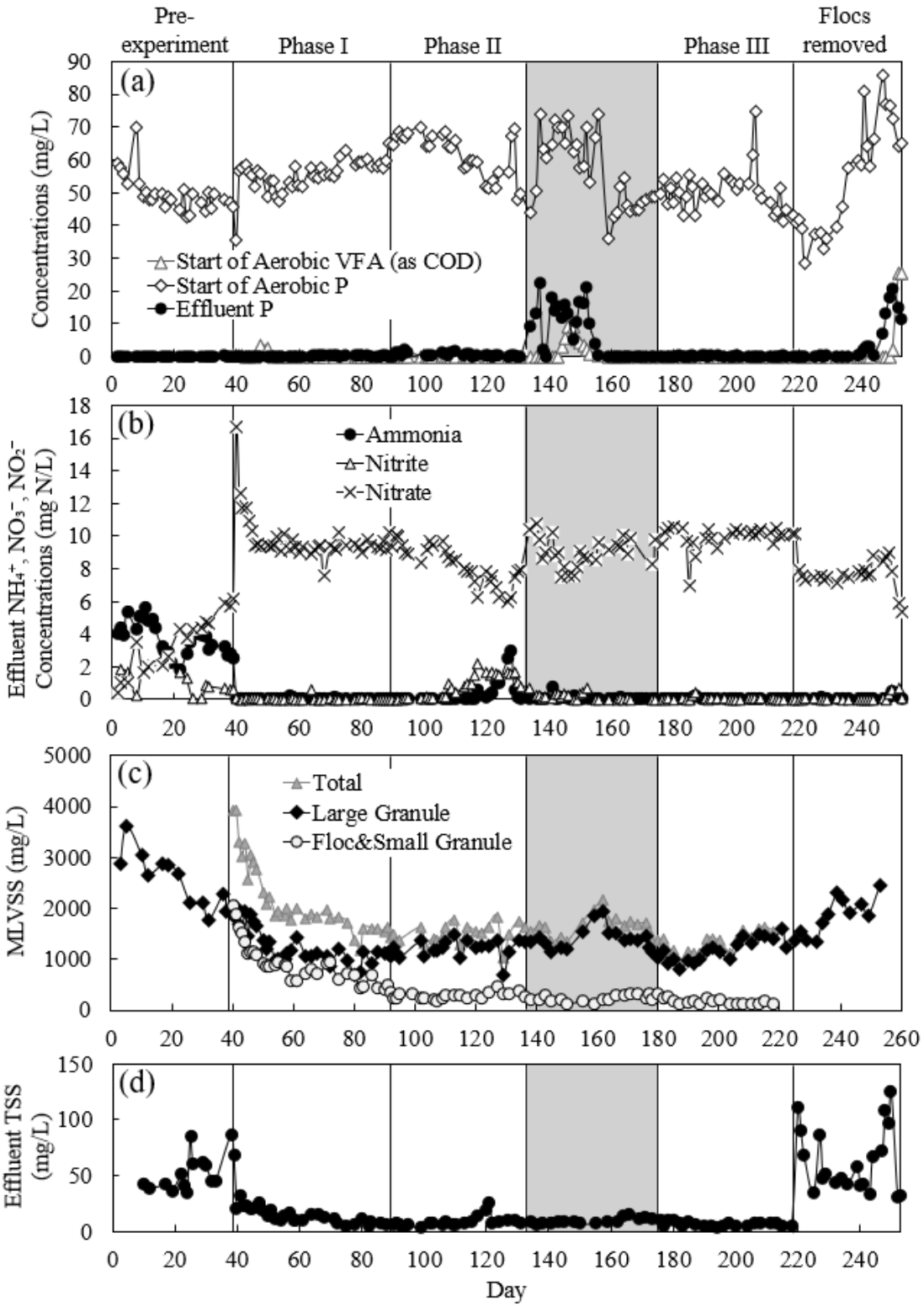

Figure 3-1. System performance data showing (a) PO_4^{3-}-P removal, (b) effluent NH_4^+, NO_3^- and NO_2^- concentrations, (c) MLVSS concentrations in the column reactor, and (d) effluent TSS.

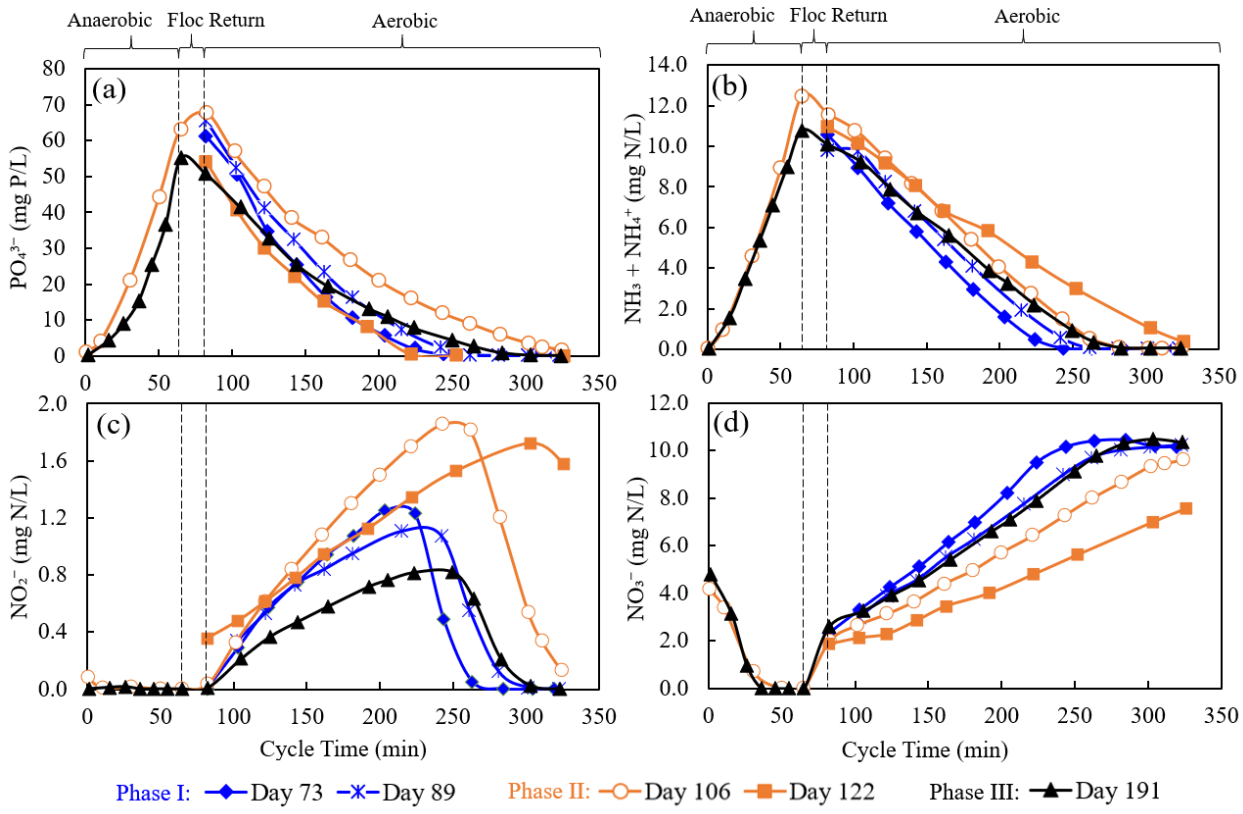

Figure 3-2. Cycle concentration profiles of (a) phosphate, (b) ammonia, (c) nitrite, and (d) nitrate in the column reactor. During the period of 65–82 minutes, the immediate change in concentrations was due to the dilution effect from the floc return flow.

Due to the higher granular SRT (20 days) than flocculent SRT (6, 4, and 2.7 days), the MLVSS of the <425 µm fraction were always significantly lower than the granule MLVSS (**Figure 3-1c**). After Phase III, the solids withdrawn from the column reactor were wasted instead of recycled back into the column, hence increasing the effluent TSS (**Figure 3-1d**). Exactly one SRT after this operational change, elevated concentrations of PO_4^{3-} started occurring in the effluent. The EBPR performance continued to deteriorate for 7 more days and reactor operation was terminated.

3.3.2 Rapid granulation of flocs

The amount of small particles decanted to the floc reactor sharply decreased from 50% at the start of Phase I to 13% in just 10 days (Fig. S3) while the SVI_5/SVI_{30} ratio dropped from 1.9 to 1.3 (Fig. S4), indicating rapid densification of the flocs. This observation was supported by microscopic images showing that flocs became small granules, exhibiting a dense core with semi-spherical morphologies (Fig. S5a). Due to the observation that the <425 μm fraction consisted of both flocs and small granules, any solids <425 μm are termed flocs and small granules (FSG) and solids >425 μm are termed large granules (LG). LG and FSG had similar ash content, which averaged 35 ± 2.6% and 36 ± 4.7%, respectively. The short granulation time for the flocs was likely enabled by the added nucleation sites from breakage of LG and PAO enrichment in the FSG (discussed in SI 2.2). As the flocs granulated, the amount of biomass bypassing the anaerobic phase became minimal, which created a condition where FSG and LG directly competed for carbon in the anaerobic phase.

3.3.3 Physical characteristics of granules

The high settleability of LG was maintained throughout the experimental period, as indicated with an SVI_5 of 66 ml/g at the end of Phase III. A reduction in granule size was indicated by the disappearance of the >2 mm size fraction since Phase II (Fig. S6), which was also apparent from the micrographs (Fig. S5b). The density of LG reduced from 1016 kg/m^3 in the pre-experimental phase down to 1008 kg/m^3 by end of Phase III, which was still within the range of typical density observed for granular sludge (Bassin et al., 2012).

3.3.4 Microbial community

The relative 16S rRNA gene abundance of the top abundant genera is shown in **Figure 3-3**. The microbial community between LG and FSG appeared to be similar (Fig. S7), showing significant differences for merely 3 out of the 362 genera ($p < 0.03$, STAMP), and the magnitude of differences were low (<0.15%) (Fig. S8). Relative abundances of the key microbial functional groups (Fig. S9) showed that the putative PAOs during Phase I-III included *Candidatus* Accumulibacter (*Accumulibacter)* (18.0–37.1%%) and *Dechloromonas* (9.3–25.5%). The PAO phenotype of *Dechloromonas* has been confirmed by many studies (Petriglieri et al., 2021; Terashima et al., 2016) but some members can behave according to the GAO phenotype (Ahn et al., 2007; McIlroy et al., 2016). It should be noted that the relative abundance of *Dechloromonas* is known to be overestimated with 16S rRNA gene amplicon sequencing, which can yield 10-folds more abundance than quantification with FISH (Stokholm-Bjerregaard et al., 2017). The only ammonia-oxidizing bacteria (AOB) genus detected in Phase I-III was *Nitrosomonas* (0.04–0.79%) while *Nitrospira* (0.0–1.9%) and *Candidatus* Nitrotoga (*Nitrotoga*) (0.06–0.33%) were the two nitrite-oxidizing bacteria (NOB) present. Analysis using comammox-specific primers indicated that the *Nitrospira* genus consisted of canonical NOB species and not comammox (Fig. S10).

To investigate the deterioration of EBPR performance after termination of floc recycling, the microbial community of Phases I–III and the "flocs removed" phase were compared. The comparison showed a decrease in *Accumulibacter* abundance ($p = 0.043$) (Fig. S11), while the relative abundances of *Leptospira* ($p = 0.00001$), *Defluviimonas* ($p = 0.00002$), and an unclassified genus under the *Sphingobacteriales* order ($p = 0.0009$) increased.

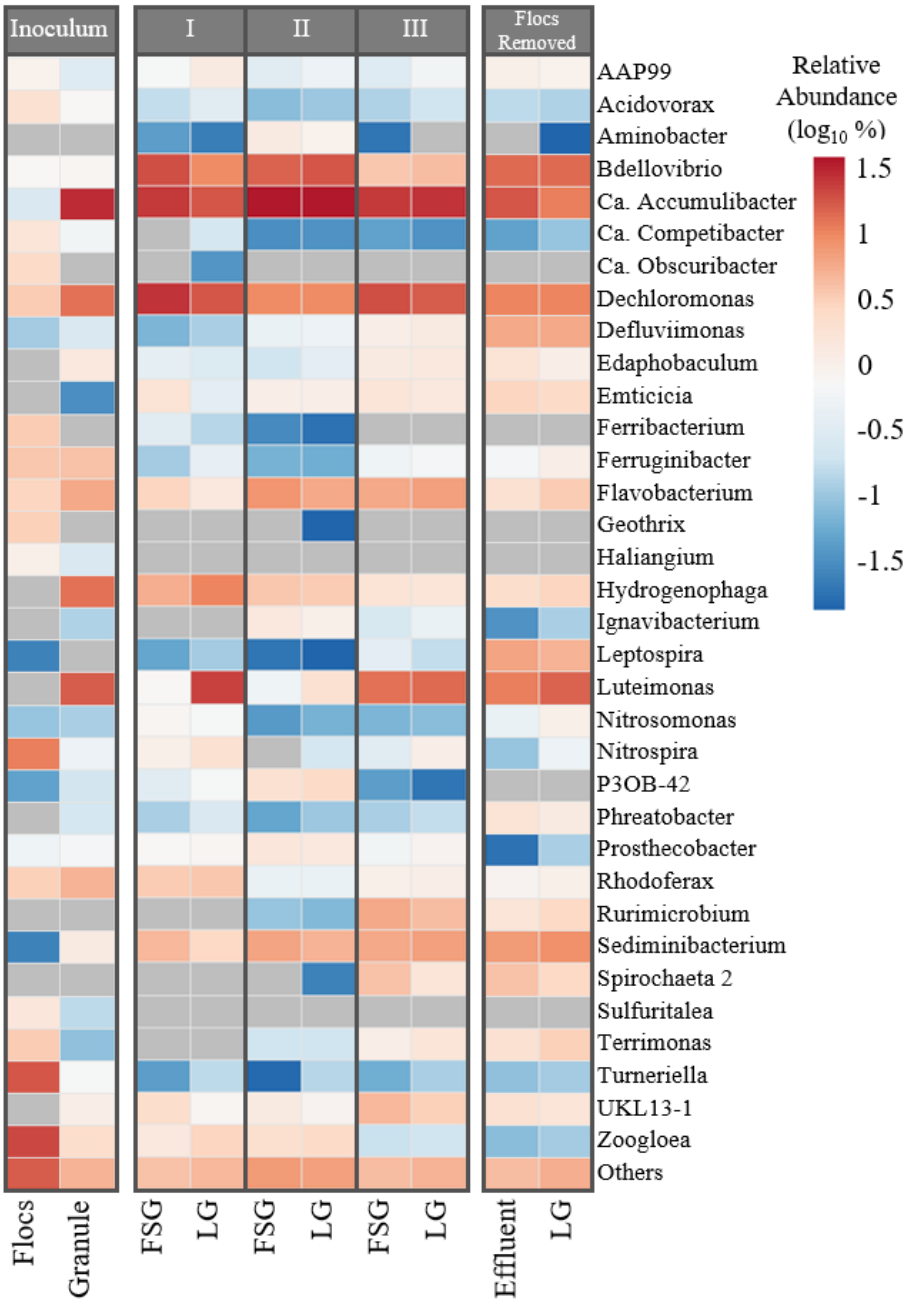

Figure 3-3. Relative 16S rRNA gene abundance at the genus level on log_{10} scale for samples taken at end of each operational phase. Genera with less than 1% relative gene abundance are grouped into "Others." Gray cells = not detected.

3.3.5 Specific PO_4-P release rates

The SPR remained constant for LG, as expected with a constant SRT at 20 days. The SPR of FSG was higher than the LG for Phases I and II by 47% and 57%, respectively (**Figure 3-4**). In Phase III, the FSG SRT was reduced to 2.7 days, which may explain the 38% reduction in FSG's SPR as the operating SRT approached the minimum SRT for EBPR of around 1.5–2.5 days at 16 °C (Brdjanovic et al., 1998; Mamais & Jenkins, 1992). As mentioned in Section 3.1, the EBPR performance failed one SRT after termination of floc recycling. A P release activity test done on the reactor biomass right before ending reactor operations showed an SPR of 27.8 mgP/gVSS·hr, which was a 52% reduction compared to Phase III.

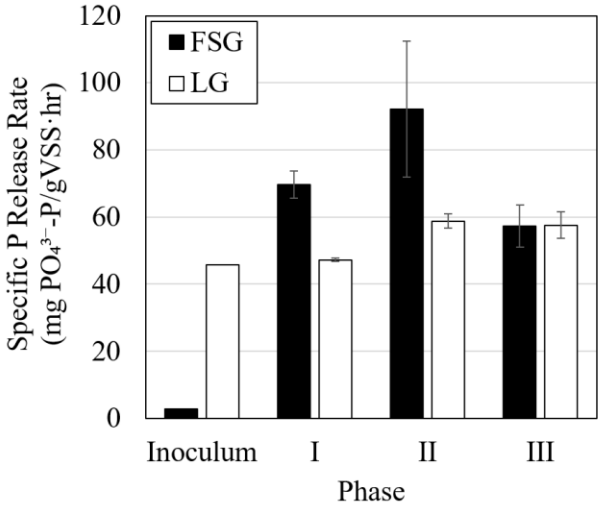

Figure 3-4. Specific PO_4^{3-} release rate of FSG and LG measured at the end of each operational phase.

3.3.6 Maximum Specific NH_4^+ and NO_2^- oxidation rates

The SARs of LG and FSG were similar in Phases I and II. The changes in SNR did not follow a clear trend (**Figure 3-5b**), but it was obvious that the SNR was higher for LG than FSG for all phases by a factor of 2–3. *Nitrospira* was the dominant NOB, except in Phase II where *Nitrotoga*

became dominant in the FSG and was as abundant as *Nitrospira* in LG (**Figure 3-5b**). The dominance of *Nitrotoga* overlapped with the highest bulk nitrite concentrations during Phase II (**Figure 3-2c**), which corroborates with other studies showing dominance of *Nitrotoga* over *Nitrospira* at higher nitrite availability (Kinnunen et al., 2017; Zheng et al., 2020). Although having the same range of maximum specific activities, *Nitrotoga* have a lower affinity for nitrite and higher tolerance for free nitrous acid than *Nitrospira* (Kitzinger et al., 2018; Wegen et al., 2019; Zheng et al., 2020), which may explain the higher *Nitrotoga* abundance at higher nitrite concentrations. In Phase III, the SAR decreased substantially for FSG due to the SRT drop to 2.7 days, which was also accompanied by a 27% SAR reduction in the LG. Based on the respective MLVSS and specific activities, the contributions of FSG and LG to the total ammonia oxidation capacity were determined (Fig. S12), which shows that FSG contributed only 3–5% of the capacity in Phase III.

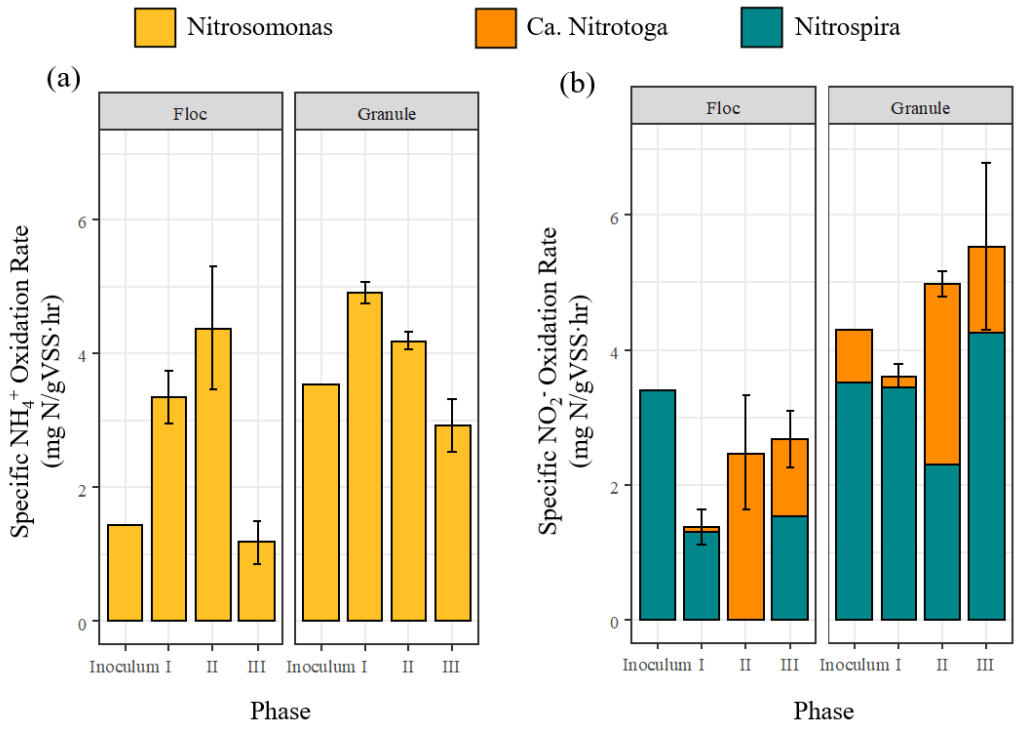

Figure 3-5. Specific rate of (a) ammonia oxidation and (b) nitrite oxidation colored by the relative gene abundance within the (a) putative AOB and (b) putative NOB groups. The height of the bars corresponds to the rate of ammonia or nitrite oxidation, while the relative heights of the colors within the bars correspond to the relative fraction of nitrifier populations.

3.3.7 Specific NOB/AOB activity ratios

To investigate the reasons behind the higher SNR rate in LG versus FSG, the ratios of maximum specific nitrite to ammonia oxidation rates (or NOB/AOB activity ratios) are plotted in **Figure 3-6** along with theoretical ratios estimated for the fully nitrifying condition. The theoretical ratios were calculated from $\mu_{max,NOB}/\mu_{max,AOB}$ using literature values while assuming the same endogenous decay for AOB/NOB and that nitrite produced by AOB was the only nitrogen source for NOB (SI 2.3). For FSG, the experimental NOB/AOB activity ratios were 14-56% lower than the theoretical values for the fully nitrifying condition; whereas for LG, the observed ratios were

within 6% for Phase I and 65-67% higher for Phase II if compared to the fully nitrifying condition.

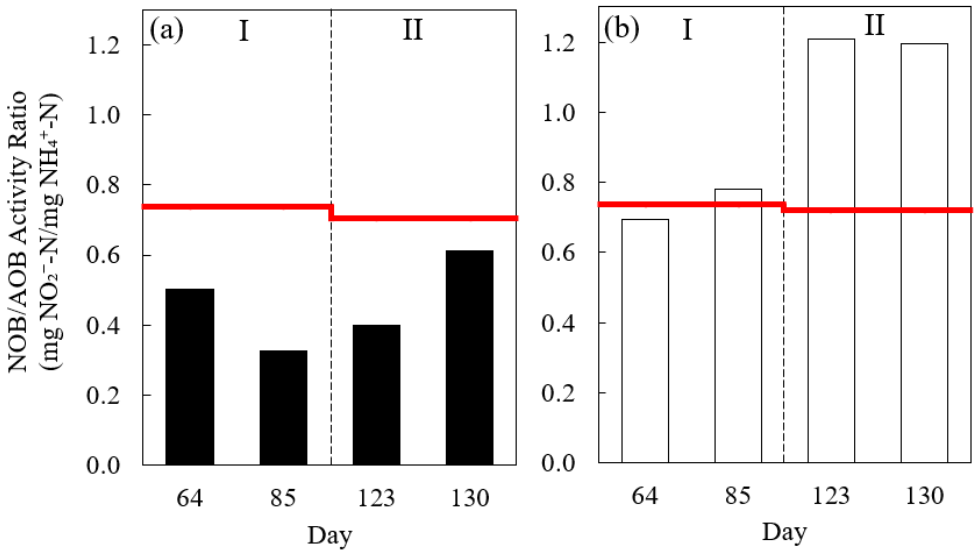

Figure 3-6. Ratios of specific nitrite-oxidizing rate (mg NO_2^--N /gVSS·hr) over ammonia-oxidizing rate (mg NH_4^+-N /gVSS·hr) in (a) FSG and (b) LG. Red line is the theoretical ratios calculated for the fully nitrifying condition using literature $\mu_{max,NOB}/\mu_{max,AOB}$ values, adjusted based on relative abundance of different NOB genera of each phase (see Table S3 and S4 for detailed calculations). Phase III was excluded due to intentional washout of AOBs in the FSG at low SRT.

3.4 Discussion

3.4.1 Carbon competition between granules and flocs

Here, we evaluated the contributions of granules and flocs to the nutrient removal performance of a CFS where the growth of granules was favored by maintaining a low floc SRT and separating a portion of the flocs from the anaerobic feed phase. In full scale, this concept could

be implemented by sending the granule fraction from a granule/floc separator to the anaerobic zone and the lighter fraction from the clarifier underflow to the aerobic phase (Fig. S1a). The fraction of biomass that bypassed the anaerobic phase via density separation was eventually low due to the rapid granulation of flocs, thus creating a condition where PAOs in LG and FSG directly competed for carbon in the anaerobic phase. This situation would be representative of a full-scale system where granule and floc separation can be achieved only partially, hence exposing flocs occasionally to anaerobic carbon addition. The consumption of carbon by PAOs in the FSG reduced the bulk liquid substrate concentration and diffusion gradient into the granule core, leading to disintegration of LG and a gradual decrease in average granule size.

The reduction in granule size led to a higher aerobic zone volume fraction at a set bulk DO level (Nguyen Quoc et al., 2021), which increased the SAR and thus also the nitrate concentration in the reactor (**Figure 3-1b**). It should be noted that the initial increase in ammonia oxidation efficiency at the beginning of Phase I was due to the higher total MLVSS after the addition of flocs into the reactor (**Figure 3-1c**), which resulted in immediate increase of effluent nitrate concentration. After the total MLVSS reduced and stabilized around 1500 mg/L by mid-Phase I, the ammonia oxidation capacity of the system was maintained due to the increase of SAR in both FSG and LG (**Figure 3-5a**). In Nereda® type SBR systems, the remaining nitrate at the end of the aeration phase is not mixed with the influent carbon due to plug flow feeding, hence allowing for anaerobic conditions even if SND is incomplete (Weissbrodt et al., 2017). To simulate continuous-flow conditions, the anaerobic phase of our system was mixed. The simultaneous presence of nitrate and carbon allowed for anoxic condition that favored the growth of heterotrophic denitrifiers, as confirmed with 0 mg/L NO_3-N measured at the end of anaerobic

phase (**Figure 3-2**d). Some strains of the *Defluviimonas* and *Emticicia* genera can perform denitrification (Foesel et al., 2011; Saha & Chakrabarti, 2006) and their gradual increase in relative abundance from Phase I to Phase III (**Figure 3-3**) corresponds to the observed increase in heterotrophic denitrification activities. On the contrary, the relative abundance of *Zoogloea*, a putative denitrifier and PHA-accumulating organism (Nierychlo et al., 2020), gradually reduced. *Zoogloea* has been suggested as an important player in granule formation by producing specific EPS (Larsen et al., 2008; Seviour et al., 2012). The reason for their gradual disappearance in our system remains unclear, but may correspond to a change in EPS composition and/or their ecological niche as large granules disintegrated.

In addition to competing with PAOs present in the flocs, PAOs in LG also had to compete with heterotrophic denitrifiers for carbon during the anaerobic phase due to the presence of nitrate. This carbon consumption by the denitrifiers caused a lower substrate diffusion gradient into the core of granules, resulting in a weakened granule structure and further contributing to their size reduction. However, the settling characteristics of the LG were maintained despite their reduction in size and density. We propose that this was likely due to the high EBPR performance and high PAO enrichment within the granules. PAO-based granules have higher settling characteristics than ordinary heterotrophic granules due to the higher density of polyphosphate, and the slow-growing metabolism of PAO leads to smooth granular morphology that further contributes to a fast-settling rate (Figdore et al., 2018; Winkler et al., 2013b).

Our results indicate that due to the diluted substrate concentrations, competition by flocs, and direct contact of nitrate with carbon, granulation in CFS can be somewhat challenging but still

achievable. Strategies such as using PAO-enriched granules as the initial seed and bypassing flocs from the anaerobic zone can be applied to maintain granule stability. Nitrate recycled to the anaerobic zone should be minimized, as in the case for all EBPR activated sludge processes. In full-scale applications, the low diffusible carbon fraction of real wastewater would make granulation even more challenging (Layer et al., 2019). The recommendation is therefore to implement process schemes that increase the substrate concentrations (e.g., mixed liquor fermentation) to support granulation in full-scale CFS.

3.4.2 Partitioning of microbial activity between FSG and LG despite similar microbial composition

The microbial community between FSG and LG were similar based on 16S rRNA gene sequencing (Fig. S7 and S8), which algins with other studies (Layer et al., 2019; Liu & Tay, 2012; Winkler et al., 2013a). Our system was unique such that the granular SRT (20 days) and flocculent SRT (6, 4, and 2.7 days) were manually decoupled and carefully controlled, and thus a similar microbial composition between granules and flocs was not expected. In a full-scale AGS SBR, Ali et al. (2019) found a lack of species-sorting between flocs (<0.2 mm) and small granules (0.2–1 mm) due to their similar SRTs (6–7 days), whereas large granules (>1 mm) had a significantly different microbial composition but at much higher SRT of 142 days. Therefore, it is possible that the difference in SRTs for FSG and LG in this study was too small to allow for a strong partitioning of core microbial communities between different-sized aggregates. In addition, previous research has shown that in a continuous-flow reactor, there can be dynamic and random processes of attachment, detachment, aggregation, and breakage between flocs and granules (Zhou et al., 2014). This constant exchange of biomass between flocs and granules could also explain their similar microbial composition, despite the difference in their SRTs.

Although the 16S rRNA gene sequencing results indicated a similar overall microbial community between the FSG and LG, partitioning of nutrient removal activities was revealed by activity batch tests (i.e., FSG had lower NOB activities and higher PAO activities than LG). These observations of microbial activity segregations led to insights for implementations of granular sludge technology in continuous flow systems (discussed in Sections 3.4.1, 3.4.3, and 3.4.4), which would have been overlooked if molecular sequencing was the only tool utilized. Indeed, 16S rRNA gene sequencing is a useful method for obtaining high-level microbial community compositions, but the compositional nature of the data cannot fully determine how the absolute abundance of individual taxa varies among samples (Barlow et al., 2020). Our results highlighted the importance of conducting physiological activity tests in addition to molecular sequencing to elucidate nutrient removal partitioning in heterogenous microenvironments (e.g., granules versus flocs) within a mixed culture.

3.4.3 Nitrite shunt in smaller particles

The lower NOB/AOB activity ratios in the FSG versus LG was an interesting observation as NOB suppression in WWTPs can lead to significant savings in aeration and carbon costs. For LG, the observed NOB/AOB ratios were either similar to (Phase I) or higher than (Phase II) values calculated for a fully nitrifying condition (**Figure 3-6b**). The higher observed NOB/AOB ratios versus the fully nitrifying values in Phase II suggested that the growth of NOB was uncoupled from the nitrite supply of AOB, which can be enabled by nitrite produced via partial denitrification (by other bacteria) or the decay products in the anoxic layer of LG (Winkler et al., 2015). The reasoning for why this uncoupled NOB growth from AOB was only observed in Phase II requires further research. For FSG on the other hand, the NOB/AOB activity ratios were

lower than the fully nitrifying condition, indicating suppression of NOB. The inhibition effect of free ammonia (FA) could be a contributing factor as NOB in the FSG were more exposed to bulk liquid ammonia concentrations whereas mass diffusion limitation would provide a more protected environment for the NOB in LG. Kent et al. (2019) observed a similar trend of decreasing NOB/AOB activity ratios with decreasing granule size in a continuous flow AGS reactor and showed that smaller granules were more sensitive to FA inhibition. Based on the ammonia concentration profile (**Figure 3-2b**) and the operational temperature/pH, the FA concentrations in our system were in the 0.05–0.1 mg NH_3-N/L range for half of the aerobic phase. However, the inhibition effect of FA on *Nitrospira* can vary widely, ranging from an inhibition threshold of 0.04–0.08 mg NH_3-N/L up to no inhibition at 10 mg NH_3-N/L, possibly due to genus-level ecophysiological diversity and other variations such as short-term effect, biomass acclimation, and competition with other microbial groups (Blackburne et al., 2007; Simm et al., 2006; Ushiki et al., 2017). In addition, *Nitrotoga* may tolerate high FA concentrations (>200 mg NH_3-N/L) (Li et al., 2020), indicating that FA inhibition may not be the reason for NOB suppression in the FSG for Phase II, during which *Nitrotoga* was the only NOB genus detected.

Previous research on aerobic granules (both PAO and nitritation/anammox types) demonstrated stratification of nitrifier guilds, such that AOBs occupy the outer granule shell while NOB are directly underneath to benefit from the localized high NO_2^- availability and protection from washout (Matsumoto et al., 2010; Poot et al., 2016; Winkler et al., 2011; Winkler et al., 2015). Such heterogeneous distribution of AOB/NOB was largely observed with FISH conducted on LG slices collected at the end of Phase II (Fig. S14). The protection from washout and access to

higher nitrite concentrations would contribute to a high NOB activity in the LG and create a nitrite sink for NOB in the FSG, as supported by the 2–3 times lower NOB activity in the FSG than LG. The reasoning behind NOB suppression in FSG requires further research, but our results indicate a potential opportunity for achieving nitritation by selecting for smaller granule sizes, as previously suggested by Kent et al. (2019). This strategy would be easier to implement in SBR-type AGS reactors than CFS as a wider particle size distribution can be expected in SBRs due to the plug-flow feeding regime.

3.4.4 Possible importance of FSG for growth of key functional groups

There were several indications that a loss of microbial activity in FSG affected the LG. In Phase III, the SAR in the FSG reduced by 69% (relative to Phase II), as expected at a 2.7-day SRT and 16 °C. The SAR of LG was also lowered by 27% even though the SRT of LG remained constant. In addition, the EBPR performance struggled after the recycling of FSG was terminated (after Phase III), and the SPR in LG reduced by 52% along with a significant reduction of *Accumulibacter* abundance (**Figure 3-3** and S11). After terminating FSG recycling, genera *Leptospira* and *Defluviimonas* showed obvious increase in their relative abundance (Fig. S11). One of the 16S rRNA gene amplicon sequences shared 100% nucleotide identity to the saprophytic *Leptospira idonii* (Numberger et al., 2019). Members of the *Defluviimonas* genus can be strict or facultative aerobes that utilize volatile fatty acids (VFA) (Foesel et al., 2011; Math et al., 2013). The role of these microbial groups during the deterioration of EBPR performance remains unknown, but it can be suspected that they competed for carbon within the community.

Even with similar microbial community between granules and flocs, flocs can exhibit higher

specific growth rates in comparison to granules due to lower substrate diffusion limitation (Liu & Tay, 2012). This phenomenon was supported by a higher SPR in the FSG than LG in Phase I and II (**Figure 3-4**), where FSG contributed to 25–57% of the reactor's P removal capacity (Fig. S13). Even in Phase III, when the FSG SRT approached the minimum value to sustain EBPR, FSG still contributed to 8% of the P removal capacity. It should be noted a higher AOB activity was not observed in the FSG as for the PAO activity. This discrepancy was likely due to the faster growth rate of PAOs than AOBs, who would benefit more from the 20-day SRT in the LG (versus the 4–6 day SRT in FSG) at 16 °C despite the lower oxygen diffusion. It is hypothesized that due to the kinetic advantages, PAO growth predominantly occurred in the FSG. Then, the recycling of FSG back into the column reactor may have enabled additional residence time for larger particles formation and attachment, thereby contributing to maintaining the PAO community in the LG biomass. By washing out the FSG, this dynamic segregation and interaction for PAO growth was disturbed, thus explaining the failed EBPR performance. The same explanation can be applied to the reduction of LG's AOB activity after AOB in the FSG was washed out (Phase III) (**Figure 3-5a**).

Although this hypothesis requires further confirmation, our observations indicated the important role of flocs and small particles in a continuous-flow system with integrated AGS technology. Due to the limited diffusible carbon penetration into the granule core, growth of PAOs may rely on flocs and smaller granules in continuous flow systems. This understanding indicated that even with a high granule abundance, recycling of flocs (and the need for clarifiers) cannot be completely eliminated in CFS as in the case for SBRs unless substrate diffusion limitations can be mitigated. In that sense, process configurations that mimic a more plug-flow feeding regime

(e.g., multiple anaerobic stages in series) would be favorable for the implementation of AGS technologies in CFS.

3.5 Conclusions

The integration of AGS into continuous-flow wastewater treatment systems is a promising technology to enhance the biological nutrient removal capacity of existing infrastructure. In this study, long-term granule stability and high nutrient removal performance were achieved in a continuous-flow setting. The respective contributions of large granules (LG) and floc/small granules (FSG) to the nutrient removal capacity were determined. FSG had higher PAO activity than LG due to the lower substrate diffusion limitation, whereas AOB activity was similar between the two biomass fractions as AOBs benefitted from the higher SRT in the LG. Nitrite shunt (NOB suppression) was observed only in the FSG but not LG. Most importantly, washing out the FSG from the system resulted in a reduction of PAO and AOB activity in the LG (and eventual failure of the EBPR performance), suggesting LG's dependency on the FSG for sustaining the PAO and (to a lesser extent) AOB populations. The scientific innovations of this study were: (1) demonstrating the feasibility of sustaining PAO-dominated granule growth in a continuous-flow system, (2) highlighting the complex partitioning and the potential competitive/cooperative relationship between flocs and granules under a continuous-flow scheme, and (3) showcasing the important role of small particles in maintaining the nutrient removal capacity of a hybrid granule/floc system.

Acknowledgements

This work was supported by the National Science Foundation (#1510665) and EPA P3 Award (#83929101).

References

Ahn, J., Schroeder, S., Beer, M., McIlroy, S., Bayly, R.C., May, J.W., Vasiliadis, G., Seviour, R.J. 2007. Ecology of the microbial community removing phosphate from wastewater under continuously aerobic conditions in a sequencing batch reactor. *Applied and Environmental Microbiology*, **73**(7), 2257-2270.

Ali, M., Wang, Z.W., Salam, K.W., Hari, A.R., Pronk, M., van Loosdrecht, M.C.M., Saikaly, P.E. 2019. Importance of Species Sorting and Immigration on the Bacterial Assembly of Different-Sized Aggregates in a Full-Scale Aerobic Granular Sludge Plant. *Environmental Science & Technology*, **53**(14), 8291-8301.

APHA. 2005. *Standard methods for the examination of water and wastewater*. *21st ed*. American Public Health Association (APHA): Washington, DC, USA.

Barlow, J.T., Bogatyrev, S.R., Ismagilov, R.F. 2020. A quantitative sequencing framework for absolute abundance measurements of mucosal and lumenal microbial communities. *Nature Communications*, **11**(1).

Bassin, J., Winkler, M.K., Kleerebezem, R., Dezotti, M., Van Loosdrecht, M. 2012. Improved phosphate removal by selective sludge discharge in aerobic granular sludge reactors. *Biotechnology and bioengineering*, **109**(8), 1919-1928.

Blackburne, R., Vadivelu, V.M., Yuan, Z.G., Keller, J. 2007. Kinetic characterisation of an enriched Nitrospira culture with comparison to Nitrobacter. *Water Research*, **41**(14), 3033-3042.

Brdjanovic, D., van Loosdrecht, M.C.M., Hooijmans, C.M., Alaerts, G.J., Heijnen, J.J. 1998. Minimal aerobic sludge retention time in biological phosphorus removal systems. *Biotechnology and Bioengineering*, **60**(3), 326-332.

Callahan, B.J., McMurdie, P.J., Rosen, M.J., Han, A.W., Johnson, A.J.A., Holmes, S.P. 2016. DADA2: High-resolution sample inference from Illumina amplicon data. *Nature Methods*, **13**(7), 581-+.

Carter, J.A. 2020. Bioaugmentation with Sidestream Granular Sludge for Nitrification in Activated Sludge Wastewater Treatment: Pilot-Scale Investigation, Vol. Master's Thesis, University of Washington.

Cotto, I., Dai, Z., Huo, L., Anderson, C.L., Vilardi, K.J., Ijaz, U., Khunjar, W., Wilson, C., De Clippeleir, H., Gilmore, K., Bailey, E., Pinto, A.J. 2019. Long solids retention times and attached growth phase favor prevalence of comammox bacteria in nitrogen removal systems. *bioRxiv*, 696351.

de Kreuk, M.K., Kishida, N., van Loosdrecht, M.C.M. 2007. Aerobic granular sludge - state of the art. *Water Science and Technology*, **55**(8-9), 75-81.

de Kreuk, M.K., van Loosdrecht, M.C.M. 2004. Selection of slow growing organisms as a means for improving aerobic granular sludge stability. *Water Science and Technology*, **49**(11-12), 9-17.

Devlin, T.R., Oleszkiewicz, J.A. 2018. Cultivation of aerobic granular sludge in continuous flow under various selective pressure. *Bioresource Technology*, **253**, 281-287.

Figdore, B.A., Stensel, H.D., Winkler, M.K.H. 2018. Comparison of different aerobic granular sludge types for activated sludge nitrification bioaugmentation potential. *Bioresource Technology*, **251**, 189-196.

Foesel, B.U., Drake, H.L., Schramm, A. 2011. Defluviimonas denitrificans gen. nov., sp nov., and Pararhodobacter aggregans gen. nov., sp nov., non-phototrophic Rhodobacteraceae

from the biofilter of a marine aquaculture. *Systematic and Applied Microbiology*, **34**(7), 498-502.
Kent, T.R., Bott, C.B., Wang, Z.W. 2018. State of the art of aerobic granulation in continuous flow bioreactors. *Biotechnology Advances*, **36**(4), 1139-1166.
Kent, T.R., Sun, Y., An, Z., Bott, C.B., Wang, Z.-W. 2019. Mechanistic understanding of the NOB suppression by free ammonia inhibition in continuous flow aerobic granulation bioreactors. *Environment International*, **131**, 105005.
Kinnunen, M., Gulay, A., Albrechtsen, H.J., Dechesne, A., Smets, B.F. 2017. Nitrotoga is selected over Nitrospira in newly assembled biofilm communities from a tap water source community at increased nitrite loading. *Environmental Microbiology*, **19**(7), 2785-2793.
Kitzinger, K., Koch, H., Lucker, S., Sedlacek, C.J., Herbold, C., Schwarz, J., Daebeler, A., Mueller, A.J., Lukumbuzya, M., Romano, S., Leisch, N., Karst, S.M., Kirkegaard, R., Albertsen, M., Nielsen, P.H., Wagner, M., Daims, H. 2018. Characterization of the First "Candidatus Nitrotoga" Isolate Reveals Metabolic Versatility and Separate Evolution of Widespread Nitrite-Oxidizing Bacteria. *Mbio*, **9**(4).
Larsen, P., Nielsen, J.L., Otzenj, D., Nielsen, P.H. 2008. Amyloid-like adhesins produced by floc-forming and filamentous bacteria in activated sludge. *Applied and Environmental Microbiology*, **74**(5), 1517-1526.
Layer, M., Adler, A., Reynaert, E., Hernandez, A., Pagni, M., Morgenroth, E., Holliger, C., Derlon, N. 2019. Organic substrate diffusibility governs microbial community composition, nutrient removal performance and kinetics of granulation of aerobic granular sludge. *Water Research X*, **4**.
Li, D., Lv, Y.F., Zeng, H.P., Zhang, J. 2016. Enhanced biological phosphorus removal using granules in continuous-flow reactor. *Chemical Engineering Journal*, **298**, 107-116.
Li, S., Duan, H., Zhang, Y., Huang, X., Yuan, Z., Liu, Y., Zheng, M. 2020. Adaptation of nitrifying community in activated sludge to free ammonia inhibition and inactivation. *Science of The Total Environment*, **728**, 138713.
Lim, J., Do, H., Shin, S.G., Hwang, S. 2008. Primer and probe sets for group-specific quantification of the genera Nitrosomonas and Nitrosospira using real-time PCR. *Biotechnology and Bioengineering*, **99**(6), 1374-1383.
Liu, H.B., Xiao, H., Huang, S., Ma, H.J., Liu, H. 2014. Aerobic granules cultivated and operated in continuous-flow bioreactor under particle-size selective pressure. *Journal of Environmental Sciences*, **26**(11), 2215-2221.
Liu, Y.Q., Tay, J.H. 2012. The competition between flocculent sludge and aerobic granules during the long-term operation period of granular sludge sequencing batch reactor. *Environmental Technology*, **33**(23), 2619-2626.
Mamais, D., Jenkins, D. 1992. THE EFFECTS OF MCRT AND TEMPERATURE ON ENHANCED BIOLOGICAL PHOSPHORUS REMOVAL. *Water Science and Technology*, **26**(5-6), 955-965.
Math, R.K., Jin, H.M., Jeong, S.H., Jean, C.O. 2013. Defluviimonas aestuarii sp nova, a marine bacterium isolated from a tidal flat, and emended description of the genus Defluviimonas Foesel et al. 2011. *International Journal of Systematic and Evolutionary Microbiology*, **63**, 2895-2900.
Matsumoto, S., Katoku, M., Saeki, G., Terada, A., Aoi, Y., Tsuneda, S., Picioreanu, C., van Loosdrecht, M.C.M. 2010. Microbial community structure in autotrophic nitrifying

granules characterized by experimental and simulation analyses. *Environmental Microbiology*, **12**(1), 192-206.
McIlroy, S.J., Starnawska, A., Starnawski, P., Saunders, A.M., Nierychlo, M., Nielsen, P.H., Nielsen, J.L. 2016. Identification of active denitrifiers in full-scale nutrient removal wastewater treatment systems. *Environmental Microbiology*, **18**(1), 50-64.
McMurdie, P.J., Holmes, S. 2013. phyloseq: An R Package for Reproducible Interactive Analysis and Graphics of Microbiome Census Data. *Plos One*, **8**(4).
Nguyen Quoc, B., Wei, S., Armenta, M., Bucher, R., Sukapanpotharam, P., Stahl, D.A., Stensel, H.D., Winkler, M.K.H. 2021. Aerobic granular sludge: Impact of size distribution on nitrification capacity. *Water Research*, **188**.
Nierychlo, M., Andersen, K.S., Xu, Y.J., Green, N., Jiang, C.J., Albertsen, M., Dueholm, M.S., Nielsen, P.H. 2020. MiDAS 3: An ecosystem-specific reference database, taxonomy and knowledge platform for activated sludge and anaerobic digesters reveals species-level microbiome composition of activated sludge. *Water Research*, **182**.
Numberger, D., Ganzert, L., Zoccarato, L., Muhidorfer, K., Sauer, S., Grossart, H.P., Greenwood, A.D. 2019. Characterization of bacterial communities in wastewater with enhanced taxonomic resolution by full-length 16S rRNA sequencing. *Scientific Reports*, **9**.
Parada, A.E., Needham, D.M., Fuhrman, J.A. 2016. Every base matters: assessing small subunit rRNA primers for marine microbiomes with mock communities, time series and global field samples. *Environmental Microbiology*, **18**(5), 1403-1414.
Parks, D.H., Tyson, G.W., Hugenholtz, P., Beiko, R.G. 2014. STAMP: statistical analysis of taxonomic and functional profiles. *Bioinformatics*, **30**(21), 3123-3124.
Petriglieri, F., Singleton, C., Peces, M., Petersen, J.F., Nierychlo, M., Nielsen, P.H. 2021. "Candidatus Dechloromonas phosphoritropha" and "Ca. D. phosphorivorans", novel polyphosphate accumulating organisms abundant in wastewater treatment systems. *Isme j*.
Poot, V., Hoekstra, M., Geleijnse, M.A.A., van Loosdrecht, M.C.M., Perez, J. 2016. Effects of the residual ammonium concentration on NOB repression during partial nitritation with granular sludge. *Water Research*, **106**, 518-530.
Pronk, M., de Kreuk, M.K., de Bruin, B., Kamminga, P., Kleerebezem, R., van Loosdrecht, M.C.M. 2015. Full scale performance of the aerobic granular sludge process for sewage treatment. *Water Research*, **84**, 207-217.
Saha, P., Chakrabarti, T. 2006. Emticicia oligotrophica gen. nov., sp nov., a new member of the family 'Flexibacteraceae', phylum Bacteroidetes. *International Journal of Systematic and Evolutionary Microbiology*, **56**, 991-995.
Seviour, T., Yuan, Z.G., van Loosdrecht, M.C.M., Lin, Y.M. 2012. Aerobic sludge granulation: A tale of two polysaccharides? *Water Research*, **46**(15), 4803-4813.
Simm, R.A., Mavinic, D.S., Ramey, W.D. 2006. A targeted study on possible free ammonia inhibition of Nitrospira. *Journal of Environmental Engineering and Science*, **5**(5), 365-376.
Stinson, B., Galvagno, G., Sears, K., Bowden, G., Margevicius, T., Craig, R. 2019. Innovative process for granulation of conventional continuous flow activated sludge – A novel cost effective Infra-stretching concept to treat more flow and remove/recover more nutrients without expanding your plant. *WEFTEC Conference Proceedings*, Chicago, IL.

Stokholm-Bjerregaard, M., McIlroy, S.J., Nierychlo, M., Karst, S.M., Albertsen, M., Nielsen, P.H. 2017. A Critical Assessment of the Microorganisms Proposed to be Important to Enhanced Biological Phosphorus Removal in Full-Scale Wastewater Treatment Systems. *Frontiers in Microbiology*, **8**.

Sturm, B., Faraj, R., Figdore, B., Willoughby, A., Ford, A., Bott, C., Shiskowski, D., McFall, L., Downing, L. 2017. Balancing Granular Sludge with Activated Sludge Systems for Biological Nutrient Removal. *WEFTEC Conference Proceedings*, Chicago, IL.

Sun, Y.W., Angelotti, B., Wang, Z.W. 2019. Continuous-flow aerobic granulation in plug-flow bioreactors fed with real domestic wastewater. *Science of the Total Environment*, **688**, 762-770.

Terashima, M., Yama, A., Sato, M., Yumoto, I., Kamagata, Y., Kato, S. 2016. Culture-Dependent and -Independent Identification of Polyphosphate-Accumulating Dechloromonas spp. Predominating in a Full-Scale Oxidation Ditch Wastewater Treatment Plant. *Microbes and Environments*, **31**(4), 449-455.

Ushiki, N., Jinno, M., Fujitani, H., Suenaga, T., Terada, A., Tsuneda, S. 2017. Nitrite oxidation kinetics of two Nitrospira strains: The quest for competition and ecological niche differentiation. *Journal of Bioscience and Bioengineering*, **123**(5), 581-589.

Wang, Q., Garrity, G.M., Tiedje, J.M., Cole, J.R. 2007. Naïve Bayesian Classifier for Rapid Assignment of rRNA Sequences into the New Bacterial Taxonomy. *Applied & Environmental Microbiology*, **73**(16), 5261-5267.

Wegen, S., Nowka, B., Spieck, E. 2019. Low Temperature and Neutral pH Define "Candidatus Nitrotoga sp." as a Competitive Nitrite Oxidizer in Coculture with Nitrospira defluvii. *Applied and Environmental Microbiology*, **85**(9).

Wei, S.P., Stensel, H.D., Quoc, B.N., Stahl, D.A., Huang, X.W., Lee, P.H., Winkler, M.K.H. 2020. Flocs in disguise? High granule abundance found in continuous-flow activated sludge treatment plants. *Water Research*, **179**.

Weissbrodt, D.G., Holliger, C., Morgenroth, E. 2017. Modeling hydraulic transport and anaerobic uptake by PAOs and GAOs during wastewater feeding in EBPR granular sludge reactors. *Biotechnology and Bioengineering*, **114**(8), 1688-1702.

Winkler, M.K.H., Kleerebezem, R., de Bruin, L.M.M., Verheijen, P.J.T., Abbas, B., Habermacher, J., van Loosdrecht, M.C.M. 2013a. Microbial diversity differences within aerobic granular sludge and activated sludge flocs. *Applied Microbiology and Biotechnology*, **97**(16), 7447-7458.

Winkler, M.K.H., Kleerebezem, R., Kuenen, J.G., Yang, J.J., van Loosdrecht, M.C.M. 2011. Segregation of Biomass in Cyclic Anaerobic/Aerobic Granular Sludge Allows the Enrichment of Anaerobic Ammonium Oxidizing Bacteria at Low Temperatures. *Environmental Science & Technology*, **45**(17), 7330-7337.

Winkler, M.K.H., Kleerebezem, R., Strous, M., Chandran, K., van Loosdrecht, M.C.M. 2013b. Factors influencing the density of aerobic granular sludge. *Applied Microbiology and Biotechnology*, **97**(16), 7459-7468.

Winkler, M.K.H., Le, Q.H., Volcke, E.I.P. 2015. Influence of Partial Denitrification and Mixotrophic Growth of NOB on Microbial Distribution in Aerobic Granular Sludge. *Environmental Science & Technology*, **49**(18), 11003-11010.

Zheng, M., Li, S., Ni, G., Xia, J., Hu, S., Yuan, Z., Liu, Y., Huang, X. 2020. Critical Factors Facilitating Candidatus Nitrotoga To Be Prevalent Nitrite-Oxidizing Bacteria in Activated Sludge. *Environmental Science & Technology*, **54**(23), 15414-15423.

Zhou, D.D., Niu, S., Xiong, Y.J., Yang, Y., Dong, S.S. 2014. Microbial selection pressure is not a prerequisite for granulation: Dynamic granulation and microbial community study in a complete mixing bioreactor. *Bioresource Technology*, **161**, 102-108.

Appendix B. Supplementary Material for Chapter 3

1.0 Materials and Methods

1.1 Conceptual scheme for combined granule and floc system. The conceptual scheme for implementing granular sludge technology in a continuous flow system is depicted in Fig. S1a. 55% of the mixed liquor flow from the aeration basin goes through a granule/floc separator, which can be a hydrocyclone, plate settler, hydraulic separator, a rotary drum screen or anything of similar function. Granular sludge is drawn from the separator and recycled back to the anaerobic zone to receive the influent COD. Flocs are directed to the clarifier where the return flocculent sludge is recycled back to the aerobic zone. This operation allows the following selection pressure for granule growth:

(1) Influent COD is preferentially fed to the granules to favor growth of PAO granules.
(2) 55% of the flocs are recycled to the aerobic zone, which reduces the competition for influent COD with the granules.
(3) Granules and flocs can be wasted from separate lines, allowing for decoupled controls for granular and flocculent SRTs.

A lab-scale reactor setup was used to simulate the same selection pressures used in the conceptual scheme, and the operational phases are outlined in Fig. S1b. Each operational phase in Fig. S1b simulates the matching number shown in Fig. S1a with the descriptions in Table S1.

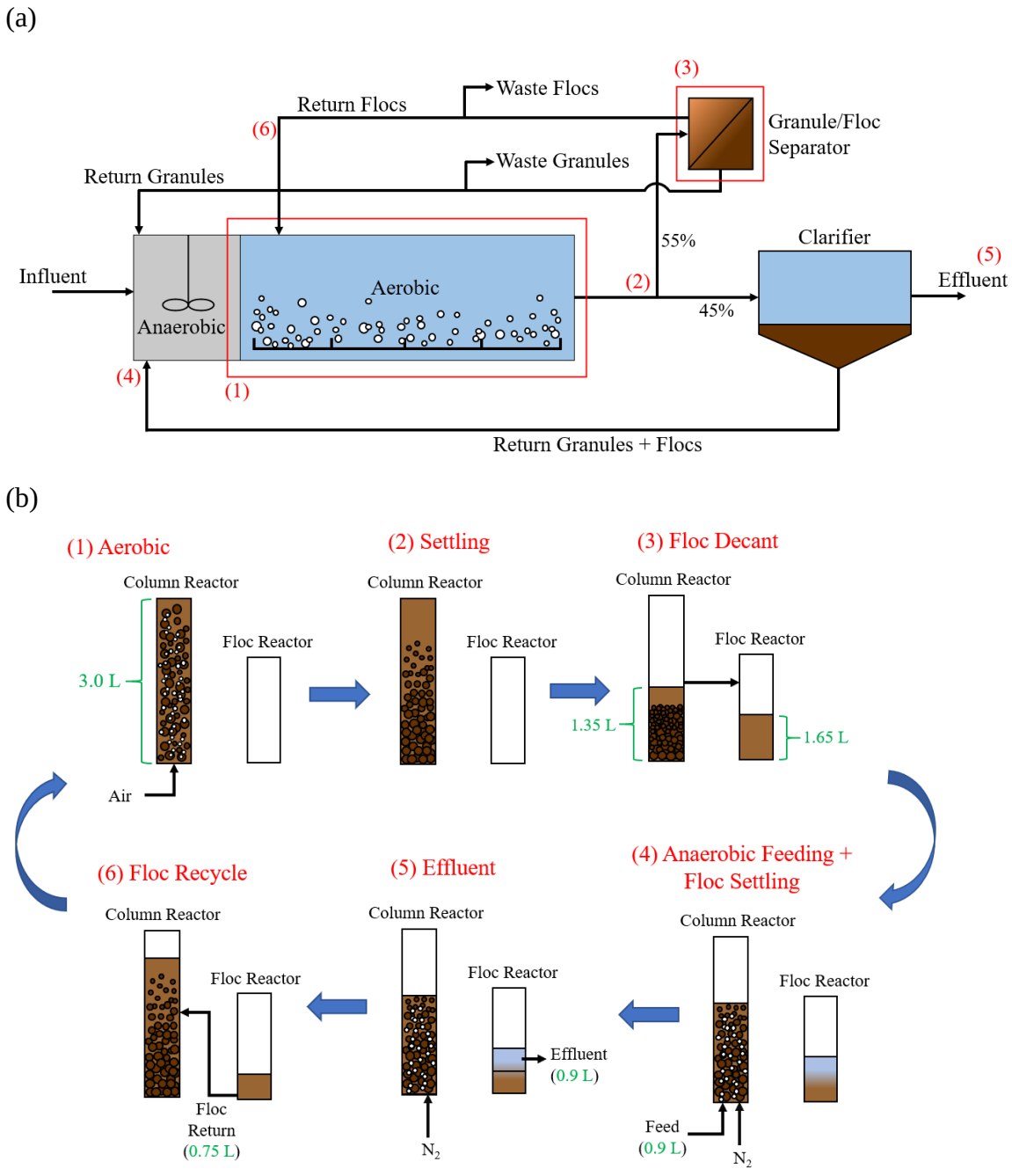

Fig. S1. (a) Conceptual scheme for integration of AGS technology in a continuous-flow system. (b) Schematic explanation for how the selection pressures utilized in the conceptual scheme (a) is simulated in a lab-scale reactor setup. The number on each red box in (a) is simulated by the matching number in (b). See Table S1 for detailed descriptions.

Table S1. Descriptions for how the selection pressures in each compartment of the conceptual scheme is represented by the reactor setup.

No.	Conceptual scheme (Fig. S1a)	Lab Reactor Simulation (Fig. S1b)		
		Phase	Description	Duration
(1)	Aerobic zone	Aerobic	Granules and flocs are aerated together in the column reactor.	242 mins
(2) and (3)	Flow split and Granule/floc separator	Settling and Floc decant	The 45/55 flow-split and the granule/floc separator are achieved together in phases (2) and (3). A short settling period is applied, then the top 55% of the liquid is decanted to the floc reactor whereas the bottom 45% stayed in the column reactor. Due to the slow settling velocity of the flocs, the top 55% decanted consists of flocs only, thus creating a separation of flocs from the granules. These two phases ensure that only 45% of the flocs are recycled back to the anaerobic zone, thereby favoring the rbCOD to the granules.	Phase (2): 3 mins. Phase (3): 3 mins.
(4)	Secondary clarifier and influent feeding to the anaerobic zone	Anaerobic feeding + floc settling	Flocs settle in the floc reactor while granules are fed COD anaerobically in the column reactor	60 mins feeding + 13 min idle
(5)	Effluent	Effluent	Effluent is drawn from the top of the floc reactor	2 mins
(6)	Recycling of flocs to the aerobic zone	Floc recycle	Remaining sludge in the floc reactor is pumped back to the column reactor	2 mins

1.2 Decoupled LG/FSG SRT control. During the last 30 minutes of the aerobic phase, a sample of roughly 20 ml was collected from the column reactor. The sample was separated into LG

(>425 μm) and FSG (<425 μM) with a sieve. The MLSS of LG and FSG in the column reactor ($MLSS_{LG,\ column\ rctr}$ and $MLSS_{FSG,\ column\ rctr}$, respectively) were then determined. A sample taken from the floc reactor was subjected to the same procedures to determine the MLSS of LG and FSG in the floc reactor ($MLSS_{LG,\ floc\ rctr}$ and $MLSS_{FSG,\ floc\ rctr}$, respectively). Effluent samples were also collected and measured for TSS, which had no particles larger than 425 μm (no LG fraction). Then, using Equations S1 and S2 below, the volumes that needed to be removed from the granule and floc reactors were determined to meet the target SRTs. Volumes were removed when the reactors were completely mixed.

$$SRT_{LG} = \frac{(MLSS_{LG,\ column\ rctr} \times V_{column\ rctr})}{(MLSS_{LG,\ column\ rctr} \times V_{column\ rctr,excess}) + (MLSS_{LG,\ floc\ rctr} \times V_{floc\ rctr,excess})}$$

Equation 1

$$SRT_{FSG} = \frac{(MLSS_{FSG,\ column\ rctr} \times V_{column\ rctr})}{\begin{array}{c}(TSS_{effluent} \times V_{effluent}) + (MLSS_{FSG,\ column\ rctr} \times V_{column\ rctr,excess}) \\ +(MLSS_{FSG,\ floc\ rctr} \times V_{floc\ rctr,excess})\end{array}}$$

Equation 2

Where,

$MLSS_{LG,\ column\ rctr}$:	MLSS of LG in the column reactor.
$MLSS_{LG,\ floc\ rctr}$:	MLSS of LG in the flocculent reactor.
$MLSS_{FSG,\ column\ rctr}$:	MLSS of FSG in the column reactor.
$MLSS_{FSG,\ floc\ rctr}$:	MLSS of FSG in the flocculent reactor.
$TSS_{effluent}$:	TSS of the effluent.
$V_{column\ rctr}$:	Volume of column reactor.
$V_{effluent}$:	Volume of the effluent.
$V_{column\ rctr,\ excess}$:	Volume of excess sludge wasted from the column reactor.
$V_{floc\ rctr,\ excess}$:	Volume of excess sludge wasted from floc reactor.

1.3 Synthetic wastewater composition. Two 10-L synthetic wastewater media were used, each consisted of (1) 16.02 g $C_2H_3NaO_2$, 11.55 g $C_3H_5NaO_2$, 5.55 g $MgSO_4 \cdot 7H_2O$ and 2.19 g KCl; and (2) 9.55 g NH_4Cl, 4.69 g K_2HPO_4, 1.83 g KH_2PO_4 and 100 ml "Vishniac and Santer" trace element solution (Vishniac & Santer, 1957). During anaerobic feeding, 150 ml of each media was fed along with 600 ml of tap water (for total feed volume of 900 ml), resulting in feed concentrations of 433 mg/L COD, 41.7 mg/L NH_4^+-N and 20.8 mg/L PO_4^{3-}-P.

1.4 Biomass-specific activity tests. Specific activity tests were performed to measure the ammonia oxidation, nitrite oxidation, and phosphorus release activities of FSG and LG separately at the end of Phases I–III, as well as for the granule/floc inoculum. All tests were conducted at 18.3 ± 0.5°C and pH of 7.2 ± 0.2. Before each activity test, a mixed liquor sample was collected from the reactor and aerated for about 1 hour in in a media consisting of 44 mg L^{-1} $MgSO_4 \cdot 7H_2O$, 17.5 mg L^{-1} KCl, and 0.5 mL of Vishniac trace element solution (Vishniac & Santer, 1957). All tests were done in 500-ml graduated cylinders with 150-ml sample volume. A 425-µm sieve was used to separate FSG and LG into different cylinders. The g of VSS in each cylinder was determined at the end of the test. For Phases I – III, activity tests were done in biological duplicates (I and III) or triplicates (II). Activity tests of granule/floc inoculum were conducted without replicates. Every time a new experimental phase began, a period of at least three FSG SRTs was passed before an activity test was conducted to ensure adequate time for microbial adaptation.

For ammonia-oxidizing bacteria (AOB) and nitrite-oxidizing bacteria (NOB) activity tests, the cylinders were spiked with 20 mg NH_4^+-N/L and 10 mg NO_2^--N/L, respectively. For the AOB test, 0.01M of phosphate buffer was added to control the pH. Under air-saturated condition, 6 samples were taken over a 50-min period and analyzed for ammonia and nitrite concentrations.

For the P release activity test, the cylinders were first sparged with N_2 gas for about 10 mins then spiked with 150 mgCOD L^{-1} of acetate. With N_2 gas purging the entire time, 6 samples were taken over a 50-min period and analyzed for acetate and phosphate concentrations. The g of VSS was determined after end of each test. The rate of ammonia oxidation, nitrite oxidation, and P release was determined from the slope of NH_4^+, NO_2^-, and PO_4^{3-} concentrations versus time, respectively. The slope was then normalized to the g of VSS to obtain the maximum specific ammonia oxidation rate (SAR), maximum specific nitrite oxidation rate (SNR), and specific P release rate (SPR), respectively.

1.5 Particle size distribution analysis. Particle size distribution of LG was determined with sieve analysis for a sample volume of roughly 70 – 100 ml collected from the granule reactor during the aeration phase. The sample was passed through a series of sieves (3-in diameter) with various mesh sizes. Starting from the sieve with the largest mesh size, a sample was passed through and only particles larger than the mesh size were retained. Gentle washing with DI water was done to help push through any particles smaller than the mesh size. All water and solids passing through the sieve were captured and the procedure was repeated with all the remaining sieves in order of reducing mesh sizes. Solids captured on each sieve was then backwashed into an individual beaker per granule size fraction and the g of TSS was measured. The particle size distribution was determined by g TSS of each size over the sum of g TSS of all sizes.

1.6 DADA2 parameters. Amplicon reads were processed following the Divisive Amplicon Denoising Algorithm 2 (DADA2) pipeline (Callahan et al., 2016) (v. 1.16) implemented in R v. 4.0.2. The forward and reverse reads were first trimmed at 243 and 215 position, respectively,

while using 2 as the DADA2 maximum expected error allowed in a read. Next, eight sub-sample sets were used to conduct iterations for estimating the error rates and sample composition until they matched. The samples were then denoised using the error parameters followed by identification of sequence variances and merging of forward and reverse reads. For merging, the sequences were constructed only if the overlap region was identical and at least 12 bases long.

1.7 PCR amplification for detection of comammox. All PCR reactions were done in 20 µl volume, consisting of 18 µl Platinum® PCR SuperMix (Invitrogen), 0.5 µl each of 10 µM forward and reverse primer, and 1 µl of 1.0 or 0.1 ng/µl of DNA template for the reactor samples or the *Nitrospira inopinata* culture, respectively. For negative control, a DNA extraction was done without biomass and 1 µl of the extraction product was used as template during PCR amplification. PCR reactions for reactor samples and controls were done in duplicates and singlets, respectively. The primer sequences and thermal profiles are listed in Table S2. Duplicates of PCR reaction were pooled and 5 µl of the product was visualized by electrophoresis on a 1.5% agarose gel stained with ethidium bromide staining in 1x TAE buffer.

Table S2. PCR primers and amplification thermal profiles used in this study

Primer	Specificity	PCR thermal profile	Reference
cmx_amoB 148F/485R	Clade A comammox	95°C/5m, 40×(95°C/15s, 52°C /45s, 72°C/60s), 72°C/10min, 4°C/∞	(Cotto et al., 2019)
NTS 232F/1200R	Nitrospira	95°C/5m, 35×(95°C /40s, 55-48°C /30s, 72°C /60s), 72°C /10min, 4°C /∞	(Lim et al., 2008)

1.8 Fluorescence in-situ hybridization (FISH). Water was first removed from the LG sample by centrifugation and removal of supernatant. Then, the pellet was resuspended in 4% paraformaldehyde and let sit on ice for 120 mins. The paraformaldehyde was washed off by centrifugation, removal of supernatant, and resuspension in 1x PBS. The final resuspension was in an ethanol and PBS solution at 1.25:1 volumetric ratio and stored at -20 °C. The sample was frozen in a tissue freezing medium at -20 °C and cut into slices of 25-µm thickness using a cryostat (Thermo Scientific CryoStar NX50). The LG slices were adhered onto gelatin-coated microscopic glass slides. The slices were then dried at 46°C and dehydrated with subsequent (3 min each) 50%, 80%, and 98% ethanol concentrations. For each well, 10 µL of hybridization buffer solution was added consisting of 0.9 M NaCl, 0.02 M Tris-HCl (pH 8.0), 35% formamide, and 0.02% sodium dodecyl sulfate (SDS). Subsequently, 1 µL of probe mix was added for each well. The probe mix included 5 µM of cy3-labelled NSO190 and NSO1225 for targeting *β-Proteobacterial* AOB (Mobarry et al., 1996), as well as 8.3 µM of fluorescein-labelled Ntspa 662 for targeting the *Nitrospira* genus (Daims et al., 2001) and Ntoga122 for targeting the *Nitrotoga* genus (Lucker et al., 2015). Hybridization step took place in a humid chamber at 46°C for 2.5 hours. Immediately after hybridization, the un-hybridized probes were washed off with a washing buffer (pre-heated to 48°C) consisting of 20 mM Tris-HCl (pH 8), 0.08 mM NaCl, 5 mM EDTA (pH 8.0), and 0.01% SDS. Washing was performed by first rinsing with the washing buffer and then immersing the slide into the washing buffer for 20 min. After a final rinse with milliQ water and air drying at room temperature, antifade fluorescent mounting medium (20 mM Tris at pH 8.0, 0.5% N-propyl gallate, and 90% glycerol) was added to each well and covered with a cover slip. Slide was observed using a confocal microscope (Zeiss Axioskop 2 MOT) fitted with a Zeiss Axiocam 503 mono camera.

2.0 Results and Discussions

2.1 Simultaneous Nitrification and Denitrification. The simultaneous nitrification and denitrification (SND) efficiency was estimated based on the feed ammonia, the amount of N removed via synthesis, and the NO_2^-+NO_3^- (NO_x-N) production. The yield of the reactor was estimated to be 0.26 ± 0.08 gVSS/gCOD based on the mg of VSS wasted per day and the COD loading. With a feed COD of 130 mg/L (concentration of normalized to the total volume of 3 L) and the assumption that roughly 12% of the biomass was composed of nitrogen, the nitrogen removed by synthesis was estimated to be around 4.0 mg N/L. Although all NO_x-N was removed in the column reactor by denitrification in the anaerobic phase, the NO_x-N contained in the floc reactor was not removed because there was no contact with the feed COD. Therefore, there was residual amount of NO_x-N from the floc reactor at the start of aerobic phase. The NO_x-N production in the aerobic phase was therefore estimated by taking the difference between effluent NO_x-N (9.6 mg/L) and the start of aerobic NO_x-N (2.3 mg/L), which was on average 7.3 mg N/L. The feed ammonia concentration was 12.5 mg N/L (normalized to the total volume of 3 L) while the average effluent ammonia concentration was 0.15 mg N/L. The amount of ammonia removed was therefore 12.4 mg N/L (12.5 – 0.15). Of the 12.4 mg N/L ammonia removed, 4.0 mg N/L (32%) was removed via synthesis and 7.3 mg N/L was oxidized to NO_x-N (59%), leaving 1.1 mg N/L (8.9%) as the amount removed by SND. Instead of using averaged values for the entire project duration, the same calculation approach was done using daily measurements of ammonia removal and NO_x-N production, the % nitrogen removed via SND was plotted in Fig. S2. The resulting average % nitrogen removed via SND from Fig. S2 was 10.5 ± 5.0%.

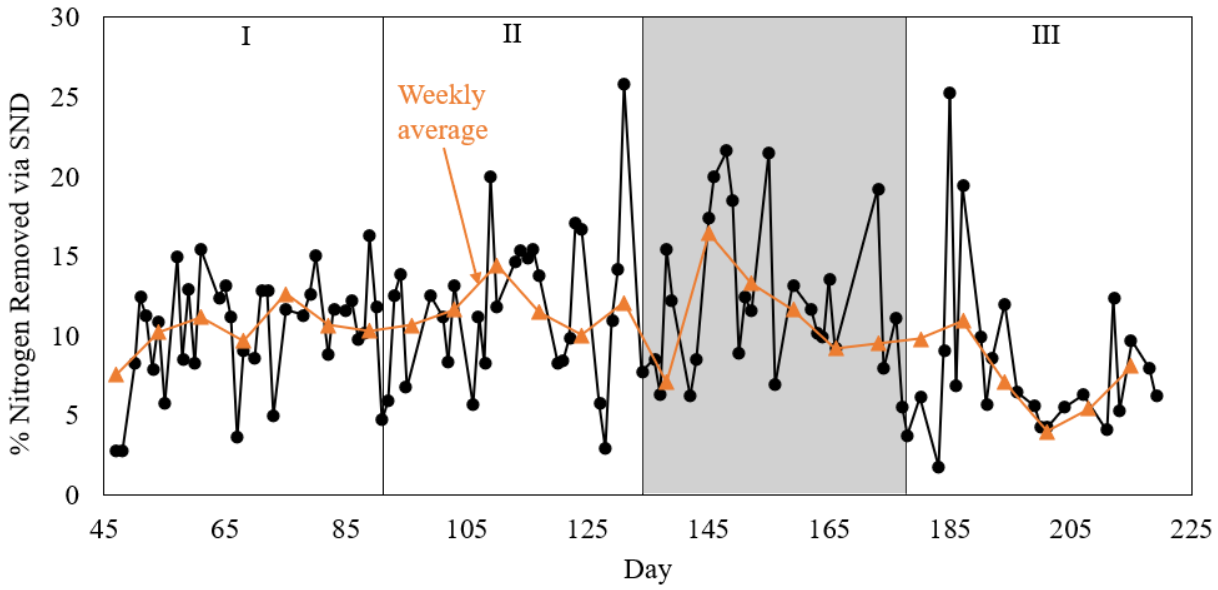

Fig. S2. Estimated % of nitrogen removal attributed to simultaneous nitrification and denitrification.

2.2 Rapid granulation of flocs

The rapid granulation of flocs can be explained by two reasons: the enrichment of PAO in the FSG and breakage from LG as nucleation sites. Since only 55% of the flocs were bypassed from the anaerobic phase, the remaining 45% was exposed to anaerobic carbon addition and promoted enrichment of *Accumulibacter* PAO in the FSG (Fig. 2 and Fig. 3), which in turn contributed to the rapid granulation of flocs. This observation aligned with previous research demonstrating that PAO cells form denser and faster-settling granules than other granule types due to polyphosphate accumulation (Figdore et al., 2018; Winkler et al., 2011; Winkler et al., 2013). In addition, there are numerous reports of spontaneous granulation observed in EBPR SBRs fed with synthetic wastewater without fast washout as a selection pressure for granulation, though it can take 40–98 days for mature granules to form (Barr et al., 2010; Ong et al., 2012; Weissbrodt et al., 2013; Wu et al., 2010). It is likely that a similar phenomenon was observed in our system

though with much shorter granulation time, which was probably due to the already established anaerobic phase that allowed for optimal conditions for rapid enrichment of PAO in the FSG. FSG are also less diffusion limited than LG, thus providing a competitive edge for PAO to access carbon in the anaerobic phase. In addition, with the observation that granules larger than 2 mm disintegrated since Phase II (Fig. S6a), we suspected that aggregates from granule breakage were likely used as nucleation sites to enable such rapid granulation of flocs. This phenomenon was confirmed by previous research using flocs and crushed granules labelled with fluorescent microbeads to show that flocs permanently attached to the surface of crushed granules during startup of an AGS SBR and reduced the time for granulation (Pijuan et al., 2011; Verawaty et al., 2012).

2.3 Theoretical NOB/AOB activity ratio. The ratio of specific nitrite oxidation rate (SNR) to specific ammonia oxidation rate (SAR) can be estimated with Eq. S3.

$$\frac{SNR}{SAR} = \frac{\mu_{max,NOB}}{\mu_{max,AOB}} \cdot \frac{(\frac{X_{NOB}}{Y_{NOB}})}{(\frac{X_{AOB}}{Y_{AOB}})} \qquad \text{Eq. S3}$$

Where μ_{max} is the maximum specific growth rate (hr^{-1}), X is the biomass concentration (mg/L), and Y is yield (g biomass/g substrate). In a fully nitrifying system with the assumptions that (1) nitrite produced from ammonia oxidation by AOB is the only source of substrate for NOB and (2) AOB and NOB have the same endogenous decay rate, it can be assumed that $X_{NOB}/X_{AOB} = Y_{NOB}/Y_{AOB}$. As a result, the last term of Eq. S3 cancel out and the SAR/SNR ratio can be simplified to Eq. S4.

$$\frac{SNR}{SAR} = \frac{\mu_{max,NOB}}{\mu_{max,AOB}} \qquad \text{Eq. 4}$$

Literature values of μ_{max} for *Nitrosomonas*, *Nitrospira*, and *Nitrotoga* are shown in Table S3. The $\mu_{max,NOB}$ was adjusted for each operational phase (Table S4) based on the relative abundances of *Nitrospira* and *Nitrotoga*. The same $\mu_{max,AOB}$ of 0.58 was used for all phases as *Nitrosomonas* was the only AOB detected. Then, the $\mu_{max,AOB}$ and weighted averaged $\mu_{max,NOB}$ was used to calculate the $\mu_{max,NOB}/\mu_{max,AOB}$ ratios (Table S4).

Table S3. Maximum specific growth rate of NOB species reported in the literature.

Species	μ_{max} (day^{-1})	Temperature (°C)	μ_{max}, corrected to 18°C (day^{-1})[c]	Reference
Nitrosomonas oligotropha[a]	0.77	21	0.63	(Park & Noguera, 2007)
Nitrosomonas europaea[a]	0.66	21	0.54	(Park & Noguera, 2007)
Nitrosomonas Average			**0.58**	
Nitrospira species[b]	0.69	22	0.52	(Park et al., 2017)
Nitrospira defluvii[a]	0.67	28	0.33	(Winkler et al., 2017)
Nitrospira Average			**0.43**	
Ca. Nitrotoga arctica[b]	0.38	17	**0.41**	(Nowka et al., 2015)

[a] Pure culture

[b] Enrichment

[c] A temperature coefficient ($\theta = 1.072$) was used for conversion

Table S4. Weighted average $\mu_{max,NOB}$ and the resulting $\mu_{max,AOB}$ / $\mu_{max,NOB}$ ratios of each phase.

Phase	Relative abundance in NOB group[a]		Weighted average $\mu_{max,NOB}$ (day^{-1})[a]	$\mu_{max,NOB}$ / $\mu_{max,AOB}$[b]
	Nitrospira	Nitrotoga		
FSG				
I	0.95	0.05	0.43	0.74
II	0.00	1.00	0.41	0.71
LG				
I	0.96	0.04	0.43	0.74
II	0.46	0.54	0.42	0.72

[a]Literature μ_{max} values for Nitrospira and Nitrotoga are 0.43 and 0.41 day^{-1}, respectively (Table S3). Weighted average was calculated by (%Nitrospira × 0.43) + (%Nitrotoga × 0.41).

[b]Literature μ_{max} of 0.58 day^{-1} (Table S3) was used for $\mu_{max,AOB}$ as Nitrosomonas was the only AOB present.

2.4 Supplementary tables and figures

Table S5. Reactor performance

	$P_{release}/C_{uptake}$	Removal Efficiencies[a], %		
	molP/molC	PO_4^{3-}	NH_4^+	Nitrogen Species[b] ($NH_4^+ + NO_3^- + NO_2^-$)
Pre-experiment	0.39 ± 0.06	99.4 ± 0.7	91.1 ± 2.4	80.5 ± 2.5
Phase I	0.42 ± 0.05	98.8 ± 1.2	99.9 ± 0.1	76.3 ± 3.3
Phase II	0.47 ± 0.05	96.2 ± 2.7	99.1 ± 1.7	77.7 ± 1.2
Phase III	0.37 ± 0.06	98.9 ± 0.9	99.8 ± 0.1	76.1 ± 1.6
Phase R	0.41 ± 0.12	78.5 ± 32.2	99.8 ± 0.2	81.5 ± 1.9

[a]Removal efficiencies were calculated by:

100× (feed concentration – effluent concentration)/ (feed concentration).

[b]This value is not indicative of the SND efficiency as a portion of the NO_3^- was removed by heterotrophic denitrification in the anaerobic phase. See Section S2.1 for discussions on SND.

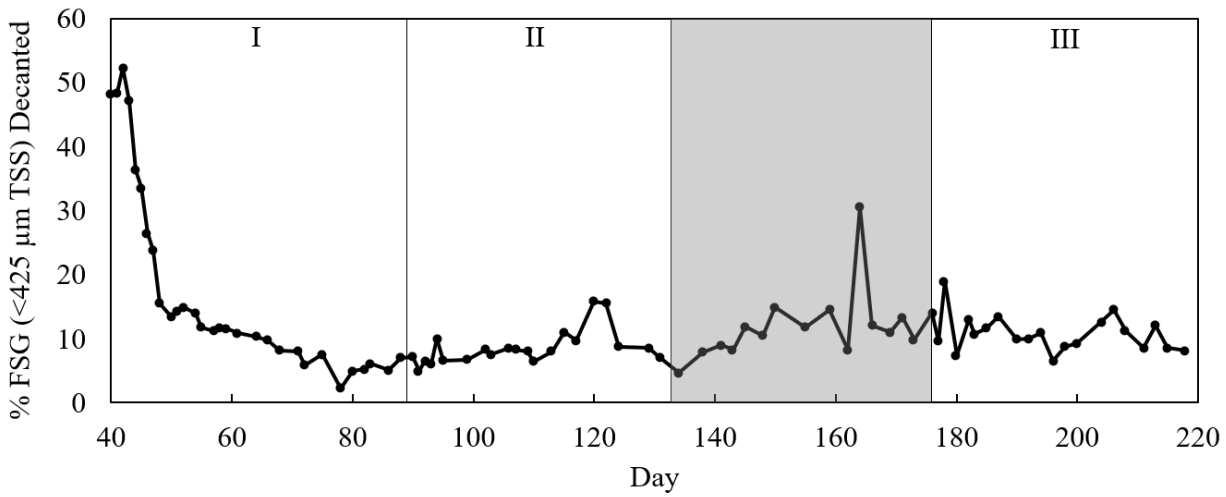

Fig. S3. The portion of total FSG (solids < 425 µm) decanted to the floc reactor. After the aeration phase, where granules and flocs were well-mixed together in the column reactor, a short settling period was applied and solids above the decant position were withdrawn to the floc reactor. The decant position was located at 45% of the column height from the bottom. Therefore, assuming that flocs were evenly distributed within the reactor during aeration, 45% of the flocs would be below the decant level at the start of the settling period. At the start of Phase 1, roughly 50% of the FSG were decanted to the floc reactor while 50% remained in the column reactor after the 3-min settling phase, which means only 5% of FSG (in addition to the 45% already on the bottom) passed the decant level.

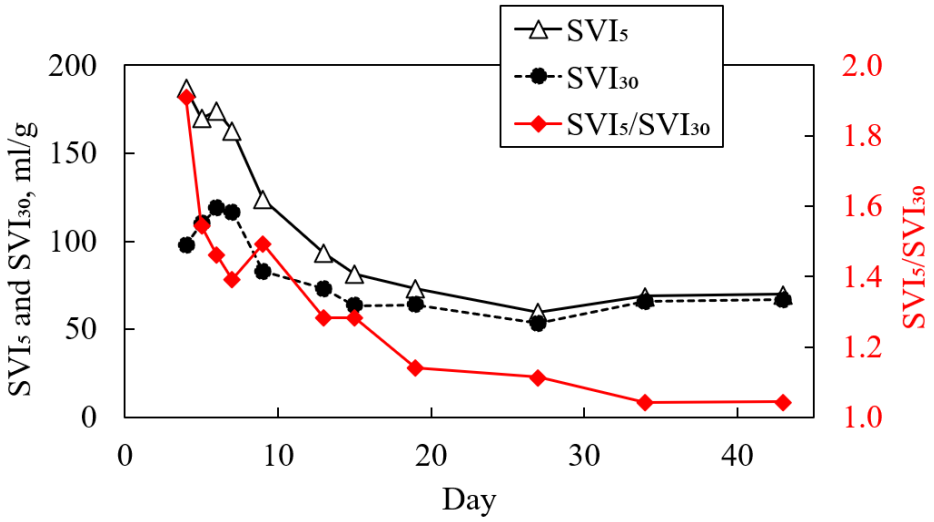

Fig. S4. Changes in SVIs of FSG during Phase I. The SVI_5/SVI_{30} ratio is an indicator of the granule fraction for a mixed liquor sample and a value of less than 1.3 indicates a mostly granular system (Figdore et al., 2017).

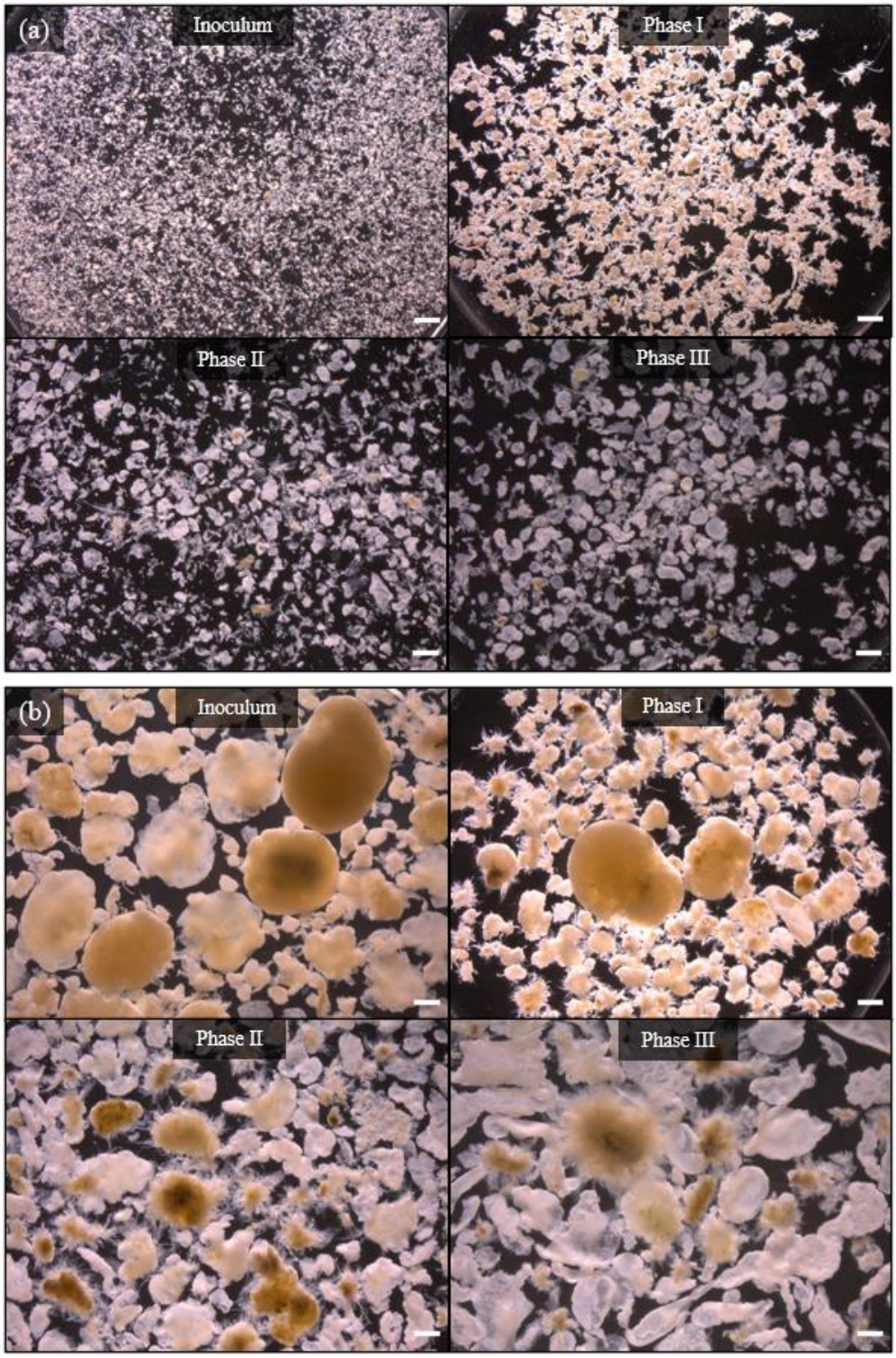

Fig. S5. Microscopic images of (a) FSG (solids < 425 µm) and (b) LG (solids > 425 µm) taken at end of each operational phase at 6.3X magnification in darkfield mode. Scale bar = 1 mm.

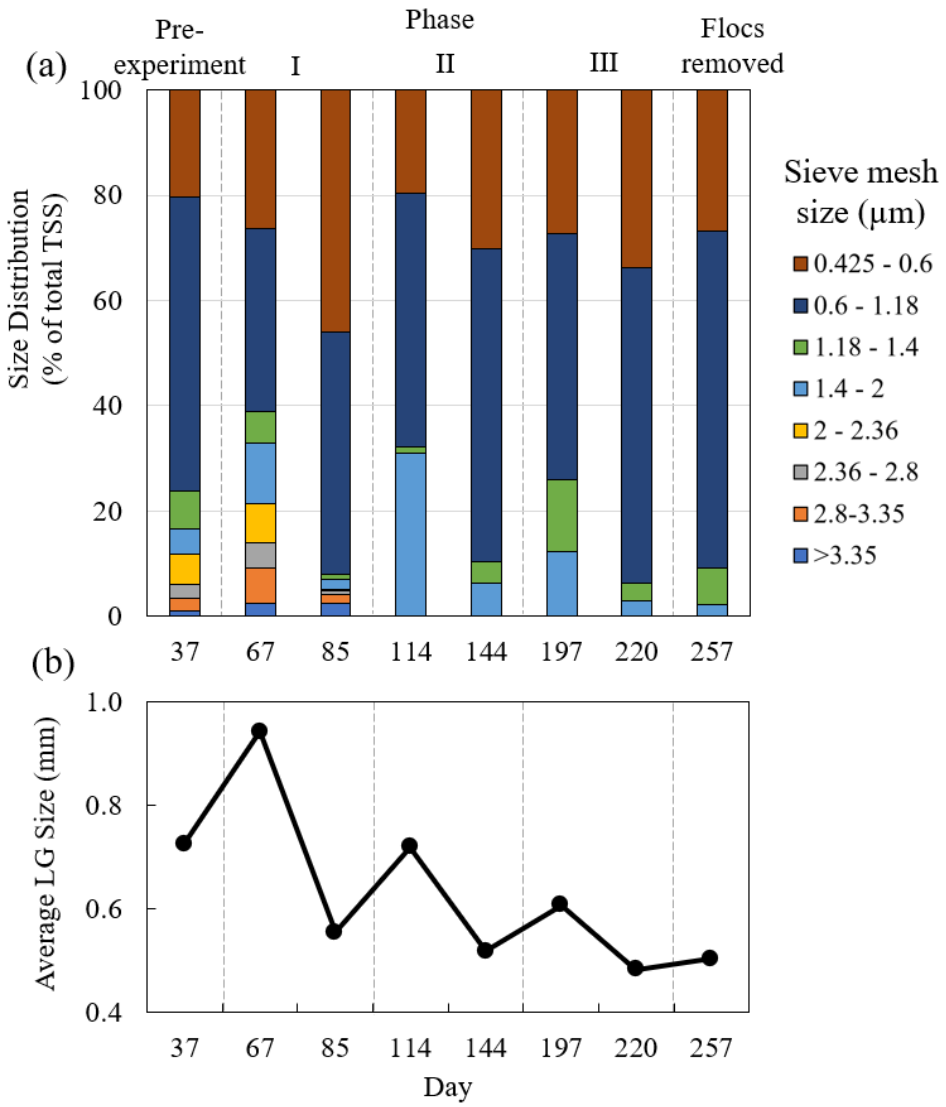

Fig. S6. (a) Size distributions of LG determined by sieving. (b) Average LG size calculated with: $\sum_1^n$(Fraction of sample total mass retained on sieve n)(Average size of opening of sieve n and sieve n − 1, mm).

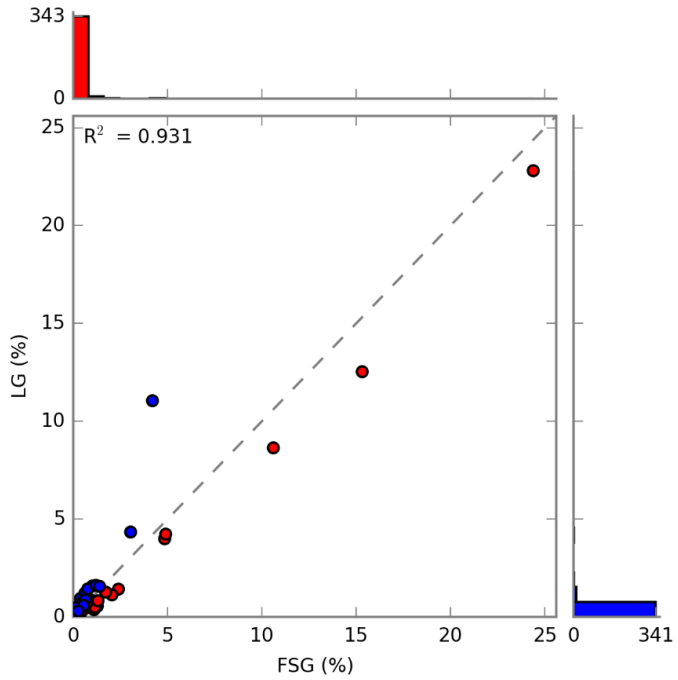

Fig. S7. STAMP scatter plot of the relative abundance profile of all 362 genera in FSG and LG. From this scatter plot, there is no clear evidence of any genus that is more enriched in LG or FSG. The bars on each side of the axis indicate the number of genera categorized in each relative abundance group. This plot illustrates that most of the genera are present in low relative abundance and are similar in LG and FSG.

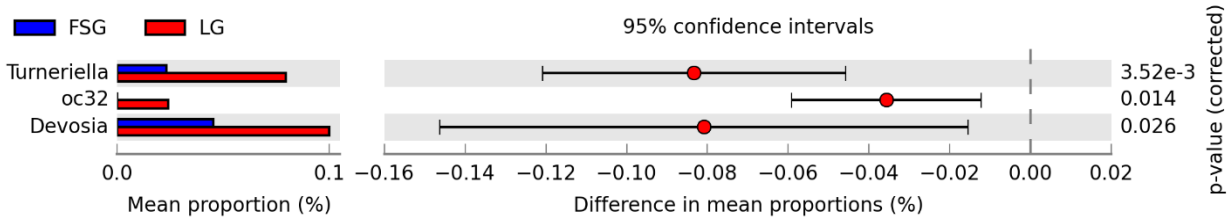

Fig. S8. STAMP plot of two-sided t-test analysis comparing the relative gene abundance profile between FSG and LG at the genus level. Most of the genera exhibited no statistical difference in relative gene abundance between LG and FSG. Only 3 out of the 362 genera (i.e., Turneriella, oc32, and Devosia) showed statistically higher abundance in the FSG than LG. Turneriella is a

member of the phylum Spirochaetes. The only isolate of the Turneriella genus is an aerobic chemoorganotrophic bacterium that grows on long-chain fatty acids and long-chain fatty alcohols (Picardeau). Oc32 is an uncultured AOB within the Nitrosomonadaceae family (Podlesnaya et al., 2020). Devosia is a Proteobacterium with variable ability to consume sugars among the different isolates (Yoon et al., 2007). There is not sufficient literature information to provide physiological explanations for the higher abundance of Turneriella, Devosia, and oc32 in the FSG versus LG. However, it is important to note that even though these three genera exhibited differences between FSG and LG, the magnitude of differences were low (<0.15%). This observation indicates that there is not enough evidence to support a clear physiological advantages of these three genera in one biomass fraction over the other.

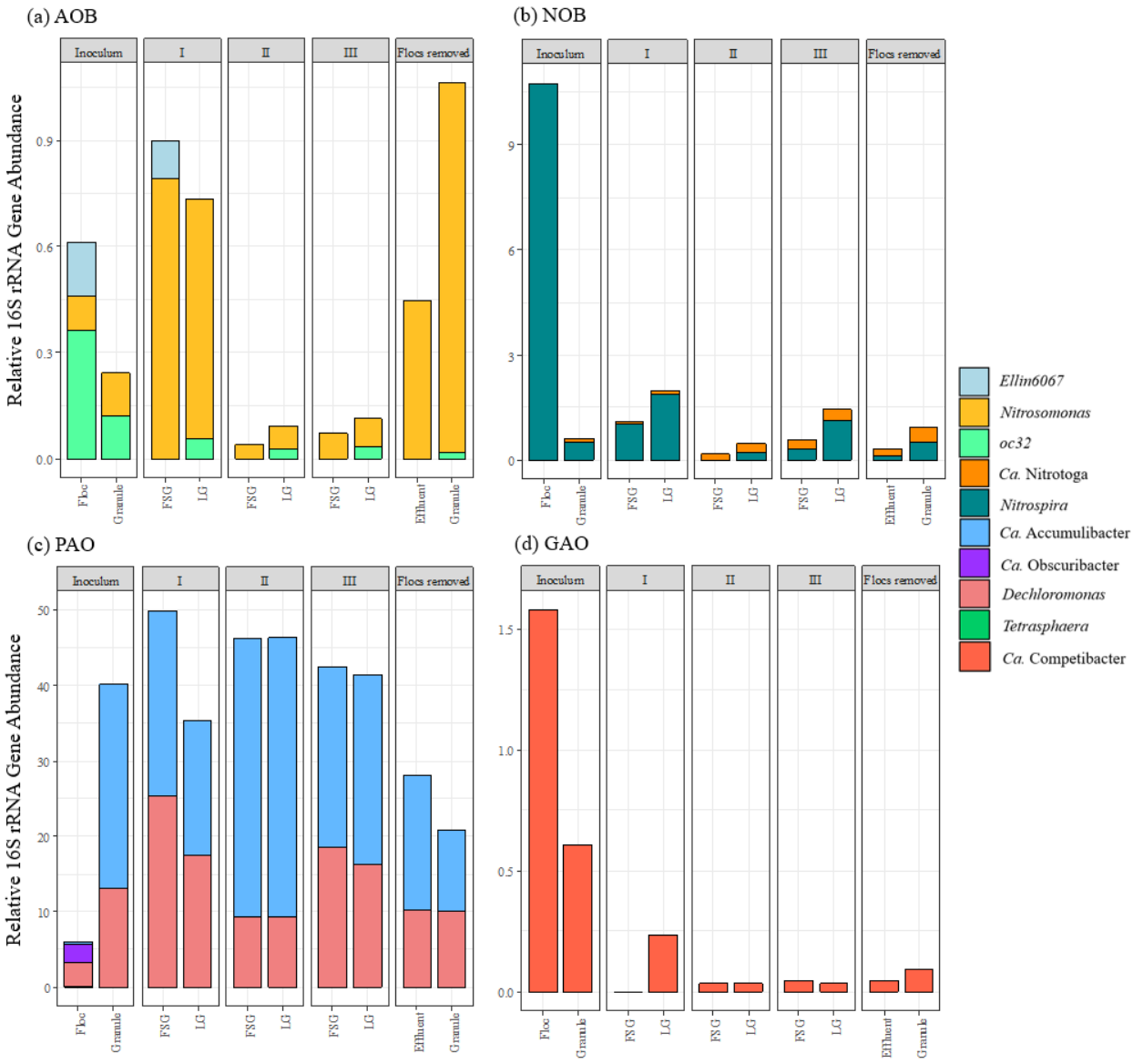

Fig. S9. Relative 16S rRNA gene abundance of putative (a) AOB, (b) NOB, (c) PAO, and (d) GAO detected in the system. The only AOB genus detected was *Nitrosomonas* (0.04–1.1%) while *Nitrospira* (0.0–10.8%) and *Candidatus* Nitrotoga (*Nitrotoga*) (0.0–0.45%) were the two NOB genera present. The putative PAOs *Tetrasphaera (0.06%)* and *Obscuribacter* (2.38%) were both present in the floc inoculum but undetected in the three experimental phases. During the experimental phases, the dominant putative PAOs were *Accumulibacter (*18.0–37.1%) and *Dechloromonas (*9.3–25.5%), while Competibacter (0.0–0.24%) was the only putative GAO

present. Some members of the *Dechloromonas* genus can also behave according to the GAO phenotype (Ahn et al., 2007; McIlroy et al., 2016). The relative abundances of *Dechloromonas* are commonly overestimated with 16S rRNA gene amplicon sequencing (Stokholm-Bjerregaard et al., 2017), partially due to its higher 16S rRNA gene copy numbers; for reference, *Dechloromonas* has 4 copies (accession no. NC_007298) versus the 2 for *Accumulibacter* (Martin et al., 2006). In EBPR systems treating complex wastewaters, *Tetrasphaera* is typically found at high abundance (up to 28%) (Lanham et al., 2013; Nielsen et al., 2019). The low abundance of *Tetrasphaera* in this study could be due to the VFA-based carbon feed that commonly enriches for *Accumulibacter* (Lanham et al., 2011; Lu et al., 2006), and the bias in standard DNA extraction procedures used in this study that results in underestimation of Gram-positive cells such as *Tetrasphaera* (Albertsen et al., 2015; Nielsen et al., 2019).

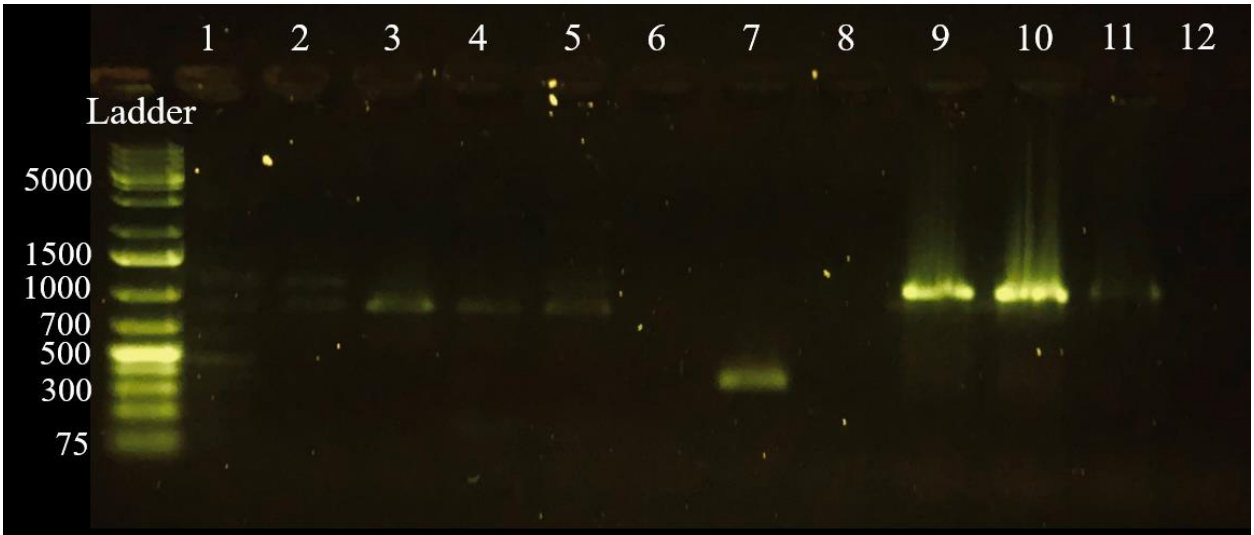

Lane	Sample	Primers	Note
1	Phase I FSG	cmx_amoB 148F/485R	
2	Phase II FSG	cmx_amoB 148F/485R	
3	Phase III FSG	cmx_amoB 148F/485R	
4	Phase I LG	cmx_amoB 148F/485R	
5	Phase II LG	cmx_amoB 148F/485R	
6	Phase III LG	cmx_amoB 148F/485R	
7	N. Inopinata culture	cmx_amoB 148F/485R	Positive control
8	DNA extraction with no biomass	cmx_amoB 148F/485R	Negative control
9	Phase I FSG	NTS 232F/1200R	
10	Phase I LG	NTS 232F/1200R	
11	N. Inopinata culture	NTS 232F/1200R	Positive control
12	DNA extraction with no biomass	NTS 232F/1200R	Negative control

Fig. S10. PCR amplification results to detect the presence of comammox. The primer set cmx_amoB 148F/485R for targeting comammox yielded bands with unexpected sizes for all experimental samples (lanes 1 - 6), whereas a clear band of expected size (337 bp) showed up for the positive control (lane 7). The primer set NTS 232F/1200R for targeting *Nitrospira* was used to confirm that this genus was present in the samples (lanes 9–10). The results indicated that members of the *Nitrospira* genus detected in this study were canonical NOB and not comammox.

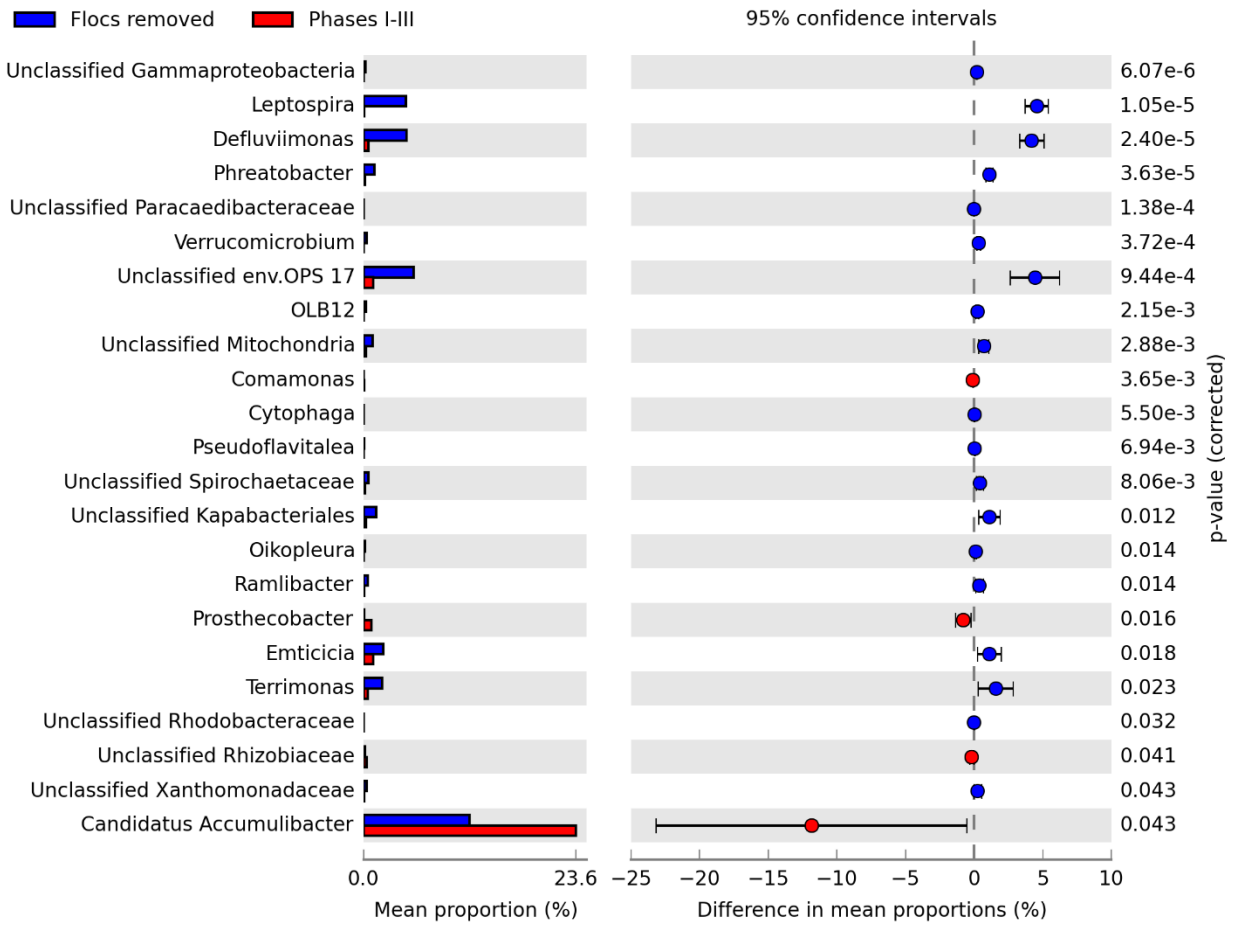

Fig S11. STAMP plot of two-sided t-test analysis comparing the relative gene abundance profile between Phases I – III and after terminating floc recycling. Genera displaying the most statistical difference included *Candidatus* Accumulibacter, *Leptospira*, *Defluviimonas*, and the unclassified env.OPS 17 (under the *Sphingobacteriales* order).

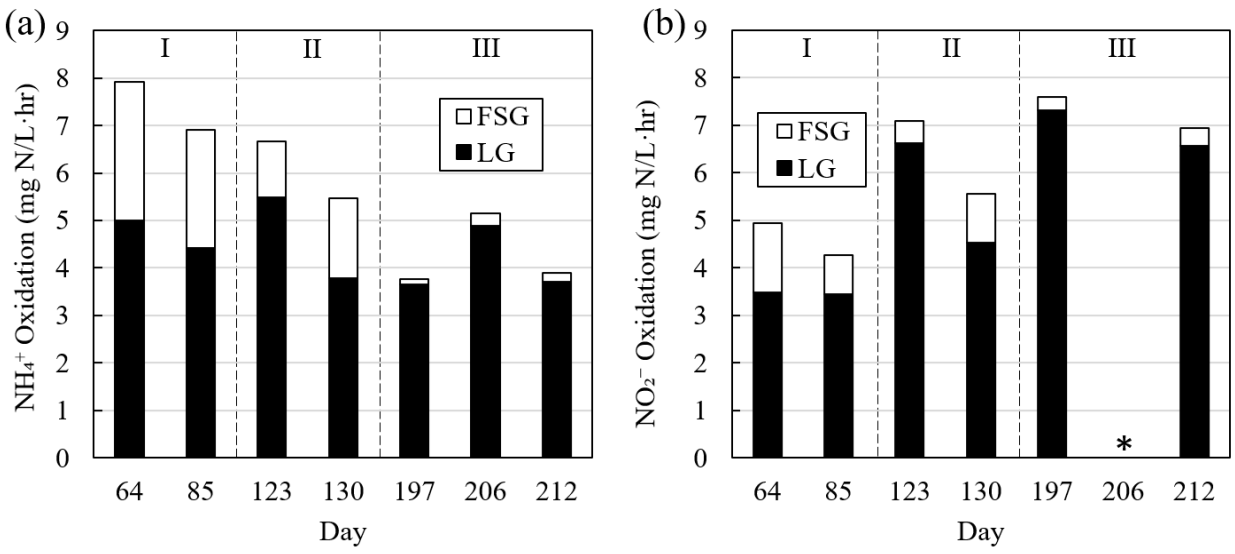

Fig. S12. Contribution of FSG and LG to the reactor's (a) ammonia oxidation capacity and (b) nitrite oxidation capacity, calculated based on the relative specific ammonia and nitrite oxidation rates and the MLVSS of FSG and LG. *Data on specific nitrite oxidation rate was not available on Day 206.

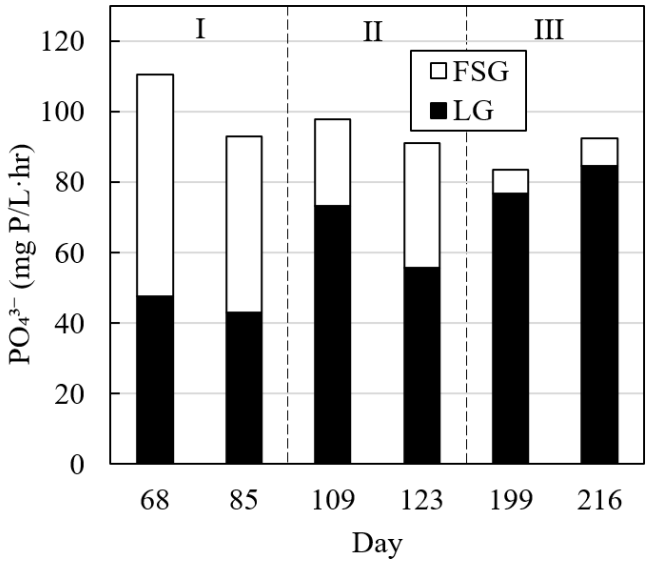

Fig. S13. Contribution of FSG and LG to the reactor's EBPR capacity, calculating based on the relative specific P release rates and the MLVSS of FSG and LG.

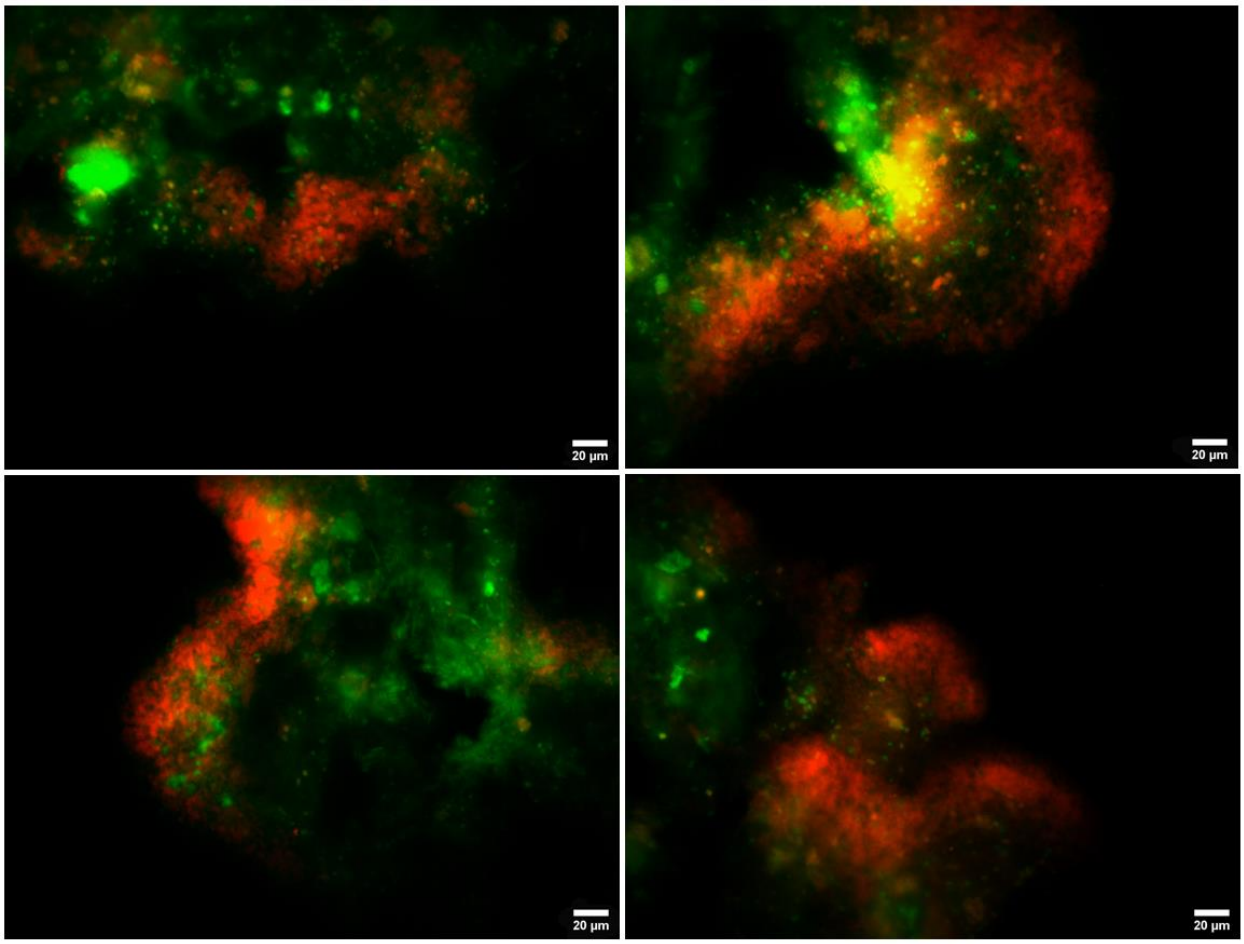

Fig. S14. FISH images of 25 µm-thick LG section collected on Day 131 (end of Phase II). Cy3 (red) = AOB (growing at granule periphery) and Fluorcein (green) = NOB (localizing behind AOB in deeper granules layers).

References

Ahn, J., Schroeder, S., Beer, M., McIlroy, S., Bayly, R.C., May, J.W., Vasiliadis, G., Seviour, R.J. 2007. Ecology of the microbial community removing phosphate from wastewater under continuously aerobic conditions in a sequencing batch reactor. *Applied and Environmental Microbiology*, **73**(7), 2257-2270.

Albertsen, M., Karst, S.M., Ziegler, A.S., Kirkegaard, R.H., Nielsen, P.H. 2015. Back to Basics - The Influence of DNA Extraction and Primer Choice on Phylogenetic Analysis of Activated Sludge Communities. *Plos One*, **10**(7).

Barr, J.J., Cook, A.E., Bond, P.L. 2010. Granule Formation Mechanisms within an Aerobic Wastewater System for Phosphorus Removal. *Applied and Environmental Microbiology*, **76**(22), 7588-7597.

Callahan, B.J., McMurdie, P.J., Rosen, M.J., Han, A.W., Johnson, A.J.A., Holmes, S.P. 2016. DADA2: High-resolution sample inference from Illumina amplicon data. *Nature Methods*, **13**(7), 581-+.

Cotto, I., Dai, Z., Huo, L., Anderson, C.L., Vilardi, K.J., Ijaz, U., Khunjar, W., Wilson, C., De Clippeleir, H., Gilmore, K., Bailey, E., Pinto, A.J. 2019. Long solids retention times and attached growth phase favor prevalence of comammox bacteria in nitrogen removal systems. *bioRxiv*, 696351.

Daims, H., Nielsen, J.L., Nielsen, P.H., Schleifer, K.H., Wagner, M. 2001. In situ characterization of Nitrospira-like nitrite oxidizing bacteria active in wastewater treatment plants. *Applied and Environmental Microbiology*, **67**(11), 5273-5284.

Figdore, B.A., Stensel, H.D., Winkler, M.K.H. 2018. Comparison of different aerobic granular sludge types for activated sludge nitrification bioaugmentation potential. *Bioresource Technology*, **251**, 189-196.

Figdore, B.A., Stensel, H.D., Winkler, M.K.H., Neethling, J.B. 2017. Aerobic Granular Sludge for Biological Nutrient Removal. Water Environment and Reuse Foundation.

Lanham, A.B., Moita, R., Lemos, P.C., Reis, M.A.M. 2011. Long-term operation of a reactor enriched in Accumulibacter clade I DPAOs: performance with nitrate, nitrite and oxygen. *Water science and technology*, **63**(2), 352-359.

Lanham, A.B., Oehmen, A., Saunders, A.M., Carvalho, G., Nielsen, P.H., Reis, M.A.M. 2013. Metabolic versatility in full-scale wastewater treatment plants performing enhanced biological phosphorus removal. *Water Research*, **47**(19), 7032-7041.

Lim, J., Do, H., Shin, S.G., Hwang, S. 2008. Primer and probe sets for group-specific quantification of the genera Nitrosomonas and Nitrosospira using real-time PCR. *Biotechnology and Bioengineering*, **99**(6), 1374-1383.

Lu, H.B., Oehmen, A., Virdis, B., Keller, J., Yuan, Z.G. 2006. Obtaining highly enriched cultures of Candidatus Accumulibacter phosphates through alternating carbon sources. *Water Research*, **40**(20), 3838-3848.

Lucker, S., Schwarz, J., Gruber-Dorninger, C., Spieck, E., Wagner, M., Daims, H. 2015. Nitrotoga-like bacteria are previously unrecognized key nitrite oxidizers in full-scale wastewater treatment plants. *Isme Journal*, **9**(3), 708-720.

Martin, H.G., Ivanova, N., Kunin, V., Warnecke, F., Barry, K.W., McHardy, A.C., Yeates, C., He, S.M., Salamov, A.A., Szeto, E., Dalin, E., Putnam, N.H., Shapiro, H.J., Pangilinan, J.L., Rigoutsos, I., Kyrpides, N.C., Blackall, L.L., McMahon, K.D., Hugenholtz, P. 2006.

Metagenomic analysis of two enhanced biological phosphorus removal (EBPR) sludge communities. *Nature Biotechnology*, **24**(10), 1263-1269.
McIlroy, S.J., Starnawska, A., Starnawski, P., Saunders, A.M., Nierychlo, M., Nielsen, P.H., Nielsen, J.L. 2016. Identification of active denitrifiers in full-scale nutrient removal wastewater treatment systems. *Environmental Microbiology*, **18**(1), 50-64.
Mobarry, B.K., Wagner, M., Urbain, V., Rittmann, B.E., Stahl, D.A. 1996. Phylogenetic probes for analyzing abundance and spatial organization of nitrifying bacteria. *Applied and Environmental Microbiology*, **62**(6), 2156-2162.
Nielsen, P.H., McIlroy, S.J., Albertsen, M., Nierychlo, M. 2019. Re-evaluating the microbiology of the enhanced biological phosphorus removal process. *Current Opinion in Biotechnology*, **57**, 111-118.
Nowka, B., Daims, H., Spieck, E. 2015. Comparison of Oxidation Kinetics of Nitrite-Oxidizing Bacteria: Nitrite Availability as a Key Factor in Niche Differentiation. *Applied and Environmental Microbiology*, **81**(2), 745-753.
Ong, Y.H., Chua, A.S.M., Lee, B.P., Ngoh, G.C., Hashim, M.A. 2012. An Observation on Sludge Granulation in an Enhanced Biological Phosphorus Removal Process. *Water Environment Research*, **84**(1), 3-8.
Park, H.D., Noguera, D.R. 2007. Characterization of two ammonia-oxidizing bacteria isolated from reactors operated with low dissolved oxygen concentrations. *Journal of Applied Microbiology*, **102**(5), 1401-1417.
Park, M.R., Park, H., Chandran, K. 2017. Molecular and Kinetic Characterization of Planktonic Nitrospira spp. Selectively Enriched from Activated Sludge. *Environmental Science & Technology*, **51**(5), 2720-2728.
Picardeau, M. Turneriella. in: *Bergey's Manual of Systematics of Archaea and Bacteria*, pp. 1-3.
Pijuan, M., Werner, U., Yuan, Z.G. 2011. Reducing the startup time of aerobic granular sludge reactors through seeding floccular sludge with crushed aerobic granules. *Water Research*, **45**(16), 5075-5083.
Podlesnaya, G., Krasnopeev, A.Y., Potapov, S., Tikhonova, I., Shtykova, Y.R., Suslova, M.Y., Timoshkin, O., Belykh, O. 2020. Diversity of nitrifying bacteria in microbial communities from water and epilithic biofilms of the Lake Baikal littoral zone. *Limnology and Freshwater Biology*, 1008-1010.
Stokholm-Bjerregaard, M., McIlroy, S.J., Nierychlo, M., Karst, S.M., Albertsen, M., Nielsen, P.H. 2017. A Critical Assessment of the Microorganisms Proposed to be Important to Enhanced Biological Phosphorus Removal in Full-Scale Wastewater Treatment Systems. *Frontiers in Microbiology*, **8**.
Verawaty, M., Pijuan, M., Yuan, Z., Bond, P.L. 2012. Determining the mechanisms for aerobic granulation from mixed seed of floccular and crushed granules in activated sludge wastewater treatment. *Water Research*, **46**(3), 761-771.
Vishniac, W., Santer, M. 1957. The thiobacilli. *Bacteriological Reviews*, **21**(3), 195.
Weissbrodt, D.G., Neu, T.R., Kuhlicke, U., Rappaz, Y., Holliger, C. 2013. Assessment of bacterial and structural dynamics in aerobic granular biofilms. *Frontiers in Microbiology*, **4**.
Winkler, M.K.H., Bassin, J.P., Kleerebezem, R., de Bruin, L.M.M., van den Brand, T.P.H., van Loosdrecht, M.C.M. 2011. Selective sludge removal in a segregated aerobic granular biomass system as a strategy to control PAO-GAO competition at high temperatures. *Water Research*, **45**(11), 3291-3299.

Winkler, M.K.H., Boets, P., Hahne, B., Goethals, P., Volcke, E.I.P. 2017. Effect of the dilution rate on microbial competition: r-strategist can win over k-strategist at low substrate concentration. *Plos One*, **12**(3).

Winkler, M.K.H., Kleerebezem, R., Strous, M., Chandran, K., van Loosdrecht, M.C.M. 2013. Factors influencing the density of aerobic granular sludge. *Applied Microbiology and Biotechnology*, **97**(16), 7459-7468.

Wu, C.Y., Peng, Y.Z., Wang, S.Y., Ma, Y. 2010. Enhanced biological phosphorus removal by granular sludge: From macro- to micro-scale. *Water Research*, **44**(3), 807-814.

Yoon, J.-H., Kang, S.-J., Park, S., Oh, T.-K. 2007. Devosia insulae sp. nov., isolated from soil, and emended description of the genus Devosia. *International Journal of Systematic and Evolutionary Microbiology*, **57**(6), 1310-1314.

Chapter 4.

Application of Aerobic Kenaf Granules for Biological Nutrient Removal in a Full-scale Continuous Flow Activated Sludge System

Abstract

Aerobic granular sludge (AGS) is a biofilm technology that offers more treatment capacity in comparison to activated sludge. The integration of AGS into existing continuous-flow activated sludge systems is of great interest as process intensification can be achieved without the use of plastic-based biofilm carriers. Such integration should allow good separation of granules/flocs and ideally with minor retrofitting, making it an ongoing challenge. This study utilized an all-organic media carrier made of porous kenaf plant stalks with high surface areas to facilitate biofilm attachment and granule development. A 5-stage Bardenpho plant was upgraded with the addition of kenaf media and a rotary drum screen to retain the larger particles from the secondary clarifier underflow whereas flocs were selectively wasted. Startup took 5 months with a sludge volume index (SVI) reduction from >200 to 50 mL g^{-1}. Most of the kenaf granules fell in the size range of 600-1400 µm and had a clear biofilm layer. The wet biomass density, SVI_{30}, and SVI_{30}/SVI_5 of the kenaf granules were 1035 g L^{-1}, 30.6 mL g^{-1}, and 1.0, respectively, which met the standards of aerobic granules. Improved stability of biological phosphorus removal performance enabled a 25% reduction in sodium aluminate usage. Microbial activities of kenaf granules were compared with aerobic granules, showing comparable N and P removal rates and presence of ammonium-oxidizing bacteria and polyphosphate-accumulating organisms in the outer 50–60 µm layer of the granule. This work is the first viable example for integrating fully

organic biofilm particles in existing continuous-flow systems.

Published as:

Wei, S. P., B. Nguyen Quoc, M. Shapiro, P. H. Chang, J. Calhoun and M. K. H. Winkler (2021). "Application of aerobic kenaf granules for biological nutrient removal in a full-scale continuous flow activated sludge system." Chemosphere **271**: 129522.

4.1 Introduction

With the growing world population, sustainable wastewater treatment and environmental preservation are faced with increasing challenges, such as the need for wastewater treatment plants (WWTP) to add treatment capacity while being limited in space and resources (Winkler & Straka, 2019). The use of biofilm technologies such as aerobic granular sludge (AGS) has been an effective way to intensify existing wastewater infrastructure. Aerobic granules are dense spherical biofilm aggregates with high thickening and fast settling characteristics, thus its application can result in significant reduction in footprint and energy demand (Pronk et al., 2015). In contrast to other attached-growth biofilm technologies, such as the integrated fixed film activated sludge process, aerobic granules are naturally occurring biofilms which do not grow on plastic carriers that need to be landfilled.

AGS systems have been well-demonstrated in sequencing batch reactors (SBR) and a critical limitation of an SBR-type AGS system is that it requires tall reactors to enable good separation of slow and fast settling particles. Such configuration is therefore not easily retrofittable into continuous flow activated sludge (CFAS) systems without major modifications and sometimes decommissioning of the existing plant. Many lab-scale studies have cultivated granules in continuous-flow reactors, but they mostly rely on some variations of complex settler design to incorporate fast washout as a selection pressure for granule growth (Kent et al., 2018), which is not convenient to implement in existing full-scale CFAS plants. The use of seeding material (e.g. crushed granules or granular activated carbon) has been shown to enhance the granulation process by acting as nucleation sites for bacterial attachment (Li et al., 2011; Pijuan et al., 2011), which could be applied in CFAS systems to facilitate granule growth. However, seeding with

granules is not always feasible for full-scale application because aerobic granules can take a long time to cultivate and are generally not available in large quantities. An attractive alternative would be an organic carrier that does not rely on plastic material or need to be cultivated beforehand. Organic carriers provide similar benefits as plastic carriers (e.g., increased treatment capacity in existing infrastructure), but are organic and may therefore undergo anaerobic digestion for sludge stabilization and resource recovery whereas plastic carriers must be land-filled.

In a CFAS system with integrated granular sludge, flocs and granules coexist and compete for substrates. Therefore, the proposed strategies for facilitating and maintaining granule growth in a CFAS system is to provide selective feeding of organic substrate to the granules and control granular sludge at higher sludge retention time (SRT) than flocculent sludge. To achieve these selective advantages for the granules, the physical separation of granules and flocs is key and research is currently focusing on sieving, hydraulic separators, or hydrocyclones (Kent et al., 2018; Sturm et al., 2017). In this work, a lignocellulosic carrier media made from kenaf plant (kenaf media) was seeded into a full-scale CFAS WWTP to facilitate biofilm attachment. Along with flocs, the kenaf media flow freely to the secondary clarifier, from which the underflow was separated into flocculent and kenaf particulate sludge with a rotary drum screen. Kenaf particles were then recycled back to the oxidation ditch and retained in the system while flocs were wasted.

The objectives of this study were to (1) explore the feasibility of the integration of granular sludge technology at an existing full-scale CFAS plant by seeding organic kenaf based carriers

and retaining large particles, (2) discuss the improvements in settling and biological nutrient removal capacities, and (3) compare the developed kenaf biofilm particulates with aerobic granules in terms of physical characteristics and activities of key microbial functional groups.

4.2 Methods

4.2.1 Plant description and upgrade

The Town of Moorfield Advanced Nutrient WWTP (WV, USA) (Plant) is a 15.5 MLD 5-stage Bardenpho plant treating roughly 10% municipal wastewater and 90% industrial wastewater from a local poultry manufacturing facility. The averaged influent data are shown in Table S1 and the time series concentrations and loading are provided in Fig. S1 and Fig. S2, respectively. The Plant was upgraded with the Nuvoda's Mobile Organic Biofilm (MOB™) process, which involved the addition of organic media carriers made of kenafs to the oxidation ditch. To aid the adaptation of the MOB™ process, other plant-specific upgrades were made, including a 68 m^3 h^{-1} rotary drum screen (mesh size 500 μm), a 3.8 m^3 waste activated sludge (WAS) holding tank, and a belt filter press dewatering system (**Figure 4-1**). Upon completion of the construction (March 9th, 2017), a single seeding event of about 50,325 kg of kenaf media was added directly to the oxidation ditch for a target fill ratio of 0.0033 kg of media per L of reactor volume. Flow from the oxidation ditch exited via a weir and moved to the center well of the secondary clarifiers. After the secondary clarifier underflow, a rotary drum screen was installed within the existing WAS line, which received on average 2.08 ML per week of flow. The cake (kenaf particles) from the rotary screen was returned to the reaeration zone of the ditch by gravity while the filtrate (flocs) was directed to sludge handling. As a result, only flocculent sludge was wasted

from the system whereas kenaf particles were retained to ensure sufficient retention time for bacterial attachment and biofilm development on the kenaf particles. The dissolved oxygen (DO) setpoint in the aerobic zone was 0.35-0.5 mg L^{-1}. Sodium aluminate was dosed at a constant speed at the primary clarifier for chemical phosphorus removal, and the feed was manually increased whenever effluent TP raised above 0.7 – 0.8 mg L^{-1} for a few days. Supplemental carbon (glycerin) was added in the post-anoxic zone based on a nitrate sensor (Hach Nitratax sc) to maintain a nitrate level below 3.5 mg L^{-1}.

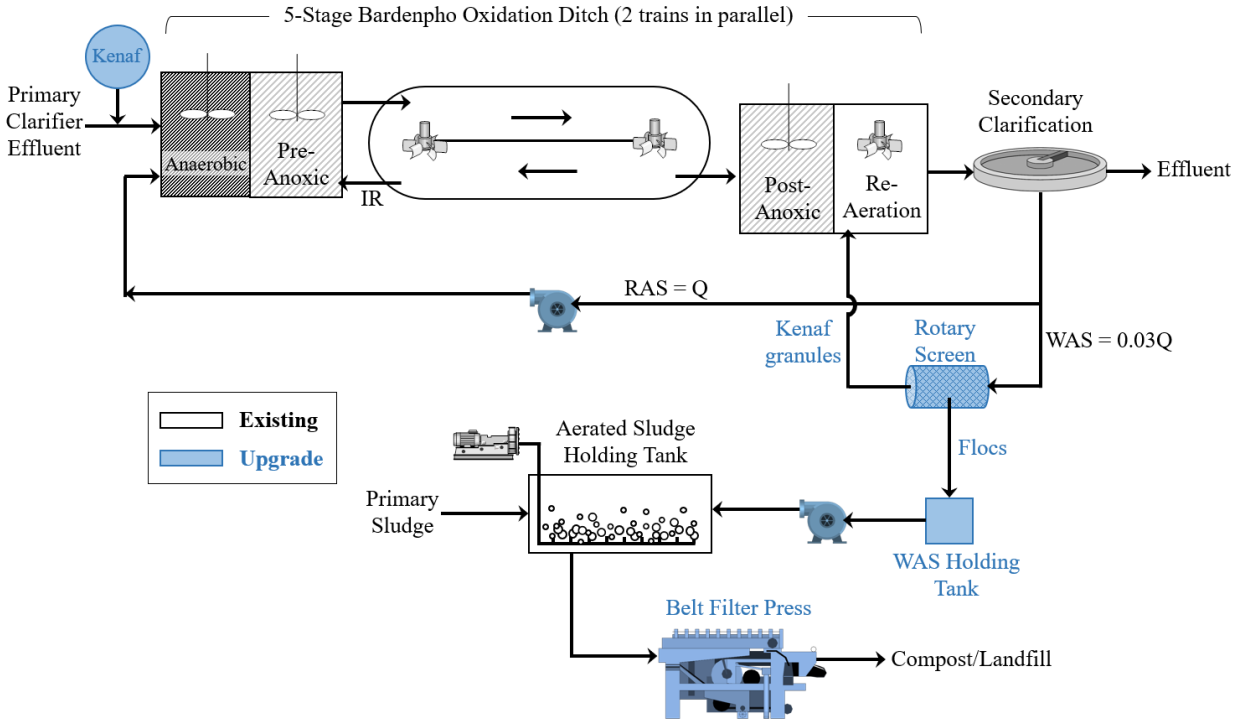

Figure 4-1. Process schematic of the Town of Moorefield Advanced Nutrient WWTP.

The kenaf media was made of renewable lignocellulosic material harvested from the kenaf plant, *Hibiscus cannabinus*, which was grown and processed at a local farm in Cameron, NC (USA). The kenaf media is approximately 1 mm in size with an estimated outer specific surface area (SSA) of greater than 20,000 m^2 $(m^3)^{-1}$ and total SSA greater than 463,000 m^2 $(m^3)^{-1}$ (Fig. S3a).

Kenaf is a fast-growing plant with high adaptation to wide range of climate conditions (Ramesh, 2016). Like other natural plant fibers, it is considered a renewable material due to its high crop yield, minimal energy requirements, and biodegradability (Akil et al., 2011).

4.2.2 Plant data and sample collection

Twenty-four months of process data (twelve months each before and after the upgrade) was collected from the plant, which included 3 or 4 measurements per week of influent and effluent flows, BOD, TP, and NH_4^+, as well as effluent TN, NO_2^-, and NO_3^-. Weekly MLSS and monthly SVI_{30} were determined from grab samples collected from the oxidation ditch at about 4 ft from the surface (1/4 of the ditch height). TSS of secondary clarifier's underflow and effluent were measured weekly and once a month, respectively. After more than two years since the upgrade, two mixed liquor samples were collected (in May and June 2019) from the oxidation ditch and shipped overnight on ice to the University of Washington. The first sample was used for physical characteristic analyses and microscopic imaging (Section 4.2.3, 4.2.4, 4.2.7, 4.2.8) and the second sample was used for biomass-specific activity tests (Section 2.5). Morphologies of the kenaf particulates were observed at 6X-10X magnification under a Zeiss Stemi 508 stereomicroscope in dark field mode.

4.2.3 Wet biomass density

Density of mixed liquor sample (flocs + kenafs) and kenafs only (screened with a 212-µm sieve) were measured with a pycnometer similar to previous research (Winkler et al., 2012a). Briefly, weight of the empty pycnometer (M_{pyc}) and pycnometer filled with water (M_{pyc+w}) were first determined. Free water in the samples was removed by passing the samples through a 0.45 µm glass filter. Using a spatula, the cake (wet biomass) retained on the filter was transferred to the

empty pycnometer and together the weight was measured (M_{pyc+b}). The pycnometer with the inserted biomass was then filled with water and the weight was determined ($M_{pyc+b+w}$). Density of the wet biomass was then calculated using Eq. 1:

$$\rho_b = \frac{M_b}{V_b} = \frac{M_{pyc+b} - M_{pyc}}{\frac{M_{pyc+w} - M_{pyc}}{\rho_w} - \frac{M_{pyc+b+w} - M_{pyc+b}}{\rho_w}} \qquad \text{Eq. 1}$$

Where:

ρ_b = density of biomass, g L^{-1}

m_b = mass of biomass, g

V_b = volume of biomass in pycnometer, L

M_{pyc+b} = mass of pycnometer containing biomass, g

M_{pyc} = mass of pycnometer, g

$M_{pyc+b+w}$ = mass of pycnometer containing biomass and water, g

ρ_{water} = density of water at temperature of experiment, g L^{-1}

4.2.4 Particle Size Distribution

The particle size distribution of the mixed liquor sample was determined with sieve analysis. Samples were passed through a series of sieves (3-in diameter) with various mesh sizes (van Loosdrecht et al., 2016). Starting from the sieve with the largest mesh size, a sample was passed through and only particles larger than the mesh size were retained. Gentle washing with DI water was done to help push through any particles smaller than the mesh size. All water and solids

passing through the sieve were captured and the procedure was repeated with all the remaining sieves in order of reducing mesh sizes. Solids captured on each sieve was then backwashed into an individual beaker per granule size fraction and the g of TSS was measured per Section 4.2.6. The particle size distribution was determined by g TSS of each size over the sum of g TSS of all sizes.

4.2.5 Specific activity tests

Specific activity tests were performed to measure the ammonia oxidation, phosphorus release, phosphorus uptake, and heterotrophic denitrification activities. All tests were conducted using separate aliquots of the same mixed liquor sample collected in June 2019. Before each activity test, the mixed liquor sample was first aerated for 1.5 – 2 hours at room temperature. A 425-µm sieve was used to screen out the flocs in the mixed liquor to ensure only large biofilm particulates (kenaf particles) were used. The kenafs were then aerated for another 15 mins in a media consisting of 44 mg L^{-1} $MgSO_4 \cdot 7H_2O$, 17.5 mg L^{-1} KCl, and 0.5 mL of Vishniac trace element solution (Vishniac & Santer, 1957). The tests were conducted in 500-mL graduated cylinders with liquid volume of 200 mL at 20°C in biological duplicates (e.g., two individual mixed liquor aliquots were subjected to the same procedures for measuring ammonia oxidation in two separate cylinders). The g of VSS in each cylinder was determined at the end of the test. For ammonia oxidation activity, 30 mgN L^{-1} of NH_4^+ was spiked into the cylinder and NH_4^+ concentrations were monitored over time while sparged with air. 0.01M of phosphate buffer was added to control pH at 7.39 ± 0.02. For the P release activity test, the cylinders were first sparged with N_2 gas for about 10 mins then spiked with 150 mgCOD L^{-1} of acetate. PO_4^{3-} and acetate concentrations were monitored over time while sparged with N_2 gas. Immediately after the P release test, granules were transferred into new media free of acetate for the P uptake activity

test. Transferring was done with N_2-parged water to provide anaerobic starting conditions. Samples were then aerated and once the DO reached saturation, 100 mg L^{-1} PO_4^{3-}-P and 6 mg L^{-1} NH_4^+-N were spiked into the cylinders. PO_4^{3-} concentrations were monitored over time while sparged with air. For heterotrophic denitrification test, the cylinders were sparged with N_2 gas first for 10 mins then spiked with 150 mgCOD L^{-1} of acetate, 30 mg L^{-1} of NO_3^--N and 6 mg L^{-1} NH_4^+-N. Concentrations of COD and NO_3^- were monitored over time while sparged with N_2 gas.

4.2.6 Analytical Methods

Suspended and volatile solids (TSS and VSS) were analyzed according to Standard Methods 2540D and 2540E. The SVI_5 and SVI_{30} (mL g^{-1}) were determined from the settled volume (mL) of a mixed liquor sample, after 5 and 30 min settling in a 1-L graduated cylinder, divided by g TSS. Using the Gallery™ Automated Photometric Analyzer and the Gallery™ system reagents (all by Thermo Fisher Scientific), concentrations of NH_4^+, NO_2^-+NO_3^-, NO_2^-, and PO_4^{3-} were measured according to ISO 15923-1, EPA 353.1, EPA 354.1, and EPA 365.1, respectively. Acetate concentrations were analyzed using the ion-chromatography Dionex ICS-5000 system with the IonPac® ICE-AS6 column (both by Thermo Fisher Scientific).

4.2.7 Determination of biomass fraction of kenaf particles

Kenaf biofilm particles (screened with a 212-µm sieve) were sparged with air for 1 hour and stained with 1.5 µl of SYTO™ 9 Green Fluorescent Nucleic Acid Stain (Thermo Fisher Scientific) per mL of cellular content, then incubated in dark for 15 minutes. Z stacks were used to image cross sections throughout the biofilm particles. To confirm z-stack cross section, a 100 µm section was sliced from a kenaf particle using a cryostat (Thermo Scientific CryoStar NX50). Staining and microscopy were done on the section following the same protocol as the whole

biofilm particles. A total of 4 z-stack images and 1 cryotome-sliced image were obtained from 2 kenaf particles. Software processing to determine biomass volume fractions was done for all 5 images using ImageJ.

4.2.8 Fluorescence in-situ hybridization (FISH)

Water was first removed from the mixed liquor sample by centrifugation and removal of supernatant. Then, the pellet was resuspended in 4% paraformaldehyde and let sit on ice for 120 mins. The paraformaldehyde was washed off by centrifugation, removal of supernatant, and resuspension in 1x PBS. The final resuspension was in an ethanol and PBS solution at 1.25:1 volumetric ratio and stored at -20 °C. Kenaf biofilm particulates were frozen in a tissue freezing medium at -20 °C and cut into slices of 25-µm thickness using a cryostat (Thermo Scientific CryoStar NX50). Kenaf slices were adhered onto gelatin-coated microscopic glass slides. The slices were then dried at 46°C and dehydrated with subsequent (3 min each) 50%, 80%, and 98% ethanol concentrations. For each well, 10 µL of hybridization buffer solution was added consisting of 0.9 M NaCl, 0.02 M Tris-HCl (pH 8.0), 35% formamide, and 0.02% sodium dodecyl sulfate (SDS). Subsequently, 1 µL of 5 µM probe mix was added for each well. The FISH probe mix included PAO462/PAO651/PAO846 for targeting *Candidatus* Accumulibacter (Crocetti et al., 2000) and NSO190/NSO1225 for targeting ammonia oxidizing bacteria (AOB) (Mobarry et al., 1996) (sequences are listed in Table S2). A recent study evaluated the widely used FISH probes for targeting ammonia oxidizing betaproteobacteria *(β*-AOB) and offered newly designed probes with better or similar coverage as the established probes (Lukumbuzya et al., 2020). For the *β*-AOB probes used in this study, Lukumbuzya et al. (2020) showed that NSO190 covers *β*-AOB incompletely whereas NSO1220 still offers excellent coverage. Hybridization step took place in a humid chamber at 46°C overnight. Immediately after

hybridization, the un-hybridized probes were washed off with a washing buffer (pre-heated to 48°C) consisting of 20 mM Tris-HCl (pH 8), 0.08 mM NaCl, 5 mM EDTA (pH 8.0), and 0.01% SDS. Washing was performed by first rinsing with the washing buffer and then immersing the slide into the washing buffer for 20 min. After a final rinse with milliQ water and air drying at room temperature, antifade fluorescent mounting medium (20 mM Tris at pH 8.0, 0.5% N-propyl gallate, and 90% glycerol) with 0.05 µg L^{-1} of DAPI was added to each well and covered with a cover slip. Slide was observed using a confocal microscope (Zeiss Axioskop 2 MOT) fitted with a Zeiss Axiocam 503 mono camera.

4.3 Results and Discussion

4.3.1 Startup and system performance

4.3.1.1 Improved treatment capacity

Once operations started in early March of 2017, there was a gradual decrease in mixed liquor SVI_{30} from >200 mL g^{-1} to below 50 mL g^{-1} in about 5 months (**Figure 4-2a**), which is similar to the startup time to reach mature granulation at pilot- or full-scale AGS facilities (Pronk et al., 2015; Pronk et al., 2017; Wagner et al., 2015). In contrast to systems using plastic carriers, which requires a screen to retain the carriers inside the aeration basin to avoid operational issues, the kenaf biofilm particles can convey freely into the secondary clarifiers to improve settling performance and lower the effluent TSS (**Figure 4-2c**). Before the upgrade, the SRT of the Plant was 26.5 ± 6.8 days. After the MOB™ process started, the average solids concentrations of the clarifier underflow (**Figure 4-2b**) and WAS flowrate (2.08 ML $week^{-1}$) did not vary over time, but only solids that passed through the rotary drum screen (flocs) were wasted and kenaf particles were retained in the system. As a result, the kenaf and flocculent SRTs were decoupled.

However, how much the SRTs were decoupled was unknown because the Plant's measurements on MLSS and waste solids did not separate kenaf particles and flocs, and thus it is recommended to obtain additional measurements to reflect the separation of SRTs. After the upgrade, less solids were wasted as kenaf biofilm particles were retained, which should ultimately lead to higher MLSS concentrations. However, the Plant reported lower MLSS (4005 ± 818 mg L^{-1}) after the upgrade in comparison to before (5655 ± 576 mg L^{-1}) (Fig. S4). In SBR-type AGS systems, it is common that the MLSS at the bottom is higher than the MLSS at the top of the reactor because the larger granules are too heavy to be evenly suspended and tend to concentrate on the bottom (Pronk et al., 2014; Winkler et al., 2011b). Such phenomenon likely occurred at this plant as well and due to the sampling location being near the top (4ft from the surface), the mixed liquor sample collected may have under-represented the actual MLSS in the oxidation ditch, emphasizing the need for better mixing, sampling, and sludge management procedures in granule type systems.

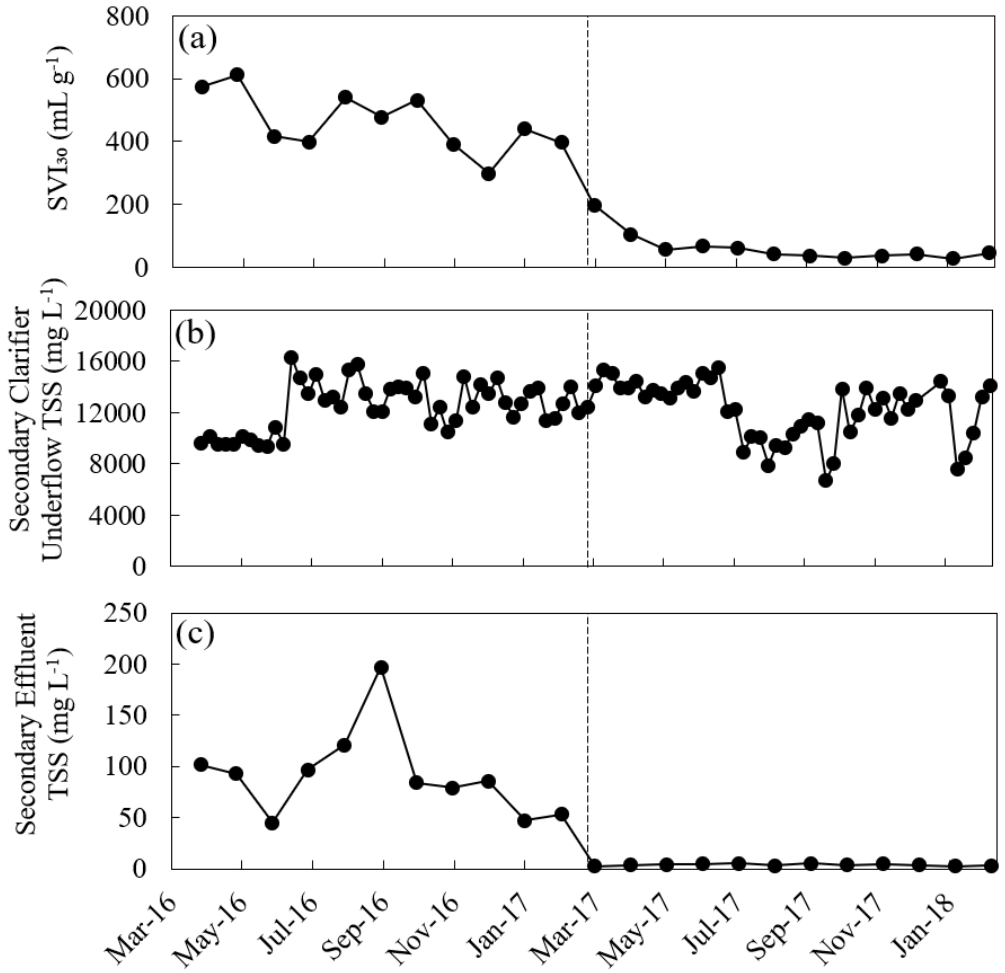

Figure 4-2. (a) Monthly SVI_{30}, (b) weekly secondary clarifier underflow TSS, and (c) monthly secondary effluent TSS; dashed vertical line indicates time of upgrade.

4.3.1.2 EBPR and nitrification capacity

There were minimal variations in influent TP loading (Fig. S2) and effluent TP concentrations (**Figure 4-3a**) before versus after the upgrade, but there was an obvious 25% reduction in the average sodium aluminate usage from 61,000 to 46,000 kg $month^{-1}$ (Fig. S5). The amount of sodium aluminate (added at the primary clarifier) was manually adjusted depending on the biological P removal performance at the oxidation ditch (based on the effluent TP concentrations), and thus a decrease in chemical usage indicated an increase in the enhanced

biological phosphors removal (EBPR) capacity. This improvement was likely due to buildup of polyphosphate-accumulating organism biomass from the increase of solids inventory that intensified the treatment capacity of existing infrastructure. In addition, biofilm systems are more tolerant to pH/temperature shocks and inhibitory substances in comparison to flocculent sludge due to shielding of microorganisms within the protective biofilm structure (Liu et al., 2015; Lourenco et al., 2015; Pronk et al., 2015). As the nitrogen loading was already below the capacity prior to the upgrade, there was no obvious changes in the nitrogen removal efficiency after the addition of kenaf carriers (**Figure 4-3** and **Figure 4-3**). The elevated effluent ammonia and nitrate/nitrite concentrations during the Winter months of 2017 might be due to a system upset in combination with low temperature, which led to a reduction in biofilm area specific removal rates. The performance recovered toward the start of Spring. Previous research had demonstrated that in a flocculent system with minimal nitrification capacity (low temperature and SRT), high ammonia oxidation efficiency can be achieved by bioaugmentation with granules (Figdore et al., 2018). Such system requires that granules be separated from flocs and retained in the system, which is feasible with the kenaf particles and rotary drum screen as shown in this study. Therefore, it is expected that the Plant can handle higher future nitrogen loading with the integration of mobile kenaf biofilm particles.

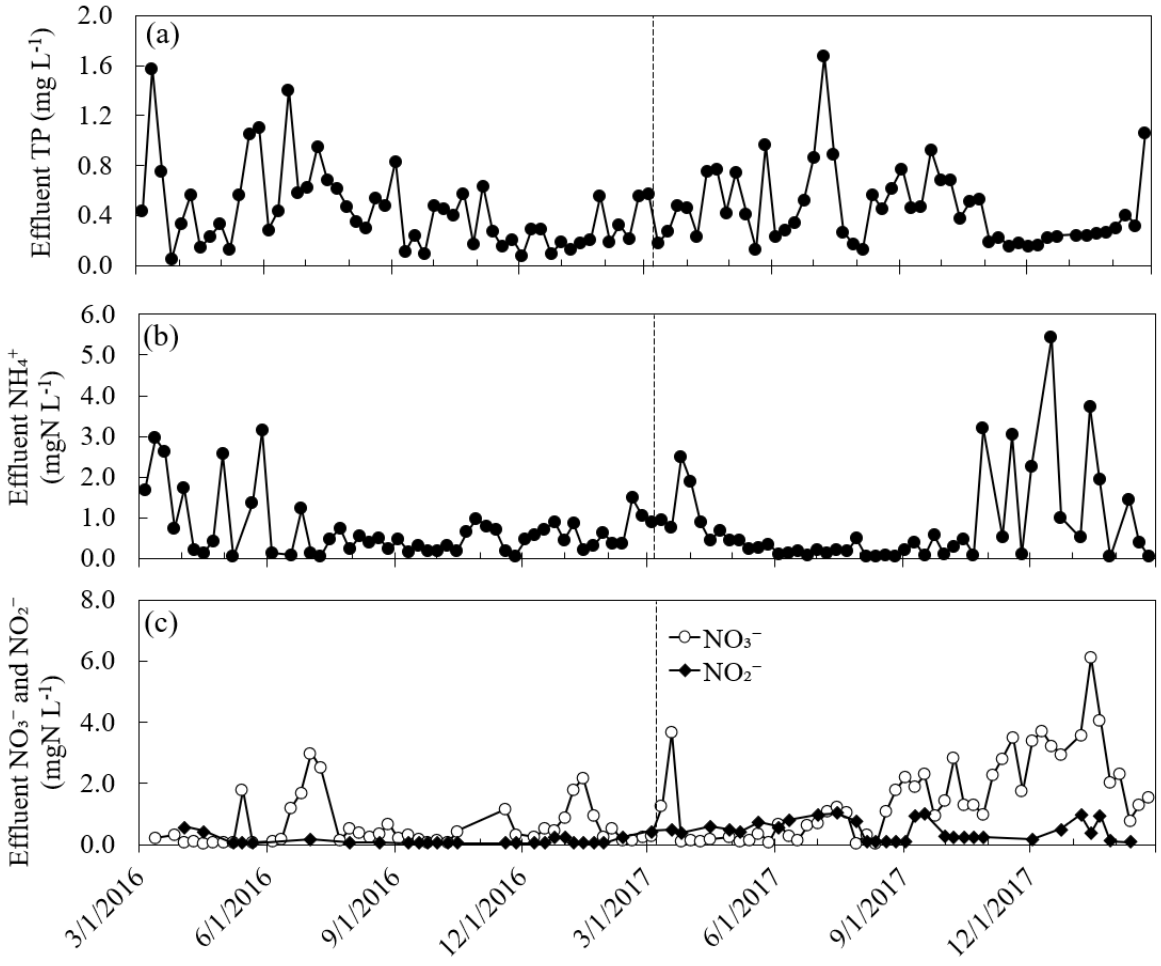

Figure 4-3. Weekly average effluent (a) TP, (b) NH_4^+, and (c) NO_3^-/NO_2^- concentrations; dashed vertical line indicates time of upgrade.

4.3.2 Physical characteristics of kenaf biofilm particulates

After more than two years since the upgrade, the kenaf particles were collected for further examinations. The kenafs had clear development of biofilm on the surface (Fig. S3b) and the cylindric-oval structure and smooth surface indicated granular morphologies (**Figure 4-4**). Microscopic image of a 25-µm thick biofilm section showed a fibrous interior structure covered by an outer bacterial layer with an average thickness of 75 µm (Fig. S6). The mechanisms of biofilm growth on the kenaf particles were not studied but according to literature, the key

processes for biofilm development likely involved cell attachment onto the media surface, microbial adhesion enhancement by production of extracellular polymeric substances, and expansion of microcolonies and biofilm matrix (di Biase et al., 2019; Winkler et al., 2018). Particles size distribution analysis showed that the majority (60%) of the kenaf granules fell in the size range of 600-1400 µm and flocs (<212 µm) accounted for 13% of the total TSS (Fig. S7). The density of mixed liquor was 1032 ± 0.4 g L^{-1} while the density for kenaf granules alone was slightly higher at 1035 ± 0.9 g L^{-1}. These densities are on the high end in comparison to values measured for lab-scale aerobic granules cultivated in EBPR SBRs, which vary from 1004 ± 4 to 1018 ± 13 g L^{-1} for granules enriched with glycogen-accumulating organisms (GAO) and polyphosphate-accumulating organisms (PAO), respectively (Winkler et al., 2011a). The higher density of the kenaf granules may be attributed to the high specific gravity of 1.059 of the media. Kenaf granules alone exhibited similar settling characteristics to granular sludge with an SVI_{30} of 30.6 mL g^{-1} and SVI_5/SVI_{30} ratio of 1.0. Interestingly, there appears to be the presence of semi-spherical granules as opposed to the elongated morphologies of the kenaf particles (**Figure 4-4**). It has been shown in previous research that in continuous-flow systems, there is a constant exchange of biomass between granules and flocs where they undergo dynamic processes of aggregation, attachment, and breakage (Zhou et al., 2014). Therefore, it is possible that these semi-spherical aggregates were formed by biofilm detachment from the kenaf granules.

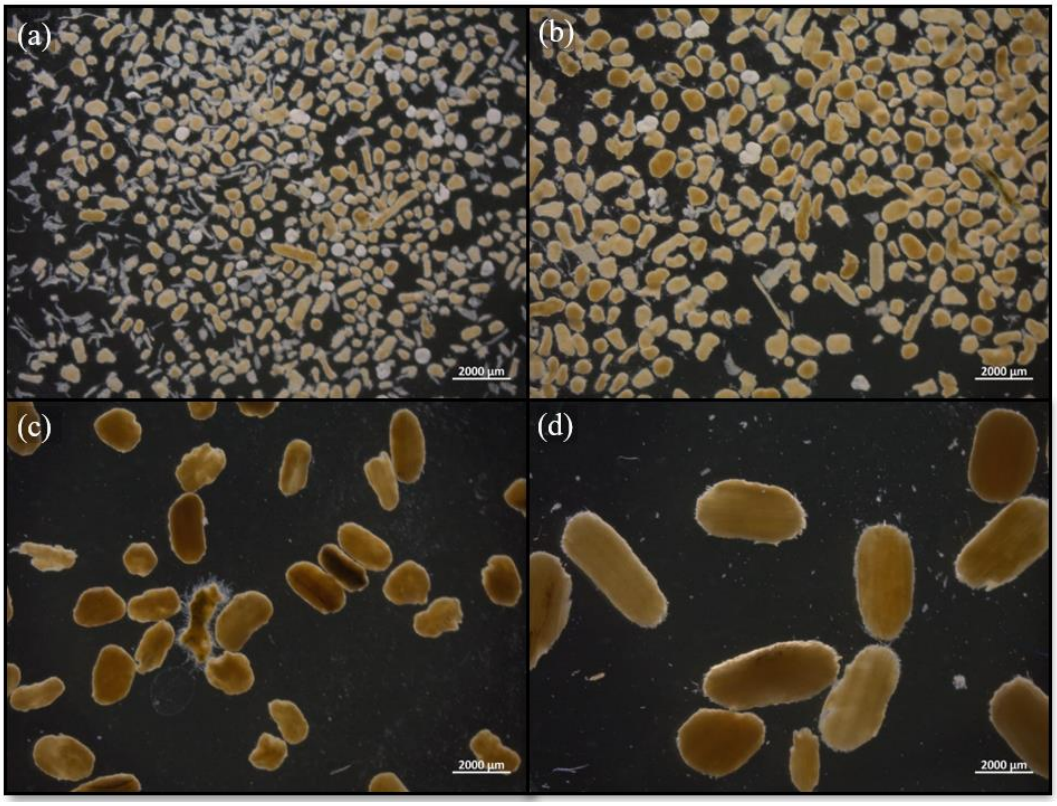

Figure 4-4. Stereomicroscopic images of kenaf granules of size ranges (a) 212 – 425 µm, (b) 425 – 600 µm, (c) 850 – 1180 µm, and (d) 1700 – 2000 µm taken in darkfield mode at 6.3X.

Due to starvation and anaerobic conditions, the core of aerobic granules is usually inactive, consisting of dead cells, proteins, and inorganic precipitates (McSwain et al., 2005). The biomass fraction of the kenaf granules was determined to be 38 ± 8%. For comparison, the biomass fraction of aerobic granules collected from a pilot-scale SBR treating centrate (Armenta et al., 2019) was also measured and the value was 34 ± 5%. It is known that endogenous decay occurs in the core of aerobic granules due to substrate diffusion limitations, and thus as granule size increases the inner structure of the granules will weaken and granule breakage will occur (Verawaty et al., 2013; Winkler et al., 2012b). Breakage of the kenaf granules was not studied. However, the core of kenaf granules consists of lignocellulose material, which is non-degradable for most of the common microorganisms found in activated sludge (de Souza, 2013). Therefore,

it is possible that the kenaf core offers a stronger backbone to withstand hydrolysis and breakage in comparison to aerobic granules, allowing for better tolerance to pumping or shearing in the rotary drum screen.

4.3.3 Specific activity of key functional groups

The specific activity of the kenaf granules are presented in

Table 4-1 in comparison with values reported in the literature for full-scale SBR-type AGS plants. The specific ammonia uptake rate (SNUR) was 50% lower than the Nereda® SBR, and a possible explanation is the high influent C/N ratio of Moorefield WWTP. Lower influent C/N ratio is known to enrich for nitrifiers due to less competition with heterotrophs for substrates and space (Bassin et al., 2012; Satoh et al., 2000). The influent BOD/TN ratio was 20 for Moorefield WWTP whereas the Nereda® SBR plant (Pronk et al., 2015) had a ratio of 4.2. The higher BOD/TN ratio of this study indicated that per unit of biomass, more heterotrophs would compete for the nitrogen and less nitrogen was available for nitrifier growth, which may explain the lower SNUR of this study. The specific phosphorus uptake rate (SPUR) of the kenaf granules was similar to or higher than the aerobic granules.

Table 4-1. Specific activity values of kenaf granules in comparison with values reported at full-scale aerobic granular sludge SBR plants.

		Kenaf granules	Aerobic granules	
	Process	Continuous flow	Nereda® SBR	SBR
	Influent	90% poultry; 10% domestic	100% domestic	30 - 40% dairy; 60 - 70% domestic
	Reference	This study	(Pronk et al., 2015)	(Świątczak & Cydzik-Kwiatkowska, 2018)
Parameter[a]	Unit	Values[b]		
DO	mg L^{-1}	>8.6[c]	1.8 – 2.5	<2.0
Temp.	°C	20	20	N/A
SNUR	mg NH_4^+-N (gVSS d)$^{-1}$	13.9 ± 0.3	28[d]	6.1
SPRR	mg PO_4^{3-}-P (gVSS d)$^{-1}$	95.3 ± 0.8	N/A	N/A
SPUR	mg PO_4^{3-}-P (gVSS d)$^{-1}$	38.2 ± 0.8	40[d]	17.2
SDNR	mg NO_3^--N (gVSS d)$^{-1}$	32.2 ± 4.7[e]	N/A	N/A

[a]SNUR = specific ammonia-N uptake rate; SPRR = specific P release rate; SPUR = specific P uptake rate; SDNR = specific heterotrophic denitrification rate.

[b]Values for AGS SBRs were estimated from the reported volumetric conversion rates measured directly from a reactor cycle.

[c]Acitivty tests were conducted at saturation DO. The process DO of the Plant was 0.35 - 0.5 mg L^{-1}.

[d]8000 mg L^{-1} MLSS and 25% ash content were used for the calculation based on available information in the paper.

[e]The acetate used per NO_3^- denitrified was 16.6 ± 2.4 gCOD gN^{-1}

The FISH images showed clusters of AOBs and PAOs randomly mixed throughout the outer 50–60 μm layer of the kenaf granules (**Figure 4-5**). In SBR-type AGS systems with no anoxic phase, denitrification must occur during the aerobic phase within the anoxic layer of the granules. This is enabled by the stratified microbial distribution where nitrifiers typically inhabit the outer oxygen-penetrated shell to oxidize NH_4^+ into NO_2^-/NO_3^-, which are then used as electron acceptors for denitrification by denitrifying PAOs (dPAO) in the anoxic inner layers, as typically observed in SBR-type AGS systems fed with VFAs (de Kreuk et al., 2005; Winkler et al., 2013). In this study the application of kenaf granules were in a continuous flow system with separated anaerobic, anoxic, and aerobic zones, thus the need for high simultaneous nitrification-denitrification (SND) efficiency in a single reactor and a stratified AOB/PAO distribution in a single granule was not necessary for meeting overall TN removal requirements. Therefore, the lack of stratified distribution of AOB/PAO observed in the kenaf granules (**Figure 4-5**) was expected.

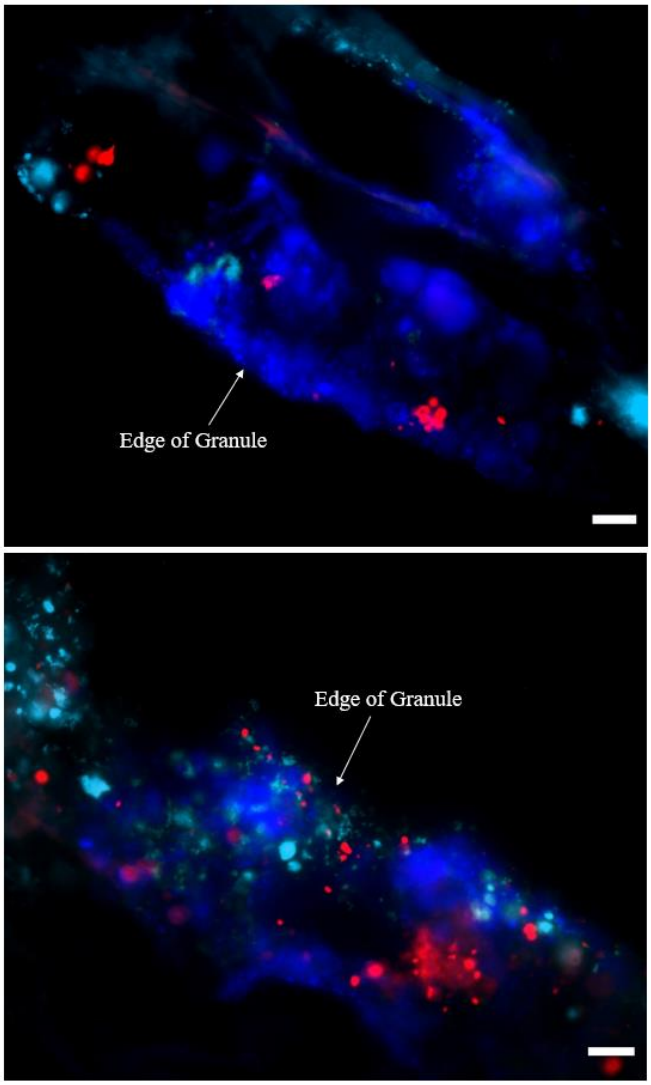

Figure 4-5. FISH images of 25 µm-thick kenaf granule sections; Cy5 (cyan) = PAO, Cy3 (red) = AOB, and DAPI (blue) = all bacteria. Scale bar = 20 µm.

This lack of stratified distribution can be explained by several factors: (1) usage of recycled nitrate by dPAO that can occur throughout the granule depth in the anoxic zone, hence eliminating the need for dPAO growth in deeper granule layers, (2) consumption of PAO's intracellular carbon storage occurred partially in the anoxic zone, leaving less carbon availability for denitrification in the subsequent aerobic zone and thus less dPAO growth in the anoxic layer, and (3) utilization of intracellular carbon and slowly biodegradable carbon by PAO and ordinary

denitrifiers, respectively, using nitrate in the anoxic zone, leading to less O_2 consumption by the heterotrophs in the aerobic phase and thus higher oxygen diffusion into the granules for AOBs growth in deeper layer. On the other hand, in SBR-type AGS systems without anoxic phase, PAOs and ordinary heterotrophs consume the carbon using oxygen in the aerobic phase, leading to less oxygen diffusion into the granule and thus less oxygen availability for growth of AOBs that share the outer-most layer with heterotrophs. In addition, it must be noted that AGS reactors treating real municipal wastewater have been shown to have much lower SND efficiencies (14 – 39%) compared to VFA-fed reactors (90%) and the availability of anoxic condition is highly dynamic and dependable upon the composition of wastewater and size of granules (Layer et al., 2020). Therefore, the assumption that a stratified distribution of microbial functional groups exists along the granule depth may not be as distinct in full-scale systems and requires further research.

4.4 Conclusions

Aerobic granular sludge is a promising technology for process intensification and its integration into continuous flow activated sludge systems is the next challenge. In this study, an appealing technology is presented that accomplished this concept with all organic mobile kenaf biocarriers, which were added to a full-scale continuous flow facility. Kenaf particles were retained in the system with a rotary drum screen fitted after the secondary clarifier underflow while flocs were selectively wasted. Biofilm developed on the kenaf media, leading to the formation of organic particles that have the same visual appearance as aerobic granular sludge. Kenaf granules had comparable settling characteristics and biomass-specific ammonia oxidation and phosphorus removal activities as aerobic granules. Furthermore, integration of the kenaf biofilm process led to lower effluent TSS concentrations and improved EBPR capacity. It is recommended that

better sludge management procedures be taken for integrated continuous flow granular sludge systems as the real solids concentrations may be significantly underestimated with the traditional MLSS measurement techniques for activated sludge. Another key benefit of these all organic biofilm aggregates is that they may not need to be landfilled as the case for other plastic carriers. This is the first full-scale application of all organic and mobile biofilm technology in continuous-flow system.

Acknowledgements

This work was supported by the University of Washington startup grant. We thank Dr. Reinhard Hübner for connecting UW with Nuvoda, making this collaboration possible, and Dr. Joshua Boltz for his comments on this manuscript.

References

Akil, H.M., Omar, M.F., Mazuki, A.A.M., Safiee, S., Ishak, Z.A.M., Abu Bakar, A. 2011. Kenaf fiber reinforced composites: A review. *Materials & Design*, **32**(8-9), 4107-4121.

Armenta, M., Stensel, H.D., Bucher, B., Sukapanpotharam, P., Nguyen Quoc, B., Winkler, M.K.H. 2019. Operation and Performance of Sidestream Aerobic Granular Sludge Nitrifying Reactor. in: *WEF Nutrient Removal and Recovery Symposium* WEF Nutrient Removal and Recovery Symposium. Minneapolis, MN.

Bassin, J.P., Kleerebezem, R., Rosado, A.S., van Loosdrecht, M.C.M., Dezotti, M. 2012. Effect of Different Operational Conditions on Biofilm Development, Nitrification, and Nitrifying Microbial Population in Moving-Bed Biofilm Reactors. *Environ Sci Technol*, **46**(3), 1546-1555.

Crocetti, G.R., Hugenholtz, P., Bond, P.L., Schuler, A., Keller, J., Jenkins, D., Blackall, L.L. 2000. Identification of polyphosphate-accumulating organisms and design of 16S rRNA-directed probes for their detection and quantitation. *Appl Environ Microbiol*, **66**(3), 1175-1182.

de Kreuk, M., Heijnen, J.J., van Loosdrecht, M.C.M. 2005. Simultaneous COD, nitrogen, and phosphate removal by aerobic granular sludge. *Biotechnol Bioeng*, **90**(6), 761-769.

de Souza, W.R. 2013. Microbial Degradation of Lignocellulosic Biomass. in: *Sustainable Degradation of Lignocellulosic Biomass - Techniques, Applications and Commercialization*, (Eds.) A.K. Chandel, S.S. Silva.

di Biase, A., Kowalski, M.S., Devlin, T.R., Oleszkiewicz, J.A. 2019. Moving bed biofilm reactor technology in municipal wastewater treatment: A review. *J Environ Manage*, **247**, 849-866.

Figdore, B.A., Stensel, H.D., Winkler, M.K.H. 2018. Bioaugmentation of sidestream nitrifying-denitrifying phosphorus-accumulating granules in a low-SRT activated sludge system at low temperature. *Water Res*, **135**, 241-250.

Kent, T.R., Bott, C.B., Wang, Z.W. 2018. State of the art of aerobic granulation in continuous flow bioreactors. *Biotechnol Adv*, **36**(4), 1139-1166.

Layer, M., Villodres, M.G., Hernandez, A., Reynaert, E., Morgenroth, E., Derlon, N. 2020. Limited simultaneous nitrification-denitrification (SND) in aerobic granular sludge systems treating municipal wastewater: Mechanisms and practical implications. *Water Res X*, **7**.

Li, A.J., Li, X.Y., Yu, H.Q. 2011. Granular activated carbon for aerobic sludge granulation in a bioreactor with a low-strength wastewater influent. *Sep Purif Technol*, **80**(2), 276-283.

Liu, Y.Q., Lan, G.H., Zeng, P. 2015. Resistance and resilience of nitrifying bacteria in aerobic granules to pH shock. *Lett Appl Microbiol*, **61**(1), 91-97.

Lourenco, N.D., Franca, R.D.G., Moreira, M.A., Gil, F.N., Viegas, C.A., Pinheiro, H.M. 2015. Comparing aerobic granular sludge and flocculent sequencing batch reactor technologies for textile wastewater treatment. *Biochem Eng J*, **104**, 57-63.

Lukumbuzya, M., Kristensen, J.M., Kitzinger, K., Pommerening-Röser, A., Nielsen, P.H., Wagner, M., Daims, H., Pjevac, P. 2020. A refined set of rRNA-targeted oligonucleotide probes for in situ detection and quantification of ammonia-oxidizing bacteria. *Water Res*, **186**, 116372.

McSwain, B.S., Irvine, R.L., Hausner, M., Wilderer, P.A. 2005. Composition and distribution of extracellular polymeric substances in aerobic flocs and granular sludge. *Appl Environ Microbiol*, **71**(2), 1051-1057.

Mobarry, B.K., Wagner, M., Urbain, V., Rittmann, B.E., Stahl, D.A. 1996. Phylogenetic probes for analyzing abundance and spatial organization of nitrifying bacteria. *Appl Environ Microbiol*, **62**(6), 2156-2162.

Pijuan, M., Werner, U., Yuan, Z.G. 2011. Reducing the startup time of aerobic granular sludge reactors through seeding floccular sludge with crushed aerobic granules. *Water Res*, **45**(16), 5075-5083.

Pronk, M., Bassin, J.P., de Kreuk, M.K., Kleerebezem, R., van Loosdrecht, M.C.M. 2014. Evaluating the main and side effects of high salinity on aerobic granular sludge. *Appl Microbiol Biotechnol*, **98**(3), 1339-1348.

Pronk, M., de Kreuk, M.K., de Bruin, B., Kamminga, P., Kleerebezem, R., van Loosdrecht, M.C.M. 2015. Full scale performance of the aerobic granular sludge process for sewage treatment. *Water Res*, **84**, 207-217.

Pronk, M., Giesen, A., Thompson, A., Robertson, S., van Loosdrecht, M. 2017. Aerobic granular biomass technology: advancements in design, applications and further developments. *Water Pract and Technol*, **12**(4), 987-996.

Ramesh, M. 2016. Kenaf (Hibiscus cannabinus L.) fibre based bio-materials: A review on processing and properties. *Prog Mater Sci*, **78-79**, 1-92.

Satoh, H., Okabe, S., Norimatsu, N., Watanabe, Y. 2000. Significance of substrate C/N ratio on structure and activity of nitrifying biofilms determined by in situ hybridization and the use of microelectrodes. *Water Sci Technol*, **41**(4-5), 317-321.

Sturm, B., Faraj, R., Figdore, B., Willoughby, A., Ford, A., Bott, C., Shiskowski, D., McFall, L., Downing, L. 2017. Balancing Granular Sludge with Activated Sludge Systems for Biological Nutrient Removal. *WEFTEC Conference Proceedings*, Chicago, IL.

Świątczak, P., Cydzik-Kwiatkowska, A. 2018. Performance and microbial characteristics of biomass in a full-scale aerobic granular sludge wastewater treatment plant. *Environ Sci Pollut Res*, **25**(2), 1655-1669.

van Loosdrecht, M.C., Nielsen, P.H., Lopez-Vazquez, C.M., Brdjanovic, D. 2016. Experimental Methods in Wastewater Treatment. *Water Intelligence Online*, **15**, 9781780404752.

Verawaty, M., Tait, S., Pijuan, M., Yuan, Z.G., Bond, P.L. 2013. Breakage and growth towards a stable aerobic granule size during the treatment of wastewater. *Water Res*, **47**(14), 5338-5349.

Vishniac, W., Santer, M. 1957. The thiobacilli. *Bacteriol Rev*, **21**(3), 195.

Wagner, J., Guimaraes, L.B., Akaboci, T.R.V., Costa, R.H.R. 2015. Aerobic granular sludge technology and nitrogen removal for domestic wastewater treatment. *Water Sci Technol*, **71**(7), 1040-1046.

Winkler, M.-K., Bassin, J., Kleerebezem, R., De Bruin, L., Van den Brand, T., Van Loosdrecht, M. 2011a. Selective sludge removal in a segregated aerobic granular biomass system as a strategy to control PAO–GAO competition at high temperatures. *Water Res*, **45**(11), 3291-3299.

Winkler, M.K.H., Bassin, J.P., Kleerebezem, R., de Bruin, L.M.M., van den Brand, T.P.H., van Loosdrecht, M.C.M. 2011b. Selective sludge removal in a segregated aerobic granular biomass system as a strategy to control PAO-GAO competition at high temperatures. *Water Res*, **45**(11), 3291-3299.

Winkler, M.K.H., Bassin, J.P., Kleerebezem, R., van der Lans, R., van Loosdrecht, M.C.M. 2012a. Temperature and salt effects on settling velocity in granular sludge technology (vol 46, pg 3897, 2012). *Water Res*, **46**(16), 5445-5451.

Winkler, M.K.H., Kleerebezem, R., Khunjar, W.O., de Bruin, B., van Loosdrecht, M.C.M. 2012b. Evaluating the solid retention time of bacteria in flocculent and granular sludge. *Water Res*, **46**(16), 4973-4980.

Winkler, M.K.H., Kleerebezem, R., Strous, M., Chandran, K., van Loosdrecht, M.C.M. 2013. Factors influencing the density of aerobic granular sludge. *Appl Microbiol Biotechnol*, **97**(16), 7459-7468.

Winkler, M.K.H., Meunier, C., Henriet, O., Mahillon, J., Suarez-Ojeda, M.E., Del Moro, G., De Sanctis, M., Di Iaconi, C., Weissbrodt, D.G. 2018. An integrative review of granular sludge for the biological removal of nutrients and recalcitrant organic matter from wastewater. *Chem Eng J*, **336**, 489-502.

Winkler, M.K.H., Straka, L. 2019. New directions in biological nitrogen removal and recovery from wastewater. *Current Opinion in Biotechnology*, **57**, 50-55.

Zhou, D.D., Niu, S., Xiong, Y.J., Yang, Y., Dong, S.S. 2014. Microbial selection pressure is not a prerequisite for granulation: Dynamic granulation and microbial community study in a complete mixing bioreactor. *Bioresour Technol*, **161**, 102-108.

Appendix C. Supplementary Material for Chapter 4

Table 1. Influent weekly average data of Moorefield Advanced Nutrient WWTP from 2016 - 2019

	Unit	Average	Min.	Max.
Influent				
Flow	MLD	9.79	6.98	18.80
BOD	mg L^{-1}	493	110	1238
TSS	mg L^{-1}	171	63	612
NH_4^+	mgN L^{-1}	24.4	10.9	57.4
TP	mg L^{-1}	11.9	3.4	18.7

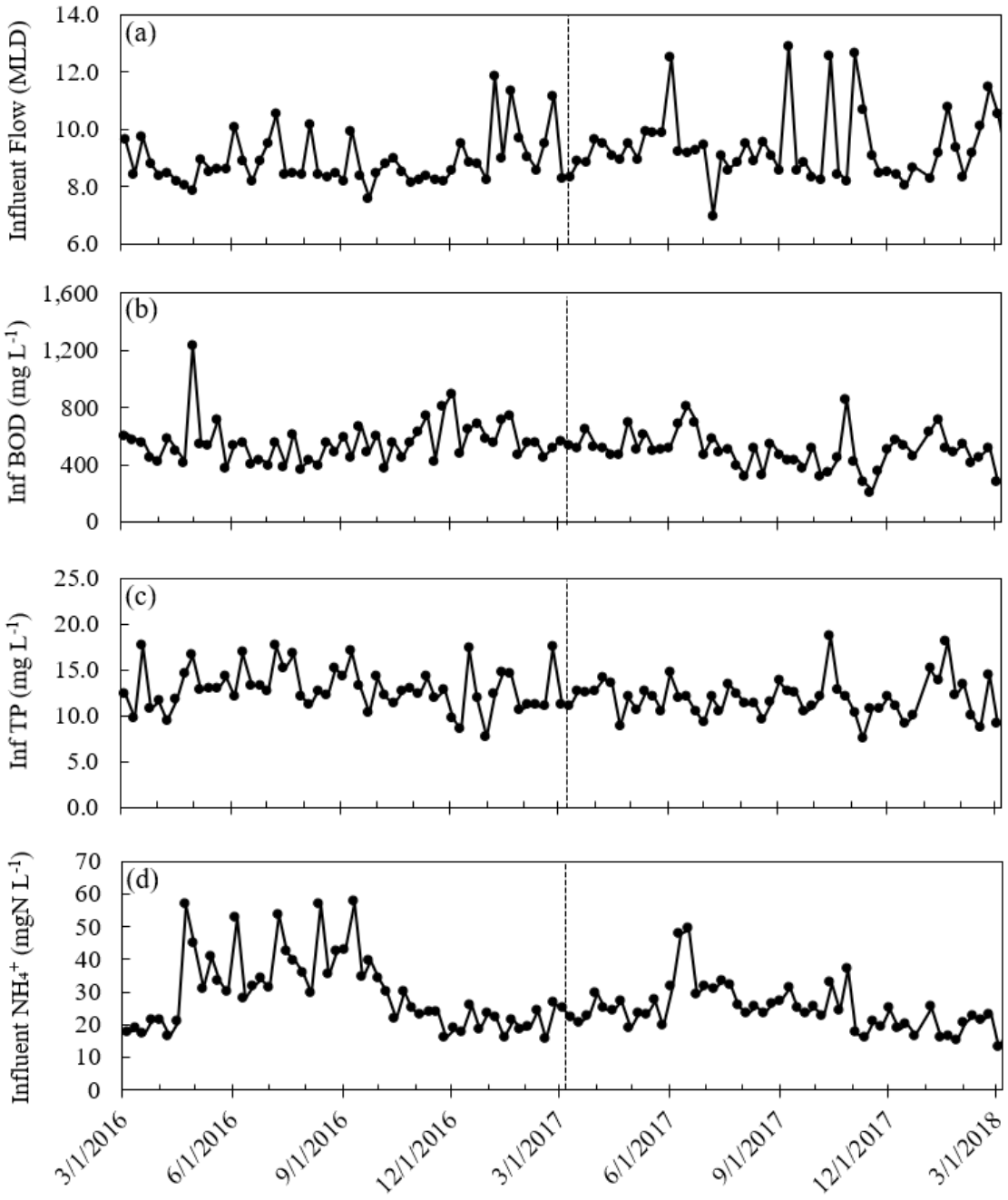

Fig. S1. Weekly average influent concentrations; dashed vertical line indicates time of upgrade.

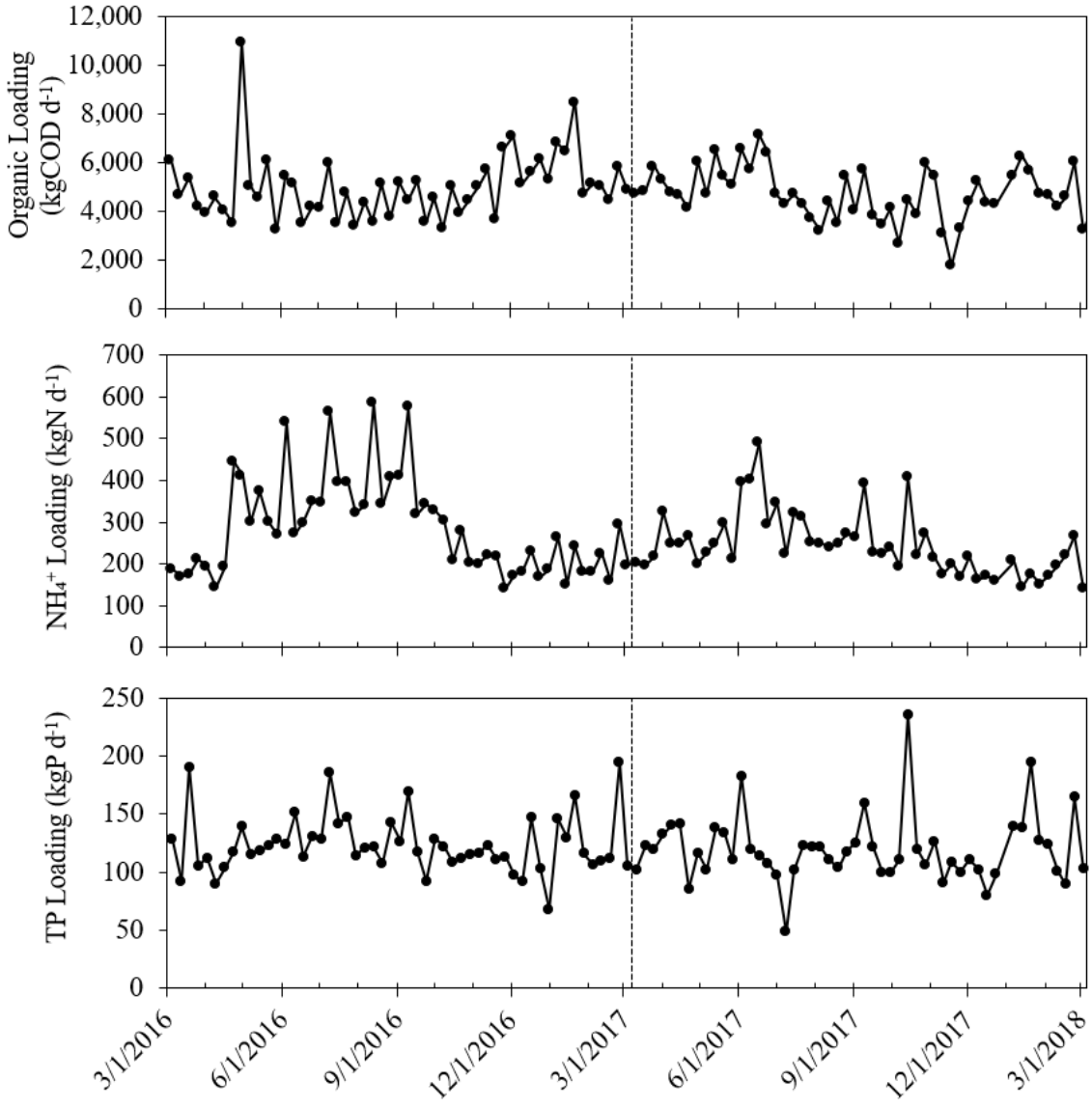

Fig. S2. Weekly average influent loadings; dashed vertical line indicates time of upgrade.

Fig. S3. (a) Dry kenaf media without biofilm growth; (b) kenaf granules after almost 2 years of biofilm buildup.

Table S2. FISH probes used in this study

Probe	Sequence	Target	Reference
PAO462	CCGTCATCTACWCAGGGTATT AAC	Most *Accumulibacter*	(Crocetti et al., 2000)
PAO651	CCCTCTGCCAAACTCCAG		
PAO846	GTTAGCTACGGACTAAAAGG		
NSO190	CGATCCCCTGCTTTTCTCC	*β-Proteobacterial* AOB	(Mobarry et al., 1996)
NSO1225	CGCCATTGTATTACGTGTGA		

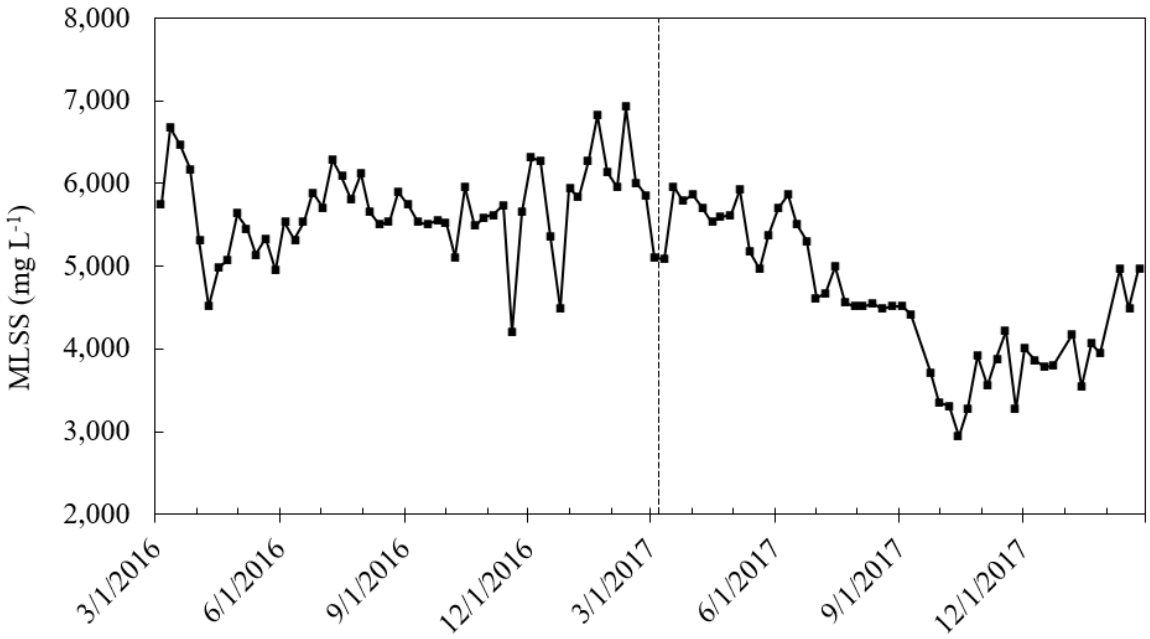

Fig. S4. Weekly MLSS data reported by the Plant. Dashed vertical line indicates time of upgrade. Section 3.1.1 of the main paper discusses why the data after upgrade may be under-representing the actual MLSS.

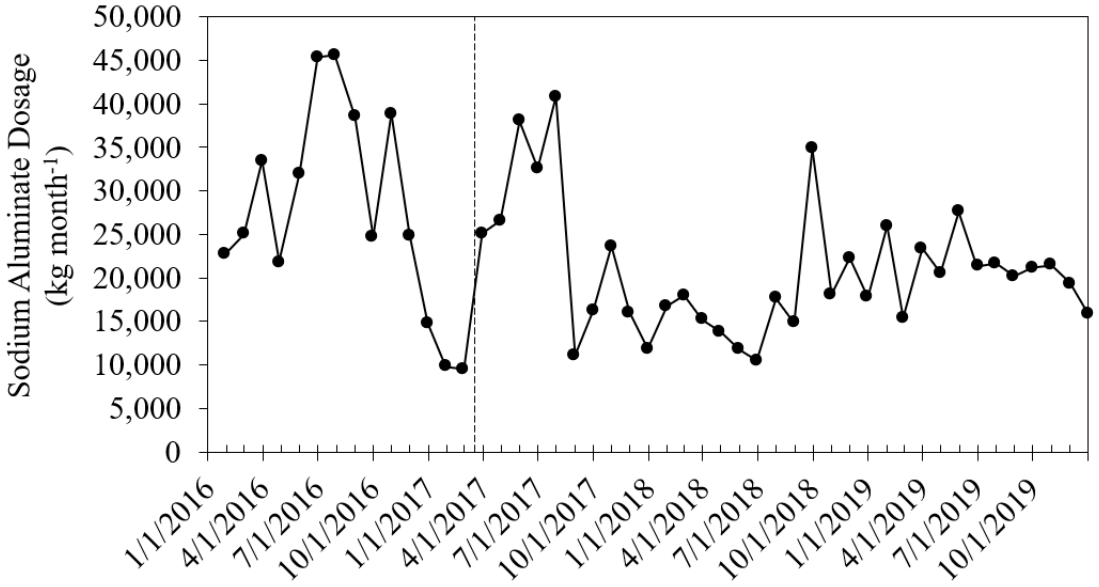

Fig. S5. Monthly usage of sodium aluminate; dashed vertical line indicates time of upgrade. The average dosages were 61,000 and 46,000 kg month^{-1} before and after the upgrade, respectively. Prior to December 2016, the sodium aluminate usage was around 20,000 – 45,000 kg month^{-1} (baseline) followed by a significant drop during the 3-month period right before the upgrade, which cannot be explained with the influent BOD/TP variations or any operational changes. This drop in dosage was likely not representative of the baseline condition because it was only a 3-month period and the dosage increased back to the 20,000 – 45,000 kg month^{-1} range in March 2017. While this increase coincidentally occurred in the month of upgrade, the addition of kenaf particles was unlikely to cause an immediate negative effect on the sodium aluminate usage. Therefore, the increase of dosage right after the upgrade was likely a return to the baseline condition. In addition, the sodium aluminate dosage started to decrease five months after the upgrade, which matched the time it took for the mixed liquor SVI_{30} to go from >200 mL g^{-1} to below 50 mL g^{-1}. Therefore, it can be concluded that the reduction of sodium aluminate was related to biofilm development on the kenaf particles and the associated improvement in EBPR capacity.

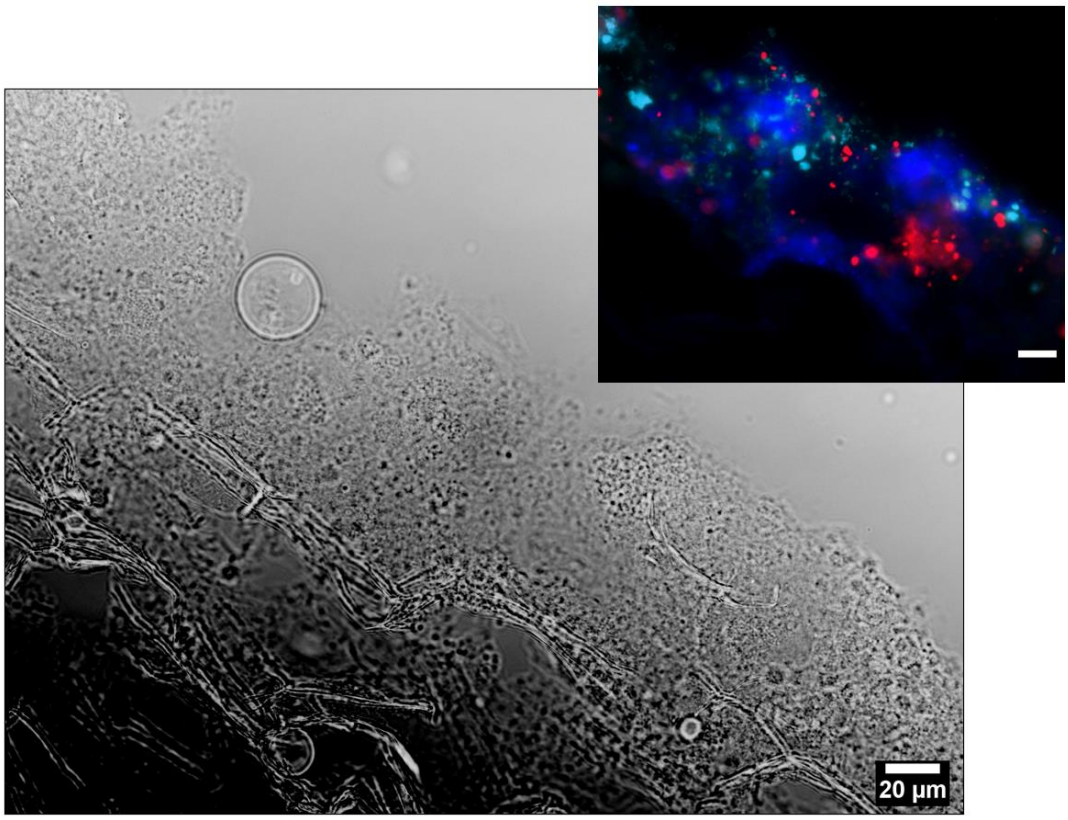

Fig. S6. Microscopic image of a 25-µm thick granule section showing the fibrous interior structure of the kenaf particles and an outer biomass layer. Fluorescence in-situ hybridization (top right, scale bar = 20 µm) was conducted on the same granule section to confirm presence of bacteria (blue = all bacteria stained with DAPI; red = ammonia oxidizing bacteria; cyan = polyphosphate accumulating organisms).

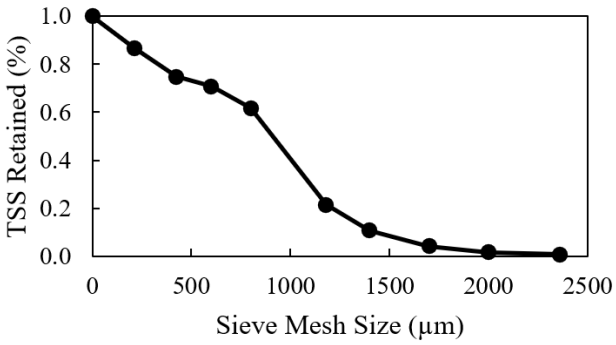

Fig. S7. Particle size distribution of the mixed liquor sample

References

Crocetti, G.R., Hugenholtz, P., Bond, P.L., Schuler, A., Keller, J., Jenkins, D., Blackall, L.L. 2000. Identification of polyphosphate-accumulating organisms and design of 16S rRNA-directed probes for their detection and quantitation. *Appl Environ Microbiol*, **66**(3), 1175-1182.

Mobarry, B.K., Wagner, M., Urbain, V., Rittmann, B.E., Stahl, D.A. 1996. Phylogenetic probes for analyzing abundance and spatial organization of nitrifying bacteria. *Appl Environ Microbiol*, **62**(6), 2156-2162.

Chapter 5.

A Concept for Nutrient Recovery from Aquaculture Waste using Aerobic Granular Sludge

Abstract

The growing global population has brought forward the intensification of fish farming practices (increased production per land area) and raised concerns about the environmental consequences caused by nutrient requirements for the fish and the more concentrated wastes. In specific, phosphorus is an essential element of the fish feed that comes from mining of the phosphate rock, which is a non-renewable resource with limiting quantities. A large portion of the phosphorus input into an aquaculture system ends up in the waste sludge, which offers an opportunity for phosphorus recovery and repurpose it as fertilizer to create a circular nutrient loop. In this study, we demonstrated a proof-of-concept for treating fish waste sludge with the enhanced biological phosphorus removal (EBPR) and aerobic granular sludge (AGS) technologies to obtain a stream with high PO_4^{3-} concentrations for struvite recovery. Waste aquaculture sludge was collected from a freshwater trout farm and subjected to fermentation to mineralize the NH_4^+, PO_4^{3-}, and volatile fatty acids (e.g., acetate and propionate). Liquid from the fermentation step was then used to cultivate aerobic granules that were enriched with polyphosphate accumulating organisms (PAOs), providing stable removal efficiencies for soluble COD (92%), PO_4^{3-} (98.5%), NH_4^+ (99.7%) and nitrogen removal (68%). The fermentation liquid did not contain sufficient metals, and thus addition of trace metals was needed to meet the metabolism of PAO and ammonia oxidizing bacteria (AOB). The granules were 0.5 – 3.0 mm in diameter with a sludge volume index at 5-minute setting of 36.5 ml/g.

Simple holding of the waste granules for 28 hours generated a stream with high PO_4^{3-} (148 – 195 mg P/L), which met the concentrations needed for struvite precipitation at economically feasible rates. A longer holding time may be needed for higher NH_4^+ mineralization or additional ammonium need to be added (e.g., with an ammonium laden side stream) to supply equimolar of N and P per the stoichiometric demand of struvite. Based on our results, a concept scheme was proposed for integrating phosphorus recovery within the context of a recirculating aquaculture system, achieved by biological means without the need for thickening equipment or anaerobic digester.

Manuscript in Preparation:

Wei, S. P., B. Roman, K. A. Hunt, K. C. Yamamoto, and M. K. H. Winkler. "A Concept for Nutrient Recovery from Aquaculture Waste using Aerobic Granular Sludge."

5.1 Introduction

Food demand of the growing global population had shaped the modern fish farming practices to intensify output (maximize fish production per land area) but comes at the cost of more concentrated waste generation. One of the major pollutants of concern are nutrients (e.g., N and P), which can contribute to eutrophication in the receiving aquatic environment. With the world's increasing population and the intensification of farming practices, aquaculture has been identified as the major source of nutrient input in some lakes and coastal waters worldwide (Aranguren-Riaño et al., 2018; Skogen et al., 2009; Wang et al., 2020). Intensive fish farming relies on artificial feeds that contain high N and P content, of which only 10 – 49% of N and 17-19% of P are retained in fish and the rest is discharged in either dissolved or solids waste (Dauda et al., 2019). Meanwhile, the linear trajectory from resource extraction to waste is unsustainable as hundreds of million tons of phosphate rocks are mined per year to produce artificial fertilizer (Jasinski, 2020), raising concerns for the lifetime of the non-renewable phosphorus resource and the need for resource recovery from waste streams (Cordell et al., 2011; Jacobs et al., 2017). A large portion of the N (up to 37%) and P (up to 55%) inputs into an aquaculture system can end up as uneaten feed and fish feces in the solid waste (Eck et al., 2019; Schneider et al., 2005). Depending on the farming practices, most of this solid waste can be efficiently removed from the fish tanks and captured, thus offering great opportunity for nutrient recovery.

In aquaculture systems, ammonia is constantly generated as a waste product of fish. To keep the ammonia concentration low in the fish-rearing tank while minimizing the use of new water, the water in the tank is constantly recycled by passing it through a biofilter (growth of nitrifying microorganisms on attached media for ammonia removal). This approach, termed recirculating

aquaculture system (RAS) allows a fish farm to continue reusing the water in the production and minimizing new water intake. In RAS, the liquid and solid wastes are separated by filtration, from which the water is passed through the biofilter and the majority of the solids (85-98%) are concentrated as waste sludge (Martins et al., 2010). Avenues for resource recovery from this waste sludge include composting and digestion. Composting is a labor-intensive process and requires large land area for moisture removal (Bao et al., 2019; Winkler et al., 2013). With the use of aerobic or anaerobic digestion, sludge mineralization produces microelements (e.g. phosphate, magnesium, and ammonium) that can be reused in aquaponics, but the accompanying high volatile fatty acids (VFAs) and ammonia are problematic if directly applied to plants (Goddek et al., 2018). Alternatively, a nutrient removal and recovery technology that is commonly employed in wastewater treatment, namely the enhanced biological phosphorus removal (EBPR) and struvite recovery process, is yet to be explored.

EBPR is a well-established activated sludge process that utilizes the polyphosphate accumulating organisms (PAO), which is a unique group of microorganisms capable of metabolizing organic carbon, nitrogen, and phosphorus. Under anaerobic conditions, PAO take up VFAs anaerobically and store it intracellularly as carbon polymer. When oxygen is available as electron acceptor, PAO respire the carbon and convert it into CO_2. In addition, PAO can also use nitrate/nitrite as electron acceptors instead of O_2 and reduce these nitrogen compounds into N_2 gas. Meanwhile, these metabolisms are fueled by the PAO's intracellular polyphosphate reserve, which is cleaved during anaerobic VFA uptake and synthesized during respiration. When PAO synthesize the polyphosphate, they take up PO_4^{3-} from the liquid, thus contributing to P removal in wastewater. To enable phosphorus recovery, sludge from the WWTP (enriched with PAO) is first thickened

and subjected to anaerobic conditions in a smaller tank where PO_4^{3-} is released back into a small volume (due to cleavage of polyphosphate), resulting in a P-rich supernatant. The PO_4^{3-} in this stream can then be precipitated out and captured in the form a struvite ($MgNH_4PO_4 \cdot 6H_2O$), a proven slow-releasing fertilizer (Le Corre et al., 2009). More recently, the use of struvite as a sustainable fire retardant (suspension of struvite powder in hydrogel carriers) has been demonstrated and considered to have higher value than struvite fertilizer (Kim et al., 2021) hence broadening its applicability.

Because high P concentration (>100 mg P/L) is needed for efficient struvite precipitation (Kehrein et al., 2020), solids thickening is required to concentrate the activated sludge prior to anaerobic phosphorus release. Alternatively, the requirement for sludge thickening can be eliminated when PAO is enriched in aerobic granular sludge (AGS) instead of activated sludge. AGS is an emerging wastewater treatment technology that promotes the cultivation of dense semi-spherical biofilm aggregates for biological nutrient removal. Each granule is colonized by a consortium of key functional microorganisms, ammonia oxidizing bacteria (AOB), nitrite oxidizing bacteria (NOB), PAO, and denitrifying bacteria, that together perform C, P, and N removal in a single reactor (Pronk et al., 2015). Due to the dense biofilm formed, aerobic granules achieve the same level of nutrient removal as conventional activated sludge but with 10-times fast settling velocity and only one-third the reactor volume requirement (Winkler et al., 2018). In addition, a high solids concentration can be achieved without specialized thickening equipment, meaning that anaerobic P release (for subsequent struvite recovery) can be done by simple holding of the waste granules. Such phosphorus recovery process is ideal for facilities that wish to reduce their phosphate discharge with minimal equipment needs.

In this research, we aim to test, for the first time, the application of EBPR and aerobic granular sludge technology using solid wastes from an aquaculture facility for phosphorus recovery. The goal of this study is to introduce the potential for struvite recovery from aquaculture sludge by (1) determining the degree of mineralization during fermentation of waste aquaculture sludge, (2) demonstrating the suitability of using the fermentation liquid to achieve stable aerobic granular sludge and EBPR performance, and (3) obtaining a phosphate-rich stream from simple holding of the aerobic granules.

5.2 Methods and Materials

5.2.1 Sludge fermentation

Raw fish sludge was collected from a freshwater trout farm in Rochester, Washington. For the first batch of fermentation, the collected raw fish sludge was split into a 4 L fermenter operated in parallel, one at 20 °C and one at 30 °C, to study the production of VFAs. The fermenters were air-tight and subjected to constant mixing for 8 days. Daily measurements of pH, VFAs, PO_4^{3-} and NH_4^+ were collected. TSS, VSS, and soluble COD (sCOD) were measured 2-3 times a week. After the fermentation period, the sludge was centrifuged at 10,000g for 30 minutes (Sorvall® RC-5C), and the supernatant (fermentate) was stored at 4°C until further processed as feed for the SBR. This same procedure was repeated for 30 L of fish sludge, which were fermented for 4 weeks to provide enough substrate for the entirety of the project.

5.2.2 Aerobic granular sludge sequencing batch reactor

A 3-L reactor column was operated in sequencing batch reactor (SBR) cycles consisting of 85 min anaerobic feeding, aeration, settling, and 5 min decant (50% volume exchange ratio), where

the aeration and settling time varied over time while fixing the cycle length at 288 minutes (5 cycles per day). The reactor was seeded with activated sludge obtained from a municipal wastewater treatment plant (South Plant, WA), an anaerobic/aerobic facility with EBPR. Before full granulation was attained, the only solids wasting was done via the effluent TSS. Over a 6-month period, the settling time was gradually reduced from 40 minutes to 3 minutes, while keeping the SRT at around 10-20 days. When the 3-minute settling was reached and the effluent TSS was not enough to keep an SRT below 20 days, manually wasting of granules was performed. The fermentate was diluted to aim for a sludge loading rate of roughly 0.2 gCOD/gVSS·day. After initial observations of poor ammonia oxidation and P removal, a solution of 6 metals (trace element solution, see Table S1 for recipe) was supplemented to the influent on day 8 at a 1:200 (v/v) ratio.

5.2.3 Metals removal experiment

To test which metals in the fermentation liquid were limiting for the PAO and AOB metabolism, the reactor was fed with raw fermentation liquid without the trace metals supplements on day 158. Then, the re-addition of Mo, Cu, and Co was done on day 164, 171, and 176, respectively. All concentrations and chemicals used were the same as the ones used in the trace element solution. With the observation that nutrient removal was unstable even after the re-addition of Mo, Cu, and Co, the trace element solution was added back into the influent.

5.2.4 Phosphate release tests

250 ml of granular MLSS was collected from the reactor at end of aeration phase and aerated for an additional 30 minutes. Then, the granular sludge was settled for 3 minutes and 130 ml of the supernatant was removed. This is to simulate a thickened granular sludge inside a fermentation tank with 60% of sludge blank to side water depth ratio. The remaining granular sludge was sparged with N_2 gas for 15 minutes. For the condition without addition of carbon, no fermentation liquid was added. For the condition with addition of carbon, a small volume of the fermentation liquid (~6ml) was added to aim for an initial VFA concentration of around 100 mg COD/L. Both conditions were done in triplicates. To provide anaerobic conditions, headspace of all bottles was sparged with N_2 gas for the entirety of the experiment. Concentrations of PO_4^{3-}, NH_3+NH_4^+ (denoted as NH_4^+ here on), NO_3^-, NO_2^-, and VFAs were monitored over 28 hours. ORP was measured with an electrode (Sensorex ORP1000) for one of the triplicate bottles for each condition.

5.3 Results and Discussions

5.3.1 Fermentation of Aquaculture Waste Sludge Provides Suitable Feed for EBPR Applications

Fermentation of the fish sludge at room temperature (20°C) achieved 22.2 mg NH_4^+-N and 10.7 mg PO_4^{3-}-P production per g of initial VSS, accompanied by a 42% VSS reduction over a 5-day period (**Figure 5-1a**). There was no enhancement of sludge hydrolysis by means of pretreatment methods or addition of hydrolyzing inoculum. The amount of VFA produced could not be normalized to g of initial VSS because fermentation likely took place in the storage tank at the aquaculture facility, as indicated by the high VFA concentration already on day 1. Phosphate concentration stopped increasing after 1 day whereas ammonia and VFA production steadily

increased and plateaued at around 6 days. The solubilization of particulate organic carbon was indicated by the increase in sCOD, of which roughly 47 - 50% consisted of VFA. The endpoint VFA consisted mainly of acetate (45%), propionate (28%), and butyrate (18%), as typically observed in fermentation of aquaculture sludge (Goddek et al., 2018; Letelier-Gordo et al., 2017). Fermentation at 30°C accelerated the release of ammonia, but the endpoint concentrations of ammonia, phosphate, and VFAs were similar as the 20°C fermenter (Figure S1). Previous studies had shown that other minerals such as K^+, Ca^{2+}, and Mg^{2+} are also mineralized and released into the liquid during fermentation of aquaculture sludge (Conroy & Couturier, 2010; Delaide et al., 2019), which could therefore lower Mg^{2+} requirements for struvite precipitation.

Our results demonstrated solids reduction and nutrient mineralization by means of simple holding of the aquaculture sludge. The resulting high VFA and PO_4^{3-} concentrations are suitable for the PAO metabolism and downstream phosphorus recovery applications. Management of the aquaculture sludge is important as the high biodegradable carbon and nutrient concentrations liberated from the solids-bounded organic molecules will leached into the aquatic environment if left untreated. Previous researchers have reported on the further treatment of this nutrient-rich fermentation liquid with applications such as aerobic treatment and constructed wetland (Brazil & Summerfelt, 2006; Sindilariu et al., 2009), but these studies provided no phosphorus recovery. This work is the first that examined the treatment of fermentation liquid from aquaculture sludge with EBPR applications, which can be conceptually followed by struvite recovery.

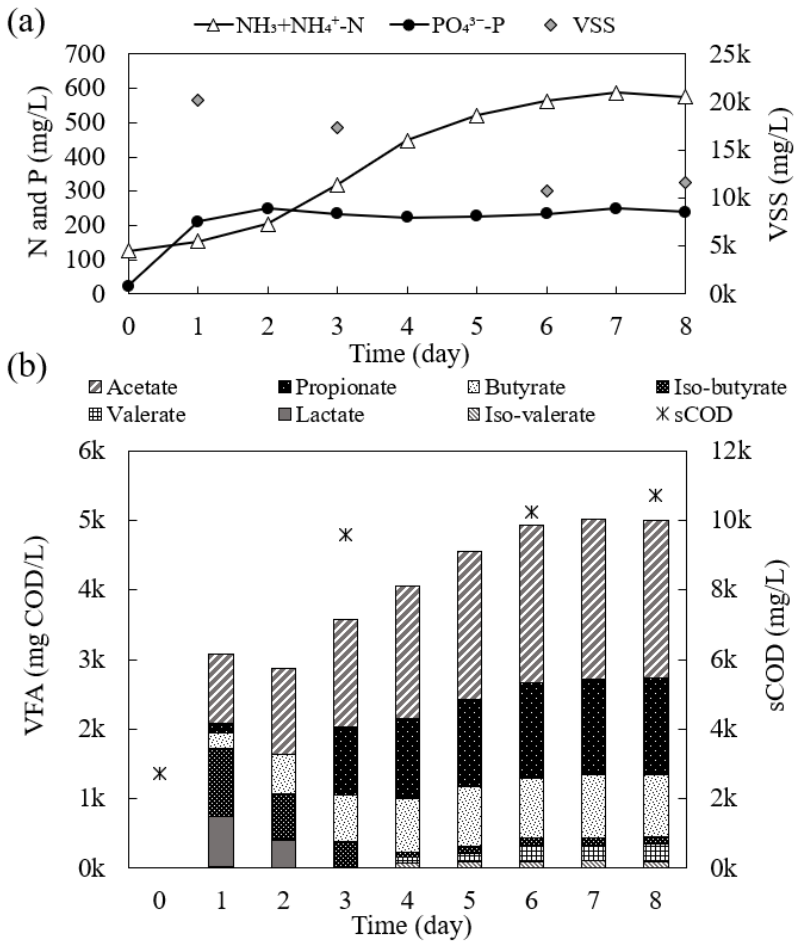

Figure 5-1. Fermentation of waste sludge from freshwater trout farm at 20 °C: (a) changes in ammonia and phosphate and VSS reduction; (b) changes in sCOD and VFA composition.

5.3.2 Stable C, P, and N Removal Performance Achieved Long-Term

After fermentation of the aquaculture sludge, the sludge was removed via centrifugation and the supernatant was used as feed for the SBR. The average influent compositions are shown in

Table 5-1. When the reactor first started, there were minimal AOB or PAO activities, as indicated by the high effluent NH_4^+ and PO_4^{3-} initially (**Figure 5-2**). It was not until the addition of trace element solution into the influent (on day 8) that both the ammonia and P removal activities improved, indicating that one or more metals were limiting for the AOB and PAO

metabolism. With the addition of trace metals, P removal performance improved immediately while ammonia oxidation activity took 13 days (roughly one SRT) to acclimate, likely due to the slower growth rate of AOB.

The average sCOD removal efficiency for the entire reactor operation was 92 ± 9%, of which 86 ± 4 % was removed during the anaerobic phase (taken up by PAO or GAO). High removal efficiencies of PO_4^{3-} (98.5 ± 1.5%) and NH_4^+ (99.7 ± 0.2%) were maintained consistently for 200 days, except a period of disturbance when we intentionally stopped adding the trace element solution (gray-shaded area in **Figure 5-2**). EBPR is a robust technology for treatment of domestic wastewater and has also been applied to efficiently capture phosphorus from many types of industrial wastewater, such as wastewaters from abattoir, food processing, and livestock production facilities (Kishida et al., 2009; Lemaire et al., 2009; Mulkerrins et al., 2004). However, no previous work has applied EBPR to fish waste hence making this the first study to successfully apply EBPR for treating aquaculture waste.

Biological nitrogen removal is achieved either via ammonia uptake for biomass assimilation or simultaneous nitrification and denitrification (SND). Due to substrate diffusion limitations across biofilm depth, different layers of redox zones exist within a granule. AOB and NOB reside the outer aerobic zone of the granules, oxidizing ammonia into nitrite and nitrate, respectively. The nitrate and nitrite can diffuse into the deeper layer of the biofilm where oxygen is depleted, creating an anoxic zone for denitrification by heterotrophic denitrifiers. This partitioning of microbial functions across the biofilm depth allows for SND within a single reactor (de Kreuk et al., 2005; Winkler et al., 2018), which is one of the many advantages of AGS over activated

sludge. However, the degree of SND varies among AGS systems, as the availability of anoxic zone is highly dynamic and fluctuates spatially and temporally with many parameters (e.g., carbon diffusibility, granule size, and bulk liquid ammonia and oxygen concentration) (Layer et al., 2019). In this study, the NOB community established slower than the AOB, as indicated by the elevated nitrite concentrations from day 23–55 (**Figure 5-1**). Then, complete nitrification was attained with effluent nitrate concentration maintained at around 7.5 mg N/L while the effluent ammonia and nitrite concentrations were <0.2 mg N/L. These values correspond to a nitrogen removal efficiency of roughly 68 ± 5%. With the high VFA:N ratio (17 ± 3) in the influent, it can be speculated that most of the N removed was attributed to biomass synthesis, and not SND.

5.3.3 Metals limitation indicates needs for higher mineralization from sludge

To test which metals in the fermentation liquid were limiting for the AOB and PAO metabolism, the metals removal experiment was performed. Addition of the trace element solution (contains 6 metals, Table S1) was stopped, and the metal components were added back in individually. PAO activity was hindered immediately after the trace elements were removed, while AOB activity started to decline after 10 days (Figure S3). Mo, Cu, and Co were likely the limiting metals due to their non-detection or low levels in the raw fermentate (Table S2). The ammonia monooxygenase, the enzyme catalyzing the ammonia oxidation metabolism in ammonia-oxidizing bacteria, is likely copper-dependent (Lehtovirta-Morley, 2018). However, even with the re-addition of all three metals (Mo, Cu, and Co) the PAO and AOB activities did not stabilized, indicating that other metals were also limited. Complete P removal and ammonia oxidation performance was resumed after re-supplementing the trace element solution. Since metals are part of the fish diet, aquaculture sludge can contain >0.4 mg/kg of the metals (Naylor

et al., 1999) essential for biological wastewater treatment. If completely liberated from the fish sludge, this amount would translate to at least 2.5 times higher than the trace element solution used in this study as supplement. However, metals are tightly bounded to the extracellular polymeric substances (EPS) of sludge via cation bridging or complexation/precipitation (Molaey et al., 2021), and thus fermentation alone achieves very low mineralization of metals from aquaculture sludge (Goddek et al., 2018). Methods exist for enhancing metals leaching from sludge, but most require chemical additions or thermal treatment (Camargo et al., 2016; Jung & Lovitt, 2011) that may not be scalable for aquaculture applications.

The removal of trace elements from the influent caused two incidents of ammonia spike in the effluent, likely due to the metals-limitation on the AOB (**Figure 5-2b**). As expected, the spike in the effluent ammonia was accompanied by a drop in effluent nitrate. Surprisingly, all nitrogen species stayed low after the re-addition of metals supplements, indicating >97% nitrogen removal efficiency. This was unexpected because all parameters stayed the same before and after the metals removal experiment, but the nitrogen removal efficiency was only 68% before the experiment. A cycle test conducted during the period of high nitrogen removal confirmed an SND profile, with intermediate accumulation of nitrate and nitrite and their gradual reduction over the cycle (Figure S4). A possible explanation for the increase in N removal efficiency is the increase in granule size before versus after the metals removal experiment.

Table 5-1. Summary of influent, effluent, and other operational data of the reactor.

Influent					Effluent		
	Unit	Min.	Max.	Average		Unit	Average
TSS	mg/L			74[a]	sCOD	mg/L	48
COD	mg/L			613[a]	NH_3+NH_4^+	mg N/L	0.15[b]

sCOD	mg/L	456	828	565	PO_4^{3-}	mg P/L	0.08[b]
VFA	mg COD/L	225	532	365			
Acetate	mg COD/L	77	193	139	Other Parameters[c]		
Propionate	mg COD/L	53	139	87			Average
Butyrate	mg COD/L	43	123	74	Effluent TSS	mg/L	73
NH_3+NH_4^+	mg N/L	14.2	28.5	21.6	MLSS	mg/L	7905
PO_4^{3-}	mg P/L	3.60	7.39	4.98	MLVSS	mg/L	6666
Cl^-	mg/L	5.8	12.0	8.6	Ash content	%	16
SO_4^-	mg/L	0.3	4.8	2.5	SVI_5	ml/g	36.5

[a]Only three data points available

[b]Not including data during removal of supplement metals in the influent

[c]Average of Day 169 – 288 (after full granulation)

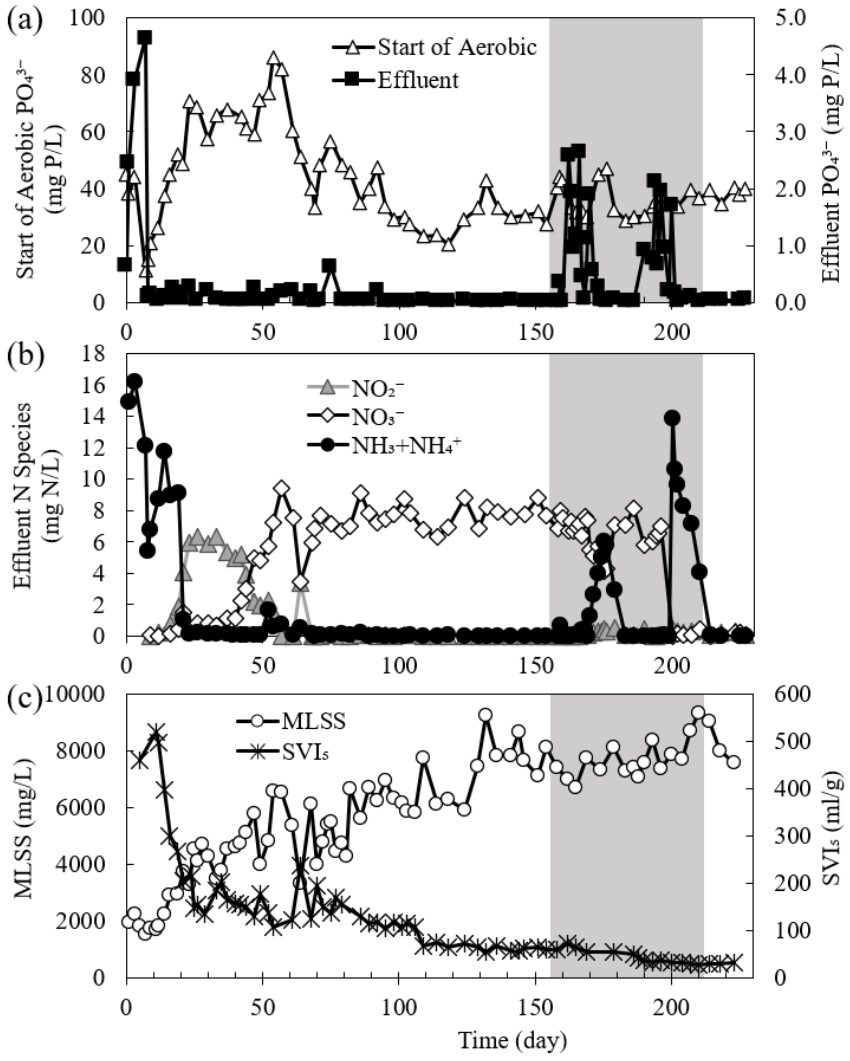

Figure 5-2. Process data of reactor: (a) phosphate and (b) nitrogen removal performance, and (c) MLSS concentration and SVI_5. Day 8: addition of trace elements. Gray area: metals removal experiment.

5.3.4 Granulation

Aerobic granulation is a gradual process of microbial self-immobilization. The selective pressures that promote the granulation process is well-documented. Under selective pressures such as alternating feast/famine conditions and shear stress, the microorganisms produce gel-like EPS that leads to microbial attachment and adhesion, which are the proposed foundational

mechanisms supporting the granulation process (Nancharaiah & Reddy, 2018; Seviour et al., 2009; Winkler et al., 2018). In this work, we applied alternating anaerobic feast and aerobic famine conditions, shear stress, and hydraulic washout of small particles to facilitate the granulation process. Since granulation relies solely on biological means of formation (i.e., without aid of carriers or surface attachment), a complete conversion from the flocculent activated sludge to granules is typically a multi-month process. It took roughly 165 days to reach full granulation, when sustained SVI_5 of <60 ml/g (**Figure 5-2c**) was achieved with minimal presence of flocs under the microscope (Figure S2). This amount of time for granulation corroborates with other studies treating real wastewater (Pronk et al., 2015; Wagner et al., 2015). The long granulation time is a drawback of the AGS technology (strategies to shorten it is an area of active research), but it does not hinder nutrient removal performance.

Our work demonstrated the cultivation of aerobic granules with stable nutrient removal performance using freshwater aquaculture waste. Relevant to the wider applications of this technology, biological phosphorus removal and successful cultivation of AGS have been demonstrated with seawater (de Graaff et al., 2020; Li et al., 2017; Wu et al., 2014), and thus applications of PAO-based aerobic granular sludge in brackish aquaculture is possible and can be explored in the future. It should be noted that the influent TSS was very low (**Table 5-1**) due to the high dilution of the fermentation liquid, and thus the effect of influent solids on the reactor performance was not evaluated in this study.

5.3.5 High P Obtained from Holding of Granules Indicates Potential for Struvite Recovery

In wastewater treatment, the first step of using waste sludge for P recovery is to concentrate the biomass so that PAO can release PO_4^{3-} in a small volume to obtain a high PO_4^{3-} concentration. The SVI_{30} of conventional activated sludge is typically >100 ml/g, meaning that the sludge can thicken to a solids concentration of less than 1% with 30-min settling. A higher solids concentration of 2-3% can be achieved with specialized equipment (e.g., gravity thickener) but it requires long detention time (18-30 hours) (U.S. EPA, 1987) and large land area. In this work, a sludge bed of 3.0 ± 0.1% solids was obtained with merely 3 minutes of settling. Phosphate release tests were conducted by simple holding of the thickened granules in anaerobic condition. After 28 hours of holding time, the phosphate concentrations were 148 and 195 mg P/L without and with fermentation liquid addition, respectively (**Figure 5-3**). The phosphate concentrations feeding a struvite recovery reactor should be at least 50 mg P/L and preferably higher than 100 mg P/L due to economic reasons (Cornel & Schaum, 2009; Kehrein et al., 2020). The reject water from anaerobic digestion at wastewater treatment plants, which is a common source of stream for struvite recovery, can have PO_4^{3-} concentration in the range from 100-350 mg P/L (Tchobanoglous et al., 2014). Our results showed that anaerobic holding of the thickened aerobic granular sludge can achieve a concentration in this range but without the need for specialized thickening equipment.

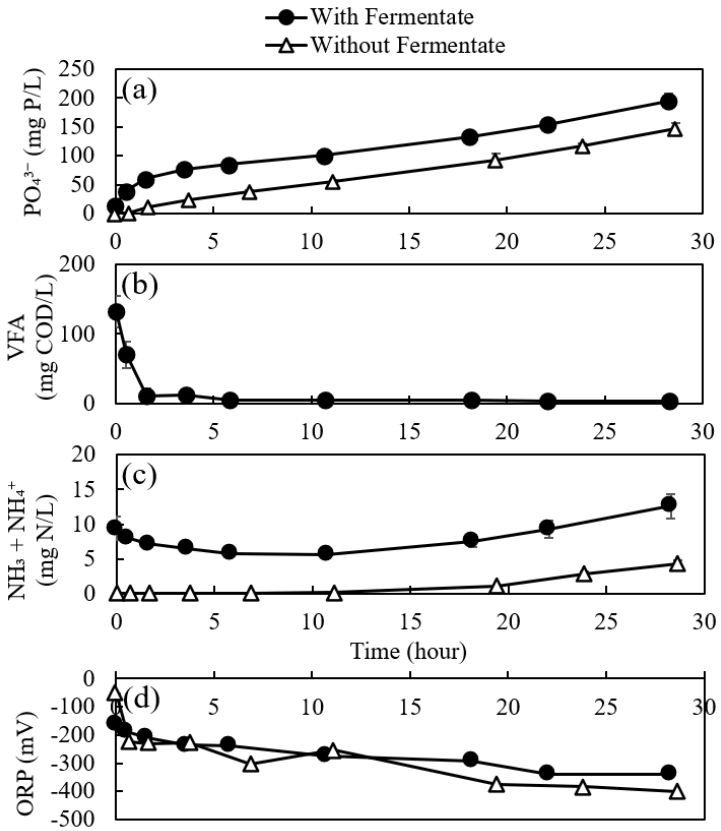

Figure 5-3. Time series measurements of (a) phosphate, (b) VFA, (c) ammonia, and (d) ORP from anaerobic holding of thickened aerobic granular sludge. The batch test with acetate added was spiked with 400 mg COD/L. pH ranged from 7.5-8.1 at the beginning to 6.7-6.8 at the end of the test.

The composition of struvite is $MgNH_4PO_4 \cdot 6H_2O$, and thus in addition to a high PO_4^{3-} concentration, NH_4^+ and Mg^{2+} ions are also needed to drive the precipitation kinetics. Mg^{2+} was not measured in this study, but its release along with PO_4^{3-} is expected since polyphosphate is composed of Mg^{2+}, K^+, and PO_4^{3-} in a 1:1:3 molar ratio (Smolders et al., 1994). Thus, during breakdown of the polyphosphate, for every mole of PO_4^{3-} ions released, 1/3 mole of Mg^{2+} and 1/3 mole of K^+ ions (secondary metabolites) are co-transported out of the PAO cells. This

amount of Mg^{2+} would only satisfy 1/3 the need for struvite, and the remaining 2/3 need to be added externally. The addition of external Mg^{2+} is commonly practiced for struvite recovery processes (Peng et al., 2018; Wei et al., 2018), and low-cost magnesium sources such as bittern and raw seawater can be utilized (Shaddel et al., 2020). Because the breakdown of amino acids is a slower process than polyphosphate cleavage, 28 hours of holding time was not sufficient for mineralization of NH_4^+ from the waste granules (**Figure 5-3c**). A higher NH_4^+ concentration can be achieved with longer detention time in the holding tank or NH_4^+ could be added from ammonium laden side streams or other sources.

5.3.6 A Resource Recovery Concept in Aquaculture Settings

Based on the demonstration of cultivating PAO-enriched aerobic granules from fish sludge and obtaining P-rich stream from the waste granules, we propose a conceptual scheme (**Figure 5-4**) to enhance resource recovery within an existing RAS. The components of the conceptual scheme are described as follows:

(a) Fermentation of the fish sludge produces high VFA and PO_4^{3-}.

(b) The fermentation liquid is used for cultivating aerobic granules with high ammonia and PO_4^{3-} removal capacity. The significance of demonstrating granulation from seed flocs is to show that every aquaculture facility can cultivate their own granules.

(c) Waste granules are held anaerobically to produce a high PO_4^{3-} stream without the need for specialized sludge thickening equipment.

(d) The high PO_4^{3-} stream can then be used for struvite precipitation.

(e) In addition to struvite recovery, the effluent from the AGS reactor, which provides complete ammonia removal and partial nitrate removal, can potentially be used as recycled water back to the fish-rearing tanks.

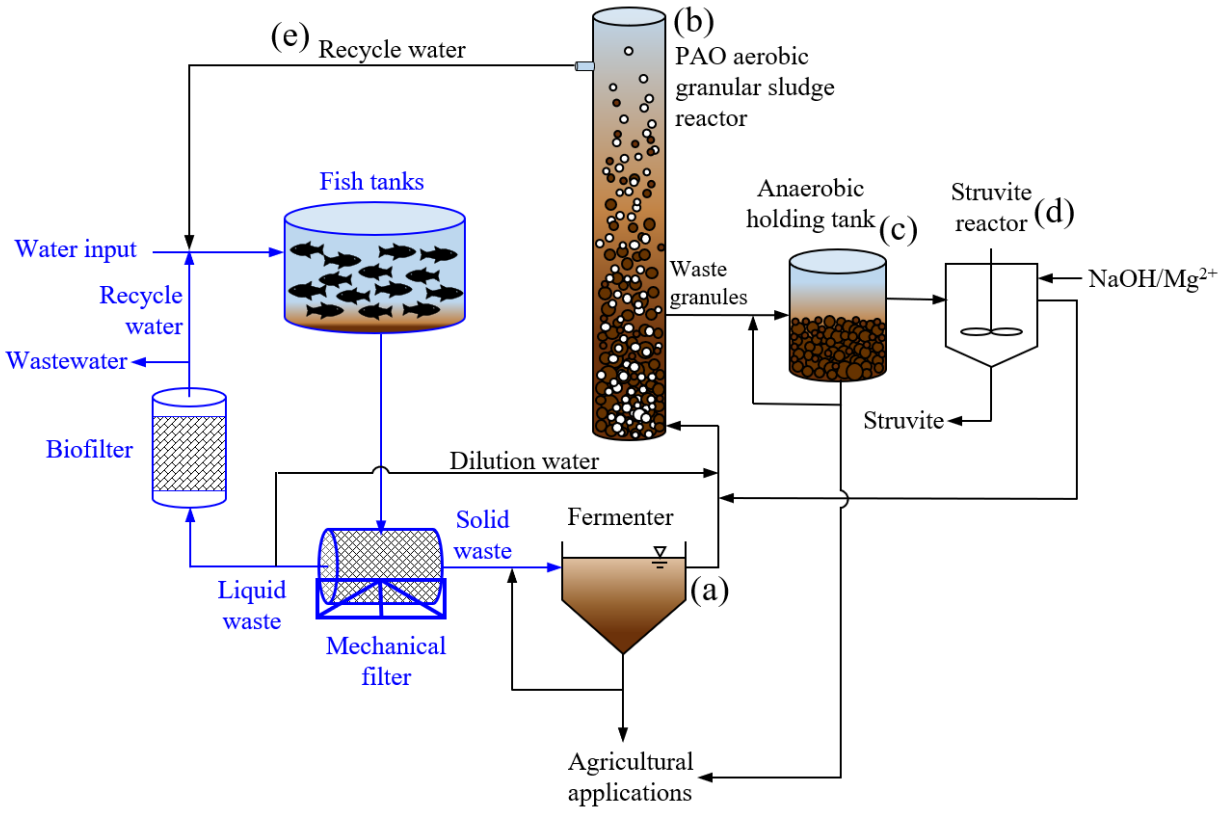

Figure 5-4. Proposed schematics of an integrated resource recovery process within a RAS; blue outline indicates tanks and piping that already exist at a typical RAS. For descriptions of (a)-(e), refer to Section 3.5.

5.4 Conclusions

Aerobic granules were cultivated using fermentation liquid of waste sludge from a freshwater trout farm, demonstrating high and stable COD, NH_4^+, and PO_4^{3-} removal efficiencies. Metals were limited in the fermentation liquid and thus exogenous supplement of trace elements was required for the PAO and AOB metabolism in the AGS reactor. The success of granulation from fish waste indicated that any RAS could cultivate granules from flocs (no seeding of carriers or granules required) and achieve biological nutrient removal with only 1/3rd the reactor volume compared to conventional activated sludge. In addition, the high thickening characteristics of the

granules were leveraged to produce a high PO_4^{3-} stream by means of simple anaerobic holding and without the need for thickening equipment or anaerobic digestion. The PO_4^{3+} concentration was in the range of 148 - 195 mgP/L, which is suitable for struvite recovery. This work demonstrated a proof-of-concept and proposed a conceptual scheme for nutrient removal and recovery within a RAS.

Acknowledgement

The authors would like to thank Dr. Pieter Candry for his counseling during startup of the fermentation and EBPR reactors. We would also like to express our gratitude to Victor Lobanov and Dr. Alyssa Joyce (University of Gothenburg) for sharing their expertise on RAS and arranging contact and picking up fish sludge for the project. Lastly, this work could not happen without the assistance of Jeff Hudson (Riverence Brood LLC), who supported our research and organized sludge pickup from his facility.

References

Aranguren-Riaño, N.J., Shurin, J.B., Pedroza-Ramos, A., Muñoz-López, C.L., López, R., Cely, O. 2018. Sources of nutrients behind recent eutrophication of Lago de Tota, a high mountain Andean lake. *Aquatic sciences*, **80**(4), 1-9.

Bao, W.J., Zhu, S.M., Jin, G., Ye, Z.Y. 2019. Generation, characterization, perniciousness, removal and reutilization of solids in aquaculture water: a review from the whole process perspective. *Reviews in Aquaculture*, **11**(4), 1342-1366.

Brazil, B.L., Summerfelt, S.T. 2006. Aerobic treatment of gravity thickening tank supernatant. *Aquacultural Engineering*, **34**(2), 92-102.

Camargo, F.P., Tonello, P.S., dos Santos, A.C.A., Duarte, I.C.S. 2016. Removal of Toxic Metals from Sewage Sludge Through Chemical, Physical, and Biological Treatments-a Review. *Water Air and Soil Pollution*, **227**(12).

Conroy, J., Couturier, M. 2010. Dissolution of minerals during hydrolysis of fish waste solids. *Aquaculture*, **298**(3-4), 220-225.

Cordell, D., Rosemarin, A., Schroder, J.J., Smit, A.L. 2011. Towards global phosphorus security: A systems framework for phosphorus recovery and reuse options. *Chemosphere*, **84**(6), 747-758.

Cornel, P., Schaum, C. 2009. Phosphorus recovery from wastewater: needs, technologies and costs. *Water Science and Technology*, **59**(6), 1069-1076.

Dauda, A.B., Ajadi, A., Tola-Fabunmi, A.S., Akinwole, A.O. 2019. Waste production in aquaculture: Sources, components and managements in different culture systems. *Aquaculture and fisheries*, **4**(3), 81-88.

de Graaff, D.R., van Loosdrecht, M.C.M., Pronk, M. 2020. Biological phosphorus removal in seawater-adapted aerobic granular sludge. *Water Research*, **172**.

de Kreuk, M., Heijnen, J.J., van Loosdrecht, M.C.M. 2005. Simultaneous COD, nitrogen, and phosphate removal by aerobic granular sludge. *Biotechnology and Bioengineering*, **90**(6), 761-769.

Delaide, B., Monsees, H., Gross, A., Goddek, S. 2019. Aerobic and Anaerobic Treatments for Aquaponic Sludge Reduction and Mineralisation. in: *Aquaponics Food Production Systems*, Springer Nature Switzerland AG, pp. 247-266.

Eck, M., Körner, O., Jijakli, M. 2019. Nutrient Cycling in Aquaponics Systems. in: *Aquaponics Food Production Systems: Combined Aquaculture and Hydropnic Production Technologies for the Future*, (Eds.) S. Goddek, A. Joyce, B. Kotzen, G.M. Burnell, Springer Open.

Goddek, S., Delaide, B.P.L., Joyce, A., Wuertz, S., Jijakli, M.H., Gross, A., Eding, E.H., Blaser, I., Reuter, M., Keizer, L.C.P., Morgenstern, R., Korner, O., Verreth, J., Keesman, K.J. 2018. Nutrient mineralization and organic matter reduction performance of RAS-based sludge in sequential UASB-EGSB reactors. *Aquacultural Engineering*, **83**, 10-19.

Jacobs, B., Cordell, D., Chin, J., Rowe, H. 2017. Towards phosphorus sustainability in North America: A model for transformational change. *Environmental Science & Policy*, **77**, 151-159.

Jasinski, S.M. 2020. Phosphate Rock, (Ed.) USGS.

Jung, I.S., Lovitt, R.W. 2011. Leaching techniques to remove metals and potentially hazardous nutrients from trout farm sludge. *Water Research*, **45**(18), 5977-5986.

Kehrein, P., Van Loosdrecht, M., Osseweijer, P., Garfí, M., Dewulf, J., Posada, J. 2020. A critical review of resource recovery from municipal wastewater treatment plants–market supply potentials, technologies and bottlenecks. *Environmental Science: Water Research & Technology*, **6**(4), 877-910.

Kim, A.H., Yu, A.C., El Abbadi, S.H., Lu, K.T., Chan, D., Appel, E.A., Criddle, C.S. 2021. More than a fertilizer: wastewater-derived struvite as a high value, sustainable fire retardant. *Green Chemistry*, **23**(12), 4510-4523.

Kishida, N., Tsuneda, S., Kim, J.H., Sudo, R. 2009. Simultaneous Nitrogen and Phosphorus Removal from High-Strength Industrial Wastewater Using Aerobic Granular Sludge. *Journal of Environmental Engineering*, **135**(3), 153-158.

Layer, M., Adler, A., Reynaert, E., Hernandez, A., Pagni, M., Morgenroth, E., Holliger, C., Derlon, N. 2019. Organic substrate diffusibility governs microbial community composition, nutrient removal performance and kinetics of granulation of aerobic granular sludge. *Water Research X*, **4**.

Le Corre, K.S., Valsami-Jones, E., Hobbs, P., Parsons, S.A. 2009. Phosphorus Recovery from Wastewater by Struvite Crystallization: A Review. *Critical Reviews in Environmental Science and Technology*, **39**(6), 433-477.

Lehtovirta-Morley, L.E. 2018. Ammonia oxidation: Ecology, physiology, biochemistry and why they must all come together. *Fems Microbiology Letters*, **365**(9).

Lemaire, R., Yuan, Z.G., Bernet, N., Marcos, M., Yilmaz, G., Keller, J. 2009. A sequencing batch reactor system for high-level biological nitrogen and phosphorus removal from abattoir wastewater. *Biodegradation*, **20**(3), 339-350.

Letelier-Gordo, C.O., Larsen, B.K., Dalsgaard, J., Pedersen, P.B. 2017. The composition of readily available carbon sources produced by fermentation of fish faeces is affected by dietary protein:energy ratios. *Aquacultural Engineering*, **77**, 27-32.

Li, X.L., Luo, J.H., Guo, G., Mackey, H.R., Hao, T.W., Chen, G.H. 2017. Seawater-based wastewater accelerates development of aerobic granular sludge: A laboratory proof-of-concept. *Water Research*, **115**, 210-219.

Martins, C.I.M., Eding, E.H., Verdegem, M.C.J., Heinsbroek, L.T.N., Schneider, O., Blancheton, J.P., d'Orbcastel, E.R., Verreth, J.A.J. 2010. New developments in recirculating aquaculture systems in Europe: A perspective on environmental sustainability. *Aquacultural Engineering*, **43**(3), 83-93.

Molaey, R., Yesil, H., Calli, B., Tugtas, A.E. 2021. Enhanced heavy metal leaching from sewage sludge through anaerobic fermentation and air-assisted ultrasonication. *Chemosphere*, **279**.

Mulkerrins, D., O'Connor, E., Lawlee, B., Barton, P., Dobson, A. 2004. Assessing the feasibility of achieving biological nutrient removal from wastewater at an Irish food processing factory. *Bioresource Technology*, **91**(2), 207-214.

Nancharaiah, Y.V., Reddy, G.K.K. 2018. Aerobic granular sludge technology: Mechanisms of granulation and biotechnological applications. *Bioresource Technology*, **247**, 1128-1143.

Naylor, S.J., Moccia, R.D., Durant, G.M. 1999. The chemical composition of settleable solid fish waste (manure) from commercial rainbow trout farms in Ontario, Canada. *North American Journal of Aquaculture*, **61**(1), 21-26.

Peng, L.H., Dai, H.L., Wu, Y.F., Peng, Y.H., Lu, X.W. 2018. A comprehensive review of phosphorus recovery from wastewater by crystallization processes. *Chemosphere*, **197**, 768-781.

Pronk, M., de Kreuk, M.K., de Bruin, B., Kamminga, P., Kleerebezem, R., van Loosdrecht, M.C.M. 2015. Full scale performance of the aerobic granular sludge process for sewage treatment. *Water Research*, **84**, 207-217.

Schneider, O., Sereti, V., Eding, E.H., Verreth, J.A.J. 2005. Analysis of nutrient flows in integrated intensive aquaculture systems. *Aquacultural Engineering*, **32**(3-4), 379-401.

Seviour, T., Pijuan, M., Nicholson, T., Keller, J., Yuan, Z.G. 2009. Gel-forming exopolysaccharides explain basic differences between structures of aerobic sludge granules and floccular sludges. *Water Research*, **43**(18), 4469-4478.

Shaddel, S., Grini, T., Ucar, S., Azrague, K., Andreassen, J.P., Osterhus, S.W. 2020. Struvite crystallization by using raw seawater: Improving economics and environmental footprint while maintaining phosphorus recovery and product quality. *Water Research*, **173**.

Sindilariu, P.D., Brinker, A., Reiter, R. 2009. Waste and particle management in a commercial, partially recirculating trout farm. *Aquacultural Engineering*, **41**(2), 127-135.

Skogen, M.D., Eknes, M., Asplin, L.C., Sandvik, A.D. 2009. Modelling the environmental effects of fish farming in a Norwegian fjord. *Aquaculture*, **298**(1-2), 70-75.

Smolders, G.J.F., Vandermeij, J., Vanloosdrecht, M.C.M., Heijnen, J.J. 1994. Model of the Anaerobic Metabolism of the Biological Phosphorus Removal Process - Stoichiometry and pH Influence. *Biotechnology and Bioengineering*, **43**(6), 461-470.

Tchobanoglous, G., Stensel, H.D., Tsuchihashi, R., Burton, F. 2014. *Wastewater Engineering: Treatment and Resource Recovery*. *5th ed*. Metcalf & Eddy, Inc., McGraw-Hill Education, New York.

U.S. EPA. 1987. Biosolids Technology Fact Sheet

Wagner, J., Guimaraes, L.B., Akaboci, T.R.V., Costa, R.H.R. 2015. Aerobic granular sludge technology and nitrogen removal for domestic wastewater treatment. *Water Science and Technology*, **71**(7), 1040-1046.

Wang, J., Beusen, A.H.W., Liu, X., Bouwman, A.F. 2020. Aquaculture Production is a Large, Spatially Concentrated Source of Nutrients in Chinese Freshwater and Coastal Seas. *Environmental science & technology*, **54**(3), 1464-1474.

Wei, S.P., van Rossum, F., van de Pol, G.J., Winkler, M.K.H. 2018. Recovery of phosphorus and nitrogen from human urine by struvite precipitation, air stripping and acid scrubbing: A pilot study. *Chemosphere*, **212**, 1030-1037.

Winkler, M.K.H., Bennenbroek, M.H., Horstink, F.H., van Loosdrecht, M.C.M., van de Pol, G.J. 2013. The biodrying concept: An innovative technology creating energy from sewage sludge. *Bioresource Technology*, **147**, 124-129.

Winkler, M.K.H., Meunier, C., Henriet, O., Mahillon, J., Suarez-Ojeda, M.E., Del Moro, G., De Sanctis, M., Di Iaconi, C., Weissbrodt, D.G. 2018. An integrative review of granular sludge for the biological removal of nutrients and recalcitrant organic matter from wastewater. *Chemical Engineering Journal*, **336**, 489-502.

Wu, D., Ekama, G.A., Wang, H.G., Wei, L., Lu, H., Chui, H.K., Liu, W.T., Brdjanovic, D., van Loosdrecht, M.C.M., Chen, G.H. 2014. Simultaneous nitrogen and phosphorus removal in the sulfur cycle-associated Enhanced Biological Phosphorus Removal (EBPR) process. *Water Research*, **49**, 251-264.

Appendix D. Supplementary Material for Chapter 5

Table S1. Recipe of the trace element solution.

Chemical	g to add for 2L volume
$EDTA{\cdot}H_2{\cdot}Na_2{\cdot}2H_2O$	100
$FeSO_4{\cdot}7H_2O$	9.98
$ZnSO_4{\cdot}7H_2O$	4.4
$CaCl_2{\cdot}2H_2O$	16.36
$MnCl_2{\cdot}4H_2O$	10.12
$Na_2MoO_4{\cdot}2H_2O$	4.36
$CuSO_4{\cdot}5H_2O$	3.14
$CoSO_4{\cdot}7H_2O$	3.22

Table S2. Concentrations of metals in the fermentation liquid and the supplements; ND = Not detectable at the Reporting Limit.

	ICP-MS Results		Reactor Feed	
Total Metals	Raw Fermentate (10X), µg/L	Reporting Limit, µg/L	Raw Fermentate* (1X), µg/L	Supplements, µg/L
Iron	421	1	42	301
Zinc	36.2	2.5	3.62	150
Manganese	491	5	49	421
Molybdenum	ND	1.5	-	259
Copper	ND	2	-	120
Cobalt	1.46	1	0.15	101

*Calculated from the 10X raw fermentate.

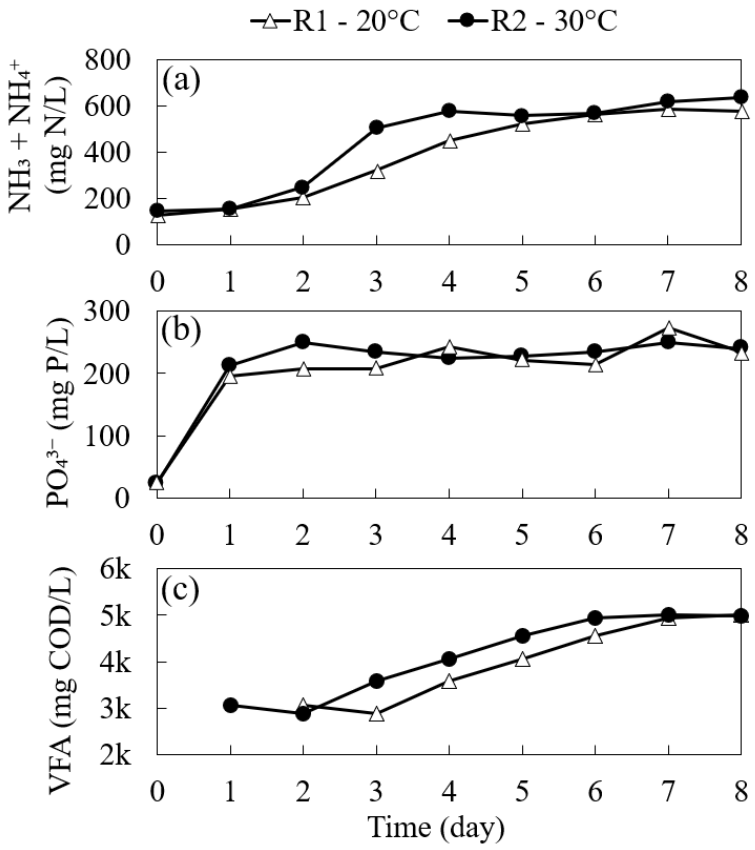

Figure S1. Comparison of (a) ammonia, (b) phosphate, and (c) VFA production between fermentation of fish sludge at 20°C versus 30°C.

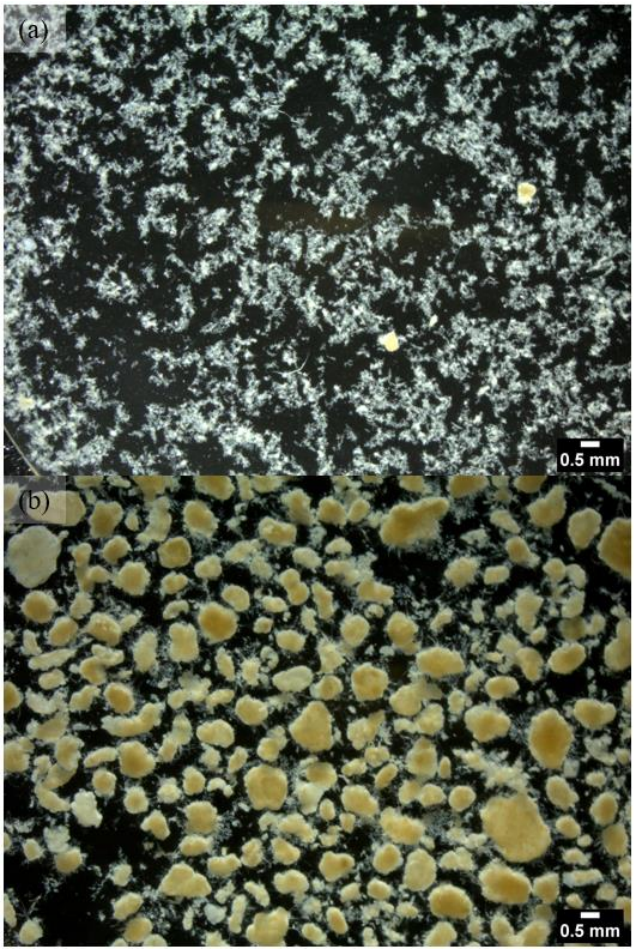

Figure S2. Microscopic images of (a) activated sludge seed and (b) granules on day 165.

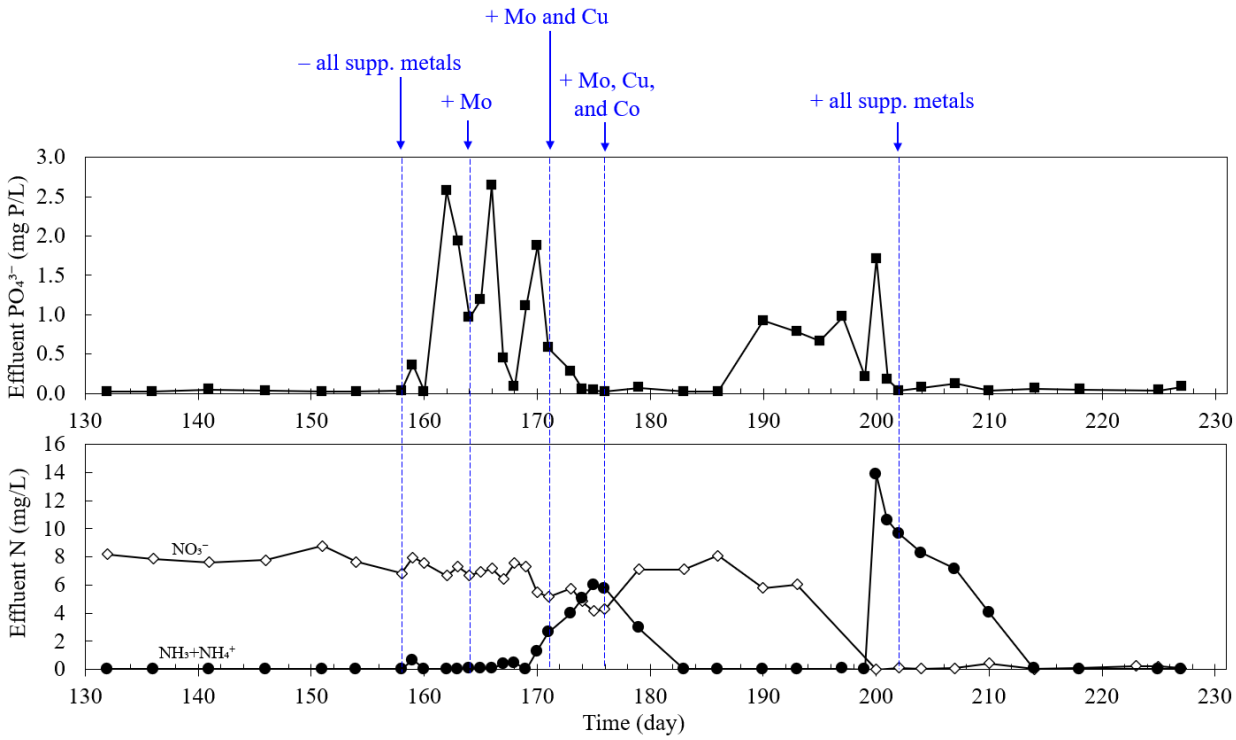

Figure S3. Reactor performance during the metals removal experiment. To test which metals in the fermentation liquid were limiting for the PAO and AOB metabolism, supplementation of the metal mixture in the influent was stopped and slowly replaced with individual metal components. The concentrations of the supplements added are shown in Table S1.

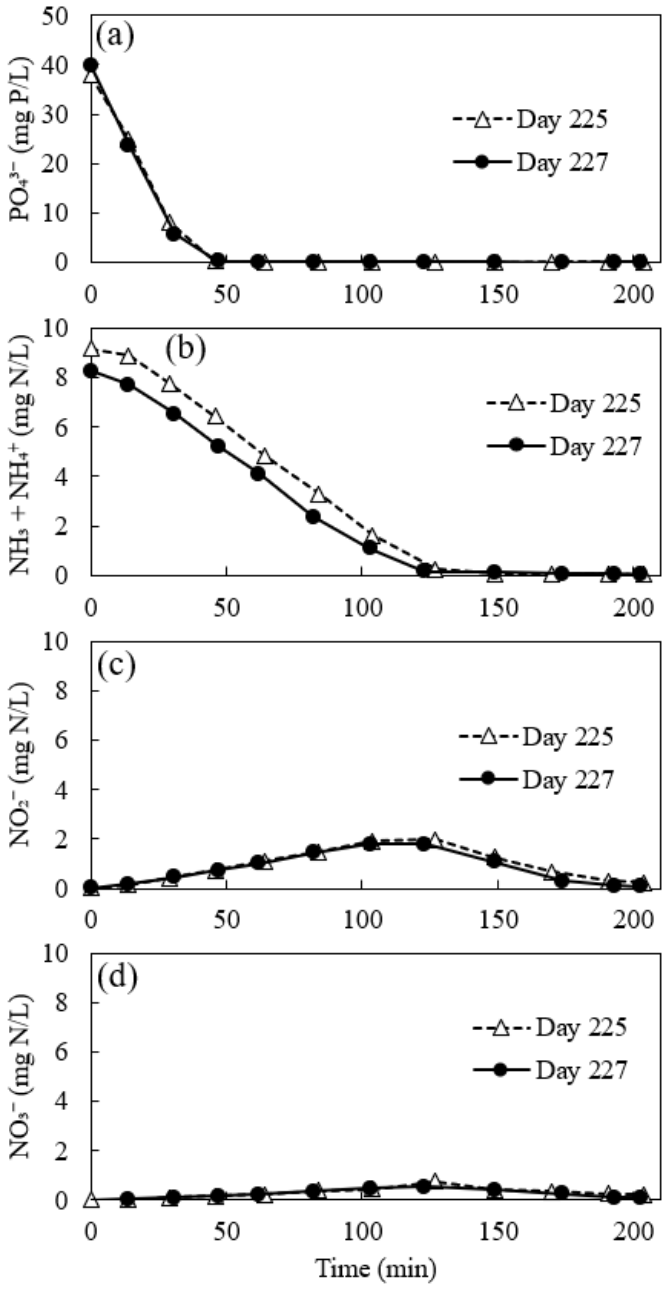

Figure S4. Cycle profile showing concentrations of (a) phosphate, (b) ammonia, (c) nitrite, and (d) nitrate during aerobic phase of reactor operation. Error bar represents coefficient of variants of data from two cycles, each collected on day 225 and 227 (during high N removal efficiency in the reactor).

Chapter 6.

Recovery of Phosphorus and Nitrogen from Human Urine by Struvite Precipitation, Air Stripping and Acid Scrubbing: A Pilot Study

Abstract

Sustainable and closed-loop nutrient cycling require the recovery of valuable resources from wastewater. Resource recovery from diluted wastewater streams is limited by diluted concentrations and unfavorable reaction kinetics. In comparison, source separated urine allows resource recovery from a highly concentrated nutrient stream, resulting in a more sustainable and efficient recovery practice. Different nutrient recovery methods from urine have been studied in lab-scale, but pilot or full-scale process evaluations remain sparse. In this study, recovery of struvite and ammonium sulfate from urine of pregnant women was demonstrated at a pilot-scale treatment facility by means of precipitation and air stripping/acid scrubbing. The system achieved 94% struvite precipitation efficiency but merely 55% of the crystals were removed and recovered. The low phosphorus recovery was due to the washout of small crystals that escaped the sieve and settling tank, hence requiring an improved method for crystals capture. The removal and recovery efficiencies for nitrogen were 93% and 85%, respectively. Composition analysis of the produced fertilizers indicated that struvite was the dominated precipitate and quality of the ammonium sulfate met European standards. Carbamazepine and diclofenac were added in the urine to measure the fate of pharmaceuticals in the treatment system. Very little of the spiked pharmaceuticals (<0.01%) accumulated in the produced struvite and ammonium sulfate. The overall energy demand of the pilot system was 1066 MJ per m^3 urine processed or

198 MJ per kg N removed. Energy efficiency was not optimized and can be improved in many ways.

Published as:

Wei, S. P., F. van Rossum, G. J. van de Pol and M. K. H. Winkler (2018). "Recovery of phosphorus and nitrogen from human urine by struvite precipitation, air stripping and acid scrubbing: A pilot study." Chemosphere **212**: 1030-1037.

6.1 Introduction

In the past decade, the focus of wastewater engineering has shifted from protecting human health and pollution control to sustainability and resource recovery. Resources such as ammonia and phosphate are essential for human food supply. Ammonia is mainly produced from the Haber-Bosch process, conducted under high pressure and temperature, which consumes more than 1% of the world's total energy (Cherkasov et al., 2015). Phosphorus is abundant in the earth's crust but its accessibility and quality are limited; Morocco and China alone account for 78% of the world phosphate rock reserves (Jasinski, 2017). Price of phosphate rocks had increased 2 to 3 folds in the last decade and the production of high-quality phosphorus reserves is estimated to peak in 20 to 70 years (Jacobs et al., 2017), where phosphorus supply starts diminishing.

After consumption of crops by humans, almost 100% of the nitrogen and phosphorus consumed are released within the excreta and discharged into our sewage systems. To avoid eutrophication within natural water bodies, wastewater treatment plants (WWTPs) are designed to remove these nutrients. The most common approach for removing nutrients from wastewater is by conventional nitrification/denitrification and metal salt precipitation, by which the nutrients are effectively removed but also lost (Coats et al., 2011; Mulder, 2003). Nitrification is also an energy-intensive process that consumes up to 60% of the operational cost (Nancharaiah et al., 2016). A more sustainable approach is a closed nutrient loop that recycles the valuable resources from human waste rather than treating them as an unwanted residual.

Efficient resource recovery from combined wastewater streams is limited to existing infrastructure, treatment technologies and unfavorable reaction kinetics at lower/diluted

concentrations (Brands, 2014; Ishii & Boyer, 2015). In terms of sustainable nutrient management, the concept of urine source separation is a more promising practice than conventional wastewater treatment systems (Larsen et al., 2007). Human urine has tremendous potential for nutrient recovery as it contributes to most of the nutrient loads (80% of TN and 45% of TP) but yet accounts to less than 1% of the volumetric flow to a WWTP (Wilsenach & van Loosdrecht, 2006). A coherent approach would be to collect the urine separately from the feces then recover the nutrients from the urine, which circumvents dilution and the need for solids/liquid separation in downstream processing. Separated urine collection allows resource recovery from a more concentrated nutrient stream, offers more flexible recovery strategies and alleviates nutrient loads on WWTPs (Larsen et al., 2009; Maurer et al., 2006; Wilsenach & van Loosdrecht, 2006).

Struvite ($MgNH_4PO_4 \cdot 6H_2O$), a proven slow-releasing fertilizer that does not burn the roots of crops, can be produced from urine. With the presence of high PO_4^{3-} and NH_4^+ in the urine, and externally added magnesium (Mg^{2+}), struvite crystals can be obtained via precipitation in a 1:1:1 molar ratio. Studies on the thermodynamics and influencing factors of struvite precipitation from human urine have been covered in lab-scale (Ronteltap et al., 2007b; Ronteltap et al., 2010; Tilley et al., 2008; Wilsenach et al., 2007). With the production of struvite, 90% PO_4^{3-} but merely 3% NH_4^+ present in the urine can be recovered due to the proportionally higher ammonium than phosphate concentrations (Etter et al., 2011; Maurer et al., 2006), and thus subsequent steps for NH_4^+ removal are required. Maurer et al. (2006) summarized the different NH_4^+ recovery methods from urine but these treatment processes rarely go beyond laboratory scale (Nancharaiah et al., 2016). Similarly, literature studies on pilot or full-scale demonstrations

for struvite recovery from urine are very sparse. Etter et al. (2011) implemented struvite reactors to study the feasibility of recovering struvite from a small village in Nepal aimed for low-cost installation and operations. The pilot study by Antonini et al. (2011) studied the efficiency of phosphorus and nitrogen removal/recovery from human urine by struvite precipitation and air stripping/acid scrubbing for ammonium sulfate production in Vietnam.

Here we present a pilot-scale urine treatment technology for combined phosphorus and nitrogen removal and recovery, built for the Dutch "Betuwse Kunstmest" project (STOWA, 2010). Phosphorus and nitrogen were recovered by struvite precipitation and ammonia stripping/acid scrubbing, respectively. This study evaluates the removal and recovery efficiencies, quality of the produced fertilizers and fate of pharmaceuticals in the system. Energy demand of the system was discussed. This study is one of the few pilot-scale studies for combined nitrogen and phosphorus removal/recovery from human urine.

6.2 Materials and Methods

6.2.1 Urine Source, Transportation and Storage

The urine source in this study came from pregnant women in the Netherlands who donated their urine for the extraction of human chorionic gonadotropin (hCG) hormone for fertility treatment among other women. Collection bottles were supplied to the pregnant women, who then filled the bottles with urine and left them by the door for pickup. The bottles were picked up by a truck and transported to the pharmaceutical company for hormone extraction. Sodium benzoate in ethanol, 1% benzoate (m/v) and 5% (v/v) ethanol, was added as urease inhibitor in the collection bottles to avoid hydrolysis during hormone extraction and transport. After removal of the hCG

hormone, the residual urine was transported to the study site (Tiel, Netherlands). The pH during transportation was adjusted with sulfuric acid to pH 7.0 to avoid undirected struvite precipitation. A lower pH was not necessary since magnesium was low in the delivered urine, leading to lower solubility and precipitation potential (Le Corre et al., 2009).

Upon truck arrival at the pilot facility, the delivered urine was treated with the stages shown in **Figure 6-1**. Except for the storage tank, the system was built under a canopy to reduce the exposure to colder outdoor temperatures and violation of odor emission. Urine was first transferred from the truck into a storage tank, where no pH control was employed. From experience gained during startup, heating of the storage tank was implemented to ensure complete hydrolysis. Temperature of the storage tank was maintained at 18-25 °C with a heat exchanger connected to cooling water (about 30 °C) from a sludge processing unit, which was at the same location but separated from the urine treatment system. The urine was then pumped from the storage tank to the subsequent treatment stages at a flowrate of 0.5 m^3/hr.

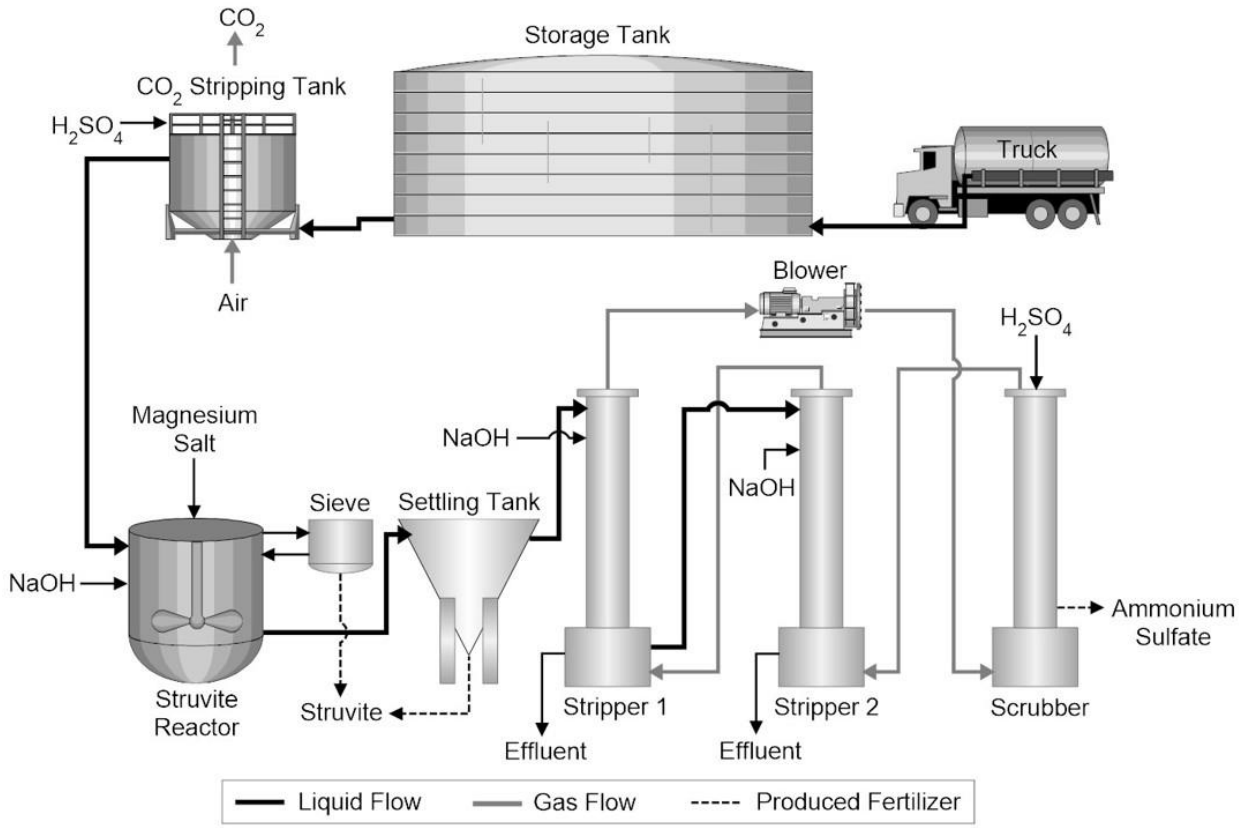

Figure 6-1. Schematic overview of the pilot facility treating human urine for simultaneous nitrogen and phosphorus removal and recovery in the form of ammonium sulfate and struvite.

Extensive sampling and analysis were conducted from February 4th to April 23rd (79 days) of 2009. First, the system was operated with undiluted urine. In real practices, diluted urine could be collected by urine-separating toilets with flushing water. For example, the NoMix toilets require flushing water that usually result in 1 - 10 dilution factor (Udert et al., 2003). Therefore, from day 51 until the end of the project, the urine already present in the storage tank and the urine delivered thereafter were diluted by a factor of 4 ($V_{urine}+V_{water}/V_{urine}$) using tap water in order to evaluate the effect of dilution on system performance.

6.2.2 CO_2 Stripping and Struvite Precipitation

The pH of the CO_2 stripping tank (7 m^3) was automatically controlled at 4.0 with H_2SO_4 (96%). At this low pH condition, all the carbonates present were stripped out of the urine as CO_2 with bubble aeration using an air blower. The purpose of CO_2 stripping was to prevent undirected phosphate carbonate precipitates in the subsequent struvite reactor.

The struvite reactor (2 m^3, 4-hour HRT) was equipped with a stirrer (0.75 kW, 690 rpm, 380 V) and dosage pumps for magnesium and sodium hydroxide (NaOH, 50%) addition. Sodium hydroxide was automatically dosed to ensure a pH of greater than 8.5. The removal of CO_2 in the previous stage reduces the buffering capacity of the urine, and thus little NaOH was needed to raise the pH to 8.5. Based on the measured phosphate concentrations in the CO_2 stripping tank, magnesium salt was dosed into the struvite reactor at a ratio of 1.6 mol Mg/mol P. The form of magnesium salt used was $MgCl_2 \cdot 6H_2O$ initially, then MgOH was used from day 7 until the end of project. With the presence of ammonium, phosphate and magnesium ions as well as sufficiently elevated pH, struvite crystals were formed in the reactor.

Effluent from the struvite reactor was recirculated over a sieve with 100 µm pore size to help capture larger struvite crystals. Smaller crystals were then captured in the settling tank (2 m^3, 4-hour HRT). During the last week of the project, phosphate concentrations in the struvite reactor were raised (by adding less MgOH) for the attempt of obtaining larger struvite crystals. Struvite crystals harvested were gathered in a drip tray and stored for further weighing. Struvite was not allowed for use on agricultural land by regulations in the Netherlands at the time, and thus the

product was stored in bags at the site. The remaining ammonia-rich aqueous solution was then passed onto the ammonium stripping steps.

6.2.3 Ammonium stripping and recovery

Three identically-configured column towers (in series: stripper 1, stripper 2 and scrubber) were used for the recovery of ammonium sulfate. Each of the three columns had a total volume of 0.75 m^3, for which 0.3 m^3 was packed with Super INTALOX® Saddles (specific surface area = 178 m^2/m^3). The columns were heated to maintain the liquid temperature at 35 - 40 °C. Stripper 1 was heated with process air from a separate sludge processing unit at the same location (Winkler et al., 2013). Stripper 2 and the scrubber were heated by the circulated process air. The two strippers were dosed with NaOH (50%) to control the pH at 9. The ammonia-rich liquid from the struvite reactor was fed from the top of stripper 1 at a flowrate of 7 m^3/hr with counter-flow of air from the bottom to strip the ammonia out of the liquid. This process was repeated in stripper 2 with 8 m^3/hr of effluent from stripper 1 to maximize the ammonia removal. Assuming a void fraction of 96% for the packed volume, the HRT was roughly 6.3 min for stripper 1 and 5.5 min for stripper 2.

Effluent from the two ammonia-stripping columns was discharged to the nearby WWTP in Tiel. The produced ammonia-rich air was then fed through the bottom of the scrubber while sulfuric acid solution (H_2SO_4, 96%) was fed from the top at 6.5 m^3/hr. With counter-flows of ammonia-rich air and sulfuric acid, liquid ammonium sulfate, $(NH_4)_2SO_4$, was produced. Air was circulated through the columns in a closed-loop cycle at a rate of 1500 m^3/h with a built-in blower. The liquid and air flowrates were not varied during the study. The produced $(NH_4)_2SO_4$

was supplied to the fertilizer market as 40% (w/v) solution. The fertilizer product was used on grassland and farmland in arable areas of the Netherlands such as Flevopolder.

6.2.4 Sample Collection and Analysis

Grab samples were collected periodically at each process stage. Number of samples over the project duration varied from 34 to 37 at different sampling locations. Upon collection, samples were immediately transported to the laboratory of Waterschap Rivierenland about 3 kilometers away. At the laboratory, pH, COD, TKN, Cl^-, NH_4^+-N, CO_3^{2-}, HCO_3^-, TP, Ca^{2+}, K^+, Mg^{2+}, Na^+, PO_4^{3-}, NO_3^--N, NO_2^--N, and SO_4^{2-} were analyzed. Struvite samples were sent to Waterschap Rivierenland for elemental composition analysis by inductively coupled plasma atomic emission spectroscopy. An ammonium sulfate sample was collected on day 50 and sent to Eurofins Analytico, NL for analysis of ammonium and sulfate compositions by spectrometry, and heavy metal contents by inductively coupled plasma mass spectrometry.

6.2.5 Pharmaceutical Experiment

After the main testing period, an additional experiment was conducted to explore the accumulation of pharmaceuticals in the produced ammonium sulfate and struvite. External carbamazepine and diclofenac were added to the urine to then later assess if the added compounds can be found in the produced fertilizers. Urine samples were collected from the storage tank prior to the experiment for analysis of background concentrations. On day 1, all pumps were stopped and carbamazepine and diclofenac were spiked in the storage tank aiming for concentrations of 50 µg/L and 100 µg/L, respectively. The added pharmaceuticals and the urine in the storage tank were mixed with recirculating pumps. Old struvite crystals were removed from the sieve. Immediately after spiking and mixing of pharmaceuticals, the system

was back online but received no more fresh urine. On day 4 (three days after spiking), urine samples were collected from all treatment stages. At the same time, new struvite crystals on the sieve and ammonium sulfate samples were collected. Samples were sent to Het Waterlaboratorium in Harlem for analysis of carbamazepine and diclofenac. The analysis was performed by ultra-performance liquid chromatography coupled with mass spectrometry. Pharmaceuticals were extracted from the samples by solid phase extraction. For struvite samples, 0.3 g of crystals were first dissolved in 100 ml of 1.5 M HCl.

6.2.6 Energy Demand Estimation

Electrical usage was obtained from electricity meter reading in kWh. Usage of H_2SO_4/NaOH was recorded at the site. Magnesium usage was estimated from the PO_4^{3-} concentration in the CO_2 stripping tank and the dosing factor 1.6 molMg/molP. Electricity and chemical usages were converted to energy consumption. Conversion factors and detailed calculations are provided in Table A4. Energy used for truck transport of collected urine was not included.

6.3 Results and Discussions

6.3.1 Urine Storage and CO_2 stripping

A total of 158 m^3 of urine was treated during the testing period. **Table 6-1** shows the fresh and stored urine compositions as well as values from the literature for comparison. The amount of COD present was higher than typical urine composition in other studies due to the added urease inhibitor (sodium benzoate in ethanol). Precipitations were found at the bottom of the storage tank, which is commonly observed as pH increases to 9.0 due to urea hydrolysis (Maurer et al., 2006). Elemental analysis of the precipitates yielded 3.6% nitrogen, 20% calcium, 4.5% magnesium and 13% phosphorus (dry solids weight), indicating the precipitates were struvite

and hydroxyapatite ($Ca_5(PO_4)_3(OH)$). These precipitates are commonly found during urine storage (Boyer et al., 2014; Udert et al., 2006), with calcite ($CaCO_3$) being another potential precipitate that is more prevalent at higher dilution factors (>18) (Udert et al., 2003). Under non-sterile conditions, complete hydrolysis was expected in the storage tank. NH_3+NH_4^+ (ammonia) constituted 91% of the TKN, which is similar to the 90% reported by Udert et al. (2006) after urea hydrolysis. The CO_2 stripping tank removed more than 99.5% of the bicarbonate and carbonate present in the storage tank.

Table 6-1. Composition of urine in this study and in the literature

		Fresh urine			Stored urine			
Parameter	Unit	This study	[a]	[b]	This study	This study	[c]	[d]
DF[e]		1	1[g]	1	1	4	1	1
pH		4.2 ± 0.3	5.6	7	8.9 ± 0.1	8.8 ± 0.2	9.3	9.1
Carbonate[f]	mM	1 ± 2	853	-	337 ± 30	90 ± 28	-	-
Ca^{2+}	mg/L	293 ± 227	89	253	267 ± 283	57 ± 29	17	0
Cl^-	mg/L	4450 ± 173	6620	-	4400 ± 253	1161 ± 185	3400	3800
COD	mg/L	14850 ± 705	7660	-	13545 ± 690	3318 ± 600	4500	10000
K^+	mg/L	1181 ± 56	1870	867	1166 ± 7	297 ± 42	1900	2200
Mg^{2+}	mg/L	49 ± 7	45.4	145	<50	7 ± 12	0.9	0
Na^+	mg/L	2300 ± 141	3240	2570	2300 ± 7	587 ± 118	2400	2600
SO_4^{2-}	mg/L	1008 ± 95	878	-	1181 ± 27	319 ± 77	800	-
TKN	mg N/L	6475 ± 82	4450[h]	-	6159 ± 299	1594 ± 198	-	9200[i]
NH_3+NH_4^+	mg N/L	443 ± 78	438	259	5615 ± 266	1447 ± 203	3700	8100
NO_3^-+NO_2^-	mg N/L	-	-	-	-	-	-	0
PO_4^{3-}	mg P/L	437 ± 10	388	327	384 ± 39	88 ± 37	223	-

[a] Rural village in Nepal (Etter et al., 2011); [b] teaching building in Beijing, China (Liu et al., 2014); [c] water-free urinals at an office (Zamora et al., 2017); [d] simulated values by Udert et al. (2006). [e] DF = dilution factor. [f] Total carbonate. [g] Slightly diluted from wash water for cleaning of urine-diverting dry toilets. [h] Urea. [i] Total nitrogen.

6.3.2 Struvite Precipitation and Nitrogen Removal

The ammonia and phosphate concentrations of the storage tank and the effluent are shown in **Figure 6-2**. The struvite precipitation efficiency of undiluted and diluted urine were 94 ± 6% and 80 ± 23%, respectively. Achieving high precipitation efficiencies (>97%) with undiluted urine is easy at Mg/P dosage ratio of more than 1.3 (Antonini et al., 2011; Liu et al., 2013; Ronteltap et al., 2010). The lower struvite precipitation efficiency of the diluted urine was largely due to reduction of Mg^{2+} addition in the struvite reactor, which was done purposely towards the end of the project for obtaining larger struvite crystals (discussed in Section 6.3.3). Due to the variability introduced from reducing the magnesium addition, we could not conclude from data

that dilution had a negative effect on the struvite precipitation performance. Theoretically, precipitation efficiency will reduce with dilution because precipitation is determined by equilibrium concentrations (Ronteltap et al., 2010; Tilley et al., 2008). Dilution can also have a negative effect on struvite precipitation efficiency by lowering the nucleation and growth rate (Le Corre et al., 2009). However, the effect of dilution on precipitation rates would not be noticeable with the long HRT of 8 hours in our struvite precipitation stage (reaction+ settling) compared to the 30-35 min reported as sufficient for struvite precipitation (Liu et al., 2013; Morales et al., 2013).

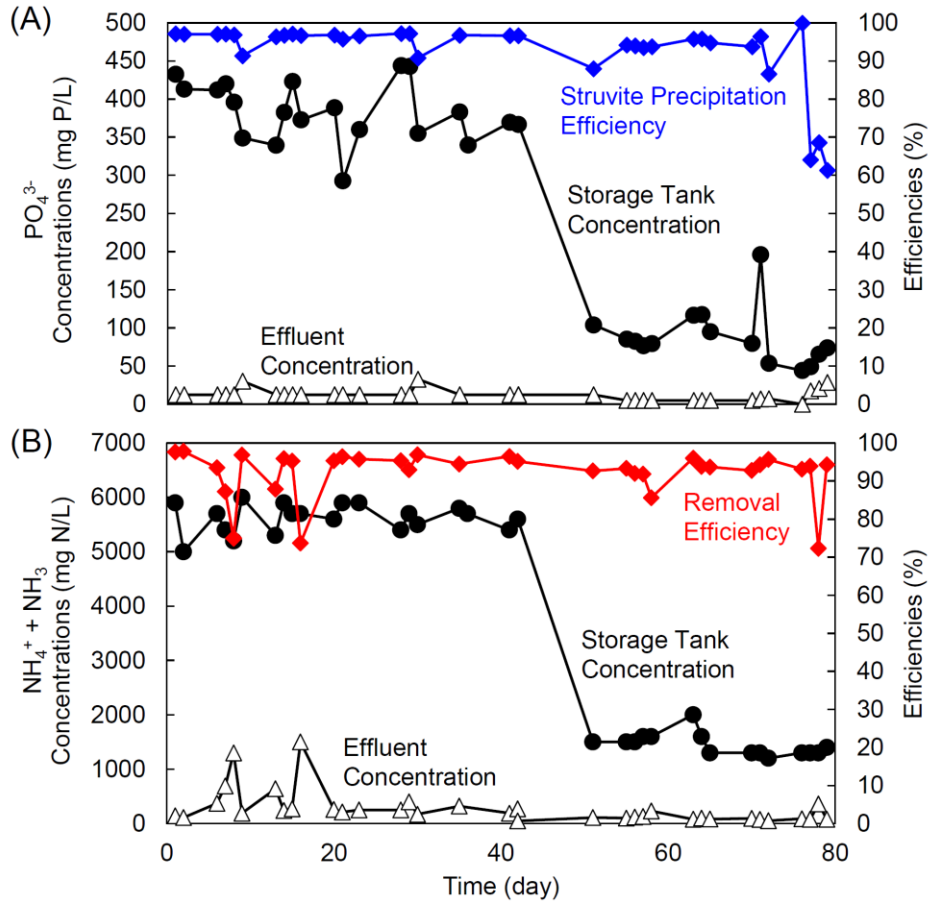

Figure 6-2. Concentrations of (a) phosphate and (b) ammonia in the storage tank and the effluent.

Similar nitrogen removal efficiencies were achieved for undiluted (93 ± 7%) and diluted urine (92 ± 6%). This corroborates findings by Liu et al. (2015) that dilution had no significant effect on NH_4^+ removal efficiency with air stripping whereas pH, temperature and air flow rate had much larger impact. Stripper 1 removed 74 ± 8% of NH_3 while stripper 2 provided additional 21 ± 5% removal. Lab-scale studies on air stripping using urine include Behrendt et al. (2002), Basakcilardan-Kabakci et al. (2007) and Liu et al. (2015), but Antonini et al. (2011) is the only pilot-scale demonstration other than this study. Antonini et al. (2011) achieved 91% NH_3 removal with one stripping tower, at 40 °C and pH 10, a Q_{air}/Q_{liquid} ratio of 13000, and a process time of 300 min. In comparison, this study achieved similar removal efficiency with two strippers at much lower Q_{air}/Q_{liquid} ratio of 188 – 214 and process time of roughly 12 mins. It should be noted that higher ammonia removal efficiencies were attainable but not required by discharge limits.

6.3.3 Recovery Efficiencies of Struvite and Ammonium Sulfate

Recovery efficiencies for phosphorus and nitrogen are listed in **Table 6-2**. A portion of the phosphorus (roughly 12% of undiluted urine) was lost via precipitation in the storage tank. Amount of P loss increases with the use of tap water because the Mg^{2+} and Ca^{2+} ions present in the tap water can form struvite and hydroxyapatite precipitates during storage (Liu et al., 2014), and thus dilution practices during urine collection and storage should be minimized. The rest of the P loss could be explained by the washout of smaller crystals. The struvite crystals formed were small and difficult to capture with the sieve (pore size of 100 μm) and the settler. It was not until close to the end of the project that raising the phosphate concentrations (by adding less magnesium) in the struvite reactor led to formation of larger struvite crystals and improved P recovery efficiency due to better capture on the sieve. Literature studies on struvite precipitations

with urine have reported crystal sizes from 12 to 100 µm (Barbosa et al., 2016; Liu et al., 2014; Morales et al., 2013; Ronteltap et al., 2010), which are smaller than the 500 to 3000 µm for struvite crystals recovered from anaerobic digester reject water (Mavinic et al., 2007; Ueno & Fujii, 2001). In general, larger struvite crystals are difficult to obtain with hydrolyzed urine due to the higher zeta-potential of struvite at high pH (Ronteltap et al., 2010). Alternative methods for recovery of small struvite crystals, other than sieving and settling, need to be further explored. Etter et al. (2011) had a similar problem where sedimentation achieved only 50% of struvite crystal capturing. The use of filter bag increased their P removal efficiency from 50% to 91%. Antonini et al. (2011) also achieved 98% P removal efficiency with a filter bag.

Table 6-2. Phosphorus and nitrogen recovery efficiencies.

Parameter	Value	Unit
Total TP processed	84	kg P
Total struvite produced	46	kg P
Phosphorus removal/recovery efficiency	55	%
Struvite produced per unit urine treated	1.7	kg/m^3
Total TKN processed	965	kg N
Total $(NH_4)_2SO_4$ produced	815	kg N
Nitrogen recovery efficiency as $(NH_4)_2SO_4$	85	%
$(NH_4)_2SO_4$ produced per unit urine treated	3.7	kg/m^3

The increase of struvite crystal size from reduction of Mg^{2+} addition can be explained with supersaturation. Both the nucleation (formation of struvite embryo) and growth (growth of the embryo into harvestable crystals) of struvite crystals are impacted by the parameter, supersaturation (Doyle & Parsons, 2002). Supersaturation is defined as the ratio between the activity of Mg^{2+}, NH_4^+ and PO_4^{3-} ions versus the struvite solubility product (Le Corre et al., 2009). At higher supersaturation ratio, nucleation dominates growth, which lead to smaller

struvite crystals; at lower supersaturation, growth dominates nucleation, which lead to larger struvite crystals (Ronteltap et al., 2010). For our case, less Mg^{2+} addition led to a lower ionic strength of the solution and lower activity of the ions, which resulted in lower superstation and ultimately, larger struvite crystals. Although larger crystals were obtained, higher effluent PO_4^{3-} concentrations and lower P removal efficiencies accompanied. Consequently, there is a tradeoff between obtaining larger struvite crystals and achieving very low effluent PO_4^{3-} concentrations. A possible future system modification would be to first recover large struvite crystals at low Mg^{2+} dosage, followed by a polishing step where the residual PO_4^{3-} is removed with high Mg^{2+} dosage.

Many studies have conducted air stripping and acid scrubbing for recovery of ammonium sulfate from high-ammonium waters, such as digester supernatant (Boehler et al., 2015), dewatered waste activated sludge (Winkler et al., 2013), landfill leachate (Ferraz et al., 2013) and dairy manure (Tao & Ukwuani, 2015). But applications using urine are limited to few (Antonini et al., 2011; Basakcilardan-Kabakci et al., 2007; Liu et al., 2015). For this study, ammonia removal efficiency was higher than 92% but only 85% of nitrogen was recovered as ammonium sulfate, indicating a 7% loss. Roughly 3% of the ammonium was removed via struvite precipitation. The remaining 4% could be due to NH_3 volatilization during CO_2 stripping or leakage out of the stripping/scrubbing towers.

6.3.4 Quality of Struvite and Ammonium Sulfate

Struvite compositions are presented in Table A1 along with the theoretical values of pure struvite. Compositions of Sample 1 were close to the theoretical composition of struvite except no elemental O was reported. Sample 2 had much higher weight percentage for magnesium,

implying presence of precipitations other than struvite. The relatively high C content (7%) could be due to flocculation of particulate organics onto the struvite crystals (Ryu & Lee, 2010). Overall, Mg, N and P represented a large portion of the samples, indicating the dominance of struvite crystals. Microscopic image of the crystals (Figure A1) shows the typical coffin shape of struvite (Barbosa et al., 2016). It is known that urine contains very small amounts of heavy metals (Spangberg et al., 2014) and that common commercial fertilizer products have higher heavy metals than untreated urine (Ronteltap et al., 2007a). Our results corroborate this understanding with the low heavy metals detected in the produced ammonium sulfate (Table A2). The produced ammonium sulfate contained only a few impurities and analysis of heavy metals showed that the quality met European and Dutch quality standards (EuropeanCommission, 1986; SDU, 1991).

6.3.5 Pharmaceuticals in Recovered Fertilizers

On average, 64% of the pharmaceuticals excreted by humans end up in urine and thus the accumulation of pharmaceuticals in fertilizers produced from urine is a general concern (Ronteltap et al., 2007a). Prior to spiking of pharmaceuticals, the concentrations in the storage tank were 10.9±0.3 and 0.7±0.1 µg/L for carbamazepine and diclofenac, respectively. These background concentrations were lower than the average concentrations in the Netherlands (Kujawa-Roeleveld & Schuman, 2008), because the urine of this study came from pregnant women, who are usually more careful in pharmaceutical consumption. Therefore, additional pharmaceuticals were spiked in the storage tank. Three days after spiking, the pharmaceutical concentrations at each process stage and the contents in the produced fertilizers were measured and are shown in Table A3. The decreasing trend of concentrations through the treatment processes can be explained by dilution from the urine already present in the system and not due

to actual removal by the treatment processes. The average HRT of the system was about 2.5 days. When samples were collected 3 days after spiking, it was likely that some amount of old non-spiked urine was still in the system. In addition, concentration reduction due to struvite precipitation would be very minimal as the measured content (18.3 µg carbamazepine and 14.8 µg diclofenac per kg of struvite) correspond to concentration reductions of less than 0.05 µg/L in the struvite reactor (Table A3).

For both pharmaceutical compounds, less than 0.01% of the spiked amount accumulated in the produced struvite and ammonium sulfate (Table A3). These results corroborate well with past research, which showed that struvite produced from urine is usually free of pharmaceutical residue with 0.1 – 0.3% of spiked carbamazepine and <0.1% of spiked diclofenac accumulated (Escher et al., 2006; Ronteltap et al., 2007b; Schurmann et al., 2012). The low pharmaceutical accumulation in the ammonium sulfate was expected since removal of carbamazepine and diclofenac by air stripping is limited due to their good solubility (Zhang et al., 2008). To our knowledge, this is the only study with reported data on the fate of pharmaceuticals in a urine treatment process for ammonium sulfate production.

This study produced nearly pharmaceuticals-free fertilizers from the urine, but the pharmaceuticals remained in the effluent will enter the receiving treatment facility if left untreated. Removal of micropollutants is not a requirement at conventional WWTPs, where typical removals for carbamazepine and diclofenac are 16% and 20%, respectively (Margot et al., 2015). Instead of upgrading the WWTPs for advanced treatments, source-separated urine offers an opportunity to remove the pharmaceuticals at higher concentrations. As reviewed by

Maurer et al. (2006), most of the pharmaceutical removal methods for urine treatment, such as nanofiltration and electrodialysis, are designed mainly for nutrient recovery, and thus separation of pharmaceuticals from the nutrients is the main mechanism. Ion exchange (Landry et al., 2015) and biochar adsorption (Solanki & Boyer, 2017) are other alternatives for pharmaceutical attenuation. Ozonation has been shown to effectively degrade micropollutants, including carbamazepine and diclofenac, but should be coupled with pre-treatment (e.g. electrodialysis or struvite precipitation) to reduce scavenging of oxidant by other species (e.g. ammonia) and include added benefits of nutrient recovery (Dodd et al., 2008).

6.3.6 Energy Demand

The energy demand of this study (**Table 6-3**) was calculated based on electricity and chemical usage data for a 16-day testing period. The energy efficiency of this period was the highest throughout the study due to turning off of canopy heating and treatment with undiluted urine. The total energy demand was 1066 MJ per m^3 urine processed or 198 MJ per kg N removed, including energy demand for fertilizer production. It should be noted that energy optimization was not a goal of the study and there are many possible improvements that can be made for energy savings. For example, blowers for NH_3 stripping/scrubbing were oversized and proper sizing would reduce electricity usage. Additionally, efficiency for CO_2 stripping can be improved by installing an actual CO_2 stripper rather than an open tank. One possibility is to eliminate the entire CO_2 stripping process. We speculate that CO_2 stripping was unnecessary prior to struvite precipitation since carbonate precipitates were not observed in other pilot studies without CO_2 stripping (Antonini et al., 2011; Etter et al., 2011). For treatment of digester supernatant, CO_2 stripping is used for the purpose of increasing pH (Boehler et al., 2015; Morales et al., 2013). But pH adjustment is not needed for hydrolyzed urine due to its high pH (> 8.5) and strong buffering

capacity (Ronteltap et al., 2007b). Removal of CO_2 reduces the buffering capacity of urine, thereby requiring high NaOH dosage during the air stripping stage when large amounts of ammonia (an alkalinity component) are stripped from the system. NaOH was the most energy consuming component (80% of total energy demand) and was mostly demanded by the ammonium processing step. The effect on energy efficiency by omitting the CO_2 stripping step cannot be estimated for this study since individual electricity and chemical consumption data separated into each process unit is not available (electricity and chemical usage were collected for the entire process). We recommend additional tests to be done to evaluate whether CO_2 stripping is necessary.

Table 6-3. Breakdown of the consumption data and calculated energy demand[a].

	Unit	Value
Consumption Data:		
H_2SO_4 (96%)	kg/kg N recovered	6.8
NaOH (pellets)	kg/kg N recovered	2.2
MgOH	kg Mg/kg P precipitated	0.42
Electricity	kWh/m^3 urine processed	36
Converted to Primary Energy:		
Chemicals	MJ/m^3 urine processed	688[b]
Electricity	MJ/m^3 urine processed	341[c]
Fertilizer Production:		
N fertilizer	MJ/m^3	32[d]
P fertilizer	MJ/m^3	5.0[d]

[a] Calculated for the testing period of day 27 - day 43. See Table A4 for detailed calculations.

[b] Using a -3.6 MJ/kg H_2SO_4 conversion factor, assuming a modern double contact process (exports 6 GJ/tonne H_2SO_4 of energy) with 60% energy recovery (EuropeanCommission, 2007); 24.3 MJ/kg 50% NaOH (Brinkmann et al., 2014); 14.9 MJ/kg Mg (Schorcht et al., 2013).

[c] Using an energy production efficiency of 38% and conversion factor of 1 kWh = 3.6 MJ (EuropeanCommission, 2009).

[d] Calculated based on energy requirements for fertilizer production reported by Maurer et al. (2003) and the recovery efficiencies of this study.

Maurer et al. (2003) compared the energy consumptions for different nutrient removal methods from urine. It was suggested that nitrogen recovery by air stripping/$(NH_4)_2SO_4$ production requires more energy in comparison to the Sharon/Anammox process (no N recovery) and N fertilizer production. Indeed, biological processes have been shown to be more cost-effective at removing nutrients from wastewater than physical processes (Siegrist, 1996). However, in this study ammonia stripping/acid scrubbing ensure well controllable and stable process performance as it does not rely on biological processes, which can fail and require a longer time to recover. In addition, biological nitrogen removal processes could be less climate-friendly than processes without nitrogen oxidation due to N_2O emissions (Larsen, 2015). Furthermore, the recovery of phosphorus in this study was particularly valuable and struvite precipitation was relatively simple and required little energy consumption. Application of struvite as fertilizer has been approved in the Netherlands since 2015 and new regulations are underway to improve production and trading of struvite between European member states (EuropeanCommission, 2017). With an increase in sales market for struvite and the potential increase of fertilizer price due to diminishing phosphorus reserves, this system can become more competitive.

6.4 Conclusions

This pilot-scale study has demonstrated that source separated urine offers a promising opportunity to recover phosphorus as struvite and nitrogen as ammonium sulfate from wastewater. The conclusions are as follows:

1. Simultaneous nitrogen and phosphate recovery was enabled by a struvite precipitation reactor for P removal/recovery, and an air stripping unit for N removal followed by an acid scrubbing unit for N recovery as ammonium sulfate.
2. The treatment system achieved high removal efficiencies of 93% for nitrogen and struvite precipitation efficiencies of 94%.
3. The recovery efficiencies were 55% for phosphorus and 85% for nitrogen. About 12% of the phosphorus was lost via precipitation in the storage tank and rest of the P loss was likely due smaller struvite crystals that escaped in the effluent. Alternative methods for more efficient capture of small struvite crystals need to be further explored.
4. Composition analysis showed that struvite was the main precipitate. The produced ammonium sulfate had very few impurities and the heavy metals content met marketable quality.
5. The pharmaceutical experiment showed that less than 0.01% of the spiked carbamazepine and diclofenac accumulated in the produced fertilizers.
6. The system's estimated energy demand was 1066 MJ per m^3 urine processed or 198 MJ per kg N removed, from which NaOH dosage for air stripping made up the most consumption. Ways to optimize energy usage were identified, such as the potential omission of the CO_2 stripping step. Although the system may not be competitive with other nitrogen removal

processes such as Sharon/Anammox in terms of energy efficiencies, it might be more robust as it does not rely on biological processes and offers added benefits for phosphorus recovery.

Acknowledgements

The presented work was carried out under STOWA's Betuwse Kunstmest project. We would like to thank STOWA and LeAF for the financial support and Waterschap Rivierenland for the excellent project cooperation. The authors would like to thank Eliza C Heery and Will King for their comments on this manuscript.

References

Antonini, S., Paris, S., Eichert, T., Clemens, J. 2011. Nitrogen and Phosphorus Recovery from Human Urine by Struvite Precipitation and Air Stripping in Vietnam. *Clean-Soil Air Water*, **39**(12), 1099-1104.

Barbosa, S.G., Peixoto, L., Meulman, B., Alves, M.M., Pereira, M.A. 2016. A design of experiments to assess phosphorous removal and crystal properties in struvite precipitation of source separated urine using different Mg sources. *Chem. Eng. J.*, **298**, 146-153.

Basakcilardan-Kabakci, S., Ipekoglu, A.N., Talini, I. 2007. Recovery of ammonia from human urine by stripping and absorption. *Environ. Eng. Sci.*, **24**(5), 615-624.

Behrendt, J., Arevalo, E., Gulyas, H., Niederste-Hollenberg, J., Niemiec, A., Zhou, J., Otterpohl, R. 2002. Production of value added products from separately collected urine. *Water Sci. Technol.*, **46**(6-7), 341-346.

Boehler, M.A., Heisele, A., Seyfried, A., Gromping, M., Siegrist, H. 2015. (NH4)(2)SO4 recovery from liquid side streams. *Environ. Sci. Pollut. Res.*, **22**(10), 7295-7305.

Boyer, T.H., Taylor, K., Reed, A., Smith, D. 2014. Ion- Exchange Softening of Human Urine to Control Precipitation. *Environ. Prog. Sustain. Energy*, **33**(2), 564-571.

Brands, E. 2014. Prospects and challenges for sustainable sanitation in developed nations: a critical review. *Environ. Rev.*, **22**(4), 346-363.

Brinkmann, T., Santonja, G.G., Schorcht, F., Roudier, S., Sancho, L.D. 2014. Best Available Techniques (BAT) Reference Document for the Production of Chlor-alkali, (Ed.) Industrial Emissions Directive, European Commission.

Cherkasov, N., Ibhadon, A.O., Fitzpatrick, P. 2015. A review of the existing and alternative methods for greener nitrogen fixation. *Chem. Eng. Process.*, **90**, 24-33.

Coats, E.R., Watkins, D.L., Kranenburg, D. 2011. A Comparative Environmental Life-Cycle Analysis for Removing Phosphorus from Wastewater: Biological versus Physical/Chemical Processes. *Water Environ. Res.*, **83**(8), 750-760.

Dodd, M.C., Zuleeg, S., Von Gunten, U., Pronk, W. 2008. Ozonation of Source-Separated Urine for Resource Recovery and Waste Minimization: Process Modeling, Reaction Chemistry, and Operational Considerations. *Environ. Sci. Technol.*, **42**(24), 9329-9337.

Doyle, J.D., Parsons, S.A. 2002. Struvite formation, control and recovery. *Water Res.*, **36**(16), 3925-3940.

Escher, B.I., Pronk, W., Suter, M.J.F., Maurer, M. 2006. Monitoring the removal efficiency of pharmaceuticals and hormones in different treatment processes of source-separated urine with bioassays. *Environ. Sci. Technol.*, **40**(16), 5095-5101.

Etter, B., Tilley, E., Khadka, R., Udert, K.M. 2011. Low-cost struvite production using source-separated urine in Nepal. *Water Res.*, **45**(2), 852-862.

EuropeanCommission. 1986. Council Directive on the protection of the environment, and in particular of the soil, when sewage sludge is ursed in agriculture (86/278/EEC), Official Journal of the European Communities.

EuropeanCommission. 2009. Reference Document on Best Available Techniques for Energy Efficiency.

EuropeanCommission. 2007. Reference Document on Best Available Techniques for the Manufacture of Large Volume Inorganic Chemicals - Ammonia, Acids and Fertilisers.

EuropeanCommission. 2017. Report on the implementation of the Circular Economy Action Plan.

Ferraz, F.M., Povinelli, J., Vieira, E.M. 2013. Ammonia removal from landfill leachate by air stripping and absorption. *Environ. Technol.*, **34**(15), 2317-2326.
Ishii, S.K.L., Boyer, T.H. 2015. Life cycle comparison of centralized wastewater treatment and urine source separation with struvite precipitation: Focus on urine nutrient management. *Water Res.*, **79**, 88-103.
Jacobs, B., Cordell, D., Chin, J., Rowe, H. 2017. Towards phosphorus sustainability in North America: A model for transformational change. *Environmental Science & Policy*, **77**, 151-159.
Jasinski, M.S. 2017. Phosphate Rock. U.S. Geological Survey.
Kujawa-Roeleveld, K., Schuman, E. 2008. Sustainable Water Management in the City of the Future: Biodegradability and fate of pharmaceutical impact compounds in different treatment processes SWITCH.
Landry, K.A., Sun, P., Huang, C.H., Boyer, T.H. 2015. Ion-exchange selectivity of diclofenac, ibuprofen, ketoprofen, and naproxen in ureolyzed human urine. *Water Res.*, **68**, 510-521.
Larsen, T.A. 2015. CO2-neutral wastewater treatment plants or robust, climate-friendly wastewater management? A systems perspective. *Water Res.*, **87**, 513-521.
Larsen, T.A., Alder, A.C., Eggen, R.I.L., Maurer, M., Lienert, J. 2009. Source Separation: Will We See a Paradigm Shift in Wastewater Handling? *Environ. Sci. Technol.*, **43**(16), 6121-6125.
Larsen, T.A., Maurer, M., Udert, K.M., Lienert, J. 2007. Nutrient cycles and resource management: implications for the choice of wastewater treatment technology. *Water Sci. Technol.*, **56**(5), 229-237.
Le Corre, K.S., Valsami-Jones, E., Hobbs, P., Parsons, S.A. 2009. Phosphorus Recovery from Wastewater by Struvite Crystallization: A Review. *Crit. Rev. Environ. Sci. Technol.*, **39**(6), 433-477.
Liu, B.X., Giannis, A., Zhang, J.F., Chang, V.W.C., Wang, J.Y. 2015. Air stripping process for ammonia recovery from source-separated urine: modeling and optimization. *J. Chem. Technol. Biotechnol.*, **90**(12), 2208-2217.
Liu, X.N., Hu, Z.Y., Zhu, C.Y., Wen, G.Q., Meng, X.C., Lu, J. 2013. Influence of process parameters on phosphorus recovery by struvite formation from urine. *Water Sci. Technol.*, **68**(11), 2434-2440.
Liu, X.N., Wen, G.Q., Wang, H.H., Zhu, X.Q., Hu, Z.Y. 2014. Fate of phosphorus in diluted urine with tap water. *Chemosphere*, **113**, 146-150.
Margot, J., Rossi, L., Barry, D.A., Holliger, C. 2015. A review of the fate of micropollutants in wastewater treatment plants. *Wiley Interdisciplinary Reviews-Water*, **2**(5), 457-487.
Maurer, M., Pronk, W., Larsen, T.A. 2006. Treatment processes for source-separated urine. *Water Res.*, **40**(17), 3151-3166.
Maurer, M., Schwegler, P., Larsen, T.A. 2003. Nutrients in urine: energetic aspects of removal and recovery. *Water Sci. Technol.*, **48**(1), 37-46.
Mavinic, D.S., Koch, F.A., Huang, H., Lo, K.V. 2007. Phosphorus recovery from anaerobic digester supernatants using a pilot-scale struvite crystallization process. *J. Environ. Eng. Sci.*, **6**(5), 561-571.
Morales, N., Boehler, M.A., Buettner, S., Liebi, C., Siegrist, H. 2013. Recovery of N and P from Urine by Struvite Precipitation Followed by Combined Stripping with Digester Sludge Liquid at Full Scale. *Water*, **5**(3), 1262-1278.

Mulder, A. 2003. The quest for sustainable nitrogen removal technologies. *Water Sci. Technol.*, **48**(1), 67-75.
Nancharaiah, Y.V., Mohan, S.V., Lens, P.N.L. 2016. Recent advances in nutrient removal and recovery in biological and bioelectrochemical systems. *Bioresour. Technol.*, **215**, 173-185.
Ronteltap, M., Maurer, M., Gujer, W. 2007a. The behaviour of pharmaceuticals and heavy metals during struvite precipitation in urine. *Water Res.*, **41**(9), 1859-1868.
Ronteltap, M., Maurer, M., Gujer, W. 2007b. Struvite precipitation thermodynamics in source-separated urine. *Water Res.*, **41**(5), 977-984.
Ronteltap, M., Maurer, M., Hausherr, R., Gujer, W. 2010. Struvite precipitation from urine - Influencing factors on particle size. *Water Res.*, **44**(6), 2038-2046.
Ryu, H.D., Lee, S.I. 2010. Application of struvite precipitation as a pretreatment in treating swine wastewater. *Process Biochem.*, **45**(4), 563-572.
Schorcht, F., Kourti, I., Scalet, B.M., Roudier, S., Sancha, L.D. 2013. Best Available Techniques (BAT) Reference Document for the Production of Cement, Lime and Magnesium Oxide, (Ed.) J.R. Centre, European Commission.
Schurmann, B., Everding, W., Montag, D., Pinnekamp, J. 2012. Fate of pharmaceuticals and bacteria in stored urine during precipitation and drying of struvite. *Water Sci. Technol.*, **65**(10), 1774-1780.
SDU. 1991. Besluit overige organische meststoffen (BOOM). Vol. Decree 613: 1-45.
Siegrist, H. 1996. Nitrogen removal from digester supernatant - Comparison of chemical and biological methods. *Water Sci. Technol.*, **34**(1-2), 399-406.
Solanki, A., Boyer, T.H. 2017. Pharmaceutical removal in synthetic human urine using biochar. *Environmental Science-Water Research & Technology*, **3**(3), 553-565.
Spangberg, J., Tidaker, P., Jonsson, H. 2014. Environmental impact of recycling nutrients in human excreta to agriculture compared with enhanced wastewater treatment. *Sci. Total Environ.*, **493**, 209-219.
STOWA. 2010. Betuwse kunstmest (ISBN 9789057734960).
Tao, W.D., Ukwuani, A.T. 2015. Coupling thermal stripping and acid absorption for ammonia recovery from dairy manure: Ammonia volatilization kinetics and effects of temperature, pH and dissolved solids content. *Chem. Eng. J.*, **280**, 188-196.
Tilley, E., Atwater, J., Mavinic, D. 2008. Recovery of struvite from stored human urine. *Environ. Technol.*, **29**(7), 797-806.
Udert, K.M., Larsen, T.A., Gujer, W. 2003. Estimating the precipitation potential in urine-collecting systems. *Water Res.*, **37**(11), 2667-2677.
Udert, K.M., Larsen, T.A., Gujer, W. 2006. Fate of major compounds in source-separated urine. *Water Sci. Technol.*, **54**(11-12), 413-420.
Ueno, Y., Fujii, M. 2001. Three years experience of operating and selling recovered struvite from full-scale plant. *Environ. Technol.*, **22**(11), 1373-1381.
Wilsenach, J.A., Schuurbiers, C.A.H., van Loosdrecht, M.C.M. 2007. Phosphate and potassium recovery from source separated urine through struvite precipitation. *Water Res.*, **41**(2), 458-466.
Wilsenach, J.A., van Loosdrecht, M.C.M. 2006. Integration of processes to treat wastewater and source-separated urine. *J. Environ. Eng-ASCE*, **132**(3), 331-341.

Winkler, M.K.H., Bennenbroek, M.H., Horstink, F.H., van Loosdrecht, M.C.M., van de Pol, G.J. 2013. The biodrying concept: An innovative technology creating energy from sewage sludge. *Bioresour. Technol.*, **147**, 124-129.

Zamora, P., Georgieva, T., Salcedo, I., Elzinga, N., Kuntke, P., Buisman, C.J.N. 2017. Long-term operation of a pilot-scale reactor for phosphorus recovery as struvite from source-separated urine. *J. Chem. Technol. Biotechnol.*, **92**(5), 1035-1045.

Zhang, Y.J., Geissen, S.U., Gal, C. 2008. Carbamazepine and diclofenac: Removal in wastewater treatment plants and occurrence in water bodies. *Chemosphere*, **73**(8), 1151-1161.

Appendix E. Supplementary Material for Chapter 6

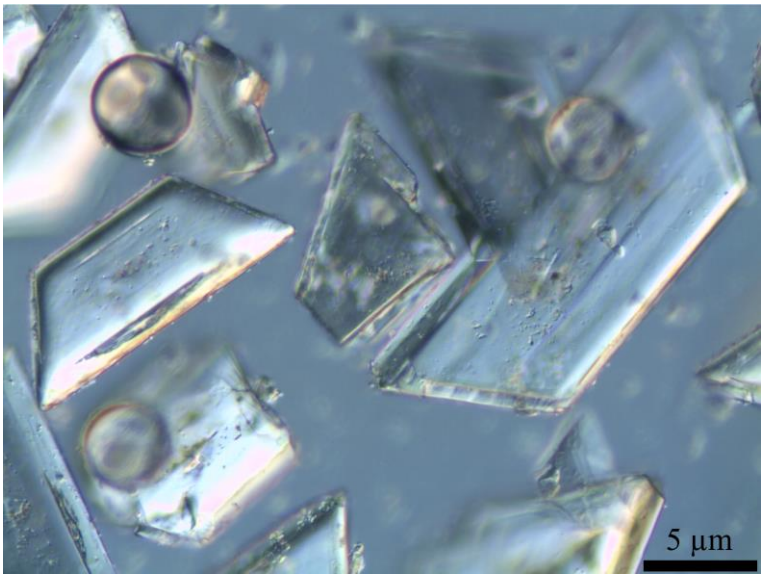

Fig. A1. Microscopic image of the produced struvite.

Table A1. Theoretical and measured weight percentages of elemental compositions in produced struvite.

	Theoretical %	Measured %	
Element	Struvite[a]	Sample 1[b]	Sample 2[b]
Mg	9.9	9.3	19.0
N	5.7	5.4	3.4
P	12.6	12.0	15.4
O	65.2	-	48.1
C	-	-	6.9
Na	-	<4	1.0
S	-	0.1	2.2
Cl	-	-	1.7
K	-	0.2	0.7
Fe	-	<0.1	-
Ca	-	0.2	1.6

[a] Calculations include bounded hydrates (6 moles of H_2O).

[b] Composition analysis was done after drying struvite at 40°C; at this temperature, hydrates remain bounded to the crystals.

Table A2. Composition of the formed ammonium sulfate (sample from March 25, 2009) and the threshold values for heavy metals under European Union sludge directive and Dutch BOOM regulations. All units in mg/kg.

Parameter	Value	EU 86/278/EEC[a]	BOOM[b]
Ammonium	180000	-	-
Sulfate	550000	-	-
Residue	675000	-	-
Arsenic	0.08	-	-
Cadmium	<0.01	20-40	1.25
Chromium	0.18	-	75
Copper	0.4	1000-1750	75
Mercury	0.03	16 - 25	-
Nickel	0.21	300-400	30
Lead	<0.125	750-1200	100
Zinc	0.33	2500-4000	300

[a] Threshold values in the European Sewage Sludge Directive for reuse of sludge in agriculture soil (EuropeanCommission, 1986).

[b] Threshold values per Dutch standards for sludge disposal on agricultural soils (SDU, 1991).

Table A3. Carbamazepine and diclofenac measured at each process stage and in the produced fertilizers.

	Unit	Carbamazepine	Diclofenac
Concentrations 3 days after spiking			
Storage tank	µg/L	67.5 ± 0.6	104.7 ± 4.0
Hydrolysis tank	µg/L	63.3 ± 0.9	85.3 ± 0.5
Struvite reactor	µg/L	54.7 ± 4.0	74.5 ± 4.7
Stripper 1	µg/L	41.0 ± 0.3	53.5 ± 0.0
Stripper 2	µg/L	34.6 ± 1.0	48.4 ± 2.8
Fertilizers[a]			
Struvite (non-washed)	µg/kg	18.3 ± 16.6	14.8 ± 7.2
Ammonium sulfate	µg/L	0.08 ± 0.0	0.05 ± 0.0
Estimated concentration reduction due to losses to struvite[b]			
	µg/L	0.04	0.03
Estimated percentage of spiked amount accumulated in the produced fertilizer			
Struvite[c]	%	0.01	0.01
Ammonium sulfate[d]	%	0.01	0.00

[a] On Day 4 of the pharmaceutical experiment (4/23/2009), a total of 4.5 m^3 urine, 0.33 kg P and 6.3 kg N were processed. Using the P recovery efficiency of 55% (**Table 6-2**), the estimated amount of P recovered was 0.18 kg (0.33 kg × 0.55) or 1.46 kg struvite. Using the N recovery efficiency of 85% (**Table 6-2**), the estimated amount of N recovered was 5.36 kg (6.3 kg × 0.85) or 50.5 kg ammonium sulfate.

[b] Carbamazepine: 18.3 µg/kg × 1.46 kg struvite ÷ 2000 L (struvite reactor volume) = 0.013 µg/L per day. Diclofenac: 14.8 µg/kg × 1.46 kg struvite ÷ 2000 L = 0.011 µg/L per day. Duration of experiment = 3 days. Carbamazepine reduction = 0.013 µg/L per day × 3 days = 0.04 µg/L. Diclofenac reduction = 0.011 µg/L per day × 3 days = 0.03 µg/L

[c] Example calculations shown for carbamazepine. If all spiked amount accumulated in struvite: 54.7 µg/L (concentration in struvite reactor) × 4.5 m^3 urine × 1000 L/m^3 ÷ 1.46 kg struvite = 168,596 µg/kg. Percentage of spiked amount found in produced struvite = 18.3 µg/kg (measured amount in struvite) × 100 ÷ 168,596 µg/kg = 0.011%.

[d] Example calculations shown for carbamazepine. If all spiked amount accumulates in ammonium sulfate: 34.6 µg/L (concentration in stripper 2) × 4.5 m^3 urine × 1000 L/m^3 ÷ 50.5 kg ammonium sulfate × 0.4 kg/L (concentration of 40% ammonium sulfate) = 1233 µg/L. Percentage of spiked amount found in produced ammonium sulfate = 0.08 µg/L (measured amount in ammonium sulfate) × 100 ÷ 1233 µg/L = 0.01%.

Table A4. Operational data for the period of 3/3/2009 (day 27) – 3/18/2009 (day 43) and the calculated energy demand.

	Unit	Value	Notes or Calculations
Operational Data			
Urine processed	m^3	35.0	
NH_4 processed	kg N	200	
NH_4 removed	kg N	189	
$(NH_4)_2SO_4$ recovered	kg N	175	Production amount recorded at treatment site
PO_4 processed	kg P	13.2	
PO_4 precipitated	kg P	12.5	
PO_4 recovered	kg P	7.30	13.2 kg of PO_4 processed × 55% struvite recovery efficiency
H_2SO_4 (96%) dosage	kg/m^3	40.0	kg of H_2SO_4 dosed recorded at treatment site ÷ 35 m^3
NaOH (50%) dosage	kg/m^3	34.0	kg of NaOH dosed recorded at treatment site ÷ 35 m^3
MgOH dosage	kg/m^3	0.42	PO_4 concentrations in CO_2 stripping tank × dosing factor 1.6 molMg/molP
Electricity Usage	kWh/m^3	36.0	Read from electricity meter ÷ 35 m^3
Normalized to kg of N or P			
NaOH (50%) dosage	kg/kg N	6.8	34 kg/m^3 × 35 m^3 urine processed ÷ 175 kg N recovered
NaOH pellets	kg/kg N	2.2	(6.8 kg 50% solution/kg N) ÷ (3.03 g 50% solution/g pellets)* *1515 g/L (density) ÷ 500 g/L (concentration) = 3.03 g 50% NaOH solution/g NaOH pellets
H2SO4 (96%) dosage	kg/kg N	8.0	40.0 kg/m^3 × 35 m^3 urine processed ÷ 175 kg N recovered
MgOH dosage	kg/kg P	1.18	0.42 kg/m^3 × 35 m^3 urine processed ÷ 12.5 kg P precipitated
Converted to Primary Energy			
H_2SO_4 (96%)	MJ/m^3	-144	40.0 kg/m^3 × -3.6 MJ/kg H_2SO_4 (100%)[a]
NaOH (50%)	MJ/m^3	826	34.0 kg/m^3 × 24.3 MJ/kg NaOH (50%)[b]
MgOH	MJ/m^3	6.3	0.42 kg/m^3 × 14.9 MJ/kg Mg[c]

Total chemicals demand	MJ/m^3	688	-144 + 826 + 6.3
Electricity	MJ/m^3	341	36.0 kWh/m^3 × 3.6 MJ/kWh ÷ 38% efficiency factor[d]
Fertilizer Production			
N needed to be produced	kg N	25	200 kg processed – 175 kg N recovered
Energy for N production	MJ/m^3	32	25 kg N × 45 MJ/kg N[e] ÷ 35 m^3 urine processed
P needed to be produced	kg P	6.0	kg P processed – kg P recovered
Energy for P production	MJ/m^3	5.0	6 kg P × 29 MJ/kg P[f] ÷ 35 m^3 urine processed
Total Energy Demand			
	MJ/m^3	1066	688 + 341 + 32 + 5
	MJ/kg N	198	1066 MJ/m^3 × 35 m^3 urine processed ÷ 189 kg N removed

[a] Using a -3.6 MJ/kg H_2SO_4 conversion factor, assuming a modern double contact process (exports 6 GJ/tonne H_2SO_4 of energy) with 60% energy recovery (EuropeanCommission, 2007).

[b] Conversion factor = 24.3 MJ/kg 50% NaOH (Brinkmann et al., 2014).

[c] Conversion factor = 14.9 MJ/kg Mg (Schorcht et al., 2013).

[d] Energy production efficiency = 38% and conversion factor of 1 kWh = 3.6 MJ (EuropeanCommission, 2009).

[e] Average N fertilizer production in Europe (Maurer et al., 2003).

[f] Average P fertilizer production in Europe (Maurer et al., 2003)

References

Brinkmann, T., Santonja, G.G., Schorcht, F., Roudier, S., Sancho, L.D. 2014. Best Available Techniques (BAT) Reference Document for the Production of Chlor-alkali, (Ed.) Industrial Emissions Directive, European Commission.

EuropeanCommission. 1986. Council Directive on the protection of the environment, and in particular of the soil, when sewage sludge is ursed in agriculture (86/278/EEC), Official Journal of the European Communities.

EuropeanCommission. 2009. Reference Document on Best Available Techniques for Energy Efficiency.

EuropeanCommission. 2007. Reference Document on Best Available Techniques for the Manufacture of Large Volume Inorganic Chemicals - Ammonia, Acids and Fertilisers.

Maurer, M., Schwegler, P., Larsen, T.A. 2003. Nutrients in urine: energetic aspects of removal and recovery. *Water Sci. Technol.*, **48**(1), 37-46.

Schorcht, F., Kourti, I., Scalet, B.M., Roudier, S., Sancha, L.D. 2013. Best Available Techniques (BAT) Reference Document for the Production of Cement, Lime and Magnesium Oxide, (Ed.) J.R. Centre, European Commission.

SDU. 1991. Besluit overige organische meststoffen (BOOM). Vol. Decree 613: 1-45.

Chapter 7.

Physiological Studies of Nitrogen Source Repression in Ammonia-Oxidizing Microorganisms

7.1 Introduction

Ammonia-oxidizing organisms (AOO) are responsible for the first step of nitrification that oxidizes ammonia to nitrite, which is subsequently oxidized to nitrate by the nitrite-oxidizing bacteria (NOB) during the second step of nitrification. One-step nitrification can also be performed by the complete ammonia oxidizer (comammox). Together, these microorganisms facilitate the nitrification process that contributes to nitrogen cycling and link the mineralization and nitrogen loss processes in the ocean, soils, and biological wastewater treatment systems (Houlton & Bai, 2009; Thamdrup & Dalsgaard, 2002; Ward et al., 2009); it also contributes to environmental damages such as nitrate leaching into the aquatic environments and the emission of the potent greenhouse gas nitrous oxide from anthropogenic nitrogen inputs (Ravishankara et al., 2009). Since the isolation of the first ammonia-oxidizing bacteria (AOB) in the early 1890s (Frankland & Frankland, 1890), many species that are affiliated to various AOO lineages have been cultured and characterized, including the first pure culture of an ammonia-oxidizing archaea (AOA) (Konneke et al., 2005) and comammox (Daims et al., 2015). Because all ammonia oxidizers primarily metabolize the same substrate (i.e., ammonia) for energy production and biosynthesis, ammonia oxidation kinetics is thought to exert major control on the niche partitioning of different AOO groups in ecosystems (Martens-Habbena et al., 2009). However, even though archaeal and bacterial ammonia oxidizers possess widely different affinities to ammonia, co-existence of high-affinity AOA and comammox and low affinity AOB

can be found in most habitats, suggesting additional physiological and metabolic traits are in play to provide alternative survival and life strategies.

In natural and engineered environments, the availability of ammonia varies temporally and spatially. Alternative nitrogen sources, such as urea and cyanate, can be hydrolyzed to ammonia first by the AOO (or other microorganisms) then utilized (Kitzinger et al., 2019). Urea is a dissolved nitrogen compound that is ubiquitous in many ecosystems. In coastal marine environments, the concentrations of urea can be in the same range or exceed the ammonia concentrations (Alonso-Saez et al., 2012; Kitzinger et al., 2019). Urea is also the most common form of synthetic nitrogen fertilizer used globally (Sigurdarson et al., 2018) and one of the major nitrogen compounds in some wastewater treatment systems (Urbanczyk et al., 2016). Genomic analyses had shown that many AOA, AOB, and comammox species contain the genes encoding the cytoplasmic nickel-dependent urease (*UreABC*) and the urease accessory proteins (*UreEFGD*) (Koch et al., 2019; Koper et al., 2004; Qin et al., 2020), and some AOB also encode the biotin- and ATP-dependent urea amidolyase (Norton et al., 2008), indicating their genomic potential to hydrolyze urea. Though urea can passively diffuse across the cell membrane, the urease-positive comammox possess the complete gene set for the active urea transporter (*UrtABCDE*) that is associated with high urea affinity (Koch et al., 2019; Palomo et al., 2018). In addition to genomic studies, the ability of AOB and AOA to grow on urea as the sole nitrogen substrate has been confirmed with pure culture batch incubation experiments (Allison & Prosser, 1991; Qin et al., 2014).

Ammonia is considered the primary substrate for both energy generation and nitrogen

requirement for AOO, and it is generally assumed that urea is an alternative source of ammonia. However, it remains to be shown whether urea is utilized only when ammonia is unavailable or both ammonia and urea can be co-metabolized in AOO. Constitutive expression of the urease gene (despite status of ammonia availability) has been suggested in some AOB species (Jiang & Bakken, 1999; Zorz et al., 2018). On the other hand, the nitrogen regulatory PII proteins appear to be widely distributed among the AOA (Qin et al., 2020), suggesting that regulatory mechanisms may be in place to facilitate selective usage of nitrogen substrates. The selective carbon-source usage and associated carbon catabolite repression regulation have been extensively studied in many model organisms (Gorke & Stulke, 2008). Conversely, little work has been conducted to study the regulation of microbial metabolism using different nitrogen sources and the available studies on nitrogen source repression are limited to the regulation of nitrogen uptake and assimilation for the purpose of microbial biosynthesis (Mobley et al., 1995; Watzer et al., 2019). The impetus for understanding nitrogen acquisition by AOO is for chemoautotrophic energy production that control the inorganic nitrogen species transformation processes and fluxes in natural and engineered ecosystems, which is completely different from the N uptake by other organisms for nutritive requirement. Yet our understanding in the nitrogen repression regulation (for both catabolism and biosynthesis) in AOO is very limited, even baseline physiological data characterizing how AOO use substrates from a mixture of different nitrogen sources are lacking.

In this work, we present physiological data that shows the indication of (or indicate the lack thereof) nitrogen source repression in different urease-containing ammonia oxidizer isolates, *Nitrososphaera viennensis* EN76 (soil AOA), *Nitrosopumilus piranensis* D3C (marine AOA),

Nitrosospira lacus APG3 (freshwater *β*-AOB), *Nitrosococcus oceani* ATCC 19707 (marine *γ*-AOB), and *Nitrospira inopinata* ENR4 (comammox). The objectives are to elucidate how the AOO selectively use ammonia and/or urea (in the presence of both substrates), to understand how the regulation of selective N source utilization vary among the phylogenetically distinct AOO, and how this variation infers their ecological niches.

7.2 Materials and Methods

7.2.1 Maintenance culture

All AOO species were maintained in liquid HEPES buffered synthetic Crenarchaeota medium (Qin et al., 2017). 200 µl of 100 mM sodium pyruvate was added for *N. viennensis* culture as a H_2O_2 scavenger. Cultures were maintained in 250-ml glass bottle with 100-ml media volume aerobically in the dark without agitation. Incubation was done at 42°C, 30°C, 20°C, 30°C, and 37°C for *N. viennensis*, *N. piranensis*, *N. lacus*, *N. oceani*, and *N. inopinata*, respectively. Growth was monitored by photometric measurements of nitrite for all AOOs except *N. inopinata*, for which nitrite plus nitrate was measured, on a Gallery Analyzer (Thermo Fisher Scientific). Contamination of all cultures were checked monthly by confirming no growth on R2A plates. Sanger sequencing was conducted every 6 months to assess purity of the strain.

7.2.2 Baseline growth experiments

Incubation experiments were set up with three different conditions: 1 mM NH_4^+, 0.5 mM NH_4^+ + 0.25 mM urea, and 0.5 mM urea. Inoculation was done with 1% transfer from the maintenance culture at mid-exponential phase. Media composition, culture volume, and growth conditions were same as the maintenance cultures. Lower concentrations of the nitrogen substrates were used for *N. lacus* due to their inhibition at NO_2^- concentration higher than 0.5 mM (Figure S1). A

negative control bottle was prepared for the 0.5 mM urea and 0.5 mM NH_4^+ + 0.25 mM urea conditions without addition of cells to confirm no non-biological degradation of urea. Samples were taken roughly at every doubling time and urea, NH_4^+, NO_2^-, and NO_3^- were monitored. Urea was measured according to Fawcett and Scott (1960). First, an aliquot was split from the original sample and treated with urease (Millipore Sigma #U1500) to convert urea into ammonia. Ammonia was measured for the urease-treated aliquot and the original sample on the Gallery Analyzer. Urea was then determined by subtracting the ammonia concentration in the original sample (untreated) from the aliquot (urease-treated).

7.2.3 Cell count and yield

A mounting medium was prepared consisting of 3 µl of 1 M ascorbic acid in 200 µl of Moviol solution (Moviol 4-88; Fluka). Cells were captured on a 0.02-µm Anopore membrane filter (Whatman) and stained with 20 µl of the mounting medium. Using a Zeiss Axioskop 2 MOT epifluorescence microscope, cell numbers were determined for 20 random fields (20 – 100 cells per field) per sample. Cell yield was then calculated by the averaged cell count per mol of ammonia oxidized.

7.2.4 Alternative nitrogen spike experiments

The response of the AOO to sudden introduction of an alternative nitrogen source was tested via two directions: (1) incubation with ammonia initially then spiked with urea and (2) incubation with urea initially then spiked with ammonia. Inoculation was done with 1% transfer from the maintenance culture at mid-exponential phase. Culture was grown on 0.5 mM (as N) of the first nitrogen substrate. Once half of the first nitrogen substrate was depleted, 0.5 mM (as N) of the second nitrogen substrate was spiked into the same culture bottle. Media composition, culture

volume, and growth conditions were same as the maintenance cultures. Samples were taken roughly at every doubling time and analyzed for urea, NH_4^+, NO_2^-, and NO_3^- concentrations.

7.2.5 Extracellular urease activity checks

Incubation experiments were conducted to check whether urease activities occurred extracellularly using three strains of AOO (*N. viennensis*, *N. inopinata*, and *N. lacus*). Cultures were incubated in 0.5 mM of urea using the same volume and growth conditions as the maintenance cultures. Upon near depletion of urea, the cells were removed via filtering with a sterile 0.02 µM filter while additional urea was re-added to the same bottle. Concentration of ammonia and urea were monitored for 8 - 10 more days to confirm no urea hydrolysis.

7.3 Results and Discussions

7.3.1 Consumption of Ammonia and Urea

The ammonia-only incubations (**Figure 7-1a**) showed typical physiology of ammonia conversion to nitrite (AOA and AOB) or nitrate (comammox). When urea was added together with ammonia as the initial substrate (**Figure 7-1b**), the AOA and comammox strains consumed the urea only after ammonia was fully exhausted or nearly depleted, indicating repression of the urea-utilizing functions when ammonia was available. Interestingly, marine AOA experienced a long lag phase between ammonia depletion and the start of urea utilization, suggesting that the urea-utilizing functions were activated only after ammonia was exhausted. The same diauxic lag was not apparent for soil AOA and comammox, which may indicate that the urea-utilizing functions were activated before full ammonia depletion. In contrast to the repression of the urea-utilizing functions under ammonia sufficiency, as was observed for the AOA and comammox strains, urea utilization proceeded in the β- and γ-AOB incubations (*N. lacus and N. oceani*) despite the

presence of ammonia.

All ammonia oxidizers could grow on media containing only urea (**Figure 7-1c**) but for *N. oceani*, whose growth on the the urea-only media resulted in a very slow specific growth rate (μ_{max} = 0.03 ± 0.005 day^{-1}; doubling time = 23 ± 4 days). Incubations with different initial ammonia-N:urea-N ratios indicated that a ratio of at least 1:1 was needed for *N. oceani* to grow at a rate comparable to ammonia-only incubation.

Although cellular localization of the urease enzyme in ammonia oxidizers is yet to be confirmed, extracellular urease activity was not observed for three of the AOO strains tested in this work (Figure S2). In addition, the ability of some neutrophilic ammonia oxidizers to grow under acidic condition with urea (but not ammonia) (Burton & Prosser, 2001; Lu et al., 2012) also support the mechanism of intracellular hydrolysis of urea and thus the cytoplasmic localization of the urease enzyme. With this assumption, the liberation of the ammonia molecules from urea would occur inside the cytoplasm and the subsequent ammonia diffusion into the periplasmic space (or pseudo-periplasmic space in the case of AOA) can be more conveniently utilized by the membrane-bound ammonia monooxygenase (AMO), if the active site of AMO is directed toward the periplasm. This description was supported by a low background ammonia concentration in the urea-only incubations for the AOA and comammox (**Figure 7-1c**), indicating rapid ammonia consumption upon urea hydrolysis. When grown on only urea, the background ammonia for *N. inopinata* and *N. piranensis* were almost un-detectable while 10 – 50 µM of background ammonia was observed in the *N. viennensis* incubation. It may be possible that AMO is constitutively active in *N. inopinata* and *N. piranensis* whereas *N. viennensis* have a strict

regulation system that switches AMO on/off depending on ammonia availability. This hypothesis corroborates with the observation that among the studied AOO in this study, *N. viennensis* experienced the largest reduction in maximum specific growth rate when grown on urea in comparison to ammonia (**Figure 7-2a**), suggesting a higher energy spent on shifting between alternative nitrogen substrates.

In contrast to the low background ammonia observed for the AOA and comammox, urea consumption by *N. lacus* was accompanied by a marked increase in bulk liquid ammonia concentration (**Figure 7-1c**), indicating a highly unbalanced ammonia production and consumption fluxes from urea hydrolysis and ammonia oxidation, respectively. The same observation can be made when both ammonia and urea were added (**Figure 7-1b**). In addition, the amount of urea-N utilized roughly equaled the amount of ammonia accumulated plus nitrite produced for both cases (**Figure 7-1b** and **Figure 7-1c**), which begs the question of whether the original ammonia (that was added in the media) was ever transported into the cells. If the original ammonia was not transported into the cells, it would indicate an inactive ammonia transporter and that the only source of ammonia for oxidation and assimilation would be from ureolysis. This hypothetical nitrogen assimilation pathway is depicted with a schematic in Figure S3, which must be confirmed with stable isotope labeling analysis and nanoscale secondary-ion mass spectrometry (NanoSIMS) analysis.

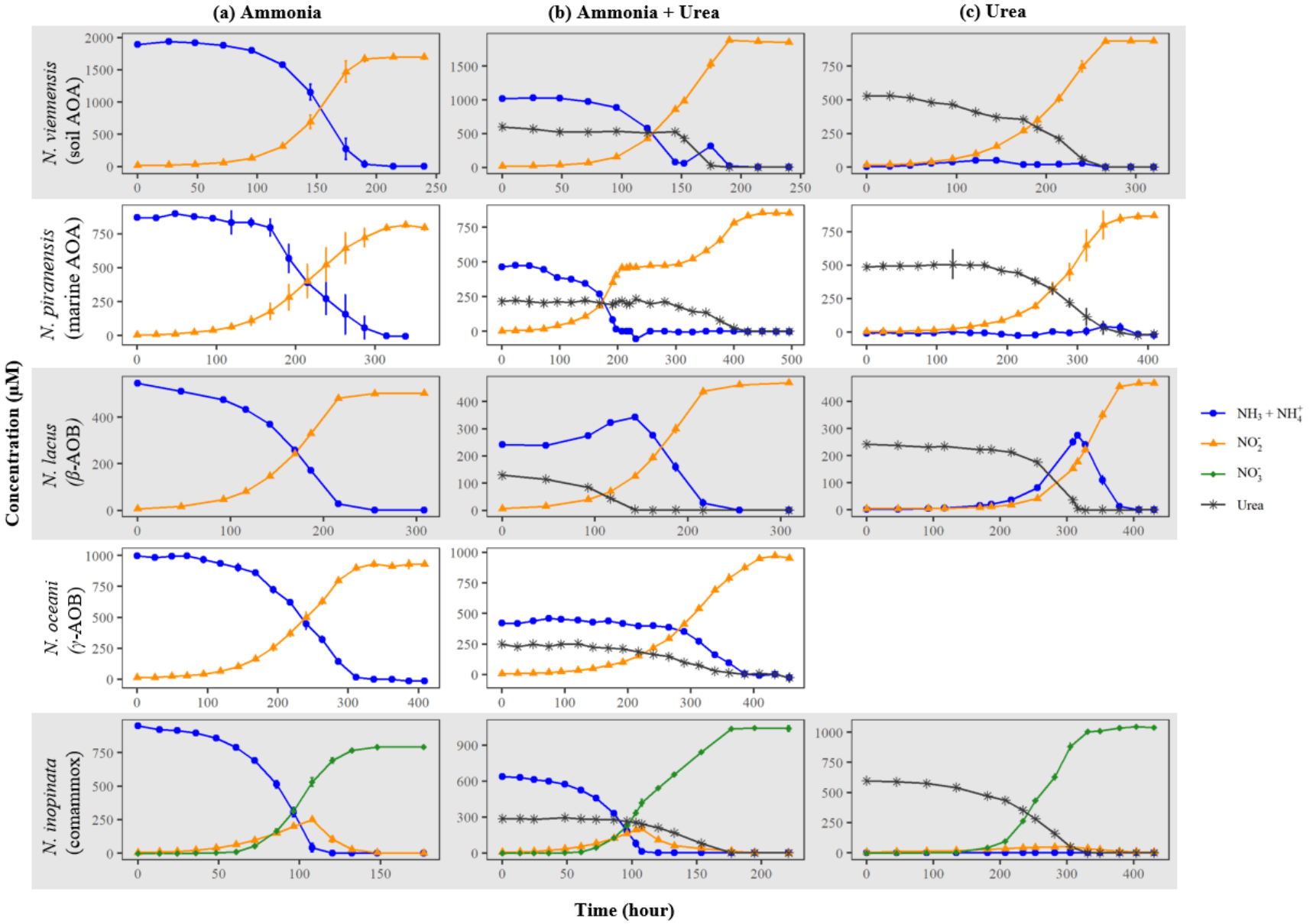
(a) Ammonia
(b) Ammonia + Urea
(c) Urea
N. viennensis (soil AOA)
N. piranensis (marine AOA)
N. lacus (β-AOB)
N. oceani (γ-AOB)
N. inopinata (comammox)
Concentration (μM)
Time (hour)
NH3 + NH4+
NO2-
NO3-
Urea

Figure 7-1. Growth of the ammonia oxidizers with ammonia and urea: (a) only ammonia, (b) ammonia + urea, and (c) only urea. All incubations were inoculated with 1% maintenance culture grown on ammonia at mid-exponential phase. Markers and error bars are average and one standard deviation of n = 3 biological replicates. The standard deviation is smaller than the marker if error bar is not visible. Urea-only incubation was not conducted for *N. oceani* due to the extremely slow specific growth rate.

7.3.2 Maximum specific growth rate and yield

The μ_{max} and yield of the incubations with different nitrogen substrates are shown in **Figure 7-2**. In comparison to the ammonia-only incubations, incubations with urea led to a significant reduction in both μ_{max} and yield for *N. viennensis*. Interestingly, for *N. piranensis*, the switch in nitrogen substrate from ammonia to urea (in the A+U incubation) imposed a greater hindrance on the μ_{max} than if the organism was grown on only urea. This low μ_{max} after switching from utilizing ammonia to urea was probably related to the long diauxic lag as discussed in Section 7.3.1. *N. lacus* was the only AOO where incubation on urea resulted in a higher μ_{max} and yield than incubation on ammonia. This observation challenges the assumption that ammonia is always the most-preferred substrate for ammonia oxidizers.

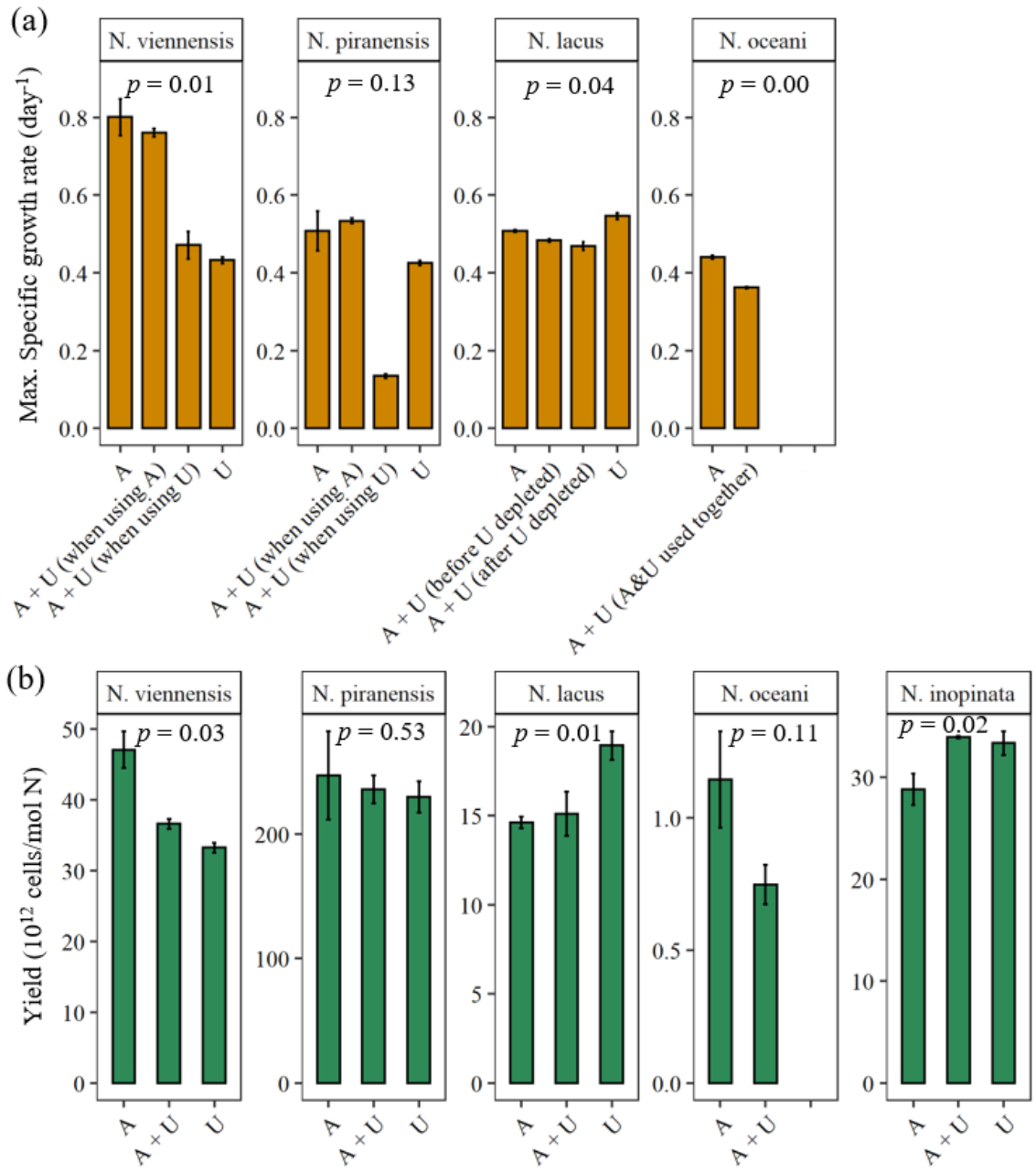

Figure 7-2. Maximum specific growth rate (μ_{max}) and yield of the ammonia oxidizers. (a) μ_{max} was determined from log linear region of NO_2^- production. The growth rate of *N. inopinata* was not calculated as it is not known whether the metabolic products (NO_2^- or NO_3^-) can be used as an indicator for comammox growth as for AOA and AOB. (b) Yield is the cell concentration at the end of the incubation divided by the initial nitrogen substrate concentration. A =

incubation with ammonia only; A + U = incubation with ammonia plus urea; U = incubation with urea only. Urea-only incubation was not conducted for *N. oceani* due to the extremely slow specific growth rate. Bar heights and error bars are average and one standard deviation of n = 3 biological replicates. The *p*-values were calculated from two-tailed t-test ($\alpha = 0.05$) for A and U incubations (or A and AU incubations in the case of *N. oceani*).

7.3.3 Response to Sudden Alternative Nitrogen Substrate Addition

To test the regulatory behavior of the ammonia- and urea-utilizing genes, we conducted experiments to observe the response of the ammonia oxidizers to a sudden introduction of an alternative substrate. When urea was spiked into the culture that was already growing on ammonia, both *N. viennensis* and *N. piranensis* would not consume the urea until ammonia was depleted (**Figure 7-3a**), indicating a repression on urea utilization. However, if these organisms were incubated with urea initially, introduction of ammonia did not stop the urea utilization but instead, ammonia and urea were consumed at the same time while accompanied by a reduction in growth rate (**Figure 7-3b**). On the other hand, preliminary results showed that even if *N. inopinata* were first growing on urea, they could switch off the urease activity within 30 hours after ammonia was spiked in. For *N. oceani*, urea hydrolysis started upon addition of urea to the ammonia incubation, without a reduction in growth rate.

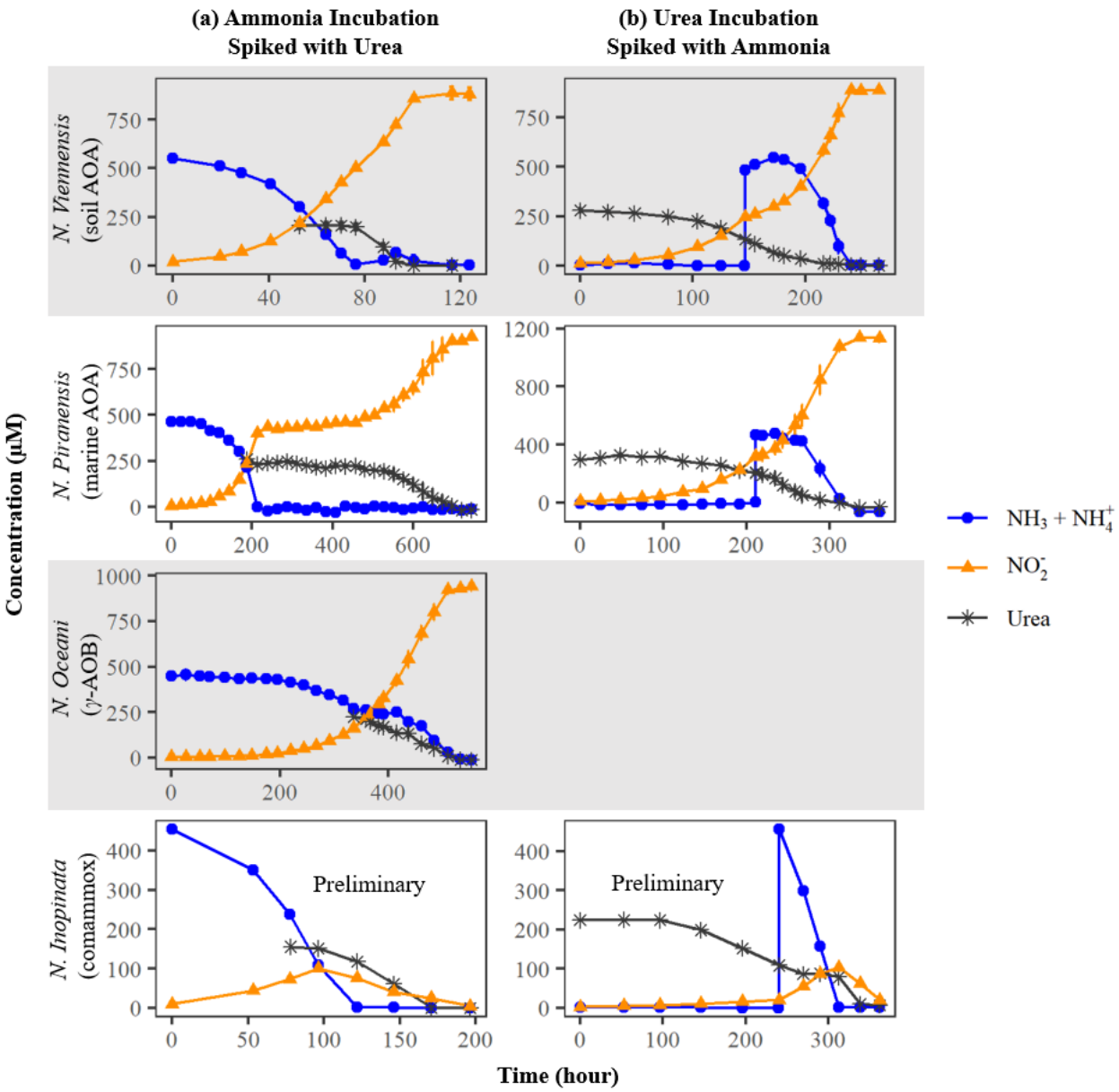

Figure 7-3. Response of the ammonia oxidizers to sudden introduction of an alternative nitrogen substrate. (a) Ammonia incubation spiked with urea. (b) Urea incubation spiked with ammonia. Urea-only incubation was not conducted for *N. oceani* due to the extremely slow specific growth rate. Markers and error bars are average and one standard deviation of n = 3 biological replicates. The standard deviation is smaller than the marker if error bar is not visible. Preliminary data for *N. inopinata* were from single incubation without replicates.

7.4 Hypotheses and Future Work

We hypothesize that for *N. viennensis* and *N. piranensis*, regulatory mechanisms are in place to repress the urease and urea transporter activities when the organisms are metabolizing ammonia. However, once the urea-utilization genes are activated, they do not have the regulatory mechanism to efficiently inactivate them. On the other hand, the urease functions of *N. inopinata* appeared to be highly regulated, being repressed whenever ammonia is available and de-repressed when ammonia is depleted. This physiological observation infers that *N. inopinata* may be more competitive in environments with alternating ammonia and urea availability. We also hypothesize that the urease and urea transporter genes are constitutively expressed in *N. lacus*. The growth rate of *N. lacus* is not affected by the type of nitrogen substrate and their metabolism on urea appears to result in a higher cell yield. However, the ammonia released into the environment can be accessed by other microorganisms, leaving *N. lacus* with less overall nitrogen substrate. The urea-utilizing genes appear to be constitutively expressed in *N. oceani* as well, but the rate of urea hydrolysis is well balanced with the rate of ammonia oxidation, which results in no background ammonia accumulation. This observation indicates that this group of AOO can benefit from urea availability given that it is not the sole nitrogen substrate.

Our work provided clear indication of nitrogen source repression among the AOO to facilitate selective usage of alternative nitrogen substrate, but where the regulation of nitrogen metabolism occur at the cellular level requires further research. The PII signal-transduction proteins are widely distributed and are known to control a variety of nitrogen regulatory functions in all three domains of life. PII proteins can regulate at different cellular levels, from acting as direct repressors/activators of gene expressions to post-translational regulation via protein-protein

interactions (Leigh & Dodsworth, 2007). Members of the PII family target a multitude of nitrogen regulatory proteins. For example, GlnB adenylylates (blocks) glutamine synthetase (GS) under condition of nitrogen sufficiency (i.e., high glutamine to α-ketoglutarate ratio) and de-adenylylates (activates) GS under nitrogen limitation (Brown et al., 1971). Other PII proteins, such as GlnK or NifI/NrpR, target the ammonia transporter or dinitrogenase in response to intracellular nitrogen availability (Coutts et al., 2002; Dodsworth & Leigh, 2006; Javelle et al., 2004; Lie et al., 2005). It was more recently identified that PII protein also regulates urea uptake in a non-diazotrophic cyanobacteria by targeting the UrtE protein (Watzer et al., 2019). Preliminary genomic analysis of the ammonia oxidizers tested in this study showed multiple copies of the PII proteins encoded in their genomes (e.g., 6 and 4 copies of the GlnB homolog in *N. viennensis* and *N. piranensis*, respectively). Further analysis is required to elucidate whether these PII protein homologs play a role in the nitrogen source repression phenomenon observed in this study.

References

Allison, S.M., Prosser, J.I. 1991. UREASE ACTIVITY IN NEUTROPHILIC AUTOTROPHIC AMMONIA-OXIDIZING BACTERIA ISOLATED FROM ACID SOILS. *Soil Biology & Biochemistry*, **23**(1), 45-51.

Alonso-Saez, L., Waller, A.S., Mende, D.R., Bakker, K., Farnelid, H., Yager, P.L., Lovejoy, C., Tremblay, J.E., Potvin, M., Heinrich, F., Estrada, M., Riemann, L., Bork, P., Pedros-Alio, C., Bertilsson, S. 2012. Role for urea in nitrification by polar marine Archaea. *Proceedings of the National Academy of Sciences of the United States of America*, **109**(44), 17989-17994.

Brown, M.S., Segal, A., Stadtman, E.R. 1971. MODULATION OF GLUTAMINE SYNTHETASE ADENYLYLATION AND DEADENYLYLATION IS MEDIATED BY METABOLIC TRANSFORMATION OF PII-REGULATORY PROTEIN. *Proceedings of the National Academy of Sciences of the United States of America*, **68**(12), 2949-&.

Burton, S.A.Q., Prosser, J.I. 2001. Autotrophic ammonia oxidation at low pH through urea hydrolysis. *Applied and Environmental Microbiology*, **67**(7), 2952-2957.

Coutts, G., Thomas, G., Blakey, D., Merrick, M. 2002. Membrane sequestration of the signal transduction protein GlnK by the ammonium transporter AmtB. *Embo Journal*, **21**(4), 536-545.

Daims, H., Lebedeva, E.V., Pjevac, P., Han, P., Herbold, C., Albertsen, M., Jehmlich, N., Palatinszky, M., Vierheilig, J., Bulaev, A., Kirkegaard, R.H., von Bergen, M., Rattei, T., Bendinger, B., Nielsen, P.H., Wagner, M. 2015. Complete nitrification by Nitrospira bacteria. *Nature*, **528**(7583), 504-+.

Dodsworth, J.A., Leigh, J.A. 2006. Regulation of nitrogenase by 2-oxoglutarate-reversible, direct binding of a PII-like nitrogen sensor protein to dinitrogenase. *Proceedings of the National Academy of Sciences of the United States of America*, **103**(26), 9779-9784.

Fawcett, J.K., Scott, J.E. 1960. A RAPID AND PRECISE METHOD FOR THE DETERMINATION OF UREA. *Journal of Clinical Pathology*, **13**(2), 156-159.

Frankland, P.F., Frankland, G.C. 1890. V. The nitrifying process and its specific ferment.—Part I. *Philosophical Transactions of the Royal Society B*, **181**, 107–128.

Gorke, B., Stulke, J. 2008. Carbon catabolite repression in bacteria: many ways to make the most out of nutrients. *Nature Reviews Microbiology*, **6**(8), 613-624.

Houlton, B.Z., Bai, E. 2009. Imprint of denitrifying bacteria on the global terrestrial biosphere. *Proceedings of the National Academy of Sciences of the United States of America*, **106**(51), 21713-21716.

Javelle, A., Severi, E., Thornton, J., Merrick, M. 2004. Ammonium sensing in Escherichia coli - Role of the ammonium transporter AmtB and AmtB-GlnK complex formation. *Journal of Biological Chemistry*, **279**(10), 8530-8538.

Jiang, Q.Q., Bakken, L.R. 1999. Comparison of Nitrosospira strains isolated from terrestrial environments. *Fems Microbiology Ecology*, **30**(2), 171-186.

Kitzinger, K., Padilla, C.C., Marchant, H.K., Hach, P.F., Herbold, C.W., Kidane, A.T., Konneke, M., Littmann, S., Mooshammer, M., Niggemann, J., Petrov, S., Richter, A., Stewart, F., Wagner, M., Kuypers, M.M.M., Bristow, L.A. 2019. Cyanate and urea are substrates for nitrification by Thaumarchaeota in the marine environment. *Nature Microbiology*, **4**(2), 234-243.

Koch, H., van Kessel, M., Lucker, S. 2019. Complete nitrification: insights into the ecophysiology of comammox Nitrospira. *Applied Microbiology and Biotechnology*, **103**(1), 177-189.

Konneke, M., Bernhard, A.E., de la Torre, J.R., Walker, C.B., Waterbury, J.B., Stahl, D.A. 2005. Isolation of an autotrophic ammonia-oxidizing marine archaeon. *Nature*, **437**(7058), 543-546.

Koper, T.E., El-Sheikh, A.F., Norton, J.M., Klotz, M.G. 2004. Urease-encoding genes in ammonia-oxidizing bacteria. *Applied and Environmental Microbiology*, **70**(4), 2342-2348.

Leigh, J.A., Dodsworth, J.A. 2007. Nitrogen regulation in bacteria and archaea. *Annual Review of Microbiology*, **61**, 349-377.

Lie, T.J., Wood, G.E., Leigh, J.A. 2005. Regulation of nif expression in Methanococcus maripaludis - Roles of the euryarchaeal repressor NrpR, 2-oxoglutarate, and two operators. *Journal of Biological Chemistry*, **280**(7), 5236-5241.

Lu, L., Han, W.Y., Zhang, J.B., Wu, Y.C., Wang, B.Z., Lin, X.G., Zhu, J.G., Cai, Z.C., Jia, Z.J. 2012. Nitrification of archaeal ammonia oxidizers in acid soils is supported by hydrolysis of urea. *Isme Journal*, **6**(10), 1978-1984.

Martens-Habbena, W., Berube, P.M., Urakawa, H., de la Torre, J.R., Stahl, D.A. 2009. Ammonia oxidation kinetics determine niche separation of nitrifying Archaea and Bacteria. *Nature*, **461**(7266), 976-U234.

Mobley, H.L.T., Island, M.D., Hausinger, R.P. 1995. MOLECULAR-BIOLOGY OF MICROBIAL UREASES. *Microbiological Reviews*, **59**(3), 451-480.

Norton, J.M., Klotz, M.G., Stein, L.Y., Arp, D.J., Bottomley, P.J., Chain, P.S.G., Hauser, L.J., Land, M.L., Larimer, F.W., Shin, M.W., Starkenburg, S.R. 2008. Complete genome sequence of Nitrosospira multiformis, an ammonia-oxidizing bacterium from the soil environment. *Applied and Environmental Microbiology*, **74**(11), 3559-3572.

Palomo, A., Pedersen, A.G., Fowler, S.J., Dechesne, A., Sicheritz-Ponten, T., Smets, B.F. 2018. Comparative genomics sheds light on niche differentiation and the evolutionary history of comammox Nitrospira. *Isme Journal*, **12**(7), 1779-1793.

Qin, W., Amin, S.A., Martens-Habbena, W., Walker, C.B., Urakawa, H., Devol, A.H., Ingalls, A.E., Moffett, J.W., Armbrust, E.V., Stahl, D.A. 2014. Marine ammonia-oxidizing archaeal isolates display obligate mixotrophy and wide ecotypic variation. *Proceedings of the National Academy of Sciences of the United States of America*, **111**(34), 12504-12509.

Qin, W., Heal, K.R., Ramdasi, R., Kobelt, J.N., Martens-Habbena, W., Bertagnolli, A.D., Amin, S.A., Walker, C.B., Urakawa, H., Konneke, M., Devol, A.H., Moffett, J.W., Armbrust, E.V., Jensen, G.J., Ingalls, A.E., Stahl, D.A. 2017. Nitrosopumilus maritimus gen. nov., sp nov., Nitrosopumilus cobalaminigenes sp nov., Nitrosopumilus oxyclinae sp nov., and Nitrosopumilus ureiphilus sp nov., four marine ammonia-oxidizing archaea of the phylum Thaumarchaeota. *International Journal of Systematic and Evolutionary Microbiology*, **67**(12), 5067-5079.

Qin, W., Zheng, Y., Zhao, F., Wang, Y.L., Urakawa, H., Martens-Habbena, W., Liu, H.D., Huang, X.W., Zhang, X.X., Nakagawa, T., Mende, D.R., Bollmann, A., Wang, B.Z., Zhang, Y., Amin, S.A., Nielsen, J.L., Mori, K., Takahashi, R., Armbrust, E.V., Winkler, M.K.H., DeLong, E.F., Li, M., Lee, P.H., Zhou, J.Z., Zhang, C.L., Zhang, T., Stahl, D.A., Ingalls, A.E. 2020. Alternative strategies of nutrient acquisition and energy conservation

map to the biogeography of marine ammonia-oxidizing archaea. *Isme Journal*, **14**(10), 2595-2609.
Ravishankara, A.R., Daniel, J.S., Portmann, R.W. 2009. Nitrous Oxide (N2O): The Dominant Ozone-Depleting Substance Emitted in the 21st Century. *Science*, **326**(5949), 123-125.
Sigurdarson, J.J., Svane, S., Karring, H. 2018. The molecular processes of urea hydrolysis in relation to ammonia emissions from agriculture. *Reviews in Environmental Science and Bio-Technology*, **17**(2), 241-258.
Thamdrup, B., Dalsgaard, T. 2002. Production of N2 through Anaerobic Ammonium Oxidation Coupled to Nitrate Reduction in Marine Sediments. *Applied and Environmental Microbiology*, **68**(3), 1312-1318.
Urbanczyk, E., Sowa, M., Simka, W. 2016. Urea removal from aqueous solutions-a review. *Journal of Applied Electrochemistry*, **46**(10), 1011-1029.
Ward, B.B., Devol, A.H., Rich, J.J., Chang, B.X., Bulow, S.E., Naik, H., Pratihary, A., Jayakumar, A. 2009. Denitrification as the dominant nitrogen loss process in the Arabian Sea. *Nature*, **461**(7260), 78-U77.
Watzer, B., Spat, P., Neumann, N., Koch, M., Sobotka, R., Macek, B., Hennrich, O., Forchhammer, K. 2019. The Signal Transduction Protein P-II Controls Ammonium, Nitrate and Urea Uptake in Cyanobacteria. *Frontiers in Microbiology*, **10**.
Zorz, J.K., Kozlowski, J.A., Stein, L.Y., Strous, M., Kleiner, M. 2018. Comparative Proteomics of Three Species of Ammonia-Oxidizing Bacteria. *Frontiers in Microbiology*, **9**.

Appendix F. Supplementary Material for Chapter 7

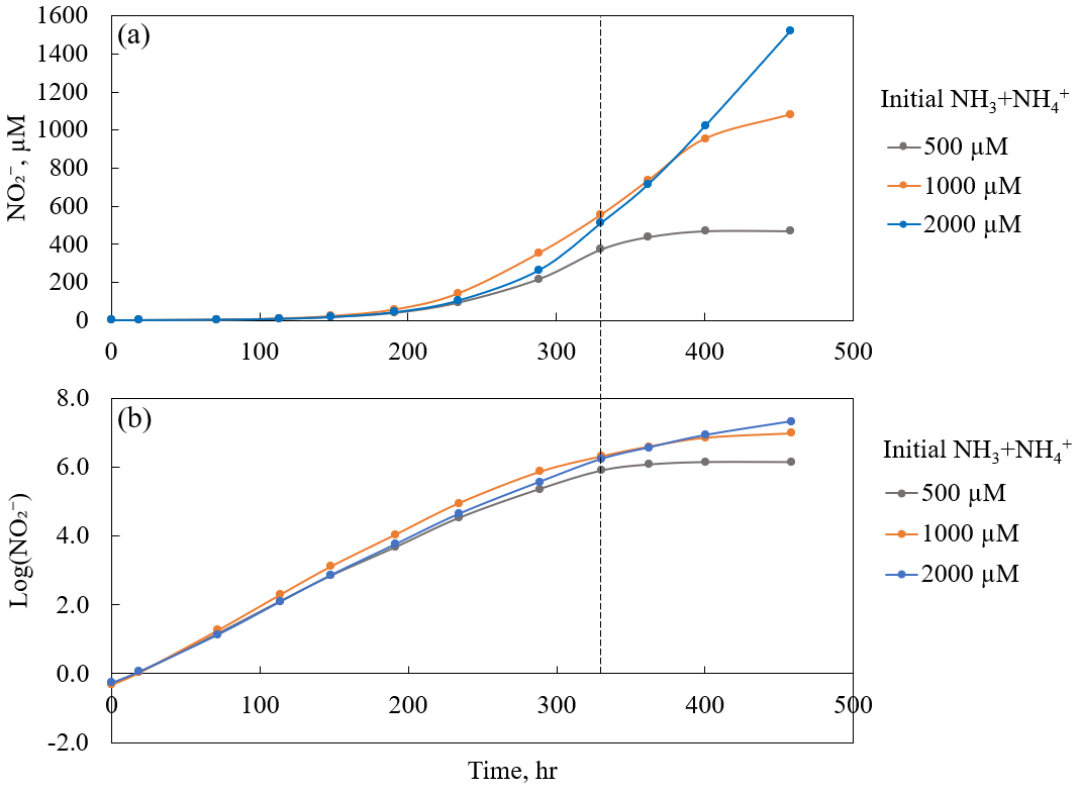

Figure S1. Effect of NO_2^- inhibition on *N. lacus*. *N. lacus* was grown at different initial ammonia concentrations to assess the effect of nitrite inhibition on the strain. (a) Nitrite concentrations and (b) nitrite concentrations on log scale. Dash line indicates where the slope of the log nitrite production curve appeared to start decreasing when NO_2^- concentration reached 500 µM.

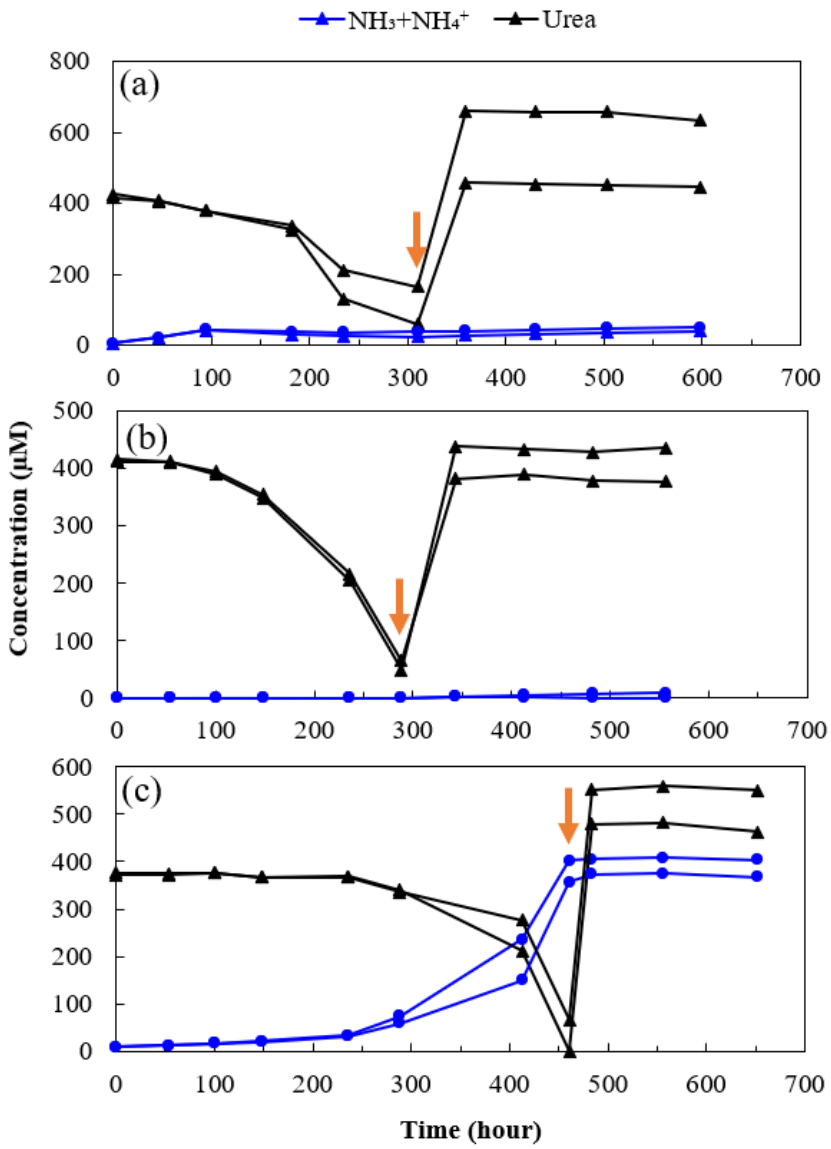

Figure S2. Extracellular urease activity checks. (a) *N. viennensis*, (b) *N. inopinata*, and (c) *N. lacus*. Arrow indicates time when cells were removed with 0.2 μm filter and re-addition of urea. The two curves with identical colors and markers are biological duplicates.

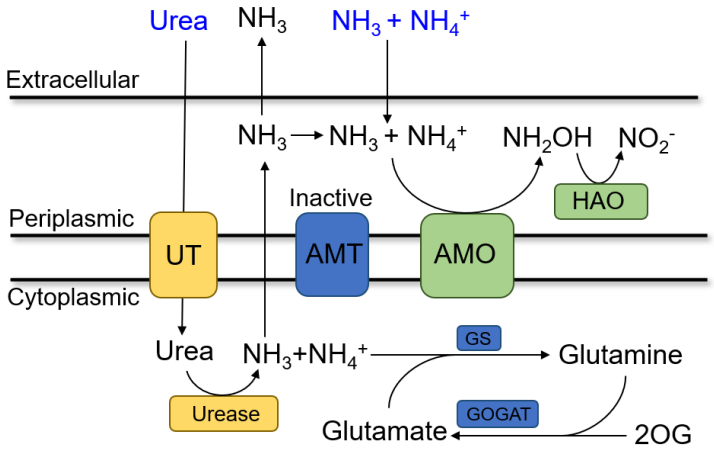

Figure S3. Schematic of substrate and metabolite flows for a hypothetical scenario where ammonia added in the media is not used by *N. lacus* for nitrogen assimilation. UT = urea transporter; AMO: ammonia monooxygenase; AMT: ammonia transporter; GS: glutamine synthetase. HAO: hydroxylamine oxidoreductase.

Chapter 8.

Conclusions and Future Outlook

The main goal of this thesis is to enhance nutrient removal and recovery by developing compact wastewater treatment solutions and inventing new concepts for nutrient recovery. The integration of AGS technology into existing CFAS infrastructure presents a new opportunity for overcoming challenges currently faced by the wastewater engineering community. To lay the groundwork for this research effort, a survey was conducted in **Chapter 2** to investigate the extent of naturally occurring granules and the operational factors necessary for granules growth at 13 full-scale EBPR continuous flow plants. It was found that granules are already present and co-exist with flocs in some CFAS systems. To understand the respective roles of granules and flocs in the nutrient removal capacity of a continuous flow system, a hybrid granule and floc reactor was operated in **Chapter 3** that highlighted the partitioning of key microbial functional groups between the two biomass fractions. Then, a method for facilitating biofilm attachment and granule growth was tested at a full-scale EBPR wastewater treatment facility by utilizing an organic carrier made of kenafs. **Chapter 4** presented the process data and discussed the applicability of this technology for improving sludge settling and nutrient removal capacity. Collectively, these chapters indicated the heigh potential for integrating AGS technology in CFAS systems. The application of AGS technology was then expanded to the realm of nutrient recovery with a hypothetical scheme of recovering struvite with minimal equipment by leveraging the high thickening characteristics of AGS. This concept was tested with an AGS reactor treating aquaculture waste in **Chapter 5**. Finally, this thesis explored nutrient recovery

from an alternative source, human urine, by evaluating the feasibility of near-complete N and P recovery via struvite precipitation and acid scrubbing (**Chapter 6**) and expanding our knowledge in the ureolytic metabolism of ammonia oxidizers (**Chapter 7**).

8.1 Major Findings and Scientific Significance

This doctoral research advanced the knowledge of integrating the AGS technology into continuous flow systems with the following significant findings:

(1) Continuous flow wastewater treatment facilities are vastly different from the SBR-type AGS system in terms of reactor configuration, feeding regime, and hydraulic washout, and thus the promotion of granule growth in continuous flow system was not generally expected. Indeed, for the 100 plus years of the activated sludge history, the presence of granules remained unexplored although some colleagues had witnessed plants with "dense floc structures". This thesis conducted the first comprehensive survey of granule occurrence at existing CFAS plants and systematically described that granules were present at every EBPR facility with SVI of less than 100 ml/g. Analyses of process data and microbial community identified that the process configurations known to favor growth of PAO and GAO (i.e., high anaerobic feeding F/M ratios and soluble COD fraction in the influent) were possible contributing factors for the granule growth. It was demonstrated that given the right operating conditions, some CFAS plants (which were initially built for activated sludge) can produce high abundance of granules (up to 80%). This work hence acts as a stepping stone and an important incentive for the engineering profession to continue developing strategies to enhance granulation in CFAS. Further, the relevant operational factors identified in this study can be adopted to complement other ongoing efforts for floc densification in continuous flow systems (e.g., with hydrocyclones (Avila et al., 2021; Sturm et al., 2017)).

(2) Building upon the indication that the growth of PAO and GAO are beneficial for granulation in CFAS system, an EBPR-based hybrid granule/floc reactor simulating a continuous flow environment was operated. It was found that PAO were more active in the smaller particles (flocs and small granules) than the large granules, while the two biomass fractions were equally important for the AOB activities. This result highlighted the importance of smaller particles for nutrient removal in a granular activated sludge system and demonstrated that granules provide a favorable environment for the slower-growing AOB, which corroborate previous research of using granules to bioaugment mainstream nitrification (Figdore et al., 2018a). Further, this study provided indication of nitrite shunt in the smaller particles, as similarly reported in previous research (Kent et al., 2019), which is a relatively new finding for EBPR-based granules that could be leveraged upon to promote NOB suppression for aeration and carbon savings.

(3) This thesis presented the first viable full-scale application of the mobile organic biofilm process by adopting the kenafs carriers for facilitating biofilm attachment in an EBPR facility. With the addition of the kenaf carrier and the selective wasting of flocs, a significant improvement in sludge settleability (a reduction in SVI_{30} from >200 to 50 ml/g) was observed within 5 months. Activity measurements showed comparable biomass specific nutrient removal kinetics between the mobile organic biofilm particles and SBR-based granules, indicating the potential of the kenaf carriers as a simple solution for promoting sludge densification/granulation in continuous flow systems.

Innovative solutions for nutrient recovery from wastewater were explored as part of this body of research, and the resulting scientific significance are as follows:

(1) A proof-of-concept for struvite recovery without the need for thickening or anaerobic digestion was presented by leveraging the high thickening characteristics of AGS. It was demonstrated for the first time that using liquid from fermentation of aquaculture sludge, stable EBPR (with long term high C, N, and P removal efficiency) and full granulation can be achieved. In addition, high phosphorus concentration (>150 mg P/L) was obtained by simple anaerobic holding of the waste granules, indicating potential for struvite recovery. Based on the results, a conceptual scheme was presented to integrate nutrient removal and recovery in a recirculating aquaculture system. This concept was integrated as part of an aquaculture facility for two reasons: (a) fish farms are generally small facilities that wish to reduce their nutrient discharge but lack specialized thickening or digestion equipment and (b) the recovery product could be used onsite if the fish-rearing tanks are integrated with other farming practices such as hydroponics.

(2) This thesis showcased one of the few pilot-scale urine treatment and resource recovery studies with struvite precipitation, ammonia stripping, and acid scrubbing. Compared to lab-scale studies, pilot-scale investigations allowed a closer estimation for the energy consumption of the technology. The technology provided near-complete nutrient removal and roughly 55% and 85% recovery efficiency for P and N, respectively. The struvite recovery could be improved by using a different method for crystal capturing (Antonini et al., 2011; Etter et al., 2011), and the process was relatively simple and required minimal electricity input. The NaOH dosage for the ammonia stripping step consumed the majority of the overall energy demand (1066 MJ per m^3 urine processed), indicating that ammonia stripping may not be an economical option for nitrogen removal from urine and that biological means of nitrogen removal/recovery may be a more feasible solution.

(3) To advance the application of nutrient recovery from urine via nitrification, the ureolytic metabolism of ammonia oxidizers was studied. Surprisingly, there is little understanding on the selective use of alternative nitrogen substrates by the ammonia oxidizers, despite the extensive amount of research done on their isolation, characterization, and physiology. Such knowledge is relevant to understand nitrogen cycling in natural and engineered systems that are exposed to varying forms of nitrogen substrate (urea and ammonia in the case of urine). This thesis presented the first characterization of ureolytic metabolism of five phylogenetically distinct ammonia oxidizers, *Nitrososphaera viennensis* (soil AOA), *Nitrosopumilus piranensis* (marine AOA), *Nitrosospira lacus* (freshwater β-AOB), *Nitrosococcus oceani* (marine γ-AOB), and *Nitrospira inopinata* (comammox). The results highlighted the differences in preference for ammonia versus urea and an indication of nitrogen catabolite repression among the ammonia oxidizers. It also challenged the perception that ammonia is the preferred substrate for biomass assimilation and energy generation for all ammonia oxidizers.

8.2 Future Outlook

- The work on integrating AGS in CFAS system all pointed to a common theme that granulation in continuous flow systems might be easier that we thought and may be accomplished by conditions that favor EBPR metabolisms (i.e., anaerobic feast/famine feeding). Indeed, PAO and GAO have been suggested as important players in the granulation process due to their slow-growing metabolism (de Kreuk & van Loosdrecht, 2004). It is also known that microbial production of EPS is the key to granulation in wastewater systems as it acts as a matrix that facilitates granule formation and maintains granule stability (Seviour et al., 2019). However, there is no direct proof of PAO/GAO's involvement in EPS production

and ultimately, granulation. Future studies should elucidate whether the different microbial functional groups present in EBPR systems are important players for EPS production and ultimately the granulation process. Such knowledge is needed to lead the direction and strategy for the expansion of AGS technology and its integration in activated sludge systems. It would also strengthen and help advocate for the case of using EBPR as a complement for sludge densification at existing infrastructure.

- Observation of granules at full-scale EBPR plants and the application of mobile organic biofilm for sludge granulation were insightful. However, the practical implications of increased granule biomass in existing infrastructure must be addressed, such as whether granules can cause problems in the recirculation piping or increase aeration/mixing energy requirements. The current development of hydrocyclones and floc/granule separator (Avila et al., 2021; Figdore et al., 2018b) can be used to maintain a certain granule/floc ratio in the system. Of particular interest is the determination of the optimal granules/floc ratio in a CFAS system for ideal nutrient removal capacity. In addition, the current work did not determine whether the naturally occurring granules or the mobile organic biofilm had capacity for simultaneous nitrification and denitrification. Overall, future research should investigate the effect of granulation in existing CF systems on mixing requirements and solids recirculation, as well as the nutrient removal capacity of the granules formed, as needed to guide practical implementations.
- The evaluation of the partitioning of nutrient removal capacity in granules and flocs was conducted based on the conceptual scheme that favored the feed of influent carbon to the granules by bypassing a portion of the flocs from the anaerobic zone. Other selection factors such as plug flow feeding or hydraulic washout were not applied as these factors cannot be

easily adopted in continuous flow configurations. Demonstration of the conceptual scheme is of high engineering value as its application can imply whether biological means of granules selection alone (i.e., selection for EBPR metabolism) is sufficient to achieve granulation in continuous flow systems. The current work used VFA-based synthetic wastewater and utilized equal amounts of granules and flocs as seed. The high diffusible carbon fraction in the synthetic wastewater was favorable for granulation, and thus even flocs turned into granules in a short period of time. It is recommended that the conceptual scheme should be tested and verified with complex wastewater and an initial biomass that contain only flocs, to evaluate the potential of the strategies adopted in the conceptual scheme for achieving granulation in continuous flow systems.

- Struvite precipitation was the technological method for phosphorus recovery in this work. Despite decades of research and development, the wide application of struvite as fertilizer has remained stagnant due to challenges with regulations and the uncertain market value (Kehrein et al., 2020). Future research should investigate alternative uses of struvite that increase its market value or elucidate the legal and economic barriers hampering its sales (de Boer et al., 2018; Kim et al., 2021). The application of phosphorus recovery within an aquaculture facility is particularly exciting as the struvite produced can be directly used in the hydroponics onsite where fish farming is integrated with hydroponics (Arcas-Pilz et al., 2021). Such application can eliminate costs associated with transportation and create a more circular food production system.
- The nitrogen catabolite repression (i.e., selective use of ammonia over urea or vice versa) observed in the ammonia oxidizers suggested a regulatory response that requires further research. Intriguingly, this regulatory mechanism appears to vary among the phylogenetically

distinct ammonia oxidizers. Where the regulation of nitrogen metabolism occurs at the cellular level (i.e., transcriptionally or post-translationally) will require further research. By identifying the regulatory machinery behind the nitrogen catabolite repression and its phenotypic variations, the information can be used to infer the ecological niche of an organism. Molecular tools such as RNA-seq or proteomics may be combined with physiological data to advance this research effort.

References

Antonini, S., Paris, S., Eichert, T., Clemens, J. 2011. Nitrogen and Phosphorus Recovery from Human Urine by Struvite Precipitation and Air Stripping in Vietnam. *Clean-Soil Air Water*, **39**(12), 1099-1104.

Arcas-Pilz, V., Rufi-Salis, M., Parada, F., Petit-Boix, A., Gabarrell, X., Villalba, G. 2021. Recovered phosphorus for a more resilient urban agriculture: Assessment of the fertilizer potential of struvite in hydroponics. *Science of the Total Environment*, **799**.

Avila, I., Freedman, D., Johnston, J., Wisdom, B., McQuarrie, J. 2021. Inducing granulation within a full-scale activated sludge system to improve settling. *Water Science and Technology*, **84**(2), 302-313.

de Boer, M.A., Romeo-Hall, A.G., Rooimans, T.M., Slootweg, J.C. 2018. An Assessment of the Drivers and Barriers for the Deployment of Urban Phosphorus Recovery Technologies: A Case Study of The Netherlands. *Sustainability*, **10**(6).

de Kreuk, M.K., van Loosdrecht, M.C.M. 2004. Selection of slow growing organisms as a means for improving aerobic granular sludge stability. *Water Science and Technology*, **49**(11-12), 9-17.

Etter, B., Tilley, E., Khadka, R., Udert, K.M. 2011. Low-cost struvite production using source-separated urine in Nepal. *Water Research*, **45**(2), 852-862.

Figdore, B.A., Stensel, H.D., Winkler, M.K.H. 2018a. Bioaugmentation of sidestream nitrifying-denitrifying phosphorus-accumulating granules in a low-SRT activated sludge system at low temperature. *Water Research*, **135**, 241-250.

Figdore, B.A., Stensel, H.D., Winkler, M.K.H., Armenta, M., Bucher, B., Sukapanpotharam, P., Smyth, J. 2018b. Aerobic Granular Sludge Bioaugmentation in Low SRT Flocculent Activated Sludge: Bench Scale Demonstration and Pilot Testing. in: *WEFTEC*. New Orleans, LA, USA.

Kehrein, P., Van Loosdrecht, M., Osseweijer, P., Garfí, M., Dewulf, J., Posada, J. 2020. A critical review of resource recovery from municipal wastewater treatment plants–market supply potentials, technologies and bottlenecks. *Environmental Science: Water Research & Technology*, **6**(4), 877-910.

Kent, T.R., Sun, Y., An, Z., Bott, C.B., Wang, Z.-W. 2019. Mechanistic understanding of the NOB suppression by free ammonia inhibition in continuous flow aerobic granulation bioreactors. *Environment International*, **131**, 105005.

Kim, A.H., Yu, A.C., El Abbadi, S.H., Lu, K.T., Chan, D., Appel, E.A., Criddle, C.S. 2021. More than a fertilizer: wastewater-derived struvite as a high value, sustainable fire retardant. *Green Chemistry*, **23**(12), 4510-4523.

Seviour, T., Derlon, N., Dueholm, M.S., Flemming, H.-C., Girbal-Neuhauser, E., Horn, H., Kjelleberg, S., van Loosdrecht, M.C.M., Lotti, T., Malpei, M.F., Nerenberg, R., Neu, T.R., Paul, E., Yu, H., Lin, Y. 2019. Extracellular polymeric substances of biofilms: Suffering from an identity crisis. *Water research (Oxford)*, **151**, 1-7.

Sturm, B., Faraj, R., Figdore, B., Willoughby, A., Ford, A., Bott, C., Shiskowski, D., McFall, L., Downing, L. 2017. Balancing Granular Sludge with Activated Sludge Systems for Biological Nutrient Removal. *WEFTEC Conference Proceedings*, Chicago, IL.

Acknowledgement

I would like to express my foremost gratitude towards my Ph.D. adviser, Prof. Mari Winkler, who has been the pillar of my personal and professional development for the past six years. I am incredibly lucky to have an adviser who inspires and motivates her students to grow, while at the same time is supportive and understanding. Thank you, Mari, for being the leader you are and the amazing research environment that you provide us in the Winkler Lab. Thank you for advocating for me during difficult times and encouraging me to go beyond my comfort zone when I had doubts. I have learned and grown so much from working with you, and I look forward to a life-long connection.

I would like to extend my appreciation to my doctoral committee, Prof. Dave Stahl, Prof. Amy Mueller, and Prof. Wei Qin. I am incredibly fortunate to have Prof. Dave Stahl be part of my research journey, guiding me with the most insightful questions that led me to become a better thinker and scientist. I would also like to thank Prof. Amy Mueller, who devoted her time and expertise to advance my research and provided guidance and support on a challenging yet exciting project. I am also lucky to have the opportunity to work closely with Prof. Wei Qin, who taught me many culturing skills with patience and provides mentorship to me both professionally and personally.

I would like to remember Prof. H David Stensel, who introduced me to the world of wastewater engineering and whose guidance helped shape the first years of my doctoral research. His brilliance and passion for the field will continue to inspire me and make an impact on my future endeavors.

Next, I would like to thank the fellow graduate students that had grown together with me and supported me over the years. I want to express special thanks to Kathryn Cogert, who had been

on this journey with me since day one. She programmed the instrumentation and control for my first reactor and taught me many skills in the lab. She has been a good friend and continues to support me until this day. “Science sisters” forever! I want to give special thanks to Bao Nguyen Quoc, who had worked with me on many projects while sharing his skills and positivity. Thank you, Bao, for supporting me in and outside the lab and always being there for me. I would also like to thank Britt Abrahamson, Zach Flinkstrom, and Brian Roman for troubleshooting with me and supporting me on various projects; and the other graduate students, Bryce Figdore, Maxwell Armenta, John Andrew Carter, Lukas Keller, Shannon Cavanaugh, Bojan Pelivanoski, Mara Roteliuk, Kota Nishiguchi, and Ting Xie, whom I had the pleasure to work alongside during my time at Benjamin Hall.

I am very fortunate to have crossed paths with many postdocs and research scientists at the Stahl/Winkler Lab who contributed immensely to my growth and development over the years. I want to express my gratitude to Kristopher Hunt, who is the role model in the lab and has provided mentorship to me both technically and professionally; and Tom Lie, who altruistically shares his knowledge and lab skills and has been a great mentor to me. Special thanks to Matthieu Landreau for his guidance and support in and outside the lab. Thank you, Matthieu, for being a mentor and a true friend. I hope you are enjoying your career in the HIV vaccine development field. I also want to thank Sam Bryson who taught me many lab and data analysis skills and provided mentorship on my writing; and Kelley Meinhardt, Frederick von Netzer, and Nejc Stopnisek, for their patience and support when I was navigating my way through the lab as a new Ph.D. student. Thank you, Pieter Candry, Raymond (Studie) RedCorn, Katya Gottshall, Levi Straka, Prakit Saingam, Bo Li, and Korena Mafune, for sharing your knowledge and discussing science with me; it was a great pleasure working alongside you. In addition, I am

grateful for the research scientists and technicians that had worked so hard to keep the lab together, Bruce Godfrey, Jessica Hardwicke, Madelyn Shapiro, and Tanisha Jain.

It was my pleasure to have worked with many master's and undergraduate students, who had contributed to my research - Xichen Gao, Kim Tran, Jianfeng Zhou, Serena Lee, and Kristina Nguyen. Special thanks to Stephanie Herrera and Karisse Chandra Yamamoto, who had spent numerous hours on tasks that were not the most fun or good smelling. Thank you for working with me and supporting the research. It was my honor being your supervisor and learning alongside you at the same time.

Lastly, I want to thank my parents Ching-Ling Wei and Cheryl Wei. 爸爸媽媽，謝謝你們這幾十年來的愛與支持。你們的女兒居然可以拿到博士，希望你們了解這也是你們的功勞。I want to thank my one-and-only sister, Jennifer Wei, whom I can always talk to and seek support during happy and difficult times. Additionally, I am incredibly lucky to have a loving family in-law, Nan, Jasmine, Charles, and Jenny, for their companionship, their support with dog-sitting, and the delicious food. I would also like to thank my dog, Mei Li, for her unconditional love and her needs for walks and treats that had been a healthy distraction for me from research.

… and thank my partner-in-life, Train, for everything else. This doctoral journey would not have begun, nor would it have been successful without you.

This work was supported by the National Science Foundation (ID# 1510665 and 1603707), the EPA P3 Award (#83929101), the Defense Advanced Research Project Agency (ID#: HR0011-17-2-0064), the Department of Energy (ID#: DE-SC0020356) and the University of Washington.

Stephany P. Wei

Curriculum Vitae

Phone: +1 206-388-8439, Email: spw6422@uw.edu

EDUCATION

Ph.D. **Environmental Engineering, University of Washington** — Expected Mar 2022
Department of Civil & Environmental Engineering, Seattle, WA

M.S. **Civil Engineering, University of Washington** — 2013
Department of Civil & Environmental Engineering, Seattle, WA

B.S. **Civil Engineering, University of Washington** — 2011
Department of Civil & Environmental Engineering, Seattle, WA

RESEARCH EXPERIENCES

Doctoral Research: University of Washington — 2015 - Present
Research Supervisor: Dr. Mari Winkler

- Integration of aerobic granular sludge technology into existing wastewater infrastructure
- Biological nutrient removal and recovery from wastewater and human urine
- Ureolytic metabolism and gene regulations of ammonia oxidizing microorganisms

Master's Research: University of Washington — 2011 - 2013
Research Supervisor: Dr. David Stensel

- Installation and operations of automatic samplers to collect composite and grab samples from three onsite wastewater nitrogen removal systems
- Conduct field measurements and common wastewater laboratory analyses
- Contributions to EPA technology verification reports

SKILLS

Laboratory Proficiency:

- Reactor operations: continuous and sequencing batch bioreactors design and operations**;** LabVIEW programming and electrical wiring for instrumentation and controls.
- Cell culture and bioprocessing: cultivation and maintenance of microbial cultures; microbiol growth curves and cell counts; flow cytometry; cell concentrating with tangential flow filtration technique; cell immobilization with hydrogel beads; biofilm sectioning with cryostat.
- Molecular biology: Quantitative and end point PCR; fluorescence in-situ hybridization; DNA/RNA/protein extraction and PCR amplification for Illumina preparation and Sanger sequencing
- Analytical: UV-vis spectrophotometry; ion chromatography; HPLC; epifluorescence and laser confocal scanning microscopy.

Bioinformatics Proficiency:

- Analysis of 16S rRNA gene amplicon libraries
- Skilled with R programming and packages (e.g., DADA2, ggplot2, tidyverse, phyloseq)
- Familiar with bioinformatics software including: BLAST, STAMP, USEARCH

Language Proficiency: Bilingual English and Mandarin Chinese

INDUSTRY EXPERIENCES

Brown and Caldwell, Seattle, WA 2013 - 2015
Environmental Engineer

- Planning, modelling, and design for wastewater treatment plants
- Wastewater characterization; hydraulic profile modelling; clarifier stress testing
- Piping system design and specifications

City of Bellevue, Bellevue, WA 2011 - 2012
Utility Systems Engineering Intern

- Water and sewer modeling: capacity analysis and input data updates
- GIS mapping to identify and display system capacity bottlenecks
- Provided alternatives for system upgrades based on modeling results

AWARDS AND HONORS

- Rossano Fellowship, UW, 2019
- Water Magic Scholarship, fully funded study abroad program, Norwegian University of Life Sciences and the University Centre in Svalbard, Summer of 2017
- Society of Women Engineers Outstanding Female Award, UW, 2017
- College of Engineering Annual Dean's List, UW, 2010-2011
- Engineer-in-Training Certification
- College of Engineering Annual Dean's List, UW, 2009-2010

SUCCESSFUL RESEARCH GRANT CONTRIBUTIONS

- Mary Gates Research Scholarship, Award: $5000, 6-month research support for an undergraduate student, 2021.
- EPA P3 Student Design Competition Grant, Online Sensor for Wastewater Phosphorus Recovery, Award: $15,000, 2018, Grant #: 83929101.

PEER-REVIEWED PUBLICATIONS

1. **Wei, S.P.**, Stensel, H.D., Ziels, R.M., Herrera, S., Lee, P.H., Winkler, M.K.H. (2021). Partitioning of nutrient removal contribution between granules and flocs in a hybrid granular activated sludge system. *Water Research*, 203.

2. **Wei, S. P.**, Nguyen Quoc, B., Shapiro, M., Chang, P. H., Calhoun, J., Winkler, M. K. H. (2021). Application of aerobic kenaf granules for biological nutrient removal in a full-scale continuous flow activated sludge system. *Chemosphere*, 271.
3. Nguyen Quoc, B., **Wei, S. P.***, Armenta, M., Bucher, R., Sukapanpotharam, P., Stahl, D.A., Stensel, H.D., Winkler, M. K. H (2021). Aerobic granular sludge: Impact of size distribution on nitrification capacity. *Water Research*, 188. ***joint first author**
4. **Wei, S. P.**, H. D. Stensel, B. Nguyen Quoc, D. A. Stahl, X. W. Huang, P. H. Lee and M. K. H. Winkler (2020). "Flocs in disguise? High granule abundance found in continuous-flow activated sludge treatment plants." *Water Research*, 179.
5. **Wei, S. P.**, F. van Rossum, G. J. van de Pol and M. K. H. Winkler (2018). "Recovery of phosphorus and nitrogen from human urine by struvite precipitation, air stripping and acid scrubbing: A pilot study." *Chemosphere*, 212.

ARTICLES UNDER REVIEW & IN PREPARATION

1. **Wei, S. P.**, B. Roman, K. A. Hunt, K. C. Yamamoto and M. K. H. Winkler (2022). "A Proof-of-Concept for Nutrient Recovery from Aquaculture Waste using Aerobic Granular Sludge." *In Preparation*.
2. **Wei, S. P.**, J. B. Abrahamson, J. Johnston, E. Choi, H. Li, Z. Flinkstrom, X. Li, X. Wan, X. Sun, Y. Zheng, M. Wells, B. Wang, K. A. Hunt, H. Urakawa, D. Wang, C. Pan, D. A. Stahl, B. B. Ward, X. Mayali, W. Martens-Habbena, W. Qin and M. K. H. Winkler (2022). "Repression of ammonia and urea utilization by nitrifying microorganisms." *In Preparation*.
3. **Wei, S. P.**, E. Y. Gottshall, M. Landreau, D. A. Stahl and M. K. H. Winkler (2022). "Nitrifying Communities and Anammox Hydrogel Beads for Nitrogen Treatment of Urine." *In Preparation*.

CONFERENCE PAPERS/PRESENTATIONS

1. **Wei, S.**, K. Yamamoto, M.K.H. Winkler (2022). Aerobic Granular Sludge with Aquaculture Waste: Expanding the Technology for Nutrient Recovery. 17th IWA Leading Edge Technology Conference, Reno, Nevada. *Poster Display.*
2. **Wei, S.**, B. Nguyen Quoc, P.H. Chang, J. Calhoun, D.A. Stahl, P.H. Lee, M.K.H. Winkler (2021). Naturally-Occurring Granules and Application of Mobile Organic Biofilm in Continuous Flow Systems. IWA Biofilm Reactors Conference, Notre Dame, Virtual. *Oral Presentation.*
3. Boltz, J. P., G. Daigger, J. Calhoun, **S. Wei**, J. A. Carter, M. Winkler (2021). Mobile Organic Biofilm (MOB) Process: Biofilm and Suspended-Growth Synergies Expand Treatment Capacity without Extensive Modification to Existing Infrastructure. WEF Innovations in Process Engineering Conference.
4. **Wei, S.**, G. Estrada, A. Perantoni, I. Wren, M. Gangestad, M. Falk, J. Neethling (2021). Beyond Liquid Treatment: Reduce Nutrient Discharge Loads by Other Means. WRF Webinar Series. *Co-Speaker.*

5. Nguyen Quoc, B., **S. Wei**, M. Armenta, R. Bucher, P. Sukapanpotharam, D.A. Stahl, H.D. Stensel, M. Winkler (2020). Effect of granule sizes on ammonia oxidation rates. WEFTEC 2020 Proceedings.
6. **Wei, S.**, H. D. Stensel, B. Nguyen Quoc, P. H. Lee, X. W. Huang and M. K. H. Winkler (2019). What's in Your Sludge? Hunting for Baby Granules in Full-Scale Activated Sludge Treatment Plants. WEFTEC, Chicago, IL. *Oral Presentation.*
7. Kitt, D., **S. Wei**, M. Winkler and R. D. Cusick (2019). Characterizing the mechanism and rate of calcium phosphate precipitation in aerobic granular sludge. WEFTEC 2019 Proceedings.
8. **Wei, S.**, H.D. Stensel, B. Nguyen Quoc, P. H. Lee, X. W. Huang and M. K. H. Winkler (2019). What's in Your Sludge? Hunting for Baby Granules in Full-Scale Activated Sludge Treatment Plants. IWA Leading Edge Conference on Water and Wastewater Technologies, Edinburgh, UK. *Technical Keynote Speaker*.
9. **Wei S.**, H.D. Stensel and M. Winkler (2017), Phosphorus Recovery Using Aerobic Granular Activated Sludge Process Without Anaerobic Digestion. WEFTEC, Chicago, IL. *Oral Presentation.*
10. **Wei S.**, M.T. Brett, G. Grinnell, and H.D. Stensel (2014) Evaluation of Modified Recirculating Gravel Filter Systems for Nitrogen Removal in Onsite Wastewater Treatment. PNCWA, Vancouver, WA. *Oral Presentation.*

WHITE PAPER CONTRIBUTIONS

1. Enhanced Recirculating Gravel Filter (2013). Evaluation of On-Site Sewage System Nitrogen Removal Technologies. EPA Environmental Technology Verification Report. Report# DOH 337-140.
2. Vegetated Recirculating Gravel Filter (2013). Evaluation of On-Site Sewage System Nitrogen Removal Technologies. EPA Environmental Technology Verification Report. Report# DOH 337-138.

TEACHING EXPERIENCES

- **Teaching Assistant**, CEWA582: Biological Treatment Systems (Instructor: Dr. Mari Winkler), **Winter 2021**
  - Graduate level course with emphasis on biological wastewater treatment processes
  - Taught two lectures: *Phosphorus Removal in Wastewater Treatment* and *Nutrient Recovery*
  - Developed homework problems
- **Teaching Assistant**, CEE482: Wastewater Reuse and Resource Recovery (Instructor: Dr. Mari Winkler), **Winter 2019**
  - Undergraduate level course with emphasis on wastewater reuse and resource recovery
  - Taught one lecture on *Phosphorus Recovery*
  - Developed calculation problems for assignments and graded final projects

COMMUNITY SERVICE & OUTREACH

- Water and Environmental Seminar Organizing Committee, 2018-2020
- Engineering Discovery Days Exhibit Volunteer, 2019
- Secretary of American Water Works Associations and Water Environment Federation Student Club, 2016-2019
- Student Representative on Faculty Search Committee, 2018
- Panelist for Introduction to Civil Engineering Session, 2017

SUPERVISION EXPERIENCES

- Karisse A Hikaru Chandra Yamamoto, 2021 – present, undergraduate research on aerobic granular sludge treating aquaculture waste
- Stephanie Herrera, 2017 – 2018, undergraduate research on aerobic granular sludge in continuous flow systems
- Xichen Gao, 2017, Master's Thesis: Improving Phosphorus Recovery in Enhanced Biological Phosphorus Removal with Alternative Feeding Methods and Using Glycerol as Carbon Source
- Bao Nguyen Quoc, 2016, Master's Thesis: Combining Ammonium-Oxidizing Archaea with Denitrifying Phosphate Accumulating Organisms in Aerobic Granular Sludge for Wastewater Nutrient Removal

PROFESSIONAL ASSOCIATIONS

Association of Environmental Engineering & Science Professors, Sep 2020 – present
Water Environment Federation, 2011-2020